Functional analysis of KLF13 in the heart

Rami Darwich

A Thesis Submitted to the
Faculty of Graduate and Postdoctoral Studies
In Partial Fulfillment of the Requirements for the Degree of
Philosophy Doctorate in Biochemistry

Department of Biochemistry, Microbiology and Immunology
Faculty of Medicine
University of Ottawa

Abstract.

Congenital heart defects (CHD) are the largest class of birth defects in humans and are a major cause of infant mortality and morbidity. Deciphering the molecular and genetic etiologies central for heart development and the pathogenesis of congenital heart diseases (CHD) is a challenging puzzle. We have previously demonstrated that the zinc-finger kruppel-like transcription factor KLF13, expressed predominantly in the atria, binds evolutionarily conserved regulatory elements known as CACC-boxes and transcriptionally activates several cardiac promoters. KLF13 loss of function in Xenopus embryos was associated with cardiac developmental defects, underscoring its critical role in the heart. In the current study, using *in vivo* and *in vitro* approaches, we examined KLF13's mechanisms of action and its interaction with other cardiac regulators. To test the evolutionary conserved role in the mammalian heart, we deleted the *Klf13* gene in transgenic mice using homologous recombination. Mice with homozygote deletion of *Klf13* were born at reduced frequency owing to severe heart defects. We also report the existence of a novel isoform of KLF13, referred to here as KLF13b. Furthermore, we report that KLF13 interacts biochemically and genetically with the T-box transcription factor TBX5 which is a key regulator of heart development. Our data provide novel insight into the role of KLF13 in cardiac transcription and suggest that KLF13 is a genetic modifier of congenital heart disease. Furthering our knowledge of protein-protein interactions and gene transcription will enhance genotype-phenotype correlation and contribute to better understanding of the etiology of CHD.

Acknowledgment.

At the end of this stage of my renaissance learning, I am adopting the engineering motto "Question everything. Learn something. Answer nothing." However, I am certain that one day I will be reading the above lines with a smirk on my face, scrutinizing my naïveté.

I would like to express my most sincere gratitude to my supervisor Dr. Mona Nemer for mentoring me and providing a creative and open environment to work in. Her vast knowledge of cardiovascular research, innovative attitude towards scientific work, and guidance throughout this project were of great importance. Thank you for paving my first stretch of road towards being an independent researcher. I would also like to express my appreciation to Dr. Ilona Skerjanc, Dr. Duncan Stewart, and Dr. Balwant S. Tuana for their constructive criticism and insights during the course of this thesis.

I owe my gratitude to all present and former members of the "Nemer Lab" for their collegial guidance and support over the years. Thank you Hiba Komati, Wael Maharsy, Abir Yamak, Jamie Whitcomb, Lara Gharibeh, Megan Fortier, and Wenjuan Li for your friendship, cooperation, and guidance during the last couple of years. Special thank you to Janie Beauregard for expert technical assistance, comic relief, and insight into life (without you I would have been studying chaos theory by now).

I would also like to extend my thanks to my friends Feras Al Ghazawii and Mamoun Al Diab for their attempts to balance my life with many regrettable activities. My deepest gratitude goes to my mother, family, and my partner Jessica, whose endless love, understanding, and confidence in me have been essential for the completion of this thesis.

Montreal, February 2016

Rami Darwich

Table of Contents

List of Figures

List of Tables

List of Abbreviations

AD 293 cells	Human embryonic kidney cells
AHF	Anterior/secondary heart fields
ANP	Atrial natriuretic factor/peptide
ASD	Atrial Septal Defect
At	Atria
ATP	Adenosine triphosphate
BSA	Bovine serum albumin
BMB	Bone Morphogenetic proteins
BNP	Brain natriuretic peptide
CARE	Cardiac response element
CATF1	Cardiac response element transcription factor 1
CBP	cAMP responsive element-binding protein binding protein
cDNA	complimentary deoxyribonucleic acid
CHD	Congenital heart diseases
CMV	Cytomegalovirus
DBD	DNA binding domain
DCM	Dilated cardiomyopathy
DMEM	Dulbecco.s Modified Eagles Medium
DMSO	dimethyl sulfoxide
dNTP	deoxynucleotide triphosphate
DNA	Deoxyribonucleic acid
DSMA1	Distal spinal muscular atrophy type 1
DTT	dithiothreitol
ED	Embryonic day
EDTA	Ethylene diamine tetraacetic acid
EMSA	Electromobility Gel Shift Assay
FCS	Fetal calf serum
FGF	Basic fibroblast growth factors
FHF	First Heart Field
FITC	Fluorescein isothiocynate
FOG	Friend of GATA
GATA	GATA binding protein
h	Hour
HA	Hyaluronic acid
HA-tag	Haemagglutinin tag
HAT	Histone acetyltransferase
HDAC	Histone deacetylase
IGHMBP2	Immunoglobulin mu binding protein 2
LV	Left ventricle
kb	Kilobase
kDa	Kilodaltons
KO	Knockout
MEF2C	Myocyte Enhancer Factor 2
MHC	Myosin heavy chain
min	Minute
ml	Millilitre

µl	Microlitre
MLC	Myosin light chain
mM	Millimolar
mRNA	Messenger ribonucleic acid
NES	Nuclear export signal
NIH 3T3	Mouse embryonic fibroblast cell line
NKX	Nirenberg and Kim X=Mammalian class
NLS	Nuclear localisation signal
NMD	Neuromuscular degeneration
NRG	Neuregulins
OFT	Outflow tract
p300	a 300kDa histone acetyltransferase
PBS	phosphate buffered saline
PCAF	p300/CBP associated factor
PCR	polymerase chain reaction
PERE	Phenylephrine response element
PEX1	Phenylephrine-induced Complex-1
PFO	Patent foramen oval
RANTES	Regulated upon Activation, Normal T-cell Expressed, and Secreted
RV	Right ventricle
Sin3	Swi-independent-3
SMARD1	Spinal muscular atrophy with respiratory distress type 1
SMC	Smooth muscle cells
TAD	transactivation domain
TAE	Tris-acetate-EDTA
TAZ	Transcriptional co-activator with PDZ-binding motive
TBS	Tris-buffered saline
TBST	Tris-buffered saline with Tween-20
TBX	T-box transcription factor
SDS	sodium dodecylsulphate
ToF	Tetralogy of Fallot
VSD	Ventricular Septal Defect
ZF	Zinc finger
ZFP	Zinc finger protein

1. Introduction

1.1 Morphology of heart development.

The heart is a four-chambered pump composed of diverse cell types (e.g. cardiomyocytes, conduction system cells, smooth muscle cells, and endothelial cells) (1). This pumping organ, the first functional organ during vertebrate embryogenesis, arises through orchestrated spatiotemporal cell fate specification, migration, differentiation, proliferation, and morphogenesis. Cardiogenesis is initiated during gastrulation as inductive signals from the underlying endoderm commit mesodermal cardiac progenitor cells into two distinct cardiac progenitor cell fields. The two cardiac fields are presently known as the first and the second heart fields (FHFs and SHFs). As development progresses, these progenitor cells undergo expansion, migration, and organization to form the cardiac crescent (**Figure 1.1**). While the first heart field is located at the medial region of the crescent, the second heart field occupies more lateral regions of the crescent (2). Later during development, the beating linear heart tube will be formed from the migration of the FHF and its fusion along the ventral midline. At this stage, the tubular linear heart consists of: 1) an interior endocardial layer of cells that lines the lumen of the heart; 2) a muscular myocardial exterior layer of cells that grant the linear heart its peristaltic contraction; and 3) a cardiac jelly composed of extracellular matrix (ECM) that separates the two last layers (1,3-9). The spatiotemporal control of cardiac jelly development is essential for the septation of the heart as well as for valvulogenesis. As development progresses, the heart tube breaks the symmetry of the early embryo by looping to the right and initiating the correct positioning of the atrial and ventricular chambers along with the aorta and the pulmonary artery (10). Looping is accompanied by the onset of cardiac ballooning to form the archetypal vertebrate four-chambered structure. The chambers will form along the outer curvature of the balloons,

and the inner curvature will form the septa and valves. Cardiac maturation will then proceed to refine the ballooned structures by further growth, septation, and trabeculation to form the definitive four-chambered heart (11-13).

In contrast to the first heart field, the temporally delayed second heart field (SHF) line of progenitor cells contributes to the heart tube at the venous and arterial poles of the tube (1,3-8). Ultimately, the FHF will form the left ventricle of the four-chambered heart, whereas the SHF will give rise to the outflow tract, right ventricle, and most of the atria (1,3-6). Furthermore, the multipotent epicardium, a simple squamous mesothelium tissue that covers the outer surface of the myocardium, is also reported to contribute to the atrial and ventricular myocardium, coronary smooth muscle, and cardiac fibroblasts (6,13,14).

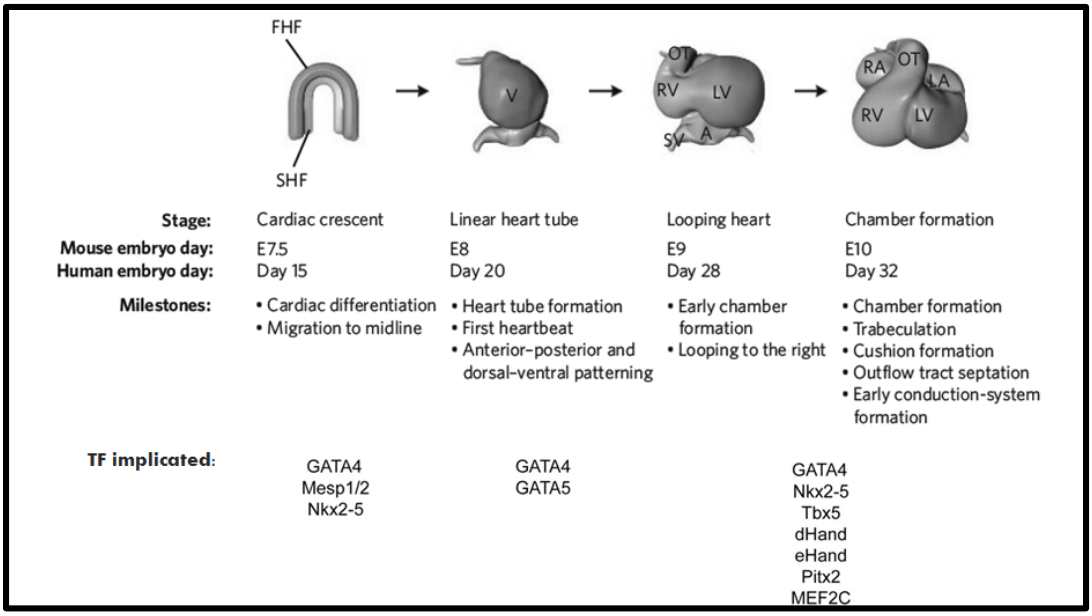

Figure 1.1: Overview of mammalian heart development.
At the earliest stages of heart formation (cardiac crescent), two pools of cardiac precursors exist. The first heart field (FHF) contributes to the left ventricle (LV), and the second heart field (SHF) contributes to the right ventricle (RV) and later to the outflow tract (OT), sinus venosus (SV), and left and right atria (LA and RA, respectively). Outflow tract septation separates the common outflow tract (OT) into the aorta (AO, connected to the left ventricle) and the pulmonary artery (PA, connected to the right ventricle). Figure modified from (6,12).

1.2 Formation of the cardiac valves.

The transition from the two chambered heart in fish, to the three chambered heart in amphibian and reptiles, to the archetypical four chambered heart in birds and mammals necessitated the formation of the cardiac valvular and septal system. Valve formation and chamber septation are necessary for proper and efficient blood flow into the pulmonary and systemic circuits (15,16).

In higher vertebrates, cardiac valves are classified as atrioventricular (AV) and outflow tract (OFT) valves. The AV valves originate from the AV cushions and separate the atria from the ventricles. While the mitral valve controls blood flow between the atrial and ventricular compartments of the left side of the heart, the tricuspid valve regulates blood flow in the compartments of the right side. The flattened laminar leaflets of the AV valves (two leaflets in the mitral and three in the tricuspid) are anchored by the annulus fibrosus and supported by a tension apparatus composed of tendinous chords and papillary muscles. In contrast to the AV valves, the semilunar OFT valves, the aortic and the pulmonary valves, control the blood flow between the left ventricle and aorta, and right ventricle and the pulmonary artery, respectively. The semilunar valves are composed of three leaflets that are formed from endocardial- and neural-crest mesenchymal cells (16,17).

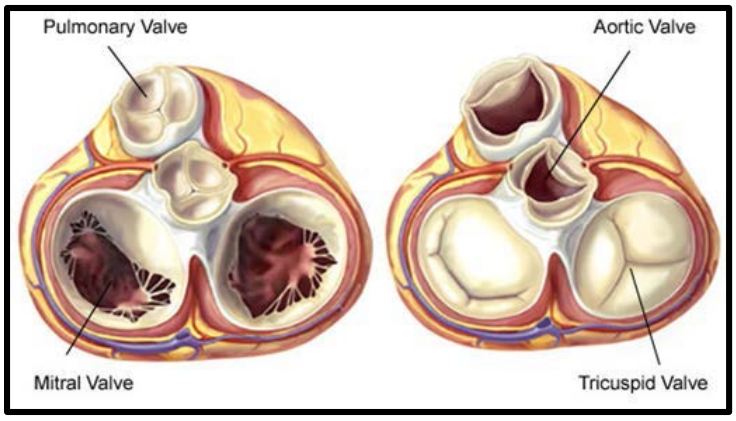

Figure 1.2: The four cardiac valves. Modified from (18)

The formation of the endocardial cushion starts with the delamination of the endocardium from the myocardium. The process is initiated and guided by the myocardium, which secretes the major components of extracellular matrix (ECM) in the AVC and OFT. The myocardium also hinders the expression of chamber-specific genes in these regions. At E9.0, the ECM can be considered as a thick, highly-hydrated and acellular basement membrane that extends from the myocardial layer to the endocardium that lines the endocardial cushions. Interestingly, at this stage the protruded or swollen endocardial cushions are able to act as a barrier to prevent the backflow of blood. The major components of this ECM include hyaluronan (HA), the proteoglycans aggregan and versican and glycoproteins like laminin, collagens (I, II, and IV), fibronectin, fibulins, fibrillins and periostin (16,17).

As cardiac development progresses, at E9.5 an evolutionarily conserved mechanism known as epithelial to mesenchymal transition (EMT) is initiated. Signaling from the myocardium and endocardium instructs the endocardial cells that line the endocardial cushions to undergo EMT. Paracrine signaling, such as TGFβ and Notch, from the myocardium instructs the endocardial cells to lose their cell polarity, to lose their cell-cell junctions, and to acquire the motile phenotype. Transcriptionally, the loss of cell-to-cell contact is facilitated by the downregulation of intercellular adhesion junction (E-cadherin and Tight Junctions) gene expression. On the other hand, the expression of EMT-inducing transcription factors, such as Snail1 and Snail2, promotes the formation of filopodia and lamellipodia by endocardial cells. In addition, the expression of extracellular matrix remodeling enzymes (such as metalloproteases) facilitates the migration of the nascent mesenchymal cell to exit the epithelium and migrate into the cardiac jelly (16,19).

Cellularization of the cushions by the proliferative mesenchymal cells prompts the fusion of the cardiac cushions and the formation of thin protruding primordial leaflets. The remodeling and maturation of the primordial leaflets into tri-stratified leaflets correctly attached to their supporting apparatus is not fully deciphered. However, it involves orchestrated events that include proliferation and apoptosis of mesenchymal cells, fusion of the cardiac cushions, and tissue maturation. The stratification of the leaflets is also manifested by their differential gene expression to form separate strata rich in elastin (ventricularis of OFT / atrialis of AV), proteoglycan (spongiosa) and collagen (fibrosa), oriented relative to blood flow. Together, these strata are required for normal valve structure and function, with dysregulation leading to disease (20). The most prominent difference between the AV and OFT valves is the presence of a supporting chordea tendineae on the ventricular side of the tricuspid and mitral valves. Furthermore, in the AV canal, EMT-derived mesenchymal cells are the sole contributor to the mitral and tricuspid valves, whereas in the OFT, endocardial and neural crest-derived EMT contribute to the formation of the aortic and pulmonary valves (16).

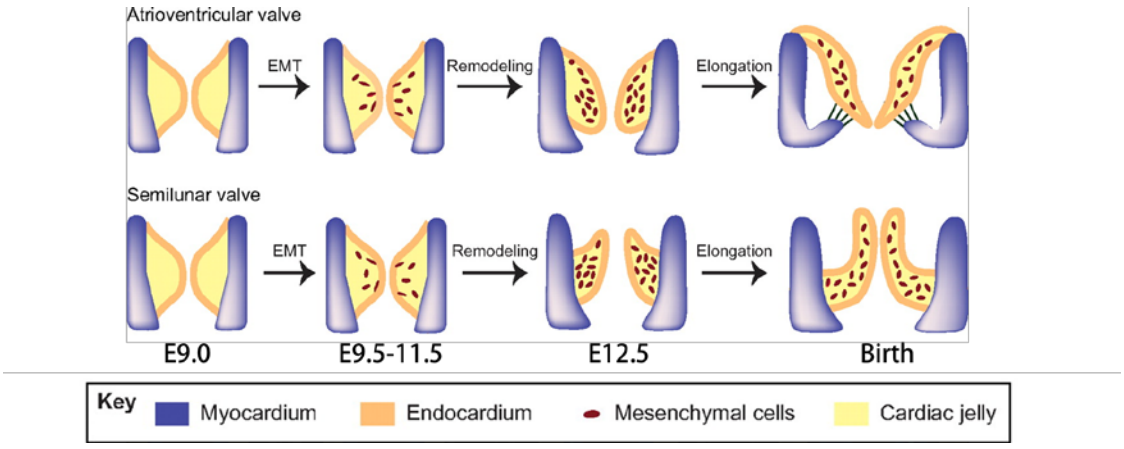

Figure 1.3: Development of the semilunar and atrioventricular valves.
Following EMT to generate mesenchymal cells that populate the cushions, the cellularized cushions remodel and elongate to from primitive valves that mature into thin valve leaflets. Modified figure from (21).

1.3 Atrial Septation.

Following the completion of cardiac looping, atrial septation is initiated around E10 (in mice). It starts with the formation and the growth of the muscular primary atrial septum (PAS), also known as septum primum, from the atrial roof downward to merge with the AV cushions. Although this septum emerges from the myocardium near the venous pole, EMT-derived mesenchyme from the adjacent rim of the pulmonary pit and the endocardium will coat the leading edge of the septum to form the mesenchymal cap. At this stage, and despite the presence of the septum, atrial communication through ostium primum maintains an adequate right-to-left shunt important for the oxygenation of the developing brain tissue. With further growth of the PAS towards the superior endocardial cushion of the AV canal, the atrial foramen gets smaller and then closes as the mesenchymal cap fuses with the superior endocardial cushion of the atrioventricular canal after E11.5. This closure is followed by myocardialization (the ingrowth of myocardial cells) of the mesenchymal cap. Interestingly, even before the completion of the septum primum, programed cell death takes place in this septum to form fenestrations that allow blood shunting between the atria. These fenestrations coalesce to eventually form the ostium secundum. At this stage, the primary atrial septum functions as a flap valve for the secondary septum. Concomitant with PAS closure, the AV endocardial cushions initiate their fusion to form separate left and right AC connections (16,22,23).

The secondary atrial septum, also known as septum secundum, grows as an infolding of the dorsal atrial wall on the right side of the existing primary septum base. However, this outgrowth never closes and an oval-shaped opening is left below its outer rim to form the foramen ovale (FO). Prior to birth, the venous blood shunts to the left atrium via the

foramen ovale for the delivery of the mother's oxygenated blood to the systemic circulation. As the lung pressure drops after birth and the pressure in the left atrium rises above that of the right atrium, the PAS flap adjoins the secondary septum's base. This closure will then be sealed by fusion of the two septa (16,22,23).

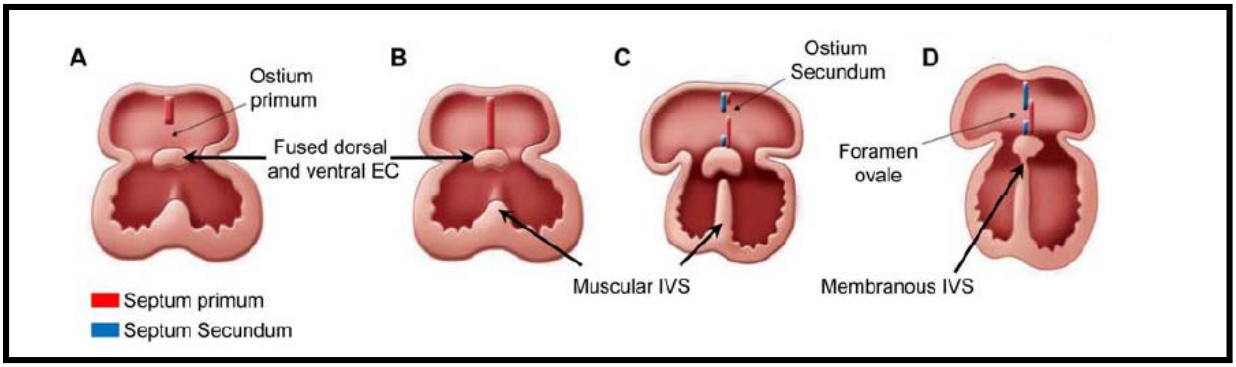

Figure 1.4: Atrial and ventricular septation

Atrial septation starts with the migration of the septum primum (red) and formation of the ostium primum (A), followed by apoptosis of the septum primum to create the ostium secundum (C) and migration of the septum secundum (blue) (C, D). In the final step, both septa fuse, leaving a foramen ovale (D). At around the same time, ventricular septation begins with the growth of the muscular IVS towards the ECs (A-C). Fusion of the IVS with the ECs closes the interventricular foramen and leads to the formation of the membranous IVS. EC: endocardial cushion; IVS: interventricular septum.

1.4 Ventricular Septation.

In addition to the inter-atrial septum, the proper division of the systemic and pulmonary circulations is also accomplished through the formation of the interventricular septum. Concomitant with the differentiation of the cardiac chambers, the development of the interventricular septum is initiated at around E10.5 with the infolding and coordinated growth of a primitive muscular interventricular septum that will eventually fuse with the endocardial cushions in the AV junction and the outflow tract at around E14.5. Initially, the primitive muscular interventricular septum is shaped as a crescent that extends posteriorly to the inferior endocardial cushion and anteriorly to the superior endocardial cushion. Proper septation of the ventricles involves the expansion and fusion of the superior and inferior endocardial cushions. As the IVS grows to septate the ventricles, an apical sinus persists between the two ventricles, known as the interventricular foramen. The membranous IVS, the last portion of the septum to be formed, is derived from the cushion tissue and it closes the foramen between the AV septum and the muscular septum. The cellular origin of the IVS is not completely deciphered yet, however, reports have pointed to the anterior heart field and trabecular myocardium as the origin (16,22-25).

1.5 Congenital Heart Diseases.

Congenital heart diseases (CHD) are a class of prenatal abnormalities affecting heart structure or function. These abnormalities are the most common developmental abnormalities in humans, afflicting nearly 1% of all live births, and are believed to be a major cause for prenatal death (6,26). Of the CHDs, abnormalities in cardiac septation and valvulogenesis are the most frequent. Septal defects range in severity from relatively minor, such as patent foramen oval (PFO), to complex malformations that require corrective

surgery to restore heart function like Tetralogy of Fallot (ToF). However, even minor, subclinical, or undiagnosed congenital defects can often lead to progressive phenotypes. Although considered minor, defects in valvulogenesis such as bicuspid aortic valves may progress to valve deterioration requiring valve replacement at a young age. Thus, early detection and interventions are crucial preventive measures for future complications such as valvular stenosis, stroke, or heart failure (12). Interestingly, cases of congenital heart diseases are frequently accompanied by secondary neurological disorders (27). Therefore, it is necessary to decipher the nature of CHDs and to understand their secondary effects on prenatal and postnatal physiology (6).

Understanding the genotype-phenotype relationship, identifying the contributing genes and molecular pathways, and deciphering the nature of variable penetrance of CHDs are essential for understanding the pathophysiology of CHDs (12). Despite sporadic random isolated cases of CHDs, patients suffering from CHDs often have a familial history. A wealth of knowledge was collected from the identification of several genomic loci linked to CHDs. Two patterns emerged from the associated defects: first, the defects are polygenic in nature meaning that a given structural defect is often linked to more than one locus; second, the mutation-linked genes are polymorphic - they are linked to multiple cardiac defects. Furthermore, the accumulated research indicates that phenotypes often display variable penetrance and expressivity, thus pointing to the influence of modifier genes and environmental influences on cardiac phenotypes (12,28). Interestingly, penetrance variability was also detected on the level of autosomal dominant diseases such as Holt-Oram Syndrome (HOS), which is caused by mutations in TBX5 (26). Within the same family, HOS affected members presented variable cardiac defects that varied from asymptomatic conduction system defects to severe structural anomalies (12) .

Heart development is an interplay of different genetic pathways and circuits. Disturbances in the intricacies of a particular circuit (e.g., ligand, receptor, transcription factor, or extracellular matrix protein) often result in correlated phenotypes. For example, in BMP signalling during atrioventricular valve formation, the conditional deletion of BMP (ligand), ALK2, 3 or 6 (receptors), or SMAD (transcription factors) were shown to result in similar cardiac defects (29). The combinatorial nature of transcription factors can also explain the polygenic nature of cardiac malformation. Many reports have indicated that the combinatorial interaction between the cardiac transcription factors NKX2.5, GATA-4 and TBX5 activates a subset of cardiac promoters. Interestingly, mutations in any of these factors are linked to similar ASD or VSD defects **(Table 1.1)** (12).

A buffering model might explain the penetrance variability of CHD (30,31). In this model, penetrance variability is attributed to: the function of a second allele, a duplicated gene, a pathway that maintains residual function, and/or from epigenetic and environmental factors. According to the model, the buffering capacity and tolerant window of loss of function of a particular gene becomes narrower by increased mutation loading on different components of a particular network (32). For example, in *Gata4-Gata6* double heterozygote mutant mice, and although mice haploinsufficient in one of the genes are viable, the compound heterozygosity of *Gata4* and *Gata6* is embryonically lethal at E13.5 due to numerous cardiovascular defects, including thinning of the ventricular walls and ventricular septal defects (33). As demonstrated by many reports, specific background and environmental factors are required for heterozygous mutation carriers to display cardiac defects (12). Thus, elucidating the genetic architecture of CHD requires the identification and characterization of: signaling pathways, downstream target genes, and cardiac transcription regulators and their interacting partners. An understanding of gene–gene as

well as gene–environment interactions is indispensable in the identification of additional regulators and effectors that are potential disease-causing genes.

With the previous points in mind, our lab has uncovered a novel role for KLF13, a member of the Kruppel-like family of zinc-finger proteins, in the transcriptional network of cardiac development. Loss of KLF13 function in *Xenopus* embryos, as well as mice, was linked to atrial septal defects and trabeculation defects similar to those observed in humans or mice hypomorphic in *Gata4* alleles (34). Thus, the analysis of KLF13's role in the genetic architecture of CHD and its underlying transcriptional networks will provide new insights for the discovery of novel molecular targets for diagnostics and therapeutics.

1.6 Molecular regulation of cardiac cushion and valve development.

Various molecules, transcription factors, and signaling pathways govern the process of valvular development as well as chamber septation including TGFβ/BMP, Notch, VEGF, NFATc1, ErbB, Wnt/β-catenin, Twist1, SOX9, TBX20, Msx1/2 and GATA4, and hyaluronic acid (16,35).

1.6.1 TGF, BMP and SMAD pathways

Members of the transforming growth factor beta (TGFβ) superfamily were among the first signaling molecules implicated in endocardial EMT. TGFβ signaling is mediated via type I and II TGFβ receptors leading to the activation of the SMAD transcription factors in the nucleus (21,36). Interestingly, multiple TGFβ isoforms are expressed in the endocardial cushions of mouse embryos. Spatially, while TGFβ1 is expressed in the endocardium, TGFβ2 is expressed in the myocardium and endocardium of the AV and OFT regions. On the other hand, TGFβ3 expression is confined to the endocardium and

mesenchymal cells after the onset of EMT. Due to the isoform's functional redundancy, disruption of multiple TGFβ ligands is often required to decipher their roles in heart development (37,38). The first direct evidence for the role of the TGFβ family in EMT came from *in vitro* AV cushion explant assays. Treatment of the explant with exogenous TGFβ1 and TGFβ2 promoted endocardial EMT and mesenchymal invasion of the collagen gel (19). Further studies demonstrated that TGFβ2 functions downstream of the NOTCH1, BMP2 and TBX2 pathways to activate Wnt/β-catenin signaling to promote EMT (16,21,38).

Expression of bone morphogenetic proteins (BMPs) is spatially and temporally correlated to the onset of EMT in the endocardial cushions. Spatially, BMP2 and BMP4 are expressed in the AV and OFT myocardium respectively; BMP6 is expressed in the myocardium of the OFT region and endothelial/mesenchymal cells of the AV canal; and BMP7 is restricted to the myocardium of the AV and OFT regions (39). Functionally, BMPs have diverse roles in valve development and cardiac septation. In the myocardium, BMP4 is essential for proper atrial and ventricular septation; as for BMP6 and BMP7, they are functionally redundant in the myocardium and in the cushion mesenchyme. While initial studies demonstrated that neither *Bmp6* nor *Bmp7* genes are required during cardiogenesis, mice that are null for both of these genes displayed hypocellular OFT cushions as well abnormal chamber septation (40). Myocardial BMP2 signaling, via Bmp type 1A receptor (Bmpr1a), induces the expression of Twist1, Msx1 and Msx2, which are all essential for EMT. In addition to that, myocardial BMP2 signaling activates the expression of the cushion extracellular matrix remodeling enzyme hyaluronic acid synthetase 2 (Has2) which is required for EMT (21). Adding to the complexity, signalling of BMP2, BMP4 and BMP7 through Bmp type 2 receptors (BMPR2) showed to have different spatial roles. Mice heterozygote for *Bmpr2* display interruption of the aortic arch (IAA), persistent truncus

arteriosus (PTA), and absent semilunar (OFT) valves. Conditional deletion of *bmpr2* in endothelial cells causes atrial septal defect (ASD), ventricular septal defect (VSD), and hyperplastic semilunar as well as AV valve leaflets, whereas *bmpr2* deletion in myocardial cells or in neural crest cells leads to septal defects characterized by double outlet right ventricle (DORV) or overriding aorta (OA)(16,21).

1.6.2 The Notch pathways

The Notch signalling pathway is essential for proper mammalian cardiac development. Dysregulation and mutations in Notch signaling were linked to human congenital heart defects such as bicuspid aortic valve disease (BAV), calcification of the heart valves, and ventricular septal defects (41). In mammals, the Notch receptor family encompasses a highly conserved family of four type I transmembrane receptors (NOTCH 1 to 4). Their ligands, five members collectively referred to as the DSL (Delta/Serrate/Lag-2), are also type I transmembrane proteins, and they include: Jagged1, Jagged2 (also called Serrate1 and Serrate2), and Delta-like 1, 3 and 4 (Dll1, Dll3 and Dll4) (42). Upon activation of Notch receptors by ligand binding at the cell surface, a series of sequential cleavages of the receptor (mediated by γ-secretase complex) ultimately releases the intracellular domain of Notch (NCID). Consequentially, NCID will then translocate to the nucleus to regulate gene transcription through interacting with the transcriptional repressor RBPJκ (recombination signal-binding protein 1 for J-κ) (41). Among Notch signaling target genes, the *Hes* (hairy enhancer of split) and *Hey* (hairy/enhancer of split-related with YRPW motif) families of basic helix–loop–helix transcription factors are the best defined (16,41).

The expressivity and the role of the different Notch signaling intricacies during cardiac development were extensively studied (43). Loss- and gain-of-function studies have

revealed the critical role of the Notch pathway in regulating cardiac development. Both *notch1*-deficient and *rbpjκ* -deficient embryos have significantly reduced EMT in the AV canal, as was determined using an *ex vivo* AV canal explant assay. In addition, these mutant mice were associated with reduced expression of TGFβ2 and its receptors, which as previously discussed, are critical initiators of EMT during heart development. Interestingly, supplementation of exogenous TGFβ2 or TGFβ3 to the mutant AV cushions in *ex vivo* explant assays was not sufficient to rescue the observed EMT defects (41,42,44). In addition, *notch1*-deficient embryos also presented with trabeculation defects due to decreased myocardial proliferation during early development. *Notch1* is highly expressed in the trabecular endocardium, where it controls myocardial differentiation and proliferation in a Neuregulin-1 (NRG-1)- and BMP10-dependent manner, respectively (42,44). The Notch target gene, *hey2*, was also found to be critical for proper heart development. *Hey2* is abundantly expressed and restricted to the endocardium of the AV canal and the compact myocardial layer of the ventricles. Studies showed its necessity for the initiation of EMT but not for the maintenance of the mesenchymal phenotype. Mice that are null for *hey2* have high postnatal mortality due to cardiovascular defects, including VSDs, pulmonic stenosis (PS), AV canal valve irregularities, and cardiac hypertrophy (16,42,45).

1.6.3 VEGF/NFAT/ Calcium signaling

Normal cardiac development is intricately dependent on the correct dosage of several growth factors including the vascular endothelial growth factor (VEGF)(46). VEGF is recognized for its role in regulating cell proliferation, vascular permeability, chemotaxis, survival of endothelial cells, and vasculogenesis as well as angiogenesis in the developing embryo (47). VEGF, also known as vascular permeability factor (VPF), is a potent secreted mitogen implicated in the activation, proliferation, and remodelling of the

endocardium (46,48). There are five VEGF isoforms in mammals: VEGF-A, VEGF-B, VEGF-C, VEGF-D, and the placental growth factor (PlGF). VEGF ligands are assembled by the homodimerization of two identical monomers associated by disulphide bonds (49). VEGF signaling is complicated and can occur by a combination of the five ligands binding to the two primary tyrosine receptors VEGFR1 (also known as FLT) and VEGFR2 (also known as FLK) with different specificities (50). The two VEGF receptors are expressed abundantly in the endocardium (16,48).

Cardiac expression of *Vegf* is induced during hypoxia, thus potentially mediating the morphogenic effects of hypoxia during cardiac morphogenesis. During early stages of cardiac development, VEGF is expressed in most endocardial cells of the primitive heart tube; however, at E9.5-10.5 its spatial expression becomes more restricted to cardiac cushions of the AV canal and OFT (51). Strikingly, VEGF has a dose and time dependent dual function in both initiating and terminating endocardial EMT. Interestingly, both gain and loss of VEGF function were associated with embryonic lethality. VEGF hypomorphism is embryonically lethal due to underdeveloped endocardial cushions, chamber malformation and compromised vascular development (52). Lethality in VEGF gain of function, a 2-3 fold increase in VEGF protein, was attributed to abnormal vasculogenesis and a myriad of heart defects including hypertrabeculation, thinner compact myocardia, and septal defects (51). In addition, conditional myocardial overexpression of VEGF at E9.5 also leads to septal and valve defects due to the abnormal expansion of the endocardial cushions (46). The aforementioned studies demonstrate the critical role of VEGF signaling, as well as its spatiotemporal expression, in regulating the proper development of the endocardial cushion and cardiac septation (16).

At E9.0, in mice, the endocardial cell transformation into mesenchymal cells requires the repression of VEGF expression in the myocardium underlying the site of prospective valve formation. This repression is mediated by calcineurin/NFATc (nuclear factor of activated T cells) signaling. Furthermore, at E11.0, a second wave of calcineurin/NFATc signaling is also required in the endocardium to direct valvular elongation and refinement (53). Calcineurin/NFATc signaling is activated by several receptors and ion channels that elevate intracellular Ca2+ leading to the activation of the Ca2+/calmodulin-dependent phosphatase, calcineurin. NFATc calcineurin-dependent dephosphorylation exposes nuclear localization signals and causes the transcription factor to translocate into the nucleus (53,54). Once NFATc is in the nucleus it forms a transcriptional complex, with the with NFAT nuclear partners (NFATn), that acts to repress or activate the expression of target genes (16,53,55).

Loss of NFATc1 in mice is embryonically lethal: the embryos die at E14.5 from hypomorphic semilunar and AV valves, as well as VSDs (56,57). However, analysis of earlier embryos showed normal endocardial cushion formation as well as normal initial septation of the OFT into aortic and pulmonary channels. Therefore, the developmental defects are likely to be due to abnormalities in the maturation of the endocardial cushions into valvuloseptal structures (56,57). Furthermore, loss of function of the myocardial factors NFATc2, NFATc3 or NFATc4 did not show abnormal valve development (16,58-60). However, compound deletions of NFATc2;c3;c4 in mice lead to significantly reduced EMT at E10.5 that was associated with a strong upregulation of VEGF expression (16,61). The precise molecular nature of Calcium-NFATc-VEGF signaling is still to be determined (16).

1.6.4 ErbB signalling

The neuregulins (NGR) are a family of four structurally related transmembrane proteins (NRG1-4). Among the family members, Neuregulin-1 (NRG-1) is the most abundant in the cardiovascular system (62). NRG-1 has approximately 30 isoforms as a result of its synthesis from different promoters and splicing variants, and these isoforms are classified into at least three subgroups (type I-III) (63). The active amino terminal domain of NRG-1 is secreted to the extracellular space through the α-secretase activity of metalloproteinase ADAMTs17 and ADAMTs19 (63,64). The active form of NRG-1 contains a cysteine-rich domain, a domain related to the epidermal growth factor (EGF), which exerts its effect in a paracrine manner. The paracrine effect of NRG-1 is mediated by binding and activating the ErbB family of tyrosine kinase transmembrane receptors that belong to the EGFR family (63). ErbB receptors are composed of an extracellular ligand-binding domain, a transmembrane domain, and a cytoplasmic tyrosine kinase domain. Binding of NRG-1 to its receptor induces dimerization and autophosphorylation events that lead to the propagation of the signal to the cytoplasm of the cell (16,62).

The distinct patterns of expression of NRG-1 signaling intricacies during cardiac morphogenesis suggest their differential functions. Around E9.0, NRG-1 is highly expressed and restricted to the endocardium. At this stage, the receptors ErbB2 and ErbB4 are highly expressed in the ventricular myocytes. On the other hand, ErbB3 is expressed in the endocardial and mesenchymal cells of the endocardial cushions (62). Interestingly, disruption of NRG-1 signaling (NRG-1 or the ErbB2, ErbB3, or ErbB4 receptors) is embryonically lethal due to numerous cardiac defects that are endocardial in nature (62). Furthermore, *erbb2* and *nrg1* null embryos die at E10.5 due to trabeculation defects and underdeveloped cushions. ErbB3 loss of function was lethal at E13.5 with severe

endocardial cushion defects that lead to blood reflux (65). On the other hand, *erbb4*-null embryos died ~E9.5 due to severe trabeculation defects but had no associated valvulogenesis defects (16,66).

The exact role of NRG-1 signaling and its mechanisms of action during cardiac development are yet to be deciphered. However, insight for its actions was acquired from studies of the function of hyaluronan synthase 2 (Has2) during AV canal formation. Has2 loss of function is embryonically lethal at E9.5 due to vasculature defects and severe reduction of cardiac jelly. Furthermore, *ex vivo* explant studies of AV canals from the mutant mice showed diminished endocardial cell migration and defective EMT. Mechanistically, the endocardial cushions of *has2* null embryos were also characterized with a reduced phosphorylation state of ErbB2 and ErbB3. Interestingly, the defects observed with the explant assay were rescued by the addition of exogenous hyaluronic acid (HA) or NRG-1 to the endocardial cushion explants which phosphorylated the ErbB receptors (67). These studies suggested that HA and NRG-1 in the cardiac jelly co-regulate ErbB2/ErbB3 signaling (16).

1.7 Cardiac transcription: Different levels of control

Cardiac progenitor populations undergo lineage commitment and expansion via coordinated positive and negative inductive signals from neighbouring endothelial, endocardial, and other mesodermal derived cells. Among these inductive signals are bone morphogenetic proteins (BMPs), basic fibroblast growth factors (FGF), and Wnt proteins. The decisive nature of these inductive signals during cardiac differentiation can be represented by the loss of FGF8 function in mice. FGF8 deficient embryos demonstrated

multiple cardiovascular lethal malformations that were related to the secondary heart field (SHF) (13,16,68,69).

Following the aforementioned inductive signaling, a number of cardiac-specific and evolutionarily-conserved transcription factors (TF) were found to be activated within the cardiac progenitor cells of the FHF and AHF. These factors include members of GATA (12), NKX2 (70), TBX (71), MEF2 (72), SRF (73) and HAND (74) factors. As an example, the zinc-finger containing factors, GATA4 and the homeodomain containing factor NKX2.5, were found to mediate BMP signalling (12). Furthermore, many of the cardiac regulators interact cooperatively to control their target promoters which express genes that control cardiac cell fates and morphogenesis. These target genes include muscle specific proteins such as α-myosin heavy chain (α-MHC), cardiac α-actin, and the A- and B-type natriuretic peptide genes (*Nppa* and *Nppb*) (75). Cardiac transcription factors also control the expression of other transcription factors via transcriptional feedback loops that stabilize and maintain proper cardiac gene programs (76). For example, GATA4 and TBX20 cooperatively activate both the NKX2.5 and MEF2C enhancers (13,77).

Chromatin remodelling and histone modification tightly control the accessibility and affinity of transcription factors to their binding sites. This layer of control adds another level of modulation to the spatiotemporal activity of cardiac transcription factors. For example, Baf60c, a unit of the BAF chromatin remodelling complex, mediates the augmentation of the transcriptional activities of GATA4, NKX2.5, and TBX5. This augmentation is mediated by the interaction between these DNA-binding transcription factors and the BAF complexes. Interestingly, embryos deficient in Baf60c demonstrated cardiac lethality at E10.0–11.0 (77). In addition, several histone modifying enzymes are

known to interact with various cardiac transcription factors (78,79). Histone acetyltransferase (HAT) proteins, for example p300, does not only control gene expression via the acetylation of lysine residues on histones but also via the acetylation of several transcription factors (e.g., GATA4). Acetylation activates and enhances the DNA-binding activity and the transcriptional activity of transcription factors (80). Treatment of embryonic stem cells with histone deacetylase (HDACs) inhibitors enhanced cardiac lineage differentiation due to the elevated levels of acetylated GATA4 (81). Therefore, multiple levels of transcriptional control regulate the accessibility and affinity of transcription factors to the downstream target genes. These levels of control ensure the proper spatiotemporal cardiac gene expression during the multiple stages of cardiac development (13,16,78,82).

1.8 Natriuretic peptides: A tool to decipher cardiac transcription.

The discoveries of the atrial natriuretic peptide (ANP), and brain natriuretic peptide (BNP) by De Bold and Sudoh, respectively, had tremendous impact on the current understanding of cardiac development and homeostasis (83,84). The two proteins are synthesized by the A- and B-type natriuretic peptide genes, *NPPA* and *NPPB*, respectively. These highly homologous polypeptides are currently used in clinical practices as biomarkers of heart failure. Natriuretic hormones are synthesized as pro-peptides, they are enzymatically cleaved to give rise to biologically active forms that can be stored in specific granules (85). These two hormones are continuously released, and deviation from the basal level of release is controlled by mechanical and neuroendocrine stimuli which modulate the rate of ANP and BNP synthesis or/and release. The activities of ANP and BNP are mediated via the natriuretic polypeptide receptors NPR-A and NPR-B which are guanylyl cyclases coupled receptors that catalyse the synthesis of cGMP from GTP. Within the cells,

cGMP targets include cGMP-dependent protein kinases, cGMP-gated ion channels, and cGMP-regulated cyclic nucleotide phosphodiesterases (PDE). In turn, these targets modulate the response to the natriuretic factors which include diuretic, natriuretic, and vasodilating actions and inhibitory effects on renin and aldosterone secretion (13,86-88).

Postnatally, ANP and BNP hormones are secreted from the atria and ventricles, respectively. While ANP functions as a modulator of blood pressure, BNP is a paracrine regulator of cardiac remodeling. In mouse models, loss of function in the murine ANP gene, Nppa, was associated with hypertension. However, loss of the BNP gene Nppb showed no signs of hypertension or ventricular chamber hypertrophy (89). However, the ventricles of the *Nppb* null mice were characterized with fibrotic lesions that were found to be aggravated in response to pressure overload (90).

The importance of natriuretic hormones for cardiac development can be demonstrated by their expression in precursor cardiac cells prior to the formation of the primitive heart (91). During the early stages of embryogenesis in mice, *Nppa* is expressed both in atrial and ventricular, but not in skeletal, muscle cells. In later stages of fetal development, *Nppa* expression is dramatically reduced in the ventricles but remains high in the atria (87,92). On the other hand, postnatal ventricular *Nppa* gene expression is reactivated in response to hemodynamic overload and cardiac abnormalities (13,87,93). Moreover, *Nppa* expression and secretion are also modulated via neural and endocrine factors including α-adrenergic agonists, β-adrenergic agonists, endothelin-1 (ET-1), glucocorticoids, prostaglandins, thyroid hormones, Nitric Oxide inhibition and angiotensin II (Ang II) (13,87,94,95). At the genetic level, analysis of the *Nppa* and *Nppb* promoters and their patterns of expression have led to the characterization of key cardiac regulators and

pathways that converge onto these sensitive markers of cardiac stress. Among these cardiac transcription factors are GATA4, TBX5, and NKX2.5, which are fundamental to cardiac development; their mutations were found to be linked to a wide array of cardiac defects (13,85). KLF13, the focus of this thesis, was identified as a cardiac transcription factor able to regulate the function of the *Nppa* and *Nppb* promoters.

1.9 Essential cardiac regulators

The use of genetic engineering to induce the loss of function of specific genes allowed for the identification of proteins involved in cardiac development and their associated congenital heart defects (CHD)(12). These mouse models also allowed for the identification of genes important to postnatal cardiac development and homeostasis (Table 1.1). The wealth of knowledge gained from developmental biology was also utilized to provide insight on studies pertaining to cardioprotection postnatal heart (86). The following section will provide an overview of some of the major cardiac transcription factors that have been shown to be important for cardiac development.

1.9.1 GATA4

GATA-binding proteins are a subfamily of zinc-finger transcription factors that are characterized by their interaction with the DNA consensus sequence A/G GATA A/T. There are six mammalian members (GATA1-6) of the GATA family. These factors share a highly conserved DNA-binding domain containing two C-X2-C-X17-C-X2-C (C2C2-type) zinc-fingers, of which 82 residues are identical across the six proteins (96,97). Several reports have indicated that while the N-terminal zinc-finger stabilizes DNA–protein interactions, DNA-binding is chiefly the function of the C-terminal zinc-finger (96,98). On

the other hand, the N-terminal zinc-finger also mediates specific protein–protein interactions.

The GATA family can be subdivided into two subfamilies based on their sequence homology and tissue expression: GATA1/2/3 and GATA4/5/6. Members of the GATA4/5/6 subfamily share two structurally related amino-terminal transcriptional activation domains (16,99). Beyond the aforementioned domains, the GATA4/5/6 proteins retain very low similarity to one another (96).

Table 1.1: Transcription factors associated with cardiac development.

Transcription Factor	Cardiac Expression	Role	Human Cardiac Phenotype	Ref.
NKX2.5	Pan-cardiac	Cardiac specification and patterning: Development of the conduction system	ASD, VSD, conduction defects	(100-105)
GATA4	Pan-cardiac	Cardiac differentiation; Ventral morphogenesis	ASD, VSD	(106)
GATA5	Pan-cardiac	Cardiac differentiation; Ventral morphogenesis	ASD, VSD, BAV	(107,108)
GATA6	LV; Epicardium; OFT	Cardiac differentiation; Ventral morphogenesis	VSD, BAV	
FOG2	Pan-cardiac	Modulator of GATA-4 activities	ASD, TOF	(109)
MEF2C	Pan-cardiac	Cardiomyocytes specification	N/A	(110)
FGF10	AHF	Ventricular patterning	N/A	(111)
Isl-1	AHF	AHF development	N/A	(112)
Hand1	LV; AVC; OFT	Cardiac patterning and proliferation	N/A	(113)
Hand2	RV; Endocardium	Cardiac proliferation; RV identity	N/A	(4,114)
TBX1	PA	AHF proliferation; Development of the OFT	Conotruncal abnormalities	(115)
TBX2	Primitive myocardium	Inhibits chamber differentiation	N/A	(116)
TBX3	Primitive myocardium; CCS	Inhibits chamber differentiation; Sinoatrial node patterning	N/A	(117)
TBX5	LV; At	Atrial and left ventricle identity	ASD, VSD, conduction defect	(118)
TBX20	Pan-cardiac	Repress TBX2; Development of the endocardial cushions.	N/A	(77)

Legend: AHF: Anterior/Secondary Heart Field; ASD: Atrial Septal Defect; At: Atria. AVC: Atrioventricular Canal; BAV: Bicuspid Aortic Valves; CCS: Central Conduction System; LV: Left Ventricle; N/A: Not Associated with Phenotype; N/R: Not Reported; OFT: Outflow Tract; PA: Pharyngeal Arches; RV: Right Ventricle; ToF: Tetralogy of Fallot; VSD: Ventricular Septal Defect; Modified from (13)

Members of the GATA family are lineage-restricted and are known to be essential during cellular growth and development (96,119). While the GATA1/2/3 subfamily is required for the proper development of the hematopoietic system, GATA4/5/6 are important for proper cardiac development and endoderm derived cells. Of the six members, GATA4/5/6 are the chief factors expressed in the cardiovascular system. While GATA4 is widely expressed in all cardiac progenitors and at all stages, GATA5 expression is restricted to endocardial cells and GATA6 is expressed mainly in myocardial and vascular smooth muscle cells (16,96,119).

By far, GATA4 is the most comprehensively studied member of the family. It was first identified as a transcriptional regulator for the BNP gene, *Nppb* (120). Several lines of evidence support GATA4's importance as a critical regulator of cardiac development as well as for regulating survival and hypertrophic growth of the adult heart (12,121,122). Firstly, GATA4 is detected as early as E7.0 in the precardiac splanchnic mesoderm, and is thus one of the earliest cardiac developmental markers (12,123). At E8.0, GATA4 is also highly expressed in the folding heart tube, both in the endocardium and the myocardium. This expression persists throughout prenatal and postnatal life (124). Secondly, GATA4 is an integral member of the positive feedback loop that controls the expression of several cardiac transcription factors and modulates the onset of cardiogenesis. For example, its combinatorial interaction with SMAD proteins, the signalling intermediates of the TGF/BMP signalling pathway, activates the expression of the early cardiac factor, NKX2.5 (125). Thirdly, GATA4 was found to directly regulate more than 30 cardiac promoters and enhancers (12). Lastly, the indispensability of GATA4 during cardiac development is evident by the numerous forms of congenital heart disease (CHD) associated with GATA4 loss of function and mutations in several animal models (12,126,127). Mouse embryos null

for *gata4* displayed severe cardiac abnormalities as early as ED 7.0. These defects included the absence of a primitive heart tube due to the failure of the FHF to migrate and fuse along the ventral midline (13,126).

Structurally and similar to other members of the family, GATA4 contains two zinc-fingers of the C2C2-type in which a zinc ion is tetrahedrally bound by four cysteine residues (127,128). While the C-terminal zinc -finger is critical for DNA binding, the N-terminal zinc-finger stabilizes and confers specificity to the protein-DNA complex (128,129). Proper nuclear localization of GATA4 is granted by the nuclear localization sequence (NLS) located within the basic domain flanking the C-terminal zinc-finger. Several cardiac transcription factors were found to combinatorially interact with GATA4 including NKX2.5 (130), TBX5 (71), and the multi zinc-finger protein friend of GATA (FOG2) (131). The majority of the elucidated protein-protein interactions were found to be mediated via the C-terminal zinc-finger of GATA4, except for FOG2 and KLF13, which are directed via the N-terminal zinc-finger of GATA4. As previously described, GATA4/5/6 contain two separate transcriptional activation domains (i.e., TAD1 and TAD2) within the N terminal of the protein. The partial conservation of the two transactivation domains between the subfamily members might explain the functional redundancy and the buffering capacity among GATA4/5/6 (129,132).

1.9.2 MEF2

Myocyte enhancer factor 2 (MEF2) proteins are members of the evolutionarily conserved MADS (MCM1, AGAMOUS, DEFICIENS, and SRF) family of transcription factors. These proteins functionally act as “transcriptional switches” and their expression is concurrent with onset of differentiation programs in their enriched tissues including cardiac

tissue (133). Structurally the four members of the MEF2 family (MEF2A, B, C, and D) are highly divergent in their C-terminal regions but have highly similar N-terminal regions; these contain the evolutionarily conserved MADS and MEF2 domains, which mediate both DNA as well as protein interactions (133). Developmentally, MEF2 proteins are characterized by a distinct spatiotemporal expression profile with highest expression in the striated muscles and the nervous system (134). MEF2C is the first family member to be expressed in the heart, as it is detected as early as E7.5 in the cardiogenic precursors of the precardiac mesoderm. The transcripts of the other members are detected shortly after, at E8.5, in the myocardium. Their activities are mediated by strongly activating or repressing gene transcription via interactions with their repertoire of cofactors (133,134).

Developmentally, loss of Mef2c function in mouse was associated with embryonic lethality at E9.5 due to failure in the cardiac looping process and right ventricular aplasia (135). Similarly, Mef2a-null mice were lost perinatally due to a range of cardiac abnormalities that included right ventricular dilation and myofibrillar fragmentation (136). MEF2 regulates the expression of numerous cardiac differentiation genes that include structural and contractile proteins. Note that examination of the developmental function of each of the MEF2 proteins in the heart is a challenge due to their overlapping spatiotemporal expression. To overcome this, a cardiac-specific overexpression of a dominant-negative MEF2 mutant (MEF2C/EnR) was generated. Overexpression of this mutant protein was associated with loss of cardiomyocyte differentiation in both transgenic mice and P19 cells. Moreover, the overexpression in P19 cells was associated with drastic loss of the expression of GATA4, BMP4, NKX2.5 and MEF2C (137). Postnatally, MEF2 proteins are involved in mediating postnatal cardiac hypertrophic growth. For example, cardiac-specific overexpression of MEF2A and MEF2C in mice was associated with higher incidence of

dilated cardiomyopathy and lengthening. Mechanistically, MEF2A and MEF2C overexpression were found to induce sarcomeric disorganization and focal elongation that were associated with altered gene expression of extracellular matrix remodeling, ion handling, and metabolic genes (138). Collectively, the aforementioned studies point to an essential role for MEF2 proteins in the proper differentiation and postnatal development of the contractile heart.

1.9.3 NKX2.5

NKX2.5 (Nirenberg and Kim X=Mammalian class 2.5) is a member of the NK-2 family of homeodomain transcription factors. The importance of this class of transcription factors in the field of development and organogenesis was first established in *Drosophila*. Azpiazu *et al*, demonstrated that *Tinman*, the founding member of the NK-2 class of homeobox genes, lacked all dorsal mesodermal derivatives, including the dorsal vessel, visceral muscle, and a subset of body wall muscles (139). It is noteworthy that the dorsal vessel is the insect equivalent of the vertebrate heart. This class of transcription factors is evolutionary conserved and is characterized by binding to the DNA consensus sequence T(C/T) AAGTG (125,127). Members of the NK-2 family are lineage-restricted and are known to play indispensable roles during cellular growth and development. Of the NK-2 genes expressed in vertebrates NKX2.3, NKX2.5, NKX2.6, NKX2.7, NKX2.8, and NKX2.10 are referred to as the cardiac group due to their high cardiac expressivity (13,125).

Among the NK-2 cardiac group, NKX2.5 is the most extensively studied member. NKX2.5 was first identified in a screen for mammalian homologues of *Drosophila's Tinman* (12,125). Species conservation of *Nkx2.5* suggests a conserved regulatory mechanism during cardiogenesis (140). During cardiogenesis in mice, NKX2.5 is expressed quite early

at E7.5, and continues to be expressed at a high level in the heart throughout adulthood (103). In contrast to the loss of *Tinman* in *Drosophila*, which exhibited complete absence of the structure equivalent to mammalian heart, *nk2.5* loss of function in mice didn't affect the formation of the linear heart tube. However, the targeted deletion of NKX2.5 was associated with embryonic lethality at E9.0-E10.0. In the mutant embryos, the linear heart tube failed to progress to the looping stage and a single ventricular chamber was present with a truncated OFT (12,125) (103). The discrepancy in the phenotype severity between *Drosophila* and mice might be due to a buffering effect from other NK factors that remains to be identified (12,16). Human mutations in NKX2.5, most within the homeodomain, were linked to septal defects, conduction abnormalities, thinning of the ventricular myocardium, and hypotrabeculation (12,13,125). At the molecular level, the expression of a number of cardiac-specific genes were down-regulated in NKX2.5 mutant mice, including *Nppa* and the basic helix-loop-helix TF (*eHand*). Although NKX2.5 expression is homogeneous throughout the heart, analysis of mutant mice suggests the necessity of NKX2.5 for proper chamber specification and septation (12). The discrepancy between NKX2.5's broad spatial expression and specific regionalization in the heart is attributed to combinatorial interaction with other cardiac regulators, such as GATA4 and TBX5 (12,130,141).

Homologous to the other members of the NK2 family, NKX2.5 is structurally comprised of four conserved motifs. Ordered from the amino terminus of the protein, these motifs are: the tinman (TN) domain, the homeodomain, the NK-2 specific domain, and the sequence GIRAW. The DNA-binding domain of NKX2.5 is attributed to the homeodomain. NKX2.5's homeodomain is composed of three helices (I/II/III) that form a hydrophobic core with a tyrosine (Y) at position 54 characteristic of the NK-2 family members. Of the three helices, helix III is responsible for DNA binding specificity (125). The homeodomain also

mediates protein-protein interaction with other cardiac transcription factors (e.g. GATA4, TBX5 and SRF) (130,142,143). The precise functions of the TN-Domain and NK-2 domain are yet to be determined; however recent reports indicate their importance in regulating the transcriptional activity of NKX2.5 (144,145). The deca-peptide TN domain, also found in some basic helix-loop-helix (bHLH) factors such as Olig2, was shown to mediate the interaction of NKX2.5 with the Groucho family of co-repressors. These co-repressors were implicated in the formation of a repressed chromatin state in several genetic loci in order to control major developmental processes ranging from body axis patterning to eye development (146,147). Interestingly, point mutations of the TN domain were linked to atrial fibrillation and were shown to modify the interactions of NKX2.5 and p300 (145,148). The characteristic domain of the NK-2 class, NK-2 domain, is localized adjacent to the C-terminal of the homeodomain and is structurally composed of a proline-rich region, a hydrophobic core, and a cluster of flanking basic amino acids. This domain likely facilitates protein-DNA interaction as well as interactions with other members of the transcriptional machinery (125,140,149). Using mutational analysis in the NK-2 transcription factor Ventral Nervous System Defective protein (VND), the NK2-domain was found to be responsible for mediating cell death upon ectopic expression of VND in various *Drosophila* tissues (150). Lastly, the function of the amino acid sequence "GIRAW" has yet to be determined (125). Interestingly, deletion of the C-terminal domain does not impair NKX2-5 activity in inducing cardiomyogenesis in P19 cells. However, it appears that the C-terminal of NKX2.5 that contains both the NK-2 domain and the GIRAW sequence has an autorepression functionality as its deletion leads to super-activation of the *Nppa* promoter (151).

Mechanistically, part of the regulatory mechanism assumed by the NK-2 proteins is attributed to the choice of the transcriptional partner. For example, while *Nppa* transcription is stimulated by the combinatorial interaction between NKX2.5 and GATA4, *Nppa* gene transcription is inhibited by NKX2.5-TBX2 transcription interaction (125).

1.9.4 TBX5

The Brachyury (T) gene family encodes phylogenetically-conserved transcriptional regulators that share a highly-conserved 180-amino acid DNA-binding domain, termed the T-box (152,153). This family plays diverse roles in metazoan embryogenesis and germ cell differentiation (154). To date, 17 T-box genes have been identified in mouse and human and are organized into five subfamilies. Seven members of these families (i.e. TBX1-5, TBX18, and TBX20) were shown to be expressed in the embryonic vertebrate heart with overlapping expression patterns (152). Loss of function of any of these seven genes is linked to embryonic/prenatal lethality due to a wide range of cardiac defects. Each of these genes has a unique spatiotemporal expression pattern within progenitor fields, including those of the early germ layers, to control a different set of developmental processes, most prominently differentiation and patterning. Furthermore, T-box genes execute their diverse function in a combinatorial or hierarchical fashion. The dose-sensitive nature of T-box genes is demonstrated by the human congenital defects associated with their haplo-insufficiency as well as their over-expression (155).

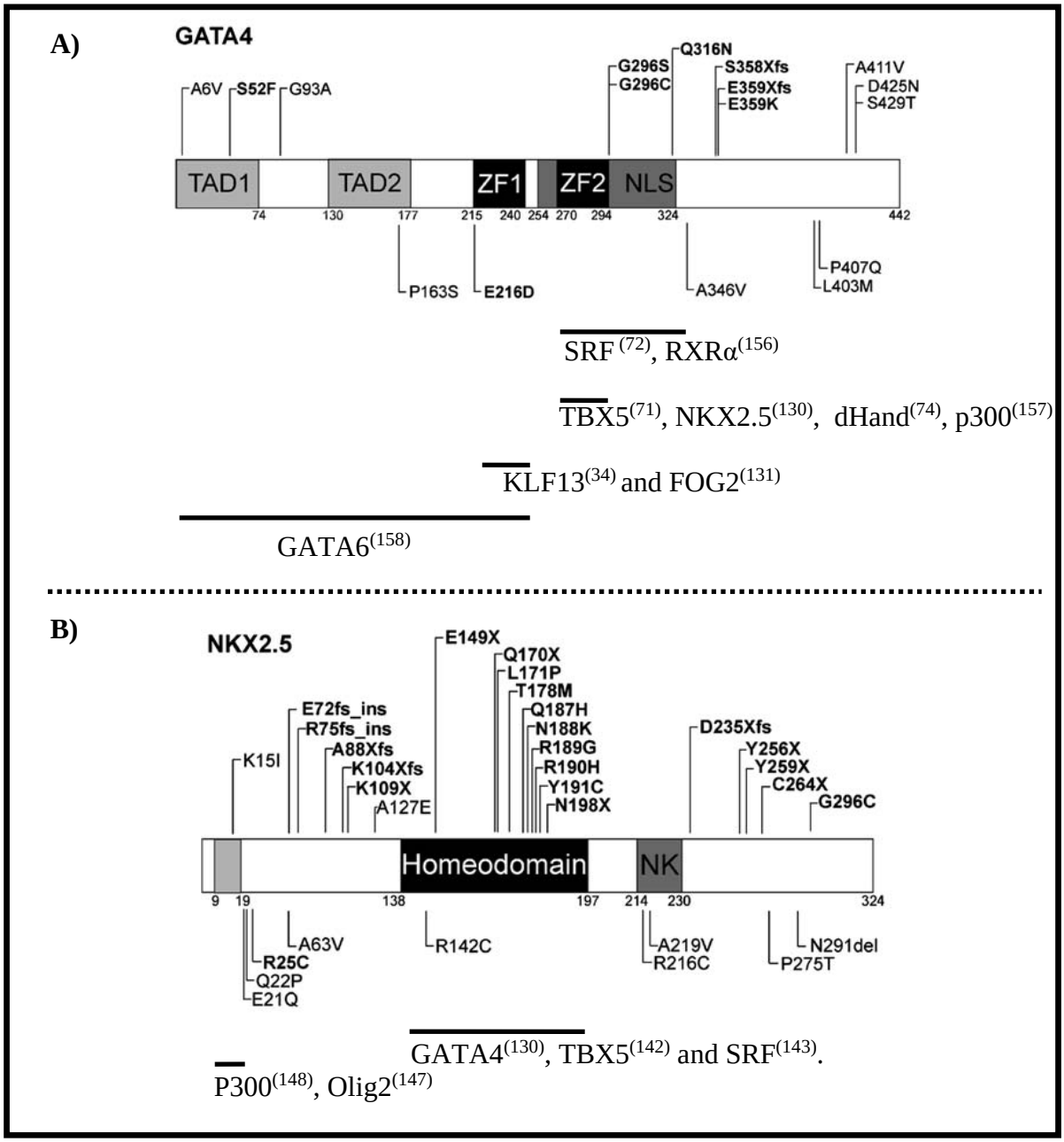

Figure 1.5: Schematic representation of A) GATA4 and B) NKX2.5 protein structure.

The exonic germline mutations related to nonsyndromic CHD are also indicated. All mutations related to ASDII are represented on the top. Mutations found in patients with CHD other than ASDII are shown below the structural domains. All mutations which were evaluated by family and/or functional studies are represented in bold letters. Somatic and intronic mutations are not included. The lines represent the regions required for the interaction with the protein identified under the line. The figure is modified from (26).

TBX5 is the most extensively studied member of the T-box genes. Uniquely, haplosufficiency in TBX5 was also found to be associated with embryonic lethality (152,159). Furthermore, TBX5 is the gene linked to human Holt-Oram Syndrome (HOS), a dominant syndrome characterised primarily by upper fore-limb defects and cardiac abnormalities (160). The latter abnormalities include chamber septal defects, tetralogy of Fallot (TOF), hypoplastic left heart, and conduction anomalies (152). TBX5 is expressed at the earliest stages of cardiogenesis, in the cardiac mesoderm, and is co-localized with other early cardiac transcription factors such as NKX2.5 and GATA4 (161). Studies on zebrafish, revealed that TBX5 expression in the anterior lateral plate mesoderm provides the required competency for the later BMP signaling that is required for proper cardiogenesis and chamber formation (162). As the heart differentiates, TBX5 expression follows the retinoic acid signaling gradient along the linear heart tube with a peak in the posterior sinoatrial segments of the heart. This gradient is thought to serve as a positional cue for the anterior-posterior cardiac axis (13,163).

Structurally, *tbx5* encodes five different isoforms, through alternative splicing of 11 exons, with differing N- and C-terminal domains (164). Most of the structure function studies were conducted on isoform TBX5a which contains a 56 amino acid N-terminal, a 180-amino acid DNA binding domain, and a 282-amino acid C-terminal (Error! Reference source not found.) (165). Beyond the T-box domain of TBX5, which is common with the other isoforms, structure-function analysis of the other regions is yet to be determined. The T-box domain is composed of a seven-stranded β-barrel domain that is closed by a smaller β-pleated sheet (166). Based on binding studies with synthetic oligonucleotides, the consensus sequence of TBX5 was defined as the following 8-bp-long DNA half-site (A/G)GGTGT(C/G/T)(A/G) (166,167). The T-box domain does not only mediate DNA-

binding, but also protein-protein interactions (168). Over 70 mutations in the TBX5 gene have been associated with Holt-Oram syndrome including: nonsense, frameshift, splice site, deletion, and missense (164). The majority of these mutations introduce a premature stop codon within the T-box domain. Hence, these mutations impact the DNA-binding properties of TBX5 to target genes, leading to deregulated transcriptional activation by TBX5 and abnormal synergistic transcriptional activation with its partners (e.g. NKX2.5, GATA4, and the MAD box cardiac transcription factor MEF2C) (165). The poorly conserved N-terminal extension (residues 1–50) of TBX5 was also shown to be necessary for interaction with MEF2C and NKX2.5 (169,170). On the other hand, the C-terminal of TBX5 possesses a transactivation domain (TAD), 339–379aa. The mechanism underlying the transactivation by the C-terminal of TBX5 is largely unknown (165,171). However, DNA-TBX5 crystallization studies conducted by Stirnimann *et al*. indicated that proper folding of the T-box domain also affects the correct orientation of the transactivation domain (166). Thus, mutations that effect the T-box structure may also impact the proper folding of the adjacent transactivation domain. In addition, the transcriptional co-activator TAZ, transcriptional co-activator with PDZ-binding motive, was also found to interact with TBX5. The co-activational properties of TAZ were found to be mediated via interactions with the histone acetyltransferases p300 and PCAF. Although TBX5 lacks a PY motif that mediates the association of other proteins with TAZ, it alternatively interacts with TAZ through multiple domains including its C-terminal structure. Interestingly, truncated HOS mutants of TBX5 lose the capacity to associate with and be stimulated by TAZ (172).

Other structural features of TBX5 include two functional nuclear localization signal (NLS) motifs, one in the DNA-binding domain and the other in the C-terminal of the protein. Furthermore, the T-box domain also contains a Crm1-dependent nuclear export

signal (NES) (169). These nuclear import and export sequences are important regulators of the TBX5 subcellular localization and availability. In addition, LMP4 protein, a member of the PDZ-LIM protein, has been identified as interacting with the C-terminal transactivation domains of both TBX5 and TBX4 to induce their re-localization from the nucleus to the cytoplasm. As LMP4 negatively regulates the nuclear availability of TBX5, it works as a modulator of the transcriptional activity of the TBX5 protein (169). Not only was *tbx5* loss of function associated with cases of HOS, duplications in chromosome 12q2, which harbour the *tbx5* gene, have also been linked to HOS (173). These observations suggest that striking a balanced level of TBX5 protein in the cell, in the nucleus in particular, is critical for its proper transcriptional activities (13,169).

Mechanistically, TBX5 interacts directly and synergistically with other conserved cardiac transcription factors, including NKX2.5 and GATA-4, to activate the expression of chamber-specific genes such as *Nppa* (152). Takeuchi and Bruneau showed that GATA4, TBX5, and Baf60c (the cardiac-specific subunit of BAF chromatin-remodeling complexes) can direct ectopic differentiation of mouse mesoderm into beating cardiomyocytes (174). Their results indicated that while GATA4 and Baf60c initiated ectopic cardiac gene expression, the addition of TBX5 allowed differentiation into contracting cardiomyocytes and repression of non-cardiac mesodermal genes (174). In addition, Garg *et al*. (2003) demonstrated that a missense mutation in GATA4 (i.e., G296S), associated with cardiac septal defects, abrogated the interaction with TBX5. Conversely, interaction of GATA4 and TBX5 was disrupted by specific human TBX5 missense mutations that are linked to similar cardiac septal defects (175). The genotype-phenotype associations with TBX5 point mutations provided a “Rosetta stone” for deciphering how disruption of the combinatorial interactions of transcription factors can lead to specific birth defects (13,71).

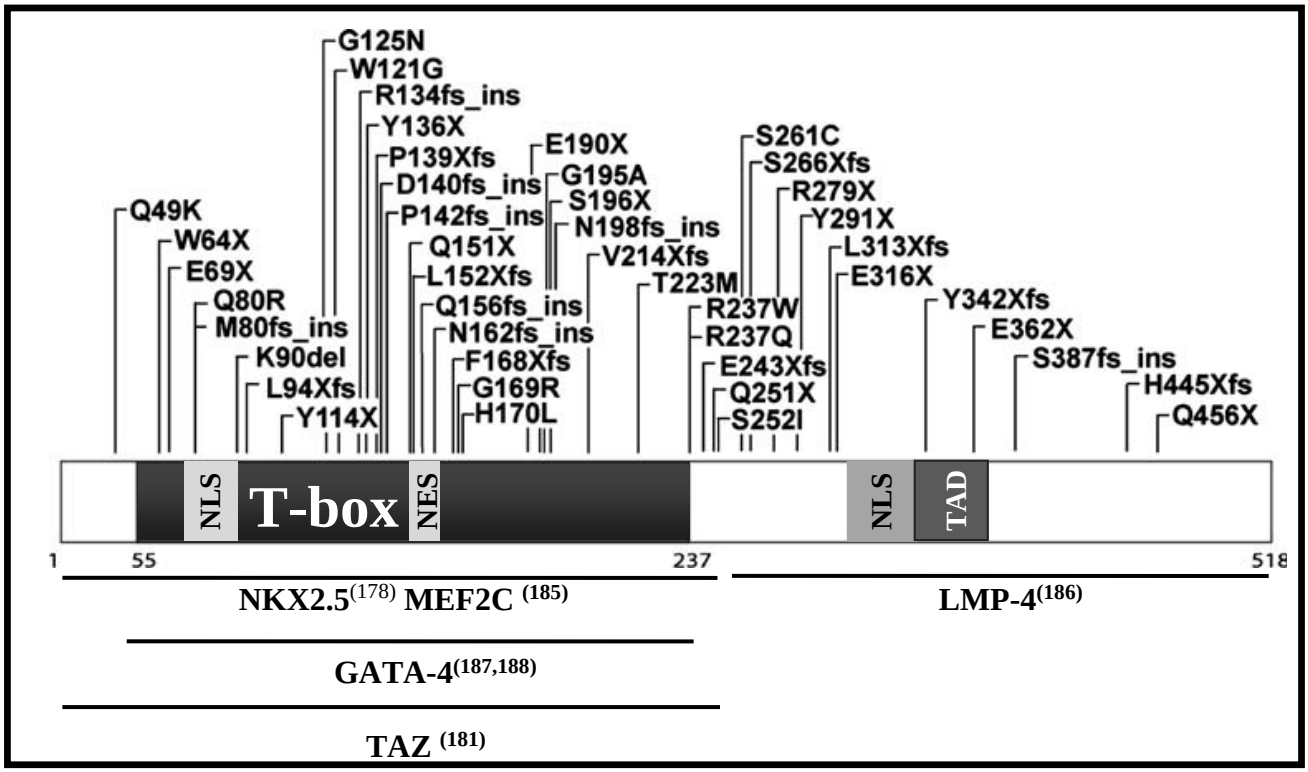

Figure 1.6: Schematic representation of TBX5a protein structure.
The exonic germline mutations related to HOS are also indicated. The majority of mutations are located in the DNA-binding T-box domain of TBX5. Intronic and somatic mutations are not included. The lines represent the regions required for the interaction with the protein identified under the line. NLS: Nuclear localization signal, NES: Nuclear export signal, TAD: Transactivation domain. The mutations are located according to reference (26).

1.9.5 PEX1

A decade ago, we reported that PEX1 (Phenylephrine-induced Complex-1), also known as ZFP260 (zinc-finger transcription factor 260), is implicated in α1-adrenergic (phenylephrine) signalling in the heart (180). Detailed spatiotemporal expression of the protein is yet to be reported, however in adult mice, the protein is expressed in the heart, skeletal muscle, and adrenal gland. In the developing heart, the expression profile of PEX1 is curiously similar to the pattern of *Nppa* gene expression, with a robust expression during cardiogenesis that decreases in postnatal ventricles. Furthermore, we found that PEX1 physically and functionally interacts with GATA4 to synergistically activate transcription of *Nppa* and other hypertrophy-induced genes. Our data identify PEX1 as a novel transcriptional regulator the heart and a nuclear effector of α1-adrenergic and Endothelin1 signaling (180,181). The role of PEX1 during cardiac development is in progress in our laboratory.

It is well established that α1-adrenergic receptors mediate catecholamine signaling to control several biological processes (e.g., myocyte growth and contractility) and the transcriptional regulation of several cardiac genes including *Nppa* (180,181). Phenylephrine response element (PERE) is essential for mediating the response of the *Nppa* promoter to the α1- adrenergic receptor agonist phenylephrine (182,183). PEX1 was identified in our screening for regulatory factors binding to the evolutionarily-conserved phenylephrine response element (PERE) on the *Nppa* promoter. Interestingly, PEX1 transcripts were also induced by the α1-adrenergic agonist phenylephrine (183). Furthermore, the transcriptional activity of PEX1 was found to be potentiated in a PKC-dependant manner by endothelin-1 (ET-1) (181). Physiologically, elevated PEX1 transcripts were detected in genetic models of hypertension and cardiac hypertrophy. Furthermore, conditional upregulation of PEX1

expression was sufficient to induce the morphological and genetic changes characteristic of cardiac hypertrophy with preserved cardiac function (181,183). On the other hand, knocking down PEX1 using an antisense strategy in cardiomyocytes eliminated the endogenous *Nppa* gene response to α1-adrenergic receptor stimulation (183). Together, our data identify PEX1 as a novel nuclear effector of α1- adrenergic receptor agonist signaling and suggest that PEX1 is a regulator of the early stages of adaptive cardiac hypertrophy. Understanding the PEX1 mechanism of action is critical in deciphering the poorly understood signaling cascade linking the α1-adrenergic receptor activation to its accompanied genetic changes (13,183).

The 407-amino-acid translated PEX1 protein is structurally characterized by the presence of thirteen C2H2-type zinc-fingers, which group the protein under the Kruppel family of zinc-finger proteins. Searching for a homologous protein in mice and humans uncovered only zinc finger (OZF), also named Zfp146, as a possible homologue. Not much is known about OZF, however it was found that the mammary gland in transgene female mice could not sustain full growth of their pups due to impaired mammary development (184). Furthermore, OZF was found to be overexpressed in the majority of pancreatic cancers and in more than 80% of colorectal cancers (185). Murine PEX1 is larger than OZF, with three additional N-terminal zinc-fingers, however they share high sequence similarity in the region containing zinc-fingers IV to XIII (13,183). Structure-function analysis of PEX1 are undergoing in our laboratory. However the protein contains several putative phosphorylation sites for PKC, PKA, and casein kinase II (13,183).

Mechanistically, PEX1 and GATA-4 are two of the few transcription factors that are required for nuclear signalling of α1-adrenergic receptors. Our data indicate that PEX1 physically and functionally interacts with GATA4 to cooperatively activate the transcription of *Nppa* and other hypertrophy-induced genes. ET-1 enhances PEX1 transcriptional activity in a PKC dependent pathway that phosphorylates the protein to potentiate its synergy with GATA4. Thus, it appears that the PEX1-GATA-4 interaction is critical for transducing the nuclear and cytoskeletal effects of α1-adrenergic agonists (181,183).

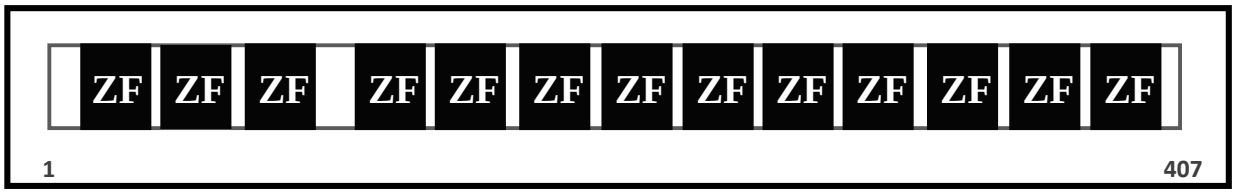

Figure 1.7: Schematic representation of PEX1 protein structure. The protein contains 13 zinc fingers of the C2H2 type and has no other identifiable domains.

1.10 The Kruppel-like transcription factor KLF13

1.10.1 Introducing the family

The Kruppel-like transcription factors (KLFs) are zinc-finger-containing transcription factors that are named for their homology to the zinc-finger (ZnF) domains found in the *Drosophila* segmentation transcriptional regulator Kruppel (186). This family is categorized along with the zinc-finger containing specificity protein (Sp) family of transcription factors under the Sp/KLF family of which there are currently 26 members. Up to the date of this thesis, there are 17 distinct mammalian members of the KLF subfamily and nine related proteins that form the SP1 subfamily. Furthermore, several members of this family exhibit splice variants (e.g., KLF6, KLF10, and KLF8) (187,188). The nomenclature rule of the KLF subfamily uses the name KLFX factors, where X corresponds to the approximate order in which the genes were described (KLF1-KLF17). The family is conserved across species with variability in numbers probably due to multiple gene-duplication events throughout evolution (**Figure 1.8** depicts a phylogenetic tree for the Sp/KLF family**)** (189).

The KLF family is structurally characterized by three consecutive C-terminal Cys2/His2 zinc-finger motifs that are connected by a conserved 7-residue linkage sequence, TGEKP(Y/F)X(190). These zinc-fingers are DNA-binding motifs that preferentially bind to the consensus sequences GC-, GT-, and CACCC-box motifs that are found in gene promoters and enhancer regions in order to mediate activation and/or repression of transcription (187,188). Although initially regarded as silencers of Sp1 transactivity, members of the KLF family are now implicated in a myriad of cellular processes including proliferation, apoptosis, differentiation, and development (186,188). Most of the Sp/KLF members display a wide spatial expression pattern, but some show a restricted

spatiotemporal pattern (**table 1.2** highlights their expression pattern and cellular function). Despite the numerous reports describing the role of KLFs in mammalian health and disease, the family's contribution to cardiac development is just emerging. Currently, there are only three published reports describing the function of KLFs in the developing heart—KLF13 in cardiomyocytes (34), KLF2 in the cardiac cushion (191) and KLF3 in cardiomyocytes (192). Interestingly, in the postnatal heart, recent publications have shown that KLF15 is an important regulator of cardiac transcription and metabolism through the recruitment of p300 to specific metabolic target genes during fasting. Interestingly, reduction of KLF15 expression was concomitant to the recruitment of p300 to pro-hypertrophic transcription factors such as GATA4 and MEF2 (193). **Table 1.3** highlights some of the published findings pertaining to KLFs in the heart and the two other muscle types. Among the three factors, only KLF13 was implicated with human cardiac malformations as heterozygote microdeletions or microduplication of the chromosomal band 15q13.3, harbouring at least seven genes including *KLF13*, are associated with cardiac defects (194).

The preferential binding of the KLF family to similar DNA consensus sequences is the function of their highly homologous C-terminal DNA binding zinc-finger domain. The diverse biochemical mechanisms and cellular functions attributed to the KLF family are due to the heterogeneity of their N-terminal domain (187,195). Physiologically, members of the KLF family can have opposing roles in the regulation of the same cellular process (**table 1.2** and **table 1.3)**. For example, while KLF5 gain of function promotes smooth muscle cell (SMC) proliferation, KLF15 gain of function inhibits SMC proliferation. Furthermore, while mice hypomorphic for KLF5 are characterized with reduced neointimal growth and perivascular fibrosis in response to vascular injury, *Klf15* null mice exhibited an exaggerated neointimal response to vascular injury (13,196). It is the N-terminal region that bestows the

functional identity to each member of this family. It is possible that these proteins have structurally evolved in a way that provided a strategic opportunity for interaction with a distinct repertoire of cofactors; not only does this allow the KLF family to regulate gene expression, but also to participate in the divergent regulation of the same gene (195). This is exemplified by the activation of the *Nppa* promoter by Sp1 in cardiomyocytes and the opposing repressive function by Sp3 on the same promoter. In addition, while KLF13 was shown to functionally interact with GATA4 to synergistically activate several cardiac promoters including *Nppa*, KLF15 repressed GATA4 DNA-binding and transcriptional activity [52, 97]. Recent reports have pointed to KLFs' regulatory effect on the expression of other family members, including the expression of KLF3 in erythroid cells (186). However, unlike other developmental regulators (e.g., Hox transcription factors) that are encoded gene clusters, the loci of Sp/KLF proteins are randomly dispersed throughout the genome and are thought to function independently except for the locus containing KLF2 and KLF3 genes. The precise gene structure of the Sp/KLF family is yet be determined (13,189).

The existence of alternative splicing isoforms for members of the Sp/KLF family bestows an additional layer of functional regulation [93, 95]. For example, while the first-discovered KLF6 transcript functions as a classic tumor suppressor, the splice variant KLF6 SV1, which lacks a nuclear localization signal, exhibits a strikingly opposite effect on cell proliferation, colony formation, and invasion (13,197).

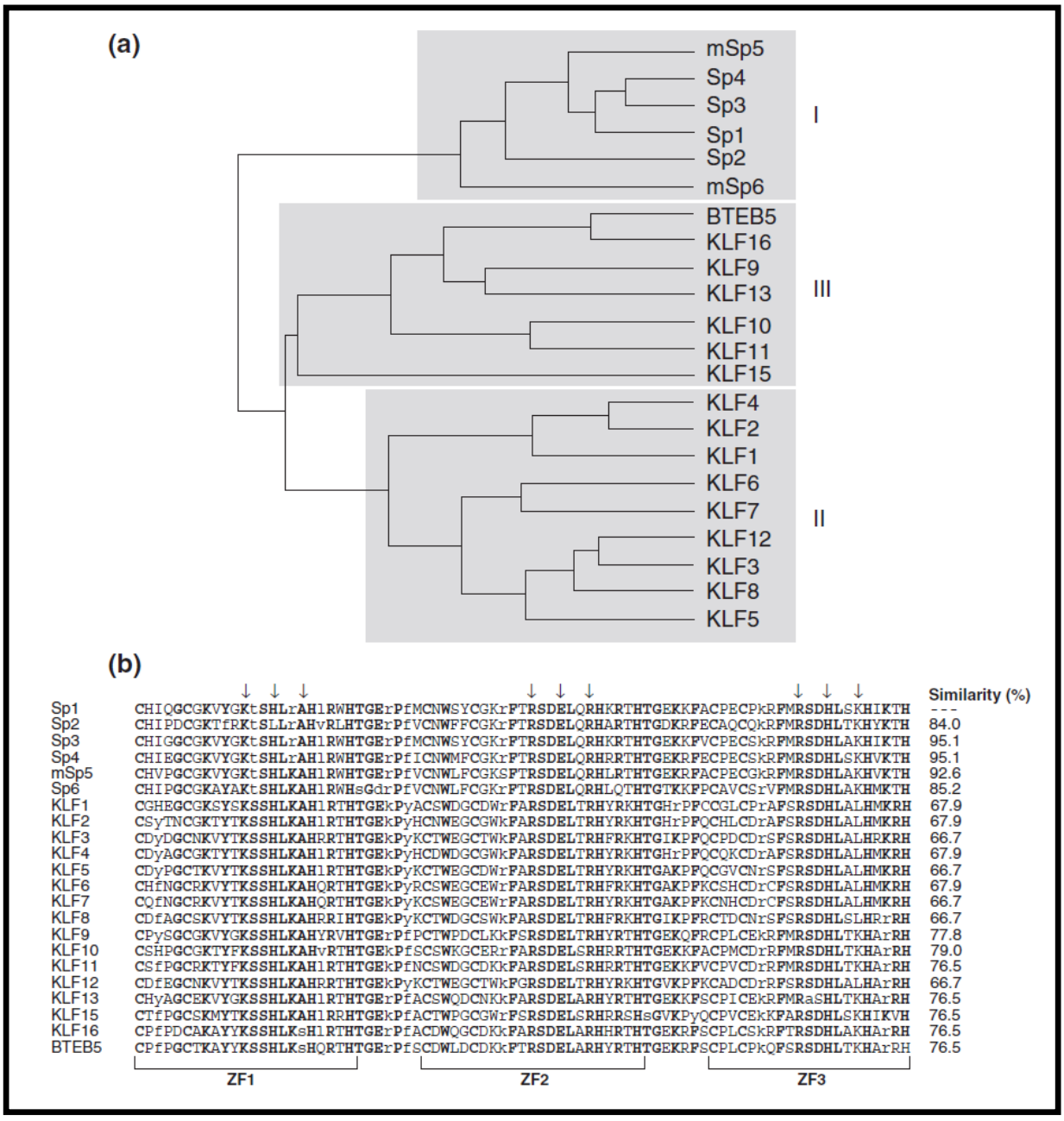

Figure 1.8: Mammalian members of the Sp1-like/KLF family.
(a) A phylogenetic tree of human Sp1-like/KLF proteins and mouse Sp5 and Sp6 (mSp5 and mSp6) identified three general subgroups. (b) Sequence alignment of the zinc-finger domains of Sp/KLF protein family members in comparison to zinc-finger motifs of human Sp1. The percentage similarity between the Sp1 and the other Sp1-like/KLF zinc-finger domains is indicated on the right. The figure is modified from (189).

Table 1.2: The functional features of Sp1-like/KLF family.

Protein*	KLF #	Expression pattern	Interacting co-activator / co-repressor	Cellular function
Sp1	-	Ubiquitous	CRSP, p300/CBP, TAFII130	Embryogenesis
Sp2	-		Unknown	Unknown
Sp3	-	Ubiquitous	Unknown	Unknown
Sp4	-	Brain-enriched	Unknown	Post-natal survival and male fertility
mSp5	-	Ubiquitous	Unknown	Unknown
Sp6	**KLF14**	Ubiquitous	Unknown	Unknown
EKLF	**KLF1**	Erythroid and mast cells	p300/CBP, PCAF, SWI/SNF and mSin3A	Erythropoiesis
LKLF	**KLF2**	Lung, blood vessels, lymphocytes	Unknown	Blood vessel, lungdevelopment, T-cell survival
BKLF	**KLF3**	Erythroid tissue-and brain-enriched	CtBP2	Unknown
GKLF	**KLF4**	Gut-enriched	p300/CBP	Anti-proliferation, survival
IKLF	**KLF5**	Gut and epithelial tissues	Unknown	Cell growth
CPBP	**KLF6**	Ubiquitous	Unknown	Putative tumor suppressor
UKLF	**KLF7**	Ubiquitous	Unknown	Cell-cycle arrest
BKLF3	**KLF8**	Ubiquitous	CtBP2	Unknown
BTEB1	**KLF9**	Ubiquitous	mSin3A	Neurite outgrowth and carcinogen metabolism
TIEG1	**KLF10**	Ubiquitous	mSin3A	Apoptosis, anti-proliferation
TIEG2/ FKLF	**KLF11**	Ubiquitous	mSin3A	Anti-proliferation
AP-2rep	**KLF12**	Brain, kidney, liver and lung	CtBP1	Unknown
BTEB3/ RFLAT-1 / FKLF-2	**KLF13**	Ubiquitous	mSin3A, p300/CBP and PCAF	Anti-proliferation and carcinogen metabolism
KKLF	**KLF15**	Unknown	Unknown	Unknown
BTEB4 / mDRRF	**KLF16**	Ubiquitous	mSin3A	Carcinogen metabolism

The table is modified from (189).

Table 1.3: The Kruppel-like Factors in muscle biology.

	Function / observation	Ref.
	Heart	
KLF2	• Expressed in endothelial cells in the developing heart • By E10.5, the AV cushions of KO mice are hypocellular, suggesting defective EMT • KLF2 ablation leads to myocardial thinning, high output cardiac failure, and death by mouse E14.5	(191)
KLF3	• Cardiac expression not reported • No cardiac defects reported in *klf3* null mice despite associated prenatal lethality • Analysis of ENU-induced mutation in the DNA-binding domain of KLF3 was linked to prenatal lethality and biventricular cardiac hypertrophy with diminished cardiac chambers. Adult survivors exhibited hypotension, cardiac hypertrophy with enlarged cardiac chambers, and aortic valvular stenosis	(192)
KLF4	• KLF4 expressed in the heart from late embryonic development through adulthood • KLF4 (−/−) mice were born at the expected Mendelian ratio but they gradually died after birth. Mice that survived beyond postnatal day 28 exhibited marked growth retardation and a significant decrease in cardiac output • KLF4 (−/−) mice had a reduction in expression of multiple cardiac genes, including GATA4	(198)
KLF5	• Expressed in cardiac fibroblasts and induced by angiotensin II • Regulates expression of PDGF-A and TGF-β • KLF5(+/−) mice have reduced hypertrophic remodeling in response to angiotensin II infusion • Interacts with retinoic acid receptor alpha whose activation modulates KLF5 function	(199)
KLF10	• Cell-specific and temporal expression within the heart not reported • KLF10(−/−) mice (males only) develop spontaneous pathologic hypertrophy by 16 months of age • Regulates expression of Pituitary Tumor Transforming Gene (Pttg1).	(200)
KLF13	• Expressed in developing cardiomyocytes with substantial reduction postnatally • Trans-activates multiple cardiac promoters, including ANP and BNP, synergistically with GATA4 • Knockdown in *Xenopus* embryos causes cardiac developmental defects (atrial septal defects and ventricular hypotrabeculation) that can be rescued by GATA4	
KLF15	• Not expressed in the heart developmentally, but upregulated postnatally in cardiomyocytes and cardiac fibroblasts • Downregulated with hypertrophic stimulation and functions as a transcriptional inhibitor of hypertrophy • Can inhibit GATA4 and MEF2 DNA-binding and transcriptional activity • KLF15(−/−) mice develop severe eccentric hypertrophy and LV dysfunction with pressure overload	(201, 202)
	Smooth muscle	
KLF4	• SMC expression is low under basal conditions but rapidly induced following vascular injury • PGDF-bb mediated repressive effects on SMC gene expression/differentiation are, in part, KLF4 dependent and may involve inhibition of myocardin • Can inhibit the TGFβ1-mediated induction of SMC differentiation markers α-SMC actin and SM22α	(203)
KLF5	• Expressed in fetal SMC but downregulated postnatally • Robust re-induction with vascular injury or angiotensin II stimulation that may involve signaling through Survivin and MAP-kinase pathways • Induces PDGF-A/B, PAI-1, iNOS, and VEGF-R and promotes SMC proliferation • KLF5(+/−) mice have reduced neointimal growth and perivascular fibrosis in response to vascular injury and angiotensin II infusion	(204)
KLF13	• Activates the minimal promoter for the SMC differentiation marker SM22α	(205)
KLF15	• Robust expression in SMC at baseline with significant downregulation after vascular injury • Overexpression prevents SMC proliferation • KLF15(−/−) mice exhibit an exaggerated neointimal response to vascular injury	(206)
	Skeletal muscle	
KLF6	• Expressed in skeletal muscle but role unknown	(207)
KLf13	• Expressed in skeletal muscle but role unknown	(208)
KLF15	• Regulates expression of glucose transporter GLUT4 • Interacts with MEF2A	(209)

The table is modified from (13,196).

1.10.2. KLF13 in embryogenesis: emphasis on cardiogenesis

The thirteenth member of the KLF family, KLF13 (also known as RFLAT1/FKLF-2/BTEB3), was initially identified as the transcriptional regulator of the chemokine RANTES in activated T lymphocytes (210). Subsequent publications have also indicated its role as a transcriptional regulator of other promoters including the human γ globin promoter, *Nppa*, *Nppb*, SV40, and SM22α promoters (34,208,211). Transcripts of *Klf13* were detected as early as E 8.0 in mice with a succeeding robust expression in the heart, cephalic mesenchyme, thymus, dermis, skeletal muscle, and epithelial layers of the gut and urinary bladder (196,212). The cardiac expression of *Klf13* was detected as early as E 9.5 with future expressions in the developing atrial myocardium, ventricular trabeculae, AV cushions, and truncus arteriosus. Postnatally, *Klf13* expression is downregulated in the heart, except for the valves and interventricular septum (196). The first report of *Klf13* knock out in mice implicated the gene in controlling erythropoiesis. Mice null for *Klf13* were born with reduced Mendelian inheritance ratios (<25%) and were characterized by reduced numbers of circulating erythrocytes and displayed a larger spleen and thymus (213).

The role of KLF13 during cardiac development was first reported by our lab (34). Our examination of *the Nppb* promoter identified an evolutionarily conserved KLF consensus sequence critical for proper promoter activity and flanked by nearby GATA sites. Interestingly, this conserved sequence was found to have a preferential transcriptional contribution in the atria compared to the ventricles. Using *in silico* analyses that were supported by *in vitro* assays, we isolated KLF13 as the most likely member of the KLF family regulating *Nppb* promoter activity. Furthermore, our luciferase reporter assay showed that KLF13 was capable of activating multiple cardiac promoters (e.g. *Nppb, Nppa, Myh7*, α-cardiac actin) synergistically with GATA4 through the N-terminal zinc finger

domain of GATA-4 (34,196,214). Knock down of klf13, using antisense morpholinos in *Xenopus* embryos revealed the importance of klf13 in the early stages of cardiac development. Loss of klf13 function was associated with ventricular hypotrabeculation, atrial septal defects, as well as delayed atrioventricular cushion formation and valve maturation. Analysis of early cardiac markers showed that klf13 is not essential for the initial specification of cardiac cell fates. The first sign of cardiac defects were detected during the linear heart tube stage which included slower pace of cardiac peristaltic beating and signs of pericardial edema. These results revealed an important role of klf13 in later stages of cardiac cell fate specification and morphogenesis. Our gene expression analysis, at the onset of cardiac tube formation, indicated severe reduction of several cardiac specific transcription factors, including GATA4, GATA5 and TBX5. Furthermore, late cardiac differentiation markers such as *Nppa* and the atrial isoform of myosin light chain (αMLC) were shown to be delayed. Our TUNEL, terminal deoxynucleotidyl transferase dUTP nick end labeling, assays for apoptotic nuclei eliminated the probability of cardiomyocyte loss. Thus, we hypothesized that klf13 is involved in cardiac cell proliferation. Supporting this hypothesis, our luciferase reporter assays found that KLF13 is a potent transactivator of the cyclin D1 promoter, which contains several KLF binding sites (34,196,214).

In addition to the aforementioned phenotypes in *Xenopus* embryos, human heterozygous for the microdeletions of the chromosomal band 15q13.3, harbouring at least seven genes including *KLF13*, are associated with cardiac defects (194). Thus, it is highly probable that KLF13 is important during mammalian and human cardiac development.

1.10.3. KLF13: A portrait of the family's structural features

To understand the function of a transcription factor, a dissection of its basic structural features and properties is necessary. A minimum of two domains are required to formulate a site-specific transcription factor - a DNA-binding domain and a transcriptional regulatory domain (195). This section will describe the structure–function aspects of KLFs with a primary focus on KLF13 features (**Figure 1.9** represents the structural features of KLF13).

As previously described, the distinguishing feature of the KLF family is the presence of a C-terminal DNA-binding domain composed of three contiguous and highly conserved Cys2/His2 zinc-fingers. The architecture and sequences of the three zinc-fingers, well conserved among the family members (**Figure 1.8**), allow the transcription factor to bind to related GC/GT rich sites on the major groove of DNA (186,187). Each of the Cys2/His2 zinc-fingers is composed of a beta-hairpin followed by an alpha-helix where a single zinc atom is tetrahedrally co-ordinated by two cysteine and two histidine moieties to form a finger-like tertiary structure (215). The consecutive three zinc-fingers are divided by the highly conserved seven-amino acid linkage sequence TGEKP(Y/F) X. Although several hypotheses were proposed to explain the necessity of three zinc-fingers, it is widely believed that each zinc-finger recognizes a nucleotide triplet, and thus the three zinc-finger repeats of the KLFs recognize nine base pairs in total (215). *In vitro* analyses have indicated that amino acids positioned at −1, 2, 3, and 6 from the N-terminal end of the α-helix in each ZF are critical for direct DNA interaction and thus for determining the consensus sequence specificity (215).

Structural analysis of non-KLF C2H2 zinc-fingers were important in our understanding and predictions of the DNA recognition modes of the ZF motifs (215,216). However, complementary *in vitro* analysis showed that some of the KLF factors prefer slightly different DNA sequences from those projected by their amino acid sequence analysis. For example, while KLF13 was predicted to bind to GC rich sequences, KLF13 binds robustly to CTCCC boxes within the RANTES promoter as well as to the CACCC boxes of γ-globin (*Hbg*), *Nppb*, and *Nppa* promoters (34,208,210). Several models were suggested to explain the discrepancies between predicted *in silico* models and actual *in vitro* DNA-binding. These included a "co-operative binding" model of the zinc-fingers and a "wobble" effect similar to that observed during peptide synthesis (195,217). In addition, the effects of post-translational modifications and combinatorial interactions with other factors are yet to be explored. Since the mammalian genome is rich in GC/GT sites, deciphering the mechanism of the zinc-fingers' wobbling DNA-binding code would be critical for studies that are focused on the mechanism of gene expression (195).

Another structural feature of transcription factors is the possible existence of nuclear localization signals (NLS). The signal is a stretch of basic amino acids that is recognized by nuclear transport proteins that target the translocation of NLS-bearing-proteins across the nuclear membrane in an ATP-dependent manner (187). Unlike the conserved three zinc-fingers of the KLF family, the location and structure of the NLSs are highly variable (195). Although some members of the KLF family possess a basic amino acid (Arg/Lys)-rich region juxtaposed to the zinc-fingers, including KLF13, they proved non-functional for nuclear localization in some KLFs including KLF1 (189,215). Interestingly, several basic moieties within the zinc-fingers that mediate the interactions with other nuclear proteins were also found to be determinants for nuclear localization (215).

As previously discussed, the heterogeneity of the N-terminal domain of the KLF factors partly explains the diverse biochemical mechanisms by which KLFs regulate transcription and influence diverse cellular processes (187,195). Analysis of these N-terminal domains revealed several activation and repression domains that interact with various co-activators and co-repressors in a context-dependent manner (187,195). The amino-terminal region of KLF13 (1–146aa) is rich in proline (24/146), serine (10/146), and alanine (30/146) moieties (187). Using luciferase reporter assays co-transfected with constructs of GAL4-DBD fused to different KLF13 deletions, a possible transactivation domain within the 1-35aa region of KLF13 was identified. Although typical transactivation domains are rich in hydrophilic amino acids, KLF13's transactivation domain is rich in hydrophobic amino acids (Ala, Pro and Val). Interestingly, this transactivation domain has a high homology to the transactivation domain of KLF9. Similar luciferase reporter studies showed that KLF13 possesses a unique repression domain (67-112aa) rich in alanine (19%) and proline (20%) (187). Proline and alanine rich domains are known to mediate protein-protein interactions. Other KLFs were also found to possess both activating and repressing domains and work as activators and repressors depending on the targeting promoters, their interacting partners, and the cellular context (187,195,196).

KLF13 also contains a serine-rich carboxyl-terminal tail (AA 250–288), but the exact function of this serine rich region is yet to be determined (187).

1.10.4. KLF13: Mechanisms of regulation

Myriad reports have linked the state of histone acetylation and deacetylation with repression and activation of transcription, respectively (189). Histone modification is thought to be the molecular switch by which Sp1/KLF proteins function as activators or repressors. With this in mind, KLF13 was shown to be a transcriptional activator for several promoters including γ globin, *Nppa*, *Nppb*, SV40, and SM22α (34,189,208,211). KLF13 was also reported to function as a transcriptional repressor for promoters such as the cytochrome P450 CYP1A1 (189,218). These studies emphasizes the promoter-dependent transcriptional activities of KLF13 (189).

Song *et al,* 2002 revealed that acetylation also modulates KLF13 transcriptional activity. The coactivators p300/CREB-binding protein (CBP) and p300/CBP-associated factor (PCAF) were found to act synergistically in stimulating KLF13 transcriptional activity (219). These findings are consistent with the previous reports linking the co-activational properties of CBP and PCAF to their acetylation of histones and/or transcription factors. Acetylation of transcription factors modulates the activity of transcription factors at multiple levels, including DNA binding, interaction with other proteins, and stability. Indeed, acetylation of KLF13 by CBP and PCAF was found to modulate its DNA binding capacity (219). PCAF was found to directly bind to and to acetylate specific lysine residues at the first and third zinc-fingers of KLF13, enhancing DNA-binding activity. Unexpectedly, acetylation by CBP was found to be disruptive for KLF13's DNA binding to its consensus sequence. These observations demonstrate that "… transcription is a very dynamic process involving the assembly and disassembly of pre-initiation, initiation or elongation complexes. Therefore, in the context of the complex process of transcriptional

regulation, CBP and PCAF may function at distinct steps of the transcription process to facilitate the assembly or disassembly of the complex through acetylation of target proteins in the complex," (219).

Several members of the KLF family, including KLF13, are also involved in the process of histone deacetylation via a mechanism that includes a direct interaction with the histone deacetylase co-repressor Swi-independent-3 (Sin3). Sin3 is a master transcriptional scaffold and corepressor that silences transcription by the recruitment of histone deacetylases (HDACs) (220). The N-terminal domain (1-114aa) of KLF13 was found to contain a sin3-interacting domain, SID, which is a hydrophobic pocket that recruits and directly interacts with Sin3 (189,195,221). Interestingly, the previously described amino-terminal activation domain of KLF13 also encompasses the SID domain (189). Thus, it is necessary to decipher the mechanistic code that dictates the recruitment of co-activators or co-repressors which eventually control KLF13's role on a given gene (189).

KLF13 was also shown to be modified via phosphorylation, suggesting that its activity is regulated by posttranslational modification. Huang *et al*. showed that PRP4, a member of the MAPK family, modulates RANTES gene expression via the control of KLF13 phosphorylation state. Although KLF13 phosphorylation by PRP4 was correlated with weaker DNA-binding, co-expression of PRP4 and KLF13 increased the nuclear localization of KLF13 and RANTES transcription (222). The exact nature of the aforementioned observation is yet to be determined. With that in mind, structural analyses of the KLF13 complex with its cofactors and transcriptional partners are necessary to decipher the molecular activities of KLF13 and the nature of its role in the processes of self-renewal, proliferation, differentiation, and development

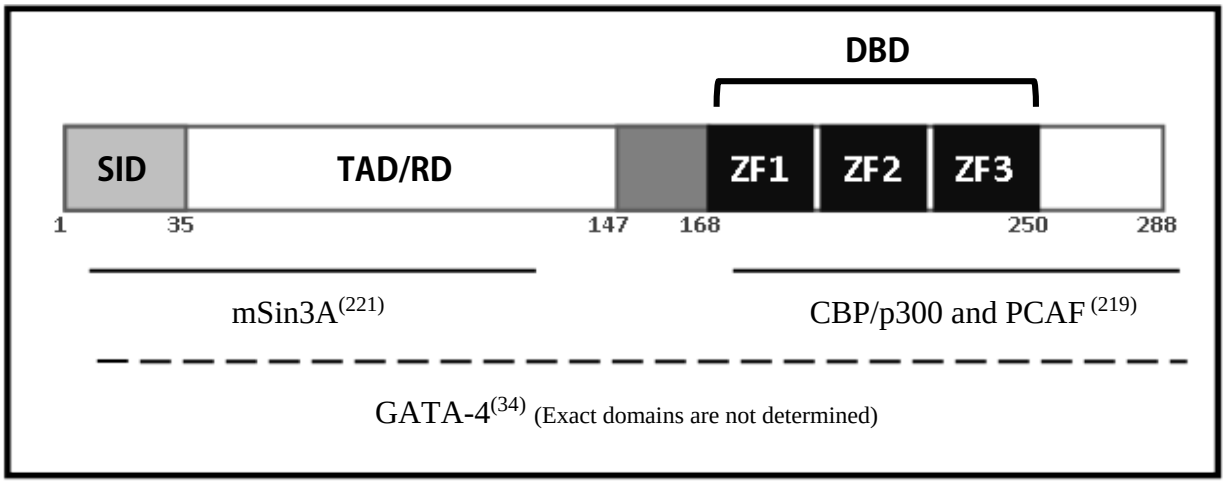

Figure 1.9: Schematic representation of KLF13 protein structure.
The lines represent the regions required for the interaction with the protein identified under the line. DBD: DNA binding domain, SID:Sin3A binding domain, TAD: Transactivation domain, RD: Repression domain.

1.11 Hypothesis and Objectives

Despite important efforts devoted to the study of chamber and tissue specific gene expression and the identification of several cardiac transcription factors (TF) involved in heart formation, the molecular mechanisms underlying the spatiotemporal regulation of transcription within the heart remain unclear. We previously showed that KLF13 is expressed predominantly in the atria and the endocardium, binds evolutionarily conserved regulatory elements known as CACC-box on several cardiac promoters (including ANP), acts as a cardiac transcriptional activator, and functionally and physically interacts with the master regulator of cardiac development, GATA-4. Furthermore, depletion of KLF13 from *Xenopus* embryos led to delayed cushion formation, septal defects, and hypotrabeculation, suggesting that KLF13 may be a disease-causing gene for CHD. However, the role of KLF13 in four chambered mammals, the mechanism by which it acts, and its spatiotemporal role are still to be determined. We hypothesize that KLF13 is an evolutionarily conserved component of the genetic circuit that controls cardiac development and that plays distinct roles in endocardial and myocardial cells. We also hypothesize that the interaction between KLF13 and other conserved cardiac transcription factors underlie its role during heart development.

The main objectives of this thesis are to use a combination of mouse models and cellular and molecular biology techniques to:

1. Explore KLF13's role and mechanism(s) of action during murine cardiac development.
2. Pursue structural and functional analysis of the two KLF13 isoforms.
3. Evaluate the genetic interactions between KLF13 and its collaborators (e.g. TBX5) and to ascertain its role as a genetic modifier of congenital heart diseases.

2. Experimental Chapter One
Essential Role for KLF13 in Heart Development

Abir Yamak[1], Salim Hayek[2], Rami Darwich[1], Wael Maharsy[1], Hiba Komati[1], Mona Nemer[1]

1- Laboratory of Cardiac Development and Differentiation, Department of Biochemistry, Microbiology, and Immunology, University of Ottawa, Ottawa (Ontario), Canada
2- Emory University, School of Medicine, Atlanta, USA

My contributions to the chapter are the following:

1- **Uncovered the atrial septal defect in the *Klf13* mutant mice (Described later as PFO by Abir Yamak in Figure 2.2 D).**
2- **carried out luciferase assays shown in Fig 6N**
3- **Dissected hearts from E11.5 embryos, prepared RNA for RNA seq and analysed data presented in Tables 2+3**
4- **Validated several transcript changes by QPCR as shown in Fig 8**

2.1. Abstract

KLF13 is a member of the Krüppel-like transcription factors that are important regulators of cell proliferation and differentiation. KLF13 is highly enriched in the developing heart where it is found in both myocardial and endocardial cells. In myocytes, it interacts with GATA4 and regulates the A- and B-type natriuretic peptide genes, Nppa and Nppb. Knock down of *Klf13* in *Xenopus* causes developmental heart defects, suggestive of an important role in heart morphogenesis. To test whether this role is evolutionary conserved in the mammalian heart, we deleted the Klf13 gene in transgenic mice using homologous recombination. Mice lacking both Klf13 alleles are born at reduced frequency owing to severe heart defects. Variable cardiac phenotypes are observed in Klf13 null mice and most are endocardial cushion defects including "Goose-neck" deformity and atrioventricular (AV) valvular abnormalities. Epithelial-mesenchymal transformation (EMT) is altered in these mice with reduced endothelial cell proliferation. Surviving Klf13 null mice have several structural cardiac anomalies including cardiomyopathies and aortic valve stenosis; and expression levels of several cardiac genes are also altered. Our data uncover a role for a new class of transcription factors in heart formation and point to KLF13 as a potential congenital heart disease causing gene in human.

2.2. Introduction

Congenital heart diseases (CHD) account for the loss of around 25% of human embryos and around 1-2% of newborns have some form of cardiac malformations (1,2). Despite the significant advances of the past two decades that have shed more light on our understanding of cardiac morphogenesis, few CHD-causing genes have been identified to date and the genetic basis of the majority of familial congenital heart diseases remain unelucidated.

Cardiac morphogenesis is a complex process whereby multiple lineages contribute to a properly developed heart. The first or primary heart field (PHF) gives rise mainly to the left ventricle and most of the atria; the secondary or anterior heart field (AHF) contributes to the right ventricle, outflow tract (OFT) and parts of the atria (3,4). One important step that takes place during heart development is epithelial-mesenchymal transformation (EMT). This is crucial for the formation of the cardiac cushions that ultimately give rise to the cardiac valves. An extracellular matrix or cardiac jelly (composed of elastin, collagen, and glycosaminoglycans) separates the endocardial from the myocardial layer in the primary heart tube. A subpopulation of cells from the endocardial layer in the atrioventricular canal (AVC) and OFT, in response to inductive signals from the overlying myocardium, undergoes EMT, thus, cellularizing the cardiac jelly and forming the endocardial cushions (EC) (5). Various signaling molecules govern this process of cardiac valve formation including VEGF, Notch, wnt/β-catenin, TGF-β, BMP and hyaluronic acid signaling (6). Malformation of the atrioventricular canal cushions result in atrioventricular septal defects (AVSDs) or endocardial cushion defects. One type of these defects is “Goose-neck deformity” that can be seen on a left ventricular angiography. It is characterized by an abnormal apical positioning of the anterior mitral valve leaflet that encroaches on the left ventricular outflow tract resulting

in a narrowing of its lumen and an anterior displacement of the aorta. The distance between the mitral valve and the apex is abnormally shorter than that between the aortic valve and the apex due to the deficiency of the IVS (7-9). Non-membranous VSDs and AV valve defects can also be observed in association with "Goose-neck deformity." The molecular basis underlying this deformity is unclear and no gene has been linked with this valvular abnormality. AVSDs account for 5% of all CHDs and are associated mainly with Down syndrome. Isolated cases are also present as an autosomal dominant trait (10,11).

KLF13 has been identified in our laboratory as a novel regulator of cardiogenesis (12). It belongs to the Kruppel-like family of transcription factors that were first identified by virtue of their similarity to Sp1, one of the first factors cloned and characterized in mammals. 21 KLF members have been identified in humans so far, of which 17 homologs are found in mice (13). They contain three highly conserved Cys_2/His_2 zinc fingers in the C-terminal region connected by a highly conserved Kruppel-link seven-amino acid sequence [TGEKP(Y/F)X]. The three zinc fingers confer specificity to KLFs to bind the consensus *GC*- and *CACCC* DNA boxes (14,15). KLF13 is expressed in the heart and the cephalic mesenchyme of the developing mouse embryo (16). A detailed spatiotemporal expression analysis of KLF13 in the developing mouse heart by Lavalleé *et al* shows that E9.5 embryos have strong expression in the heart and the epidermis. At E10.5, KLF13 is highly detected in the atrial myocardium and the endocardium. By E12.5, its expression is stronger in the atria yet is also highly detected in the ventricular trabeculae. KLF13 is downregulated in the postnatal heart where the highest levels are found in the interventricular septum and the atrioventricular valves (12). A similar expression pattern is also observed in the *Xenopus* (12). Knockdown of *xKlf13* in *Xenopus* results in a cardiac phenotype. Although early heart formation up to the heart tube stage appears normal in these embryos, several defects are observed shortly after looping and

chamber formation. Among others, the single ventricle is often hypoplastic, atrioventricular cushion formation and valve maturation is delayed and several cardiac markers are altered in these knock down embryos (12); these findings are suggestive of a role of KLF13 in amphibian heart morphogenesis (12).

In this study, we tested the role of KLF13 in mammalian cardiogenesis. We show that Klf13 null mice have defective heart morphogenesis and postnatal viability. Endocardial cushion defects including “Goose-neck” deformity and AV valvular anomalies are observed. The mechanism underlying these defects involves altered EMT with reduced endothelial cell proliferation and excessive mesenchymal differentiation in the AV cushion. Surviving $Klf13^{-/-}$ mice have several structural cardiac abnormalities and the expression of several genes involved in EMT is altered. Our data point to a novel role of KLF13 in endocardial cell proliferation and heart formation and identify KLF13 as a potential CHD causing gene.

2.3. Materials and Methods

Animals. All animal experiments were carried out in accordance with institutional guidelines for animal care. Experiments were approved by the International Animal Care and Use Committee (IACUC) of the University of Ottawa, which conforms to that of the US National Institute of Health (NIH) (Assurance number for University of Ottawa: A5043-01). At end points, mice were anesthetized with 2.2µl/g i.p KXA cocktail (Ketamine 42.86 mg/ml, Xylazine 8.57 mg/ml, and Acepromazine 1.43 mg/ml) and sacrificed. For euthanasia, CO_2 and cervical dislocation (CD) was used. CD without prior anesthesia is required for embryo collection in mice.

Generation of Klf13 knockout mice. The knockout mice were generated by targeted deletion of the 2nd exon as described (in chapter 4). The mice were kept on the C57/BL6 background. Pregnant mothers or newborn litters were sacrificed at various embryonic and postnatal time points. The morning a vaginal plug was observed was considered as embryonic day (E) 0.5.

Histology. Adult heart tissues or staged embryos were fixed in 4% paraformaldehyde at 4^{o}C overnight, processed, paraffin embedded and sectioned at 4µm intervals as previously described (17). Masson Trichrome and Alcian blue staining were done as previously described (18,19).

Echocardiography analysis. Mice were anesthetized (2.0% isoflurane, 80 ml/min 100% O_2) and two-dimensional guided M-mode echocardiography was performed using a Visual-Sonics VEVO 700 and a 30-MHz linear array transducer as described by Aries *et al.*, 2004 (20).

Real-Time PCR analysis. Total RNA was isolated from mouse tissues using TRIZOL reagent (Invitrogen). Transcript levels of the various markers were determined by real-time PCR as previously described (21).

Cell Cultures. NIH3T3 cells were maintained in culture and transfected as previously described (12). Transient transfections were conducted in 24-well plates and the amount of luciferase-reporter was kept at 1.0 μg per well and the total amount of DNA was kept constant (usually 1.25 μg). After overnight incubation, the medium and precipitates were removed and replaced with fresh medium. At 48 h post-transfection, cells were harvested, lysed, and luciferase activity was assayed with a GloMax®-96 Microplate Luminometer. The preparation KLF13a expression vector was obtained by subcloning the amplified reverse transcription (RT)-PCR cDNA constructs into the CMV-driven pCGN vector in phase with the hemagglutinin (HA) epitope as previously described (12).

RNA-Sequencing. The embryonic hearts of three wild type and five klf13 null mice at E11.5 were carefully dissected. Total RNA was isolated from mouse tissues using TRIZOL reagent (Invitrogen). Total RNA concentration and 260/230 and 260/280 ratios were estimated by Nanodrop spectrometer N1000 (Thermo Scientific). RNA integrity was estimated by resolving 1 μg of sample in a 1 % (m/v) ethidium bromide agarose gel. The RNA library was built using the Illumina TruSeq RNA library preparation protocol. The library was sequenced on a Illumina HiSeq 2500 (at the Centre for Applied Genomics, Hospital for Sick Children, Toronto, Canada) using a paired end recipe (2x100-bases) with TruSeq v3 chemistry. RNS-sequencing was also provided by the aforementioned centre. Adaptors were trimmed using "Trim Galore!" and low quality read ends were removed based on the Phred score ($t < 20$). TopHat was used to align reads to the reference genome

UCSC mm10. Resulting alignments from TopHat were then processed to extract raw read counts for genes and exons using HTSeq. Raw gene counts were loaded and sample-normalized using DESeq. PCA (Principal Component Analysis) was also performed to assess relation among samples; an empirical permutation-based procedure was used to identify informative principal components. Atwo-condition differential analysis for genes was also conducted using DESeq; we discarded genes whose max sample-normalized count across samples was lower than the 25% quantile of max sample-normalized counts (this was intended to remove genes that werenot expressed). Raw exon counts were then loaded and sample-normalized using DEXSeq. Atwo-condition differential analysis for exons was also done using DEXSeq; we discarded exons whose max sample-normalized count across samples was lower than the 25% quantile of max sample-normalized counts (this was intended to remove exons that were not expressed).

Immunohistochemistry. Immunohistochemistry on heart sections from each mouse group was performed as previously described (20). The antibodies used were: Ki67 (Clone SP6, Rabbit Monoclonal, Thermo Scientific RM-9106-S0), phospho histone H3 (Ser 10, Rabbit polyclonal, Millipore 06-570).

Cell count. Image J software was used to count the endocardial and mesenchymal cushion cells.

Statistics. The data are presented as mean ± SEM; $p<0.05$ by student two-tailed *t*-test is considered statistically significant.

2.4. Results

2.4.1. Klf13$^{-/-}$ mice have a cardiac phenotype.

The mouse Klf13 gene consists of two exons. We generated the Klf13$^{-/-}$ mice through targeted deletion of exon 2, which encodes the 2nd and 3rd zinc fingers and the entire C-terminus (please refer to experimental chapter 3). Klf13 heterozygous mice were intercrossed to generate Klf13$^{-/-}$ mice and were kept on a C57BL/6 genetic background. Quantitative PCR analysis (QPCR) confirmed the deletion of exon 2 in the knockout mice. Transcript levels from the first coding exon were reduced by 80% (**Figure 2.1**).

First, we examined the survival of the Klf13 null mice. Even though they were viable, the null mice were born at almost half the expected Mendelian ratios. Three to five litters were analyzed at each stage (**Figure 2.2 A-C**). Anatomical examination revealed a cardiac phenotype in a subset of the surviving mutant mice: right ventricular dilation and left ventricular hypertrophy were observed (**Figure 2.2 D** upper panel). Patent foramen ovale (PFO) was also observed in 35-45% of the live knock out mice (**Figure 2.2 D**, lower panel). Quantitative PCR (QPCR) analysis on RNA from adult hearts showed that the expression levels of various cardiac genes were altered in Klf13$^{-/-}$ mice as compared to wild types: ACTA1, SERCA, HAND2 and GATA4 transcript levels were significantly increased (**Figure 2.2 E**) (n=5 for Wt; n=6 for Klf13$^{-/-}$). Further examination by echocardiography analysis revealed a statistically significant increase in the mean pressure gradient across the aortic valve in ~ 60% of the mutant mice (**Figure 2.3 F**). Other cardiac functions appeared normal (**Figure 2.3 A-E**) (n=6 for Wt, n=7 for Klf13$^{-/-}$). These results suggest that a subset of the Klf13 null mice suffer from aortic valve disease and/or left ventricular dysfunction.

2.4.2. AVC and myocardial defects in Klf13$^{-/-}$ neonates.

As mentioned earlier, up untill embryonic day 18.5 (E18.5), Klf13$^{-/-}$ mice were obtained at normal Mendelian ratios. Around 35% of the mice die shortly after birth at postnatal day 0.5 (P0.5) and only half of them survive to adulthood. Consequently, we analyzed the hearts at P0; hence, including in our analysis those that do not survive. Anatomical examination revealed variable penetrance of myocardial and atrioventricular cushion (AVC) defects in these mice with higher incidences of AVC defects (n=4 for Wt; n=27 for Klf13$^{-/-}$) (refer to **Table 2.1** for percentages of incidence). Serial sections were thoroughly examined to confirm the observed phenotypes. Among the myocardial defects seen were ventricular hypertrophy (**Figure 2.4 E-F**); right ventricular dilation (**Figure 2.4 I**), right atrial dilation and right atrial hypertrophy (**Figure 2.4 K-L**). The AVC defects observed were thick AV valves (**Figure 2.4 D**) and "Goose-neck" deformity (**Figure 2.4 G**) which was sometimes accompanied by a membranous or AV type VSD (AVSD) (**Figure 2.4 H**). Ventricular hypertrophy and right atrial dilation were also observed at earlier stages of development E13.5-14.5 (**Figure 2.5 B and 5 D**) (n=6 for Wt; n=14 for Klf13$^{-/-}$). These results point to a defective endocardial and/or myocardial development in these mice. Note that the dilation of the right atria in some cases and its hypertrophy in others point to dysregulated proliferation in the hearts of these mice. No cardiac defects were observed in Klf13$^{+/-}$ neonates (n=6) (data not shown).

2.4.3. Reduced proliferation and early differentiation in Klf13$^{-/-}$ AVC.

To determine the origin of the AVC defects in these mice, we analyzed embryos at E11.5. Immunohistochemistry for the proliferation marker Ki67 and the mitosis marker phH3 was done on wild type and knockout sections. Less staining of both markers was observed in the AVC of the Klf13 null embryos (**Figure 2.6 B, C, E, F**). This decrease was also seen at

E14.5 in the endocardial cushion (EC), mitral valve (MV) and tricuspid valve (TV) (**Figure 2.6 J-L**). We then counted the numbers of Ki67 and phH3 positive cells in the AVC of three wild type and eight knockout E11.5 embryos. Cell counts indicated reduced levels of both endocardial and mesenchymal Ki67 and phH3 positive cells in the $Klf13^{-/-}$ AVC. Proliferation of the endocardial cells seemed to be affected more dramatically (**Figure 2.6 M**). Moreover, co-transfection of KLF13 and cyclin D1-luciferase expression vectors shows that KLF13 activates the cyclin D1 promoter in a dose dependent manner (**Figure 2.6 N**). This is consistent with our previous results (Lavallee *et al*, EMBO 2006) and further confirms a role of KLF13 in cellular proliferation.

Cardiac jelly is critical for development of the EC. It arises from epithelial-mesenchymal (EMT) transformation of a subset of endocardial cells that undergo proliferation, migration and differentiation into mesenchymal cells inorder to invade and cellularize the extracellular matrix (ECM). Altered proliferation of endocardial cells in the AVC of KLF13 knockout mice suggests a defective EMT in the hearts of these mice. Moreover, the delamination of a subset of endocardial cells from the endocardium and their transformation into mesenchymal cells is a complex process governed by various signaling molecules and involves a large subset of genes. QPCR analysis on RNA from P0 hearts revealed altered expression levels of several EMT regulating genes (**Figure 2.7**). *Vegf, Ctgf, Hif1α,* and *Adamts2* transcript levels were significantly reduced in the knockout hearts as compared to wild types. RNA sequencing on hearts from E11.5 knockout mice vs wild type littermates revealed profound genetic reprogramming (1572 genes significantly up-regulated and 1607 genes significantly down regulated) suggesting that KLF13 is involved in multiple processes during heart formation. Of the altered genes are those involved in cellular proliferation, migration and EMT including: *Ccnd2* (gene encoding cyclin D2); *Adamts*

(metalloprotease), *Bmpr2* (encoding Bone morphogenetic protein receptor), *Vcan* (gene encoding Versican); *Erbb3* and *Erbb4* (receptor tyrosine kinases); *Vegf* ; *Notch1* (**Table 2.2**). Several other myocardial and endocardial genes were also affected some of which were verified by QPCR (**Figure 2.8**). A list of all the genes that were significantly ($p<0.05$) up (fold change ≥ 1.5) or down (fold change ≤ 0.66) regulated is available upon request.

Collectively, these results point to an important role of KLF13 in mammalian heart development and endocardial cell proliferation. They indicate that KLF13 is essential for proper EMT and AV cushion development. Moreover, the data suggest that loss of KLF13 in mice results in AV cushion defects and in 50% of these cases causes perinatal death.

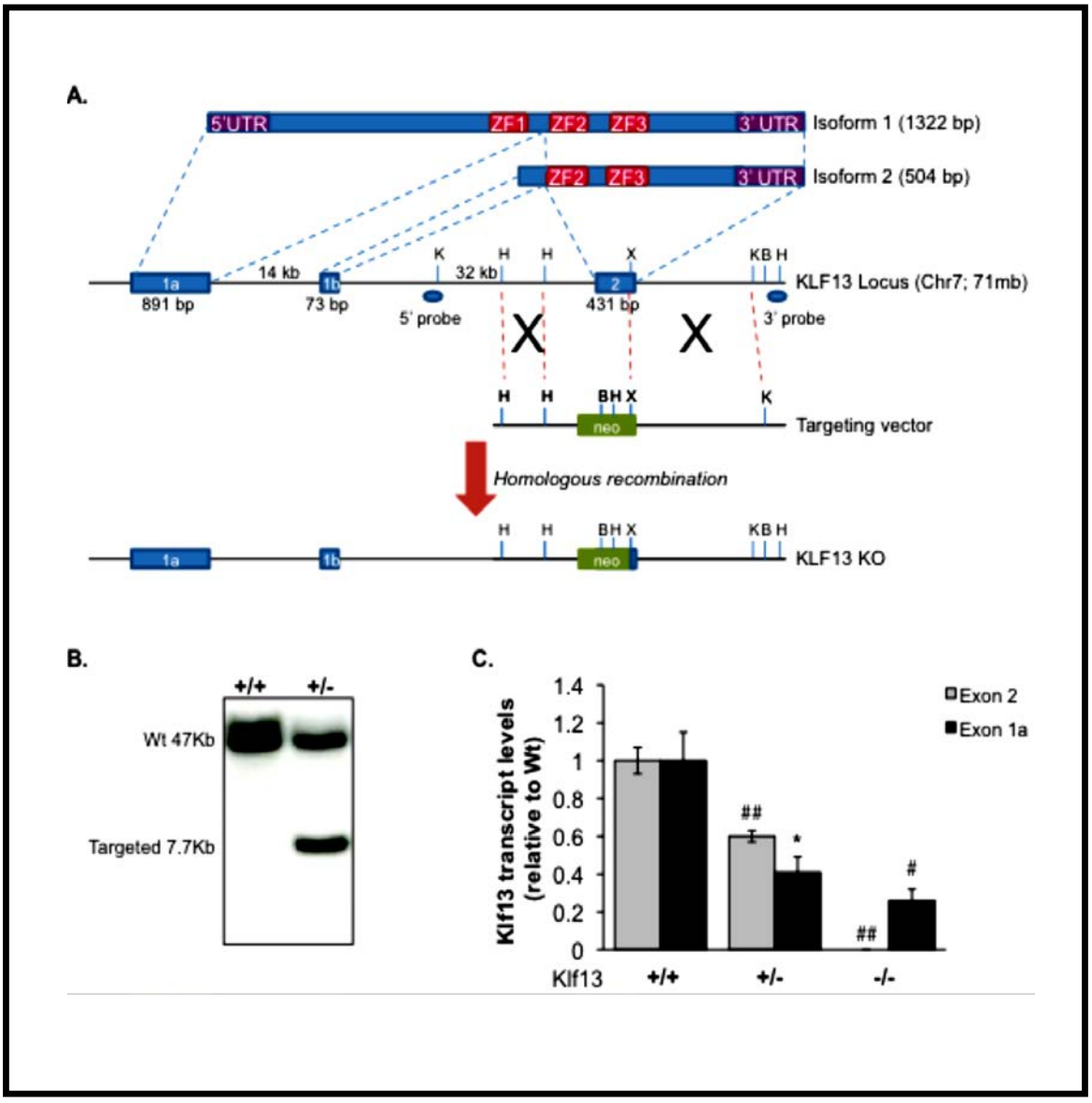
A.
5'UTR
ZF1
ZF2
ZF3
3' UTR
Isoform 1 (1322 bp)
ZF2
ZF3
3' UTR
Isoform 2 (504 bp)
K
H
H
X
KB H
1a
14 kb
1b
32 kb
2
KLF13 Locus (Chr7; 71mb)
891 bp
73 bp
5' probe
431 bp
3' probe
H
H
BH X
K
neo
Targeting vector
Homologous recombination
H
H
BH X
KB H
1a
1b
neo
KLF13 KO
B.
+/+
+/-
Wt 47Kb
Targeted 7.7Kb
C.
Klf13 transcript levels (relative to Wt)
1.4
1.2
1
0.8
0.6
0.4
0.2
0
Exon 2
Exon 1a
##
*
#
##
Klf13
+/+
+/-
-/-

Figure 2.1: Generation of Klf13-null allele.

A. Klf13 locus and targeting strategy. Positions of the 5' and 3' probes used in southern blot are shown. Homologous recombination deletes most of exon2 replacing it with a neo cassette. ZF: zinc finger; UTR: untranslated region; Wt: wild type. **B.** Southern blot analysis of targeted ES cells. Genomic DNA was digested with Hpa1 and hybridized to the 3' probe. Note the appearance of a 7.7Kb fast migrating band in $Klf13^{-/+}$ mice sample in comparison to wildtype mice. This band represents the deletion of exon 2 and the flanking region of the Klf13 gene. **C.** QPCR analysis of Klf13 transcripts in hearts of adult mice. Results confirm complete absence of exon 2 and 80% reduction of exon 1a in $Klf13^{-/-}$ mice. TBP was used as an internal control. * $p<0.05$; # $p<0.005$; ## $p<0.0001$ vs. $Klf13^{+/+}$.

A.

Wt/KO X KO/KO

E18.5	+/-	-/-
Expected	50%	50%
Observed	48.6%	51.4%

B.

Wt/KO X Wt/KO

P0	+/+	+/-	-/-
Expected	25%	50%	25%
Observed	43.3%	40%	16.7%

C.

Wt/KO X Wt/KO

Postnatal	+/+	+/-	-/-
Expected	25%	50%	25%
Observed	31.6%	54.5%	14.0%

D.

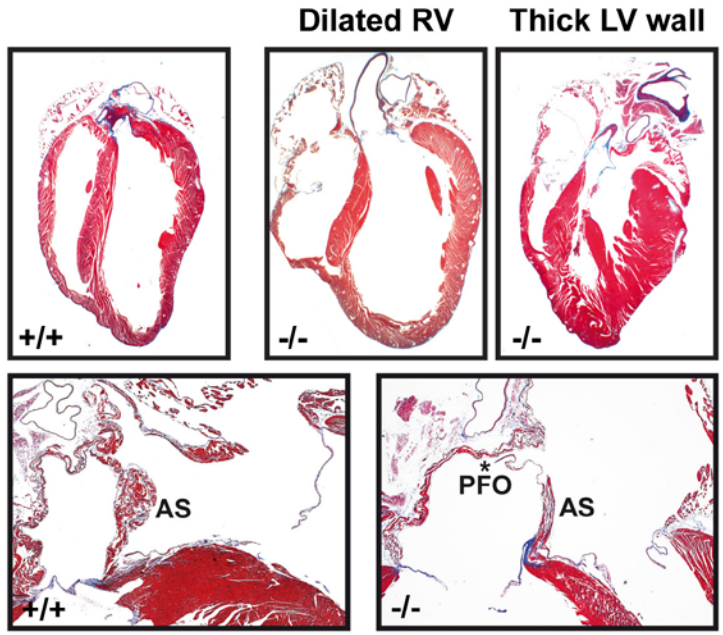

E.

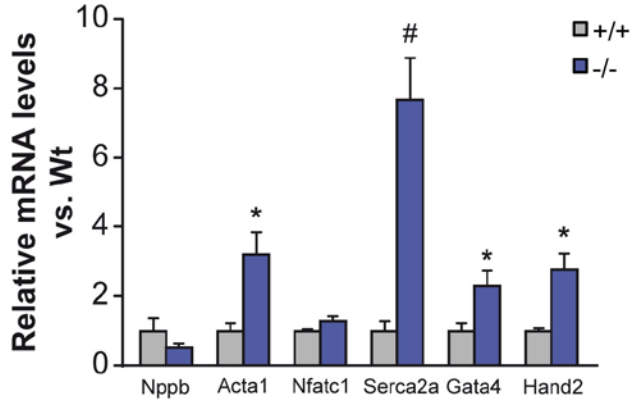

Figure 2.2: Postnatal death in Klf13-/- mice.

A-C Expected Mendelian ratios of Klf13 genotypes at E18.5, P0 and postnatally. Three to five litters were used at each stage. Note the lower than expected ratios of $Klf13^{-/-}$ at P0 and postnatally. **D.** Trichrome staining of whole heart frontal sections of $Klf13^{+/+}$ and $Klf13^{-/-}$ mice. Dilation of the right ventricle, thickening of the left ventricular wall and PFO were seen in a subset of the analyzed $Klf13^{-/-}$ mice. RV: right ventricle; LV: left ventricle; PFO: Patent foramen ovale. **E.** QPCR analysis using RNA from heart tissue of ~100-day-old mice (n=5-6 for each group). Note the statistically significant change in the transcript levels of ACTA1, SERCA2A, GATA4 and HAND2. *p<0.05; #p<0.005; ##p<0.0001 vs. $Klf13^{+/+}$.

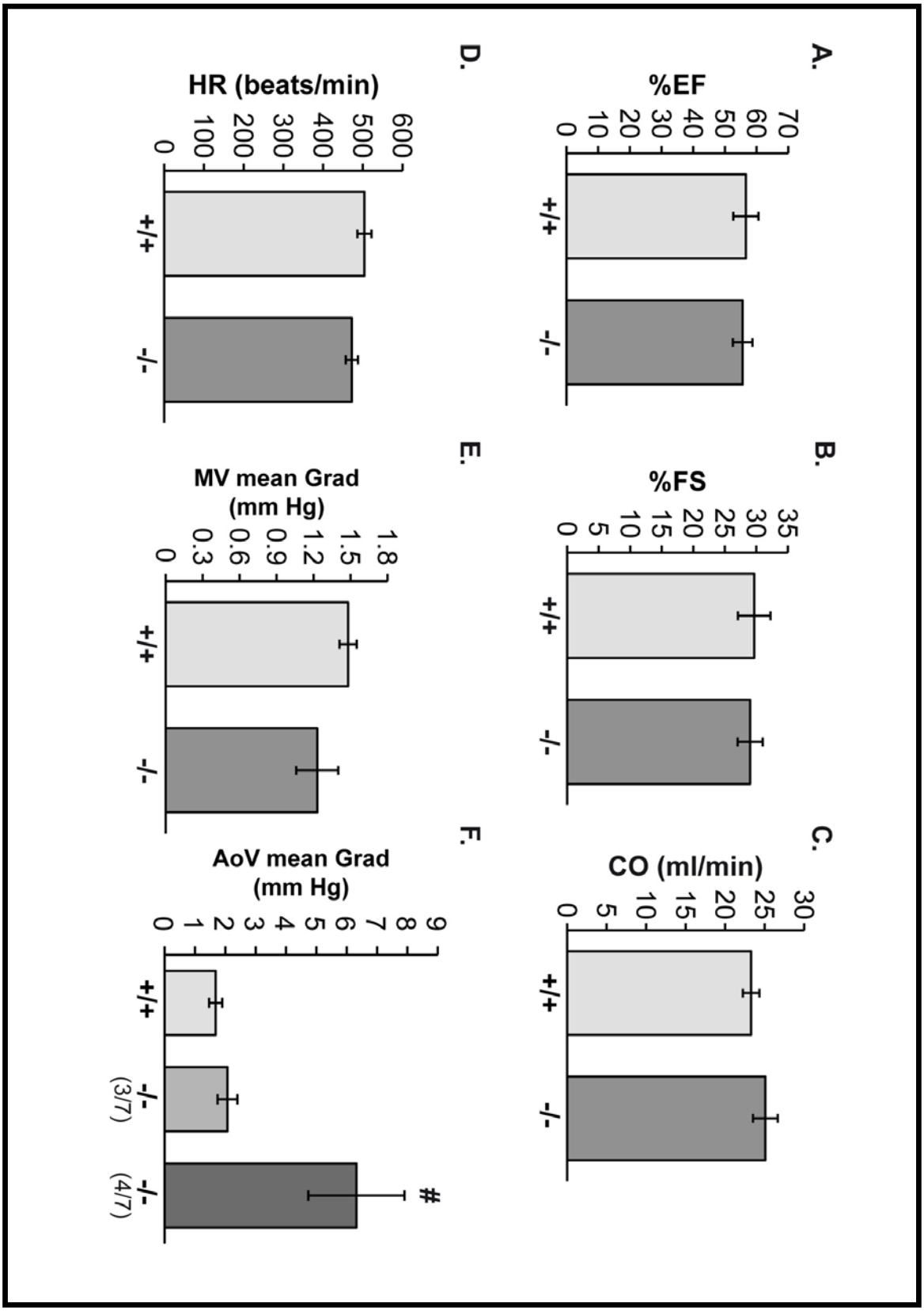
A.
%EF
70
60
50
40
30
20
10
0
+/+
-/-
B.
%FS
35
30
25
20
15
10
5
0
+/+
-/-
C.
CO (ml/min)
30
25
20
15
10
5
0
+/+
-/-
D.
HR (beats/min)
600
500
400
300
200
100
0
+/+
-/-
E.
MV mean Grad
(mm Hg)
1.8
1.5
1.2
0.9
0.6
0.3
0
+/+
-/-
F.
AoV mean Grad
(mm Hg)
9
8
7
6
5
4
3
2
1
0
+/+
-/-
(3/7)
-/-
(4/7)
#

Figure 2.3: Cardiac functional analysis in Klf13$^{-/-}$ mice

Echocardiography analysis of 265-day-old Klf13$^{+/+}$ and Klf13$^{-/-}$ mice (n=6 Wt; n=7 KO). Note the statistically significant increase in the mean pressure gradient across the aortic valve of a subset of the Klf13$^{-/-}$ mice. # $p<0.005$ vs. Klf13$^{+/+}$. EF: ejection fraction; FS: fractional shortening; CO: cardiac output; HR: heart rate; MV: mitral valve; AoV: aortic valve; Grad: gradient.

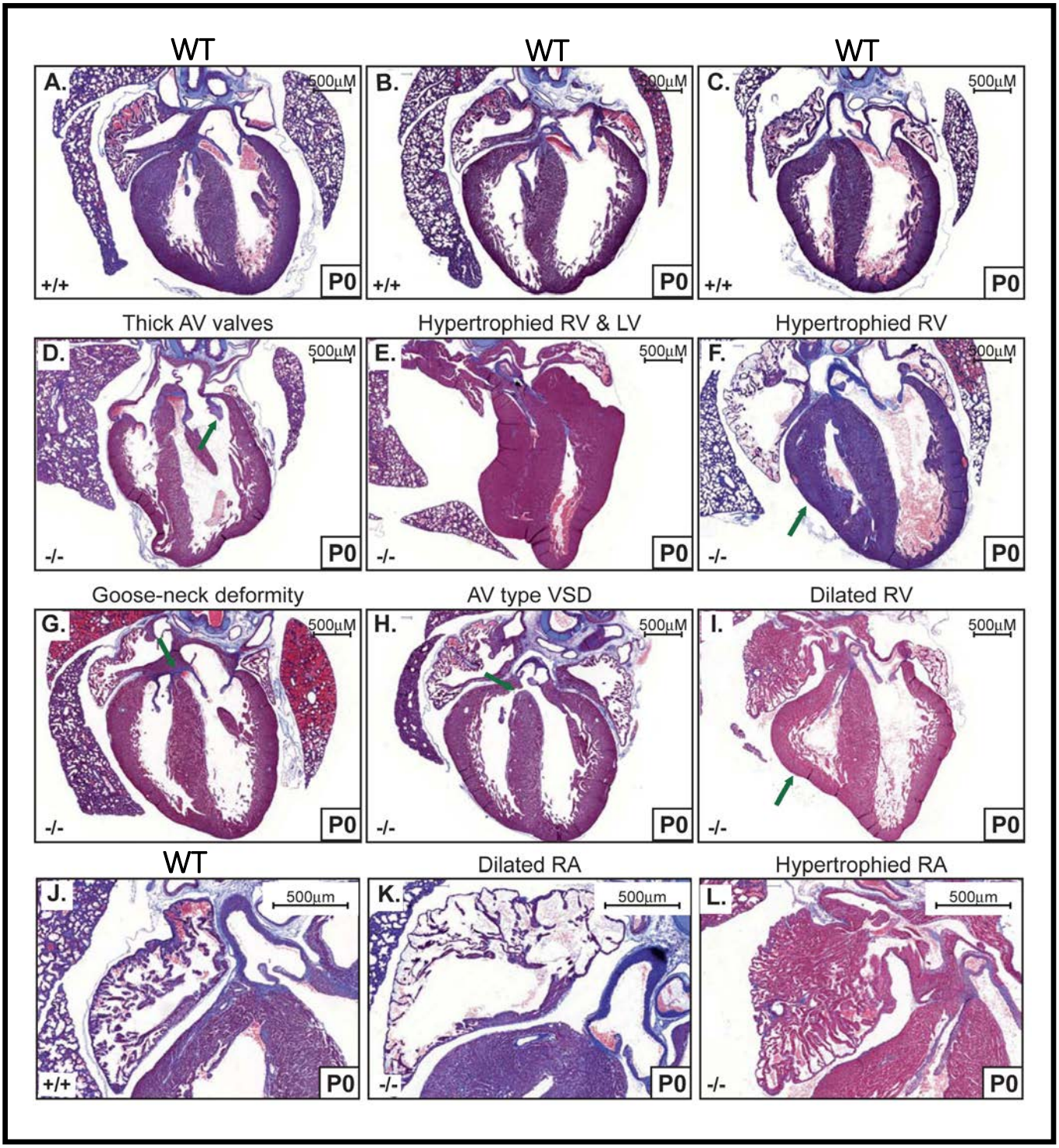
WT
WT
WT
A.
B.
C.
500µM
+/+
P0
Thick AV valves
Hypertrophied RV & LV
Hypertrophied RV
D.
E.
F.
-/-
Goose-neck deformity
AV type VSD
Dilated RV
G.
H.
I.
WT
Dilated RA
Hypertrophied RA
J.
K.
L.
500µm

Figure 2.4: Variable cardiac morphogenetic defects in Klf13$^{-/-}$ neonates.

A-L Trichrome staining of frontal heart sections of *Klf13*$^{+/+}$ and *Klf13*$^{-/-}$ P0 mice. Note the variable cardiac defects in the Klf13$^{-/-}$ neonates (D-L). AV: atrioventricular; VSD: ventricular septal defect; RA: right atrium.

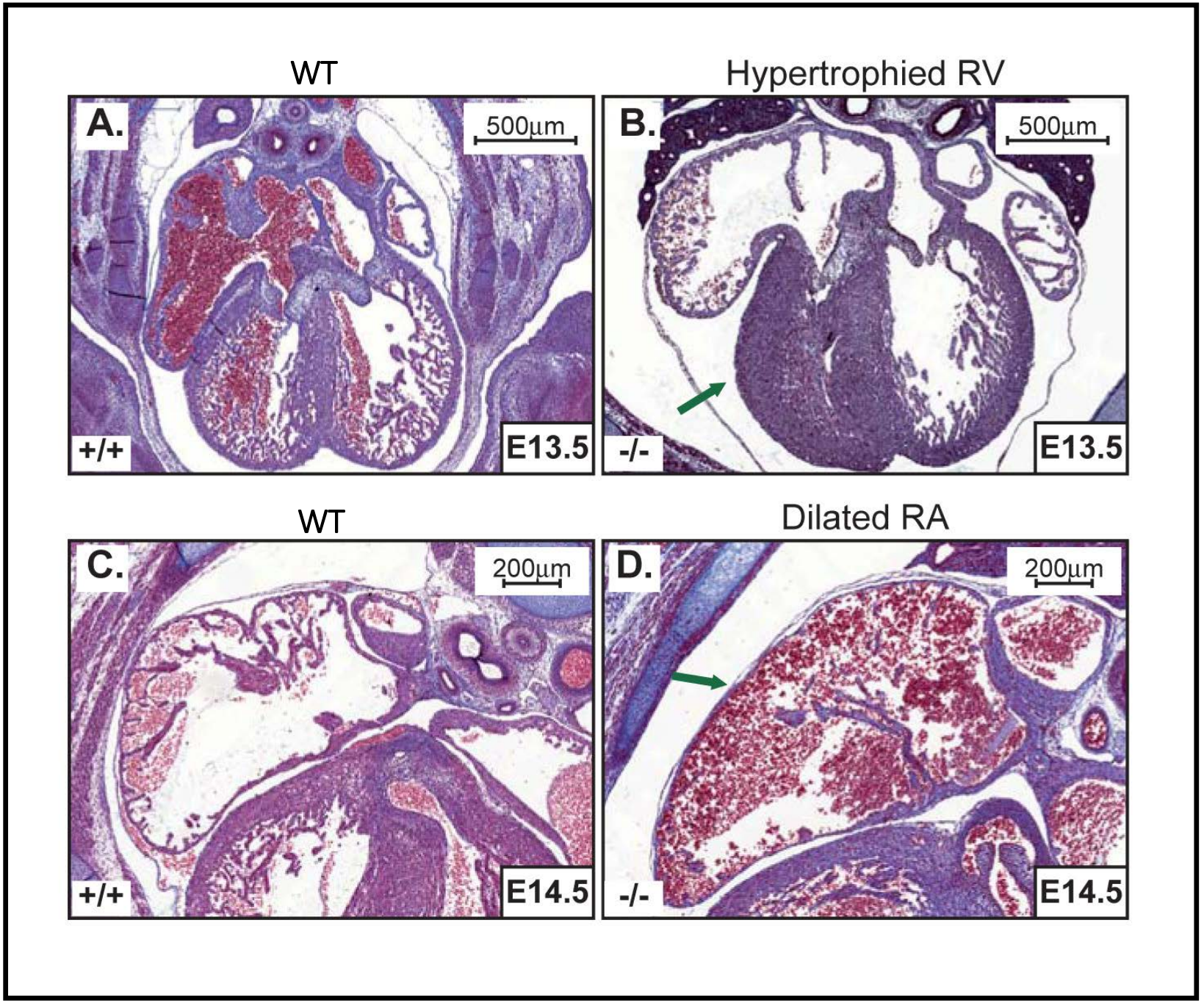
WT
Hypertrophied RV
A.
500µm
+/+
E13.5
B.
500µm
-/-
E13.5
WT
Dilated RA
C.
200µm
+/+
E14.5
D.
200µm
-/-
E14.5

Figure 2.5: Anatomical analysis of Klf13$^{+/+}$ and Klf13$^{-/-}$ at E13.5-14.5.

A-D Trichrome staining of frontal sections of Klf13$^{+/+}$ and Klf13$^{-/-}$ E13.5 (A-B) and E14.5 (C-D) embryos. Note the hypertrophied right ventricle (B) and the dilated right atria (D) in the knockout embryos.

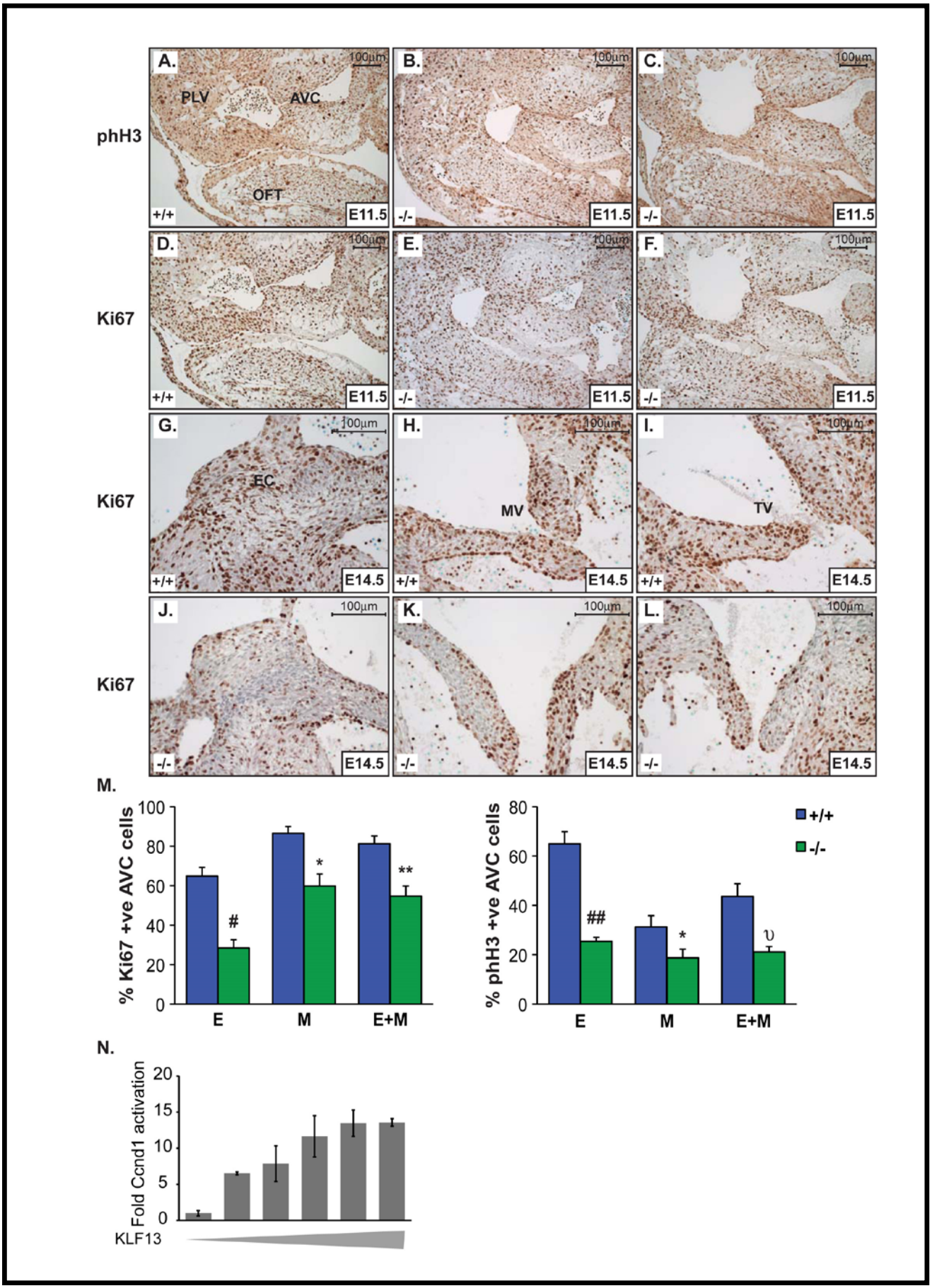
A.
B.
C.
D.
E.
F.
G.
H.
I.
J.
K.
L.
100μm
PLV
AVC
OFT
EC
MV
TV
phH3
Ki67
Ki67
Ki67
+/+
-/-
E11.5
E14.5
M.
% Ki67 +ve AVC cells
% phH3 +ve AVC cells
+/+
-/-
E
M
E+M
#
*
**
##
*
υ
N.
Fold Ccnd1 activation
KLF13

Figure 2.6: Reduced proliferation in the AVC of Klf13$^{-/-}$ embryos.

A-F Immunohistochemistry analysis of Ki67 and phH3 proliferation markers in E11.5 Klf13$^{+/+}$ and Klf13$^{-/-}$ mice. Note the reduced level of positive nuclei in the AVC of the knockout embryos (B-C and E-F). G-L Immunostaining of Ki67 on Klf13$^{+/+}$ and Klf13$^{-/-}$ embryos at E14.5. Note decreased staining in the EC (J), the mitral valve (K) and the tricuspid valve (L) of the knockout embryos. M. Percent of Ki67 and phH3 positive endocardial and mesenchymal cells in the AVC of E11.5 Klf13$^{+/+}$ and Klf13$^{-/-}$ embryos (n=3 for Wt; n=8 for KO). Note the significant decrease in the percent of proliferating mesenchymal and endocardial cells. N. Transient activation of *Ccnd1*-luciferase by increasing doses of KLF13 expression vector (25, 50, 100, 200, and 400ng).
* $p<0.05$; ** $p<0.01$; υ $p<0.001$; # $p<0.0005$; ## $p<0.0001$ vs. Klf13$^{+/+}$.PLV: primitive left ventricle; AVC: atrioventricular cushion; OFT: outflow tract; EC: endocardial cushion; MV: mitral valve; TV: tricuspid valve; E: endocardial; M: mesenchymal.

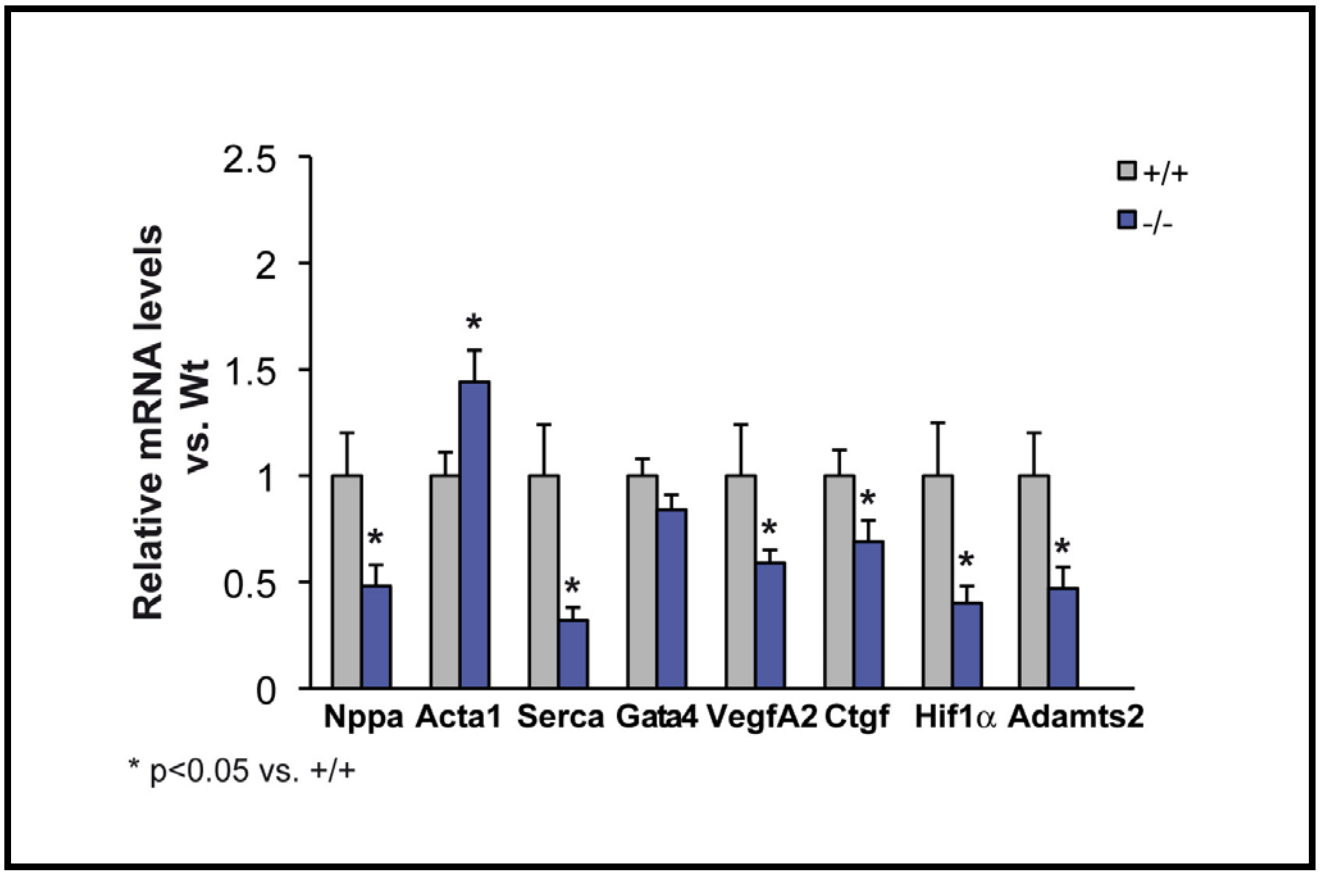
Relative mRNA levels vs. Wt
2.5
2
1.5
1
0.5
0
+/+
-/-
Nppa
Acta1
Serca
Gata4
VegfA2
Ctgf
Hif1α
Adamts2
* p<0.05 vs. +/+

Figure 2.7: Altered cardiac gene markers in Klf13$^{-/-}$ neonates.

QPCR analysis using RNA from heart tissue of P0 day old mice (n=5 for each group). Note the statistically significant change in the transcript levels of the analyzed markers in the knockout mice. *$p<0.05$ vs. Klf13$^{+/+}$.

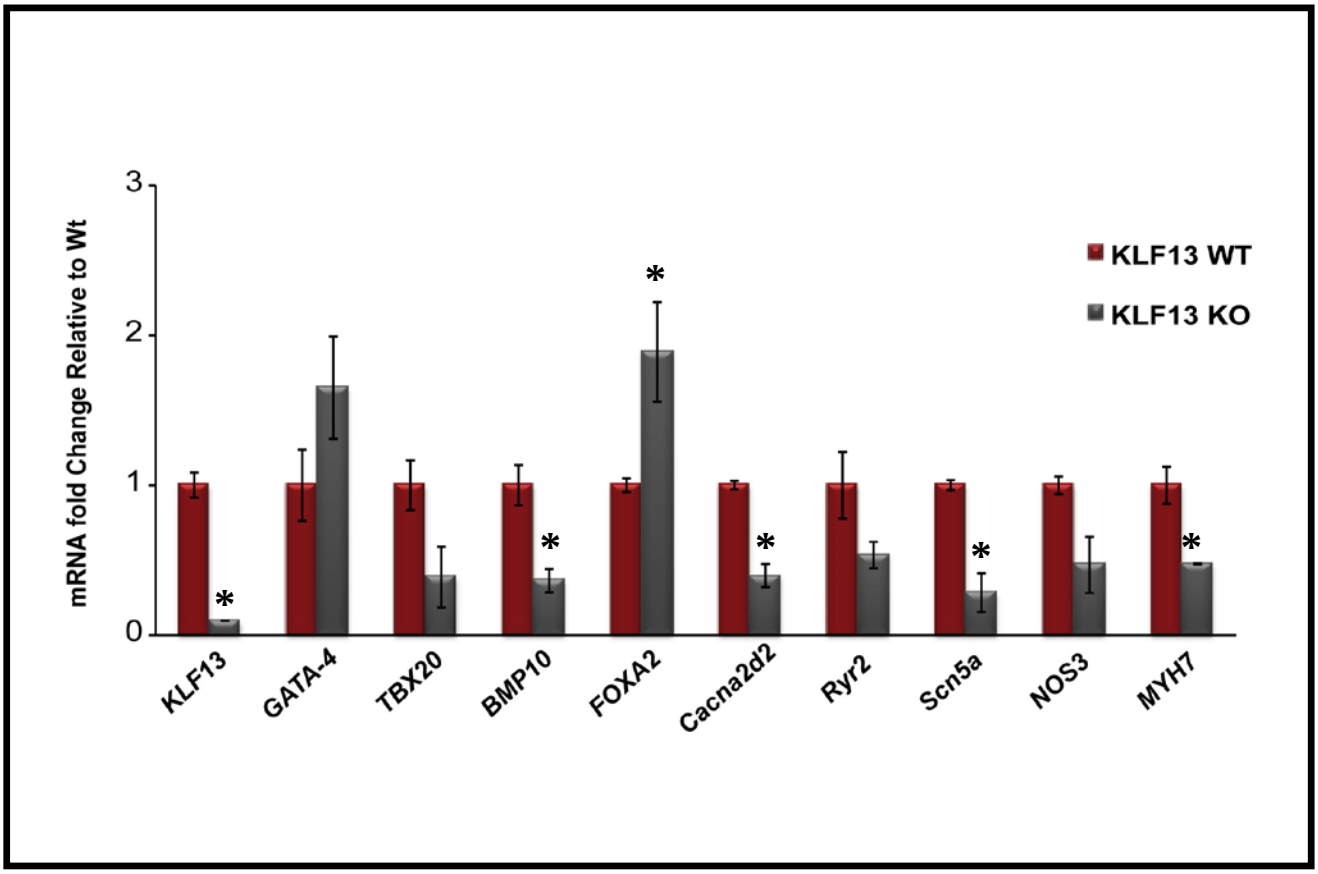
mRNA fold Change Relative to Wt
3
2
1
0
KLF13 WT
KLF13 KO
*
KLF13
GATA-4
TBX20
BMP10
FOXA2
Cacna2d2
Ryr2
Scn5a
NOS3
MYH7

Figure 2.8: Validation of a subset of RNA sequencing altered genes.

QPCR analysis using RNA from hearts of E11.5 wild type and knockout littermates. Note the statistically significant change in the transcript levels of the analyzed markers in the knockout mice. *$p<0.05$ vs. $Klf13^{+/+}$.

Table 2.1: Percentages of incidence of the indicated cardiac phenotypes in Klf13$^{-/-}$ P0 mice subdivided into myocardial and AVC defects. AVC: atrioventricular cushion. N=27.

	Defect	% of incidence
Myocardial defects	Thicker ventricular wall(s)	14.8%
	Hypertrophy of right atrium	3.7%
	Dilatation of RA	22.2%
	Dilatation of RV	7.4%
AVC defects	Thicker AV valves	22.2%
	AV type VSD	11.1%
	Goose-neck deformity	20%
	Normal	29.6%

Table 2.2: Subset of the EMT altered genes in RNA sequencing analysis on hearts from E11.5 wild type and Klf13$^{-/-}$ mice.

Gene	Fold change	P-value
Ccnd2, Ccnd3	0.43, 0.66	0.02, 0.047
Adamts6, Adamts9, Adamts14, Adamts15, Adamts17	0.3, 0.49, 0.42, 0.56, 0.44	0.008, 0.017, 0.03, 0.017, 0.012
Bmpr2	0.27	1.39E-06
Vcan	0.4	0.014
Erbb3, Erbb4	0.44, 0.2	0.035, 0.0006
Vegfc	1.65	0.04
Notch1, Notch2	0.4, 0.57	0.0004, 0.003

2.5. Discussion

In this study, we show that KLF13 is a novel regulator of the EMT and of endocardial cell proliferation. KLF13 is a member of the KLF family of DNA binding proteins that contain three Cys_2His_2 residues. The first evidence for their role in cardiovascular development came from gene disruption studies that revealed the essential role of KLF2 in blood vessel integrity (22). KLF2 was later reported to be important for vascular smooth muscle cell migration (23). Another KLF member, KLF5, was also detected in developing blood vessels albeit it plays a distinct role from that of KLF2 therein. $Klf5^{+/-}$ mice showed attenuated cardiac remodeling and decreased levels of arterial-wall thickening in response to external stress (24). Other KLF members involved in the heart include KLF10 and KLF15. Klf10 null mice developed signs of pathologic hypertrophy (25). KLF15 was reported to act as a negative regulator of cardiac hypertrophy and was later shown to inhibit smooth muscle cell proliferation; $Klf15^{-/-}$ mice had an exaggerated response to vascular damage (26,27).

An early report by Lavalleé *et al* showed that KLF13 is predominantly expressed in the developing mouse heart and knocking it down in *Xenopus* revealed its critical role in heart development (12). The Klf13 null embryos developed ventricular hypotrabeculation, atrial septal defects (ASDs) and delayed AV cushion formation pointing to KLF13 function in both the endocardium and the myocardium (12). In the present manuscript, we used mouse genetics to determine the role of KLF13 in the mammalian heart. $Klf13^{-/-}$ mice were viable; however, postnatal death was observed and the mice were obtained at almost half the expected Mendelian ratio. Dilatation of the right ventricle or hypertrophy of the left ventricular wall was seen in a subset of the surviving Klf13 null adult mice. PFO was observed in 35-45 % of the surviving knockout mice consistent with the *Xenopus* phenotype thus suggesting

evolutional conservation. It is important to note that this percentage as well as the severity of the PFO does not include the knockout mice that don't make it to adulthood. Increased aortic valve mean pressure gradient and left ventricular mass was also seen in 50-60% of the analyzed hearts. When examined at P0, myocardial and AV cushion defects were observed with variable penetrance; higher percentages were seen in the AV cushion defects. Among the AV cushion defects was "Goose-neck deformity." This is usually accompanied with anterior displacement of the aorta, non-membranous VSDs, and valvular defects (7-9), which were also seen in the analyzed hearts. One outcome of AV cushion defects is left ventricular outflow tract obstruction in the adults (28), which could explain the increased aortic valve mean pressure gradient observed in the surviving mutant mice. This in turn could lead to the ventricular hypertrophy seen in these mice. The complex process of cardiac cushion formation starts at E9.5 in the mouse and involves interaction between the myocardium and the endocardium. The presence of both myocardial and cardiac cushion defects in the Klf13 knockout hearts reflect cross talk between the endocardium and the myocardium. However, it could also point to a distinct role of KLF13 in both the myocardium and the endocardium.

Formation of the endocardial cushion starts with the deposition of extracellular matrix (ECM) components. This is then followed by EMT to cellularize the cushions, leading to their maturation and remodeling. Defective ECM organization has been linked to endocardial cushion defects. Various proteases, including the ADAMTS family of metalloproteases, are required for degradation of ECM molecules, a significant process for ventricular trabeculation and endocardial cushion maturation (29-31). Two ECM components that have been reported to be important for heart development include hyaluronan (HA) and versican. Versican is cleaved by matrix metalloproteinases (MMPs) and members of the ADAMTs family of metalloproteinases (29,30). Decreased Adamts2 and versican transcript levels were detected

in the hearts of Klf13 mutants suggesting an abnormal ECM and/ or EMT process. Other EMT markers, such as hypoxia inducible factor *Hif1α*, connective tissue growth factor *Ctgf* and vascular endothelial growth factor *Vegf* were also altered. Moreover, immunostaining for the proliferation markers Ki67 and phH3 showed decreased proliferation of both the endocardial and mesenchymal cells in the AVC of the KLF13 mutants; the proliferation of endocardial cells was more dramatically affected. Collectively, these results point to a novel role of KLF13 in the process of endocardial to mesenchymal transformation.

The natriuretic peptide genes, *Nppa* and *Nppb*, encoding ANF and BNP respectively, are known *in vitro* targets of Klf13 (12) and were down-regulated in the Klf13 null hearts. On the other hand, transcript levels of the cytoplasmic calcium pump, SERCA, were downregulated in the P0 mutant hearts suggesting cardiac stress. SERCA levels were, on the other hand, upregulated in the surviving adult Klf13 null hearts. Thus, the absence of KLF13 also has profound effects on adult heart homeostasis.

Altogether, these results point to KLF13 as a novel regulator of mammalian cardiac development and more specifically in the development of the AV cushion and in endocardial cell proliferation. Based on these data, it is tempting to speculate on the role of KLF13 as a novel congenital heart disease causing or modifier gene in humans.

Acknowledgments

We thank Megan Fortier, Nathalie Bouchard and Pierre Paradis as well as the histology core at the University of Ottawa for technical assistance. This work was funded by the Canadian Institutes of Health Research and RD is a recipient of the Canada Vanier and Ontario Graduate Scholarships.

2.6. References

1. Bruneau, B.G. (2008) The developmental genetics of congenital heart disease. *Nature*, **451**, 943-948.

2. Nemer, M. (2008) Genetic insights into normal and abnormal heart development. *Cardiovasc Pathol*, **17**, 48-54.

3. Rose, B.A., Force, T. and Wang, Y. (2010) Mitogen-activated protein kinase signaling in the heart: angels versus demons in a heart-breaking tale. *Physiol Rev*, **90**, 1507-1546.

4. Srivastava, D. (2006) Making or breaking the heart: from lineage determination to morphogenesis. *Cell*, **126**, 1037-1048.

5. Markwald, R.R., Fitzharris, T.P. and Manasek, F.J. (1977) Structural development of endocardial cushions. *Am J Anat*, **148**, 85-119.

6. Armstrong, E.J. and Bischoff, J. (2004) Heart valve development: endothelial cell signaling and differentiation. *Circ Res*, **95**, 459-470.

7. Blieden, L.C., Randall, P.A., Castaneda, A.R., Lucas, R.V., Jr. and Edwards, J.E. (1974) The "goose neck" of the endocardial cushion defect: anatomic basis. *Chest*, **65**, 13-17.

8. Towbin, R. and Schwartz, D. (1981) Endocardial cushion defects: embryology, anatomy, and angiography. *AJR Am J Roentgenol*, **136**, 157-162.

9. Ferguson, E.C., Krishnamurthy, R. and Oldham, S.A. (2007) Classic imaging signs of congenital cardiovascular abnormalities. *Radiographics*, **27**, 1323-1334.

10. Ransom, J. and Srivastava, D. (2007) The genetics of cardiac birth defects. *Semin Cell Dev Biol*, **18**, 132-139.

11. Zeigler, V.L. (2008) Congenital heart disease and genetics. *Crit Care Nurs Clin North Am*, **20**, 159-169, v.

12. Lavallee, G., Andelfinger, G., Nadeau, M., Lefebvre, C., Nemer, G., Horb, M.E. and Nemer, M. (2006) The Kruppel-like transcription factor KLF13 is a novel regulator of heart development. *EMBO J*, **25**, 5201-5213.

13. Kaczynski, J., Cook, T. and Urrutia, R. (2003) Sp1- and Kruppel-like transcription factors. *Genome Biol*, **4**, 206.

14. Bieker, J.J. (1996) Isolation, genomic structure, and expression of human erythroid Kruppel-like factor (EKLF). *DNA Cell Biol*, **15**, 347-352.

15. Dang, D.T., Pevsner, J. and Yang, V.W. (2000) The biology of the mammalian Kruppel-like family of transcription factors. *Int J Biochem Cell Biol*, **32**, 1103-1121.

16. Martin, K.M., Metcalfe, J.C. and Kemp, P.R. (2001) Expression of Klf9 and Klf13 in mouse development. *Mech Dev*, **103**, 149-151.

17. Nemer, G. and Nemer, M. (2003) Transcriptional activation of BMP-4 and regulation of mammalian organogenesis by GATA-4 and -6. *Dev Biol*, **254**, 131-148.

18. Georges, R., Nemer, G., Morin, M., Lefebvre, C. and Nemer, M. (2008) Distinct expression and function of alternatively spliced Tbx5 isoforms in cell growth and differentiation. *Mol Cell Biol*, **28**, 4052-4067.

19. Laforest, B., Andelfinger, G. and Nemer, M. (2011) Loss of Gata5 in mice leads to bicuspid aortic valve. *J Clin Invest*, **121**, 2876-2887.

20. Aries, A., Paradis, P., Lefebvre, C., Schwartz, R.J. and Nemer, M. (2004) Essential role of GATA-4 in cell survival and drug-induced cardiotoxicity. *Proc Natl Acad Sci U S A*, **101**, 6975-6980.

21. Debrus, S., Rahbani, L., Marttila, M., Delorme, B., Paradis, P. and Nemer, M. (2005) The zinc finger-only protein Zfp260 is a novel cardiac regulator and a nuclear effector of alpha1-adrenergic signaling. *Mol Cell Biol*, **25**, 8669-8682.

22. Kuo, C.T., Veselits, M.L., Barton, K.P., Lu, M.M., Clendenin, C. and Leiden, J.M. (1997) The LKLF transcription factor is required for normal tunica media formation and blood vessel stabilization during murine embryogenesis. *Genes Dev*, **11**, 2996-3006.

23. Wu, J., Bohanan, C.S., Neumann, J.C. and Lingrel, J.B. (2008) KLF2 transcription factor modulates blood vessel maturation through smooth muscle cell migration. *J Biol Chem*, **283**, 3942-3950.

24. Shindo, T., Manabe, I., Fukushima, Y., Tobe, K., Aizawa, K., Miyamoto, S., Kawai-Kowase, K., Moriyama, N., Imai, Y., Kawakami, H. *et al.* (2002) Kruppel-like zinc-finger transcription factor KLF5/BTEB2 is a target for angiotensin II signaling and an essential regulator of cardiovascular remodeling. *Nat Med*, **8**, 856-863.

25. Rajamannan, N.M., Subramaniam, M., Abraham, T.P., Vasile, V.C., Ackerman, M.J., Monroe, D.G., Chew, T.L. and Spelsberg, T.C. (2007) TGFbeta inducible early gene-1 (TIEG1) and cardiac hypertrophy: Discovery and characterization of a novel signaling pathway. *J Cell Biochem*, **100**, 315-325.

26. Fisch, S., Gray, S., Heymans, S., Haldar, S.M., Wang, B., Pfister, O., Cui, L., Kumar, A., Lin, Z., Sen-Banerjee, S. *et al.* (2007) Kruppel-like factor 15 is a regulator of cardiomyocyte hypertrophy. *Proc Natl Acad Sci U S A*, **104**, 7074-7079.

27. Lu, Y., Haldar, S., Croce, K., Wang, Y., Sakuma, M., Morooka, T., Wang, B., Jeyaraj, D., Gray, S.J., Simon, D.I. *et al.* (2010) Kruppel-like factor 15 regulates smooth muscle response to vascular injury--brief report. *Arterioscler Thromb Vasc Biol*, **30**, 1550-1552.

28. Bedard, E., Shore, D.F. and Gatzoulis, M.A. (2008) Adult congenital heart disease: a 2008 overview. *Br Med Bull*, **85**, 151-180.

29. Kern, C.B., Twal, W.O., Mjaatvedt, C.H., Fairey, S.E., Toole, B.P., Iruela-Arispe, M.L. and Argraves, W.S. (2006) Proteolytic cleavage of versican during cardiac cushion morphogenesis. *Dev Dyn*, **235**, 2238-2247.

30. Kern, C.B., Norris, R.A., Thompson, R.P., Argraves, W.S., Fairey, S.E., Reyes, L., Hoffman, S., Markwald, R.R. and Mjaatvedt, C.H. (2007) Versican proteolysis mediates myocardial regression during outflow tract development. *Dev Dyn*, **236**, 671-683.

31. Stankunas, K., Hang, C.T., Tsun, Z.Y., Chen, H., Lee, N.V., Wu, J.I., Shang, C., Bayle, J.H., Shou, W., Iruela-Arispe, M.L. *et al.* (2008) Endocardial Brg1 represses ADAMTS1 to maintain the microenvironment for myocardial morphogenesis. *Dev Cell*, **14**, 298-311.

3. Experimental Chapter Two

Alternate promoter usage produces two KLF13 isoforms with distinct functions

Rami Darwich[1,*], Hiba Komati, and Mona Nemer[1,*]

[1] Molecular Genetics and Cardiac Regeneration Laboratory, Department of Biochemistry, Microbiology and Immunology, University of Ottawa, Ottawa, K1H 8M5, Canada.
* To whom correspondence should be addressed. Tel: 1-613-562-5270; Fax: 1-613-562-5271; Email: mona.nemer@uottawa.ca

Contributions: In this chapter I have performed all the reported results. The chapter was written with the contribution of my supervisor.

3.1. Abstract.

KLF13, a member of the krüppel-like factor family is a dosage sensitive regulator of several biological processes including haematopoiesis and cardiogenesis. Dysregulated KLF13 expression is associated with congenital heart disease in human and in animal models. Unfortunately, the mechanisms regulating KLF13 levels or activity remain incompletely understood. Here we report that KLF13 exists as two isoforms with distinct spatiotemporal distribution and biochemical properties. Alternate promoter use resulting in distinct exon1 sequences is the mechanism responsible for the production of KLF13 proteins that share 2 of the 3 zinc finger domains but diverge in their N-terminal regions. Both isoform retain the ability to bind sequence specific DNA but differ in transcriptional activation of target promoters. Gain of function experiments in cardiac cells reveal that the two isoforms have overlapping as well as divergent gene targets likely reflecting differential interaction with other cardiac transcription factors. We identify NKX2.5 as a novel KLF13 co-activator and show that both KLF13a and b physically interact with NKX2.5, however only KLF13a has a strong synergistic interactions with NKX2.5 on the *Nppa* promoter. The results uncover a novel interaction between a member of the KLF family and a new homeobox containing protein that regulates transcriptional activity in cardiac and possibly other cells. They also reveal that KLF13 function can be modulated at the transcription level through the use of alternate promoters. This finding may help understand the phenotype manifestations of microdeletions involving the *KLF13* locus.

3.2. Introduction

The Krüppel-like transcription factor KLF13 is a member of the krüppel-like factors (KLFs), so named for their homology to the *Drosophila* segmentation gene product Krüppel (1-3). There are 18 distinct members of the KLF family in mammals; all are characterized by their three C-termini Cys2/His2 zinc-finger motifs that confer preferential binding to GC/GT rich sequences in gene promoters and enhancers in order to mediate activation and/or repression of transcription (1). The N-terminus region bestows the functional identity to each member of this family and its heterogeneity may explain in part the diverse biochemical mechanisms by which KLFs regulate transcription (4). Thus, differential interactions with a distinct repertoire of cofactors not only allow the various Sp/KLF members to regulate a distinct subset of genes, but also to participate in the divergent regulation of the same genes (4). For example, while KLF15 can inhibit the cardiac transcription factor GATA4 DNA-binding and transcriptional activity (5), KLF13 was shown to transactivate multiple cardiac promoters synergistically with GATA4 (6).

Although initially regarded as silencers of Sp1 transactivity, the KLF family has emerged as a critical regulator of a broad range of cellular processes including proliferation, apoptosis, differentiation, and organogenesis. For example, during the last decade, several reports have implicated KLF13 in multiple biological processes including cardiac development (6-8), haematopoietic development (9), establishment of uterine receptivity and implantation success (10), tumorigenesis of oral squamous cell carcinoma (11), and development of hereditary schizophrenia (12). In the heart, knocking-down KLF13 in *Xenopus* embryos leads to delayed cushion formation and valve maturation, septal defects, and hypotrabeculation, suggesting that KLF13 is important for amphibian heart morphogenesis (6). In human, heterozygous microdeletions and duplications of the

chromosomal band 15q13.3 (harboring *Klf13*) are associated with a wide range of cardiac defects that include Tetralogy of Fallot, mitral valve prolapse, and hypoplasia of the right side of the heart (7;13). In the circulatory system, KLF13 is involved in the development of B and T cells at multiple stages and the differential activation of macrophages and inflammation (9;14). In ovarian granulosa cells KLF13 functions as potent gonadal transregulator of genes encoding proteins that mediate sterol uptake and steroid biosynthesis (10;15). In oral cancer, KLF13 is overexpressed and is linked to the overexpression of several oncogenes including the chemotactic chemokine *CCL5* (RANTES) and the cell cycle regulator cyclin D1 *(*CCND1) (8;11). Biochemically, and similar to the well-known bi-functional EKLF subfamily (KLF1, KLF2, and KLF4), KLF13 can act as an activator or repressor of transcription depending upon the targeting promoters, the interacting proteins, and the cellular context. KLF13 is an activator of several promoters including *Hbg* (encoding human γ *globin), Nppa* (encoding the atrial natriuretic peptide ANP), *Nppb* (encoding the b-type natriuretic peptide BNP), SV40 (encoding the Simian virus 40), and adult smooth muscle SM22α promoters (6;16-18). KLF13 was also shown to repress promoters such as cytochrome P450 enzyme, *Cyp1a1* (18;19).

Given the biological importance of KLF13 in multiple physiological systems, understanding its regulation is of paramount importance. Several studies have addressed post-transcriptional KLF13 regulation. In T cells, the eukaryotic translation initiation factor eIF4E-dependent translation of KLF13, which is further regulated by ERK-1/2 and p38 MAP kinases, allows T cells to rapidly adjust RANTES expression in response to changes in the cellular environment (e.g, stress and/or growth factors) (223). In addition, microRNA-125a (miRNA-125a) has been reported to regulate a KLF13-dependent inflammatory response (20). Interestingly, oral squamous cell carcinoma (OSCC) cell lines are associated

with significantly elevated levels of KLF13 and substantially lower levels of miRNA-125b (11). Post-translationally, Song *et al* demonstrated that the coactivators p300/CREB-binding protein (CBP) and p300/CBP-associated factor (PCAF) act synergistically in stimulating KLF13 transcriptional activity indicating that both acetyltransferases are involved in KLF13 activation (21). In addition to acetylation, Huang *et al* reported that PRP4, a MAPK family member, phosphorylates KLF13 leading to increased nuclear localization and RANTES transcription in human T lymphocytes (22).

Little is known regarding transcriptional regulation of KLF13 including the possible existence of stage-specific promoters or even the presence of alternative transcription start sites (TSS) which can further contribute to fine tuning KLF13 levels and/or activity through differential regulation of mRNA production and/or the generation of protein isoforms with unique functions. In this respect, it is interesting to note that alternatively spliced isoforms of several KLF family members were recently reported (23) and two of them, KLF4 and KLF6, were analyzed for their isoforms distribution and biochemical properties (24;25). For example, while the wild-type KLF6 acts as a classic tumor suppressor, the splice isoform KLF6 SV1, which lacks a nuclear localization signal, displays a markedly opposite effect on cell proliferation, colony formation, and invasion (26). Similarly, while KLF4 is associated with tumor suppression, the cytoplasmic isoform KLF4α promotes cell cycle progression and *in vivo* tumour formation by decreasing the expression of the cyclin-dependent kinase inhibitors. We now report that KLF13 exists as 2 isoforms that are generated through the usage of alternative transcription start sites of the *Klf13* gene. The new isoform, KLF13b, lacks the entire N-terminal domain of KLF13a as well as the first zinc finger but can still bind KLF13 response elements. The 2 isoforms have distinct spatiotemporal distribution and transcriptional activities. Moreover, we identify

novel KLF13 coactivators and show that physical and functional interaction between KLF13 and different transcription factor families occurs through distinct protein domains some of which are absent in KLF13b. These results provide novel insight into KLF13 regulation and help to further elucidate its mechanisms of action in development and disease (24).

3.3. Material and Methods

Animals. Wildtype C57/B6 mice were utilized for tissue extraction. All animal experiments were carried out in accordance with institutional guidelines for animal care. Experiments were approved by the International Animal Care and Use Committee (IACUC) of the University of Ottawa, which conforms to that of the US National Institute of Health (NIH) (Assurance number for University of Ottawa: A5043-01). For euthanasia, CO_2 and cervical dislocation (CD) was used. CD without prior anesthesia is required for embryo collection in mice.

Cell Cultures. Primary cultures of cardiac myocytes were prepared from 4-day-old Sprague -Dawley rats as previously described (27). NIH3T3, AD293, TC13 cells, and HL-1 cells were maintained in culture and transfected as previously described (28-30). For transient transfections in 10 cm dishes, 10 µg DNA was used per dish; in the 24-well plates, the amount of luciferase-reporter was kept at 1.0 µg per well and the total amount of DNA was kept constant (usually 1.25 µg). After overnight incubation, the medium and precipitates were removed and replaced with fresh medium. At 48 h post-transfection, cells were harvested, lysed, and luciferase activity was assayed with a GloMax®-96 Microplate Luminometer. Atrial and ventricular cardiomyocyte primary cultures were prepared from 4- to 5-day-old Sprague-Dawley rats (Charles River) as previously described (32).

Plasmids. KLF13a, GATA4, NKX2.5 and PEX1 expression vectors were obtained by subcloning the amplified reverse transcription (RT)-PCR cDNA constructs into the CMV-driven pCGN vector in phase with the hemagglutinin (HA) epitope as previously described (6;31). Similarly KLF13b coding sequences were PCR amplified using a 5' oligonucleotide against the predicted exon1b and a 3' oligonucleotide spanning the stop codon in exon2 and the cDNA was cloned in the pCGN vector. Internal N- and C-terminal

KLF13 deletions were generated in the same pCGN vector using PCR-mediated mutagenesis. Mutant *Nppa* -luciferase and *Nppb*-luciferase constructs were generated using PCR-mediated mutagenesis utilizing the wild type *Nppa* and *Nppb* promoter constructs. All constructs were confirmed by sequencing. All other luciferase constructs were previously described (6;29;32-34).

Adenoviral Constructs. Two recombinant replication-deficient type 5 adenoviruses expressing Flag-tagged KLF13a and KLF13b were generated using the AdEasy XL Adenoviral Vector system (Stratagene). In summary, a 3XFlag-KLF13 construct was subcloned into a shuttle vector (pshuttle-CMV), and the adenovirus was generated through recombination with the pAdEasy-1. The cloning and production of adeno-LacZ and pShuttle controls were reported previously (27). The viruses were produced in bulk, and titers were determined as described (27). Cardiomyocytes were infected at a multiplicity of infection (MOI) of 1or 5 as indicated.

Protein analysis. Immunofluorescence microscopy on primary cardiomyocytes and AD293 were performed as previously described (30). Anti-HA antibody (Y-11 sc-805; Santa Cruz) was used at a dilution of 1/1000; anti-Flag antibody (M-2 2368; Cell Signaling) was used at a dilution of 1/1000; Ki67 (clone SP6 RM9106-S1; Thermo Scientific Medicorp.) was used at a dilution of 1/1000; phospho histone H3 (DAM1545035; Millipore) was used at a dilution of 1/1000. The coverslips were mounted onto cover slides using ProLong Gold antifade reagent (P36930, Invitrogen) and observed on Zeiss AxioObserver.D1 microscope. Slides were stored for up to 3 months at -20°C. For Ki67 and phospho histone H3 immunostatining an average of 10 random fields were counted per condition. Image J software was used to count the cells.

For Western blots, anti-HA, anti-flag, and anti-KLF13 (C-terminal C2C3 GTX104837; GeneTex) antibodies were used at a dilution of 1/1000 and revealed with peroxidase-tagged secondary antibodies. Co-immunoprecipitations and gel shift assays were performed as described before (6).

Electrophoretic mobility shift assays. Nuclear or whole-cell extracts from 293T cells overexpressing KLF13a, KLF13a deletion constructs, or KLF13b were used. Binding reactions were carried out at room temperature in the presence of 1 μg of poly(dI-dC). The probes used were double-stranded synthetic oligonucleotides containing wild-type or mutant CACCC elements of the rat BNP promoter (5'-ATAACCCCACCCCTACTC-3') that were radioactively end-labeled using [γ-32P] ATP by T4-polynucleotide kinase (T4-PK, New England BioLabs). The mixture was incubated at 37°C for 30 min in a binding buffer (1 μg of poly-(dI-dC)·(dI-dC) containing 10 mM HEPES pH 7.9, 1 mM MgCl2, 50 mM KCl, 1 mM DTT, 0.1 mM EDTA, 10 % glycerol, 0.025 % NP-40, 0.25 mM PMSF and 1 μM of aprotinin, leupeptin, and pepstatin. Reactions were carried out at room temperature for 20 minutes and protein-DNA complexes were separated by electrophoresis on 5 % polyacrylamide gel in 0.5 × Tris-borate-EDTA buffer (TBE) at +4 ºC. Nonlabelled double-stranded oligonucleotides were also used as specific (wild type) and non-specific (mutant) competitor DNAs.

RNA analysis. Total RNA was isolated from cardiomyocytes, wild type mouse tissue from a C57BL/6 genetic background, TC13 and HL-1 cells with TRIzol (Invitrogen). Reverse transcription was done using Omniscript RT kit (Qiagen). Semi-quantitative PCR and qPCR were carried out on 1:20 diluted cDNA. qPCR was conducted using Qiagen qPCR kits where DNA template and 300 nM oligonucleotides were used at an annealing temperature of 58 °C using the Quantitect SYBR Green PCR kit (Qiagen) in a Corbett Rotor-Gene™ 6000 machine (Qiagen). Primer sequences are available upon request.

Statistics. The data are presented as mean ± SEM; $p<0.05$ by student two-tailed *t*-test is considered statistically significant.

3.4 Results

3.4.1. The Klf13 gene produces two protein isoforms with distinct biochemical properties.

Using the ENSMBL database built on Human and Vertebrate Analysis and Annotation (HAVANA) manual curation, our *in silico* analysis of the *Klf13* gene in mouse (as well as in human and rat) revealed the possible existence of an alternative first exon (exon1b) within the large KLF13 intron. Since *exon1a* encodes the N-terminal domain of KLF13a as well as the first zinc-finger, alternate use of exon1b would generate a shorter isoform lacking these domains but containing the last two zinc fingers and a shorter new N-terminal domain (**Figure 3.1A**). Two pairs of oligonucleotides designed to span the splice junctions were utilized to assess the presence of the corresponding two Klf13 transcripts in different tissues during development. As shown in **Figure 3.1C**, *Klf13a* mRNA was detected at E11.5 in heart, lung, brain, limb, and liver whereas Klf13b transcripts were found in brain and lung tissues, but not in heart, limb, or liver tissues. As development proceeded, the ratio of *Klf13b/Klf13a* transcripts increased in all expressing tissues notably in the heart, brain, and limb. Interestingly, postnatal expression of the two isoforms was differentially regulated. For example, *Klf13a* transcripts (but not *Klf13b*) were upregulated in the brain, whereas both isoforms were re-expressed in the liver. Conversely, *Klf13b* transcripts showed a more robust expression in the kidney and liver then in the lung where they were barely detectable. No other intermediary bands were detected with either primer pairs. These results suggest the presence of two distinct *Klf13* transcripts derived from alternative first exons that maybe differentially used in a spatiotemporal manner during development.

To further confirm the presence of the alternate *Klf13b* transcript, we used primers corresponding to the 5' end of *exon1b* and the 3'end of the common *exon2* (which contains the stop codon and the 3'untranslated region) to amplify the entire *Klf13b* cDNA

from adult mouse heart. Isolated clones were sequenced and analysis of the DNA sequence perfectly matched the predicted exon usage. The cDNA was then sub cloned in a eukaryotic expression vector to produce an HA-epitope tagged protein of the expected molecular weight (16kD) as shown in **Figure 3.2A**. This recombinant protein retained the ability to bind the KLF13a binding site on the *Nppb* promoter as shown in **Figure 3.2B**. Immunocytochemical analysis revealed that, like KLF13a, KLF13b was mostly nuclear but diffuse cytoplasmic staining was also observed (**Figure 3.2C**). Of note, deletion of amino acids (AA) 1-195 of KLF13a, which are encoded by exon1a, also results in increased cytoplasmic localization. In contrast, deletion of AA1-147 which removes the N-terminal domain but keeps the three zinc fingers maintains the protein mostly in the nucleus. These results suggest that the first zinc finger, which is missing in KLF13b, contributes to the nucleo-cytoplasmic localization of KLF13a.

Next, we tested the ability of KLF13b to transactivate the *Nppb* promoter which is a known KLF13a target. Unlike KLF13a, increasing concentration of KLF13b failed to significantly activate the *Nppb*-luciferase reporter either alone or in presence of KLF13a (**Figure 3.2D** and **Figure 3-2F**). In fact, KLF13b dose dependently reduced KLF13a activation suggesting that, on this promoter, it acted to antagonize KLF13a (**Figure 3.2D)**. To test whether KLF13b was transcriptionally inactive, we co-transfected it with several other KLF13a target promoters. On a subgroup of promoters, which included those of Cyclind1/2 (*Ccnd1* and *Ccnd2*), KLF13b was unable to mediate transcriptional activation (**Figure 3.3 top row**). However, on another subgroup which included myosin heavy chains 6/7 (*Myh6* and *Myh7*), KLF13b activated transcription albeit at generally lower level than KLF13a (**Figure 3.3 bottom row**). Together with the tissue distribution, these results suggest that KLF13 isoforms may have distinct but also partially overlapping functions.

3.4.2. KLF13 isoforms have differential effects on cardiac cells.

Previously, we showed that the *Klf13* gene is expressed in both cardiomyocytes and endocardial cells of the heart (6). To assess the role of KLF13 isoforms on cardiomyocytes function and gene expression, we tested the effects of their gain of function on primary neonatal rat ventricular cardiomyocyte cultures. For this we generated two adenovirus vectors, each expressing one of the KLF13 isoforms (FLAG-tagged), and used them to infect primary cardiomyocytes isolated from 4-day neonatal rats. Infecting the myocytes at a multiplicity of infection (MOI) varying from 1-5 led to a significant increase in the corresponding mRNA and protein levels, as assessed by qPCR (**Figure 3.5A**) and Western blots (**Supplemental Figure 3.1**). Of note, KLF13a is the predominant isoform in these primary cultures. Mammalian cardiac myocytes rapidly divide during fetal life but have very minimal proliferative capacity soon after birth; during the post-natal stage of development, cardiomyocyte growth is accomplished essentially by cardiac hypertrophy and nuclear division (karyokinesis) without cell division (cytokinesis). The switch to hypertrophic growth occurs in about a week after birth in rodents (35). Postnatal upregulation of GATA4, which cooperates with KLF13a in heart development (6), leads to cytoskeletal reorganization and cardiomyocyte hypertrophy (33). Unlike with GATA4, no myofibrillar reorganization and/or cell hypertrophy were present in the KLF13a or KLF13b infected cells in comparison to LacZ infected control cells. Moreover, no changes in cell number or shape were detectable. To further analyze the effect of KLF13 isoforms on cardiomyocyte growth, we used immunofluorescence microscopy with alpha-actinin staining that identify cardiomyocytes and Ki67 staining to identify active nuclei. Quantitative analysis showed that Ki67-positive cardiomyocytes were increased in KLF13a infected cells, but not in KLF13b infected cells, as compared to the pShuttle control. Since

Ki67 marks cells that are active in all phase of the cell cycle - with the exception of G_0 phase, we also stained the cardiomyocytes with anti phosphohistone H3 (PHH3) antibody to evaluate cell division. No detectable change in PHH3 positive cardiomyocytes was found in KLF13 infected cardiomyocytes (**Figure 3.4B** and data not shown). The increase in Ki67 positive cardiomyocytes may be due to the significant increase in the transcript levels of cyclinD2 (*Ccnd2*) in KLF13a but not KLF13b infected cells (**Figure 3.4C**). QPCR analysis revealed that other transcripts were differentially affected by KLF13 isoforms including *Nppb* and *Myh6.* Interestingly, serum response factor (*Srf*), was similarly increased by both KLF13 isoforms. We conclude that neither KLF13 isoform has detectable effect on cardiomyocyte hypertrophy and that the two isoforms induce distinct changes in postnatal cardiac gene expression including cell cycle, contractile and hormone coding genes.

To gain further insight into the differential role of the two isoforms on embryonic-like cardiac cells, we analyzed KLF13 isoform gain of function in the endocardial progenitor cell line TC13 and the atrial myocyte immortalized cell line HL1, both of which express the *Klf13* gene. First, we tried to establish stable transfectants using retroviral infection but were not successful at obtaining cell lines overexpressing either isoform suggesting that cell growth may be inhibited by elevated levels of KLF13. We next tried infecting the cells with KLF13 isoforms encoding adenovirus and harvested the cells 8hrs post infection. This approach was successful at achieving transient overexpression of both isoforms as evident by QPCR and western analysis (**Figure 3.5 and Supplemental Figure 3.1)**. In HL1 atrial cardiomyocytes, both isoforms overexpression resulted in suppression of *Ccnd1*, *Ccnd2*, and *Nfatc1* transcripts and upregulation of *Nppa* and *Myh7*. Additionally, isoform specific effects were observed- for example KLF13a but not KLF13b

significantly decreased *Gata4* and *Gata5* transcripts whereas KLF13b but not KLF13a reduced *Tbx5* transcripts level by half. Lastly, as in primary cardiomyocytes, KLF13a gain of function induced *Vegfa* transcription (**Figure 3.5A)**. However, in TC13 cardiac progenitors, both isoforms induced *Vegfa* transcript levels and concomitantly decreased those of *Vegfr2* and *Gata4* mRNA levels and increased Twist transcripts (**Figure 3.5B).** Of all the genes tested, only *Nfatc1* expression was differentially regulated by KLF13a overexpression. Given that *Gata4* and *Vegfr2* signaling are critical for endothelial/endocardial proliferation, the results suggest that KLF13 gain of function disrupts normal proliferative pathways in these cells.

On the basis of the genes analyzed, and unlike primary cardiomyocytes, our data indicate a partial functional redundancy in the role of the two KLF13 isoforms in the transcriptional program of TC13 and HL-1 cells. Our results also reveal that KLF13 effects are promoter and cell context dependent likely reflecting differences in protein-protein interactions for the 2 isoforms.

3.4.3. Identification of two novel KLF13a specific co-activators.

Given the spatiotemporal co-expression of *Klf13* and *Nppa* in the atria, and our previous report showing that the *Nppa* promoter is activated by KLF13a (6), we selected this promoter to further analyze differential interaction of the two KLF13 isoforms with promoter bound transcription factors. The first 699bp of the *Nppa* promoter are rich in regulatory sequences and their analysis has provided key insight into the combinatorial interaction among cardiac transcription factors (31;36;37). **Figure 3.6A** depicts the known and evolutionary conserved regulatory elements within this region. First we tested the response of the *Nppa* promoter to the two KLF13 isoforms. Whereas KLF13a was able to

potently induce (up to 60 fold) transcription of the *Nppa*-Luciferase reporter, the maximal response to KLF13b was a modest 5 fold activation (**Figure 3.6B**). Fine mapping of KLF13 response elements, using deletion analysis, suggested the presence of at least three regions that contribute to the maximal response (**Figure 3.6C**). Importantly, the proximal promoter which contains, among other, conserved GATA, NKX2.5 and PEX1 (also termed ZFP260) binding sites was activated over 20 fold by KLF13a. Given that PEX1 and NKX2.5 are also enriched in the atrial cardiomyocytes we tested for the existence of cooperative interaction between these factors and KLF13. Co-transfections of KLF13a with increasing dose of NKX2.5 or PEX1 resulted in a significant 3-fold synergy in transcriptional activation (**Figure 3.6D**). Interestingly, KLF13b was unable to support significant synergy with either proteins. Synergy with GATA4 was carried out as control; consistent with previous reports, KLF13a further enhanced GATA4 dependent transcription (**Figure 3.6D**). Pull-down analysis indicated that KLF13a directly interacts with both NKX2.5 and PEX1 (**Figure 3.6E**).

To further elucidate the molecular basis for the differential effects of KLF13a and KLF13b on NKX2.5 dependent transcriptional activation, we carried out a structure-function analysis to determine the KLF13 domains required for physical and functional interaction with NKX2.5. Various KLF13 deletion constructs were generated and sequenced, and all were tested for protein expression using western analysis, nuclear localization using immunofluorescence microscopy, and DNA binding using electromobility gel shift analysis (**Supplemental Figure 3.2).** When the KLF13 mutant proteins were tested in pull-down assays, removal of the last two zinc fingers but not removal of the N- or C-terminal domains interfered with the physical interaction with NKX2.5. In fact the last two zinc fingers (ZF2 and ZF3), maintained the capacity to bind to NKX2.5. Consistent with

this, KLF13b was as efficiently pulled down as KLF13a by NKX2.5 (**Figure 3.7A**). KLF13 contacted NKX2.5 via its homeodomain which was sufficient to pull-down KLF13 (**Figure 3.7B**). Next we tested which KLF13 domains were required for synergistic interaction with NKX2.5 and the other cardiac transcription factors. Analysis of the various KLF13 deletion constructs using either *Nppa* or the minimal *Nppb* promoters revealed the presence of three transactivation domains (TAD) in KLF13a; two within the N-terminal domain (TAD1: AA1-67 and TAD2:AA67-147) and one in the C-terminal (TAD3) at AA 250-288. Of these, only the C-terminal TAD is present in KLF13b (**Figure 3.7C)**. The various mutants were then tested for their ability to synergize with GATA4, PEX1 or NKX2.5. Maximal synergy with GATA4 required all KLF13 TADs and removal of either TAD2 or TAD3 reduced synergy by half whereas deletion of TAD1 decreased synergy by 33% (**Figure 3.7D).** Interestingly, KLF13b retained the ability to potentiate GATA4 activation albeit to half the extent of KLF13a. In the case of NKX2.5, removal of TAD3 significantly enhanced synergy whereas removal of TAD1 and TAD2 abrogated it; not surprisingly, KLF13b was unable to support synergy with NKX2.5 (**Figure 3.7E).** Lastly, functional cooperativity with PEX1 was most dependent on TAD1 and its deletion reduced synergy to 1.5 fold vs 5.5 fold for intact KLF13a protein. Interestingly TAD3 contributed to maximal synergy and its deletion reduced synergy by 30%; the presence of TAD3 in KLF13b likely contributed to the modest but significant 1.5 fold synergy with PEX1. These results indicate that the various domains of KLF13 differentially contribute to its combinatorial interactions with other transcription factors and provide a mechanism that explains –at least in part- the distinct effects of the two isoforms on gene transcription and cell fates.

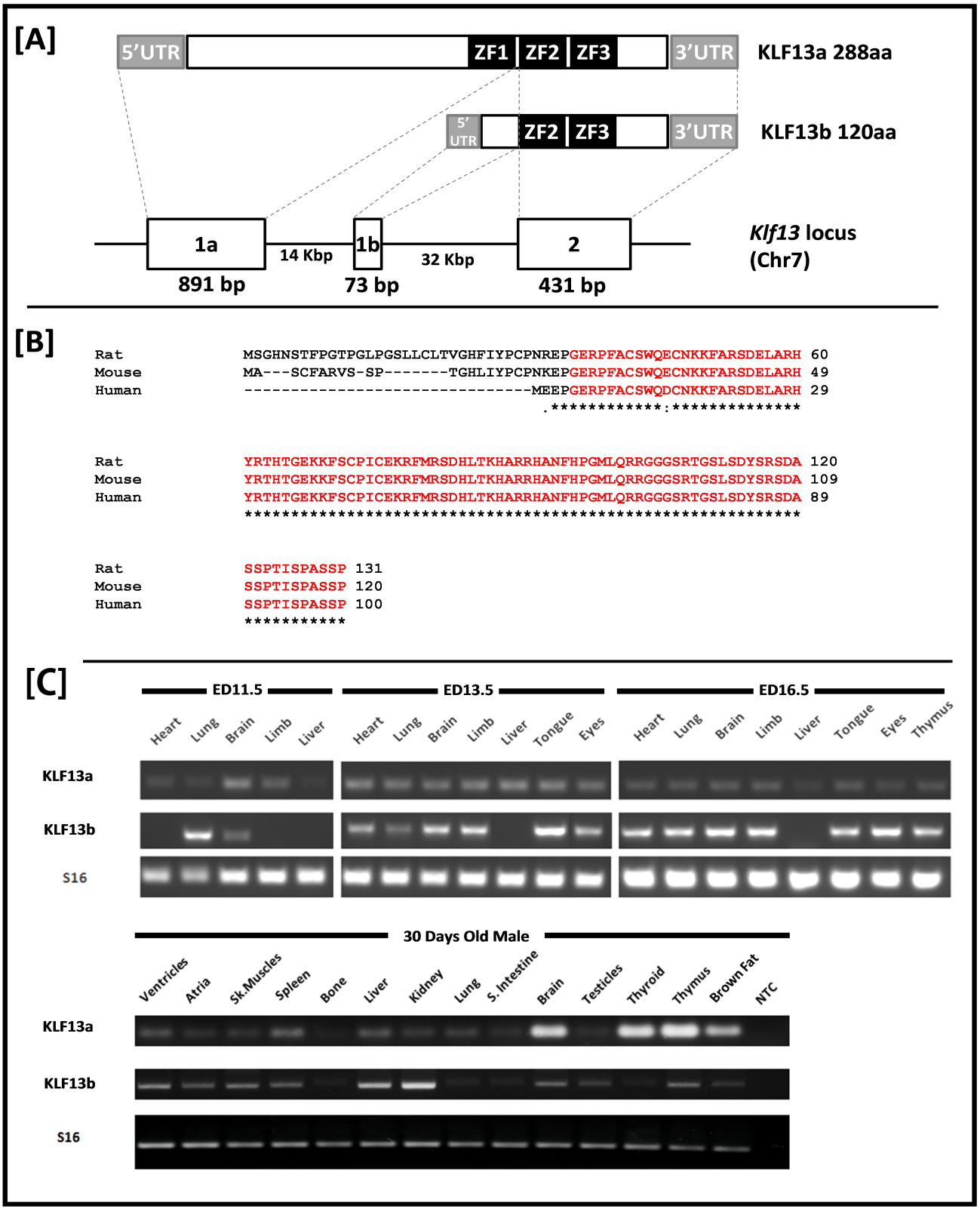
[A]
5'UTR
ZF1
ZF2
ZF3
3'UTR
KLF13a 288aa
5' UTR
ZF2
ZF3
3'UTR
KLF13b 120aa
1a
14 Kbp
1b
32 Kbp
2
Klf13 locus (Chr7)
891 bp
73 bp
431 bp
[B]
Rat MSGHNSTFPGTPGLPGSLLCLTVGHFIYPCPNREPGERPFACSWQECNKKFARSDELARH 60
Mouse MA---SCFARVS-SP-------TGHLIYPCPNKEPGERPFACSWQECNKKFARSDELARH 49
Human ------------------------------MEEPGERPFACSWQDCNKKFARSDELARH 29
.************:**************
Rat YRTHTGEKKFSCPICEKRFMRSDHLTKHARRHANFHPGMLQRRGGGSRTGSLSDYSRSDA 120
Mouse YRTHTGEKKFSCPICEKRFMRSDHLTKHARRHANFHPGMLQRRGGGSRTGSLSDYSRSDA 109
Human YRTHTGEKKFSCPICEKRFMRSDHLTKHARRHANFHPGMLQRRGGGSRTGSLSDYSRSDA 89
****
Rat SSPTISPASSP 131
Mouse SSPTISPASSP 120
Human SSPTISPASSP 100
****
[C]
ED11.5
ED13.5
ED16.5
Heart Lung Brain Limb Liver
Heart Lung Brain Limb Liver Tongue Eyes
Heart Lung Brain Limb Liver Tongue Eyes Thymus
KLF13a
KLF13b
S16
30 Days Old Male
Ventricles Atria Sk.Muscles Spleen Bone Liver Kidney Lung S. Intestine Brain Testicles Thyroid Thymus Brown Fat NTC
KLF13a
KLF13b
S16

Figure 3.1: KLF13 exists as 2 distinct isoforms.

A) Schematic representation of the *Klf13* locus. This organization is conserved across species. When exon1a. encoding the transactivation domain and the N-terminal zinc-finger, is used, the 288AA KLF13a isoform is generated; when the alternative exon1b is used, it generates KLF13b an isoform with only two C2H2-type zinc-fingers and a novel short N-terminal. B) Multiple sequence alignment (ClustalW) of KLF13b isoforms from different species. An * (asterisk) indicates positions which have a single, fully conserved residue; a : (colon) indicates conservation between groups of strongly similar properties; a . (period) indicates conservation between groups of weakly similar properties. C) RT-PCR carried out using primers specific to each of the isoforms in different tissues during development (E 11.5, 13.5, and 16.5).

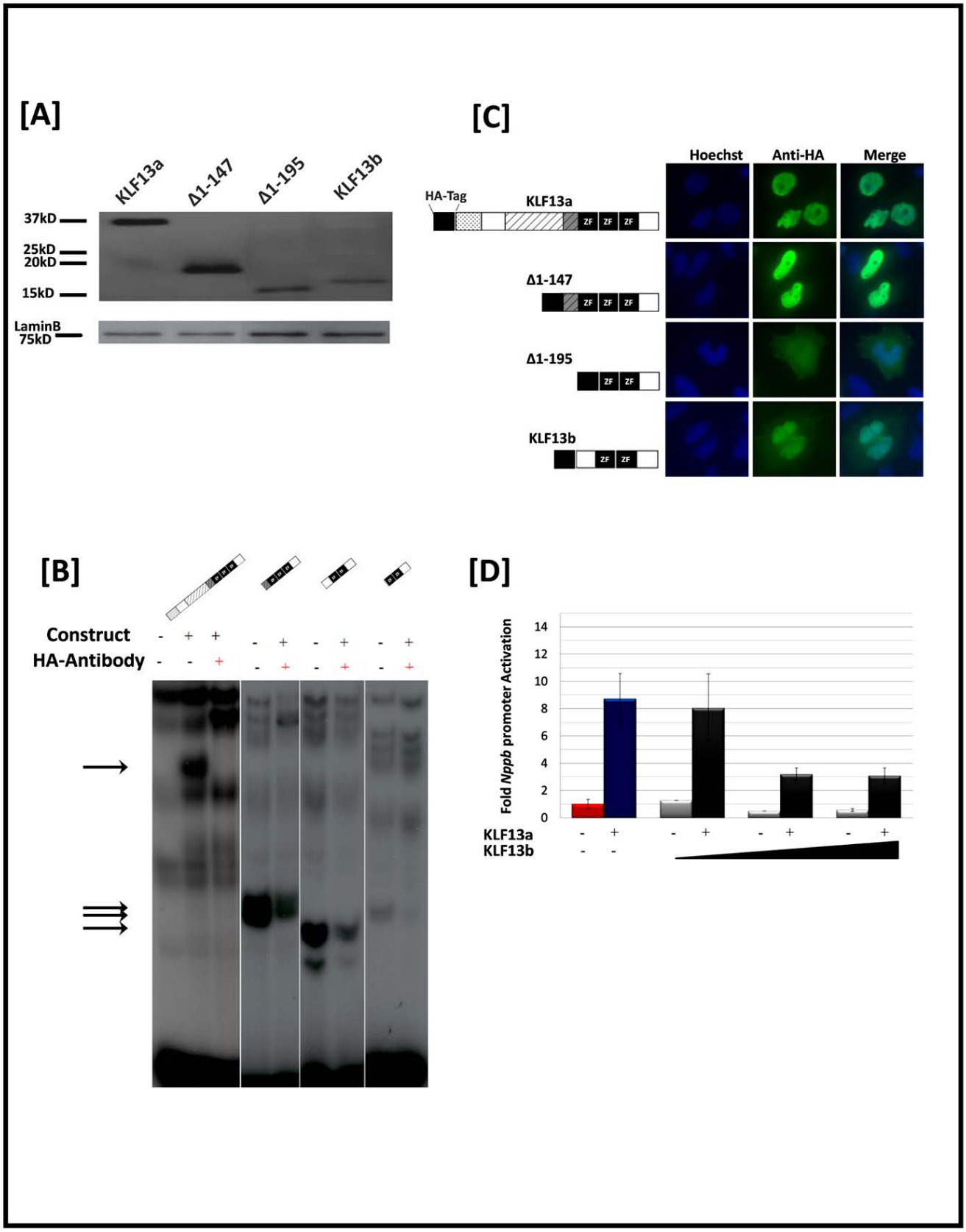
[A]
KLF13a
Δ1-147
Δ1-195
KLF13b
37kD
25kD
20kD
15kD
LaminB
75kD
[C]
Hoechst
Anti-HA
Merge
HA-Tag
KLF13a
ZF ZF ZF
Δ1-147
ZF ZF ZF
Δ1-195
ZF ZF
KLF13b
ZF ZF
[B]
Construct
HA-Antibody
[D]
Fold Nppb promoter Activation
14
12
10
8
6
4
2
0
KLF13a
KLF13b

Figure 3.2: Distinct biochemical properties of the two KLF13 isoforms

A) Western blot using anti HA antibody showing expression of recombinant HA tagged KLF13 isoforms (KLF13a and KLF13b) as well as deletion constructs (Δ1-147 and Δ1-195) in transfected AD293 cell nuclear extracts. B) KLF13b is capable of binding sequence specific DNA. Electrophoretic mobility shift assays (EMSA) of several HA-tagged KLF13 constructs as indicated above the corresponding lanes. The DNA probe utilized is derived from the proximal CACCC element of the *Nppb* promoter. The radioactive probes were incubated with either the nuclear extract of control or KLF13 transfected AD293 cells. The arrowheads shows the binding of the different KLF13 constructs to the radioactive probes. Note that antibody super-shift/band disappearance confirms the identity of the KLF13 containing bands. The arrows represent protein-DNA complexes of different sizes which are due to size differentials of the utilized KLF13 constructs. C) Immunofluorescence localization of the HA-tagged KLF13 recombinant proteins transfected into cells. The green color shows the Alexa 488 conjugated secondary antibodies against the anti-HA antibody. The nuclei are blue as visualized with Hoechst 33424 autofluorescence. D) KLF13b antagonizes KLF13a transcriptional activity on the -120bp *Nppb* minimal promoter. The study was conducted with a constant dose of (50ng) for KLF13a and different doses of the KLF13b (25ng, 50ng and 75ng). The data are the mean of n=3±SEM.

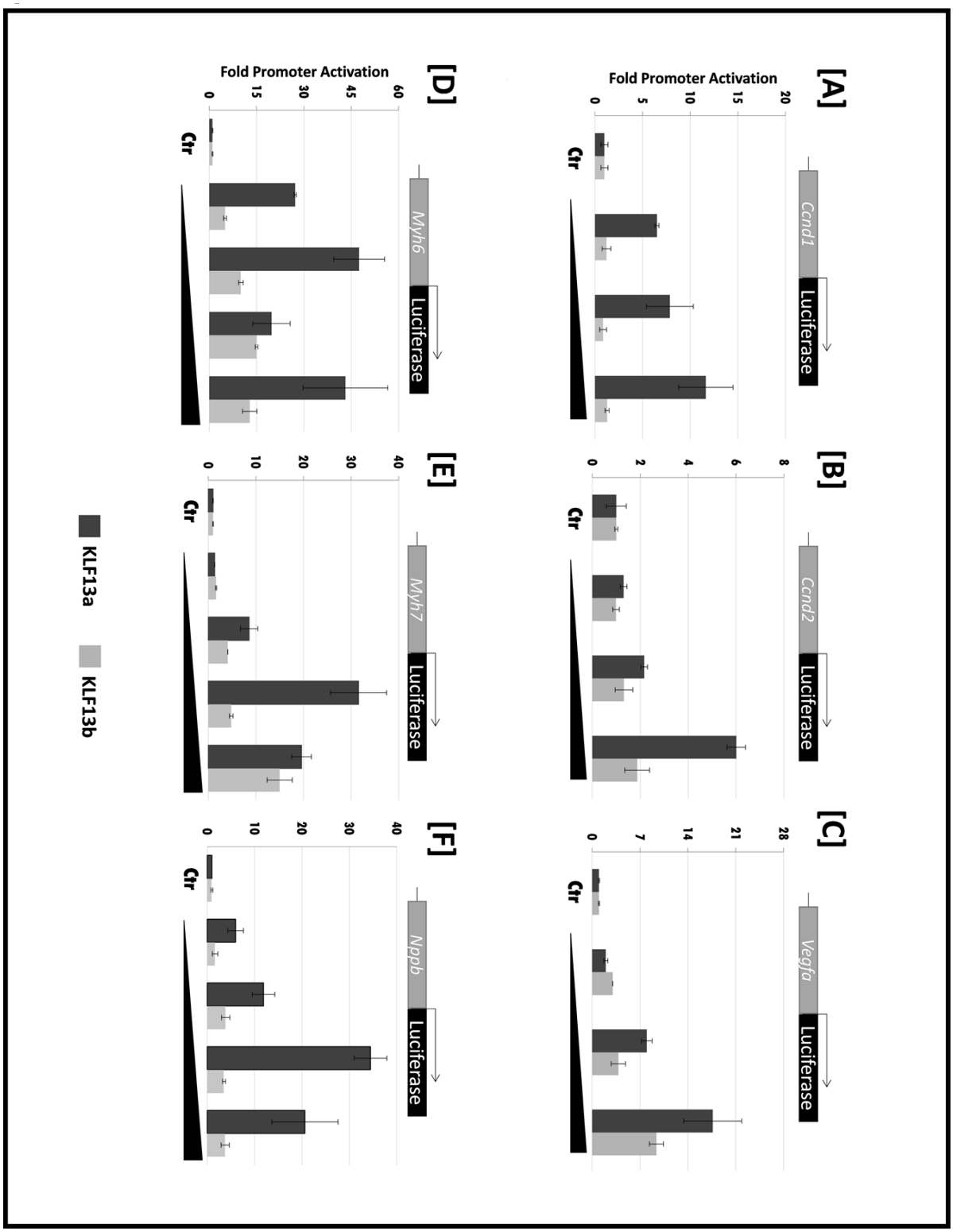
[A]
Ccnd1
Luciferase
Fold Promoter Activation
Ctr
[B]
Ccnd2
Luciferase
[C]
Vegfa
Luciferase
[D]
Myh6
Luciferase
[E]
Myh7
Luciferase
[F]
Nppb
Luciferase
KLF13a
KLF13b

Figure 3.3: Analysis of KLF13 isoforms transcriptional activity on different cardiac promoters.

Transfections were carried out in NIH 3T3 with increasing doses of KLF13 isoforms. In panels A-C we used 25, 50, or 100ng, and in panels D-F we used 25, 50, 100, or 250g. Note that the total amount of DNA was kept constant (2500ng) using an empty pCGN vector. Fold promoter activity was expressed as the fold change relative to the control. The data shown are from one representative experiment carried out in duplicate. Ccnd1: cyclinD1 promoter, Ccnd2: CycinD2 promoter, Myh6: α-Myosin heavy chain promoter, Myh7: β-Myosin heavy chain promoter, Nppb: BNP promoter,

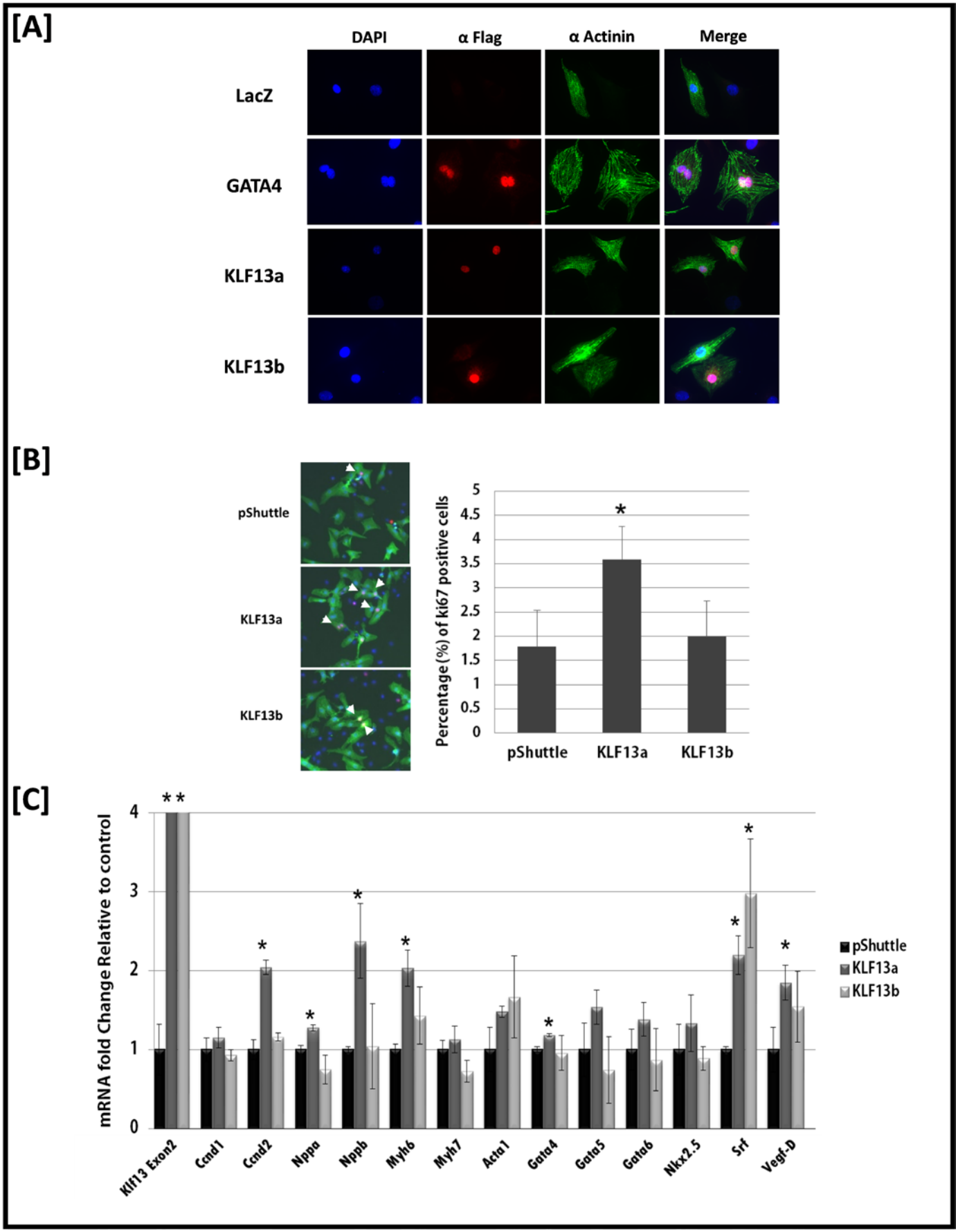
[A]
DAPI
α Flag
α Actinin
Merge
LacZ
GATA4
KLF13a
KLF13b
[B]
pShuttle
KLF13a
KLF13b
Percentage (%) of ki67 positive cells
5
4.5
4
3.5
3
2.5
2
1.5
1
0.5
0
pShuttle
KLF13a
KLF13b
[C]
mRNA fold Change Relative to control
4
3
2
1
0
Klf13 Exon2
Ccnd1
Ccnd2
Nppa
Nppb
Myh6
Myh7
Acta1
Gata4
Gata5
Gata6
Nkx2.5
Srf
Vegf-D
pShuttle
KLF13a
KLF13b

Figure 3.4: Gain of KLF13 function in postnatal cardiomyocytes.

A) Fluorescence microscopy of cardiomyocytes infected with Flag-tagged KLF13a, KLF13b, GATA4 or LacZ adenoviral vectors. Exogenous KLF13 isoforms and GATA4 were detected using anti-Flag antibody (red). The nuclei were visualized by Hoechst 33424 autofluorescence (blue) and the cardiomyocytes were visualized with anti-alpha-actin in antibody (green). Note how only GATA4 induces cytoskeletal reorganization of cardiomyocytes. B) Ki67 staining of of cardiomyocytes infected with Flag-tagged KLF13a, KLF13b, or pShuttle adenoviral vectors. The left panel shows representative fields with Ki67 positive (red) cardiomyoctes. Indicated by arrowheads, the nuclei a blue and the cardiomyocytes (green) marked by alpha-actin in staining. The right panel represents the data quantification for the different infected groups (n=5 for each group). *$p<0.05$. C) QPCR analysis using RNA extracted from primary rat neonatal cardiomyocyte cultures infected with Flag-tagged KLF13a, KLF13b, or pShuttle adenoviral vectors (n=3 for each group). *$p<0.05$.

[A]

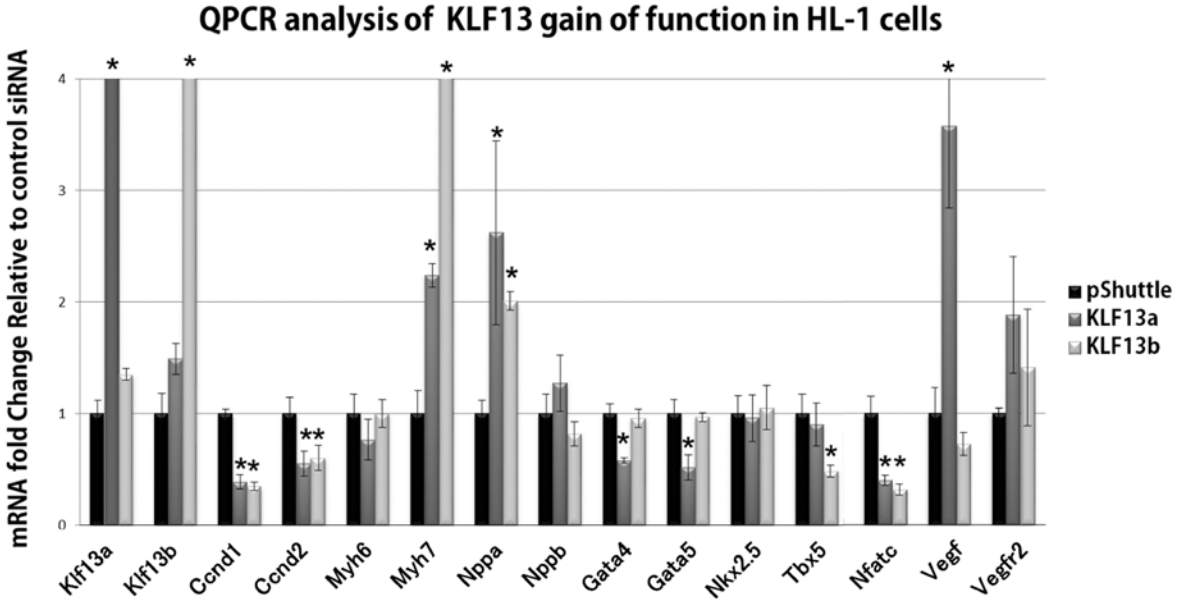
QPCR analysis of KLF13 gain of function in HL-1 cells
mRNA fold Change Relative to control siRNA
0
1
2
3
4
Klf13a
Klf13b
Ccnd1
Ccnd2
Myh6
Myh7
Nppa
Nppb
Gata4
Gata5
Nkx2.5
Tbx5
Nfatc
Vegf
Vegfr2
pShuttle
KLF13a
KLF13b

[B]

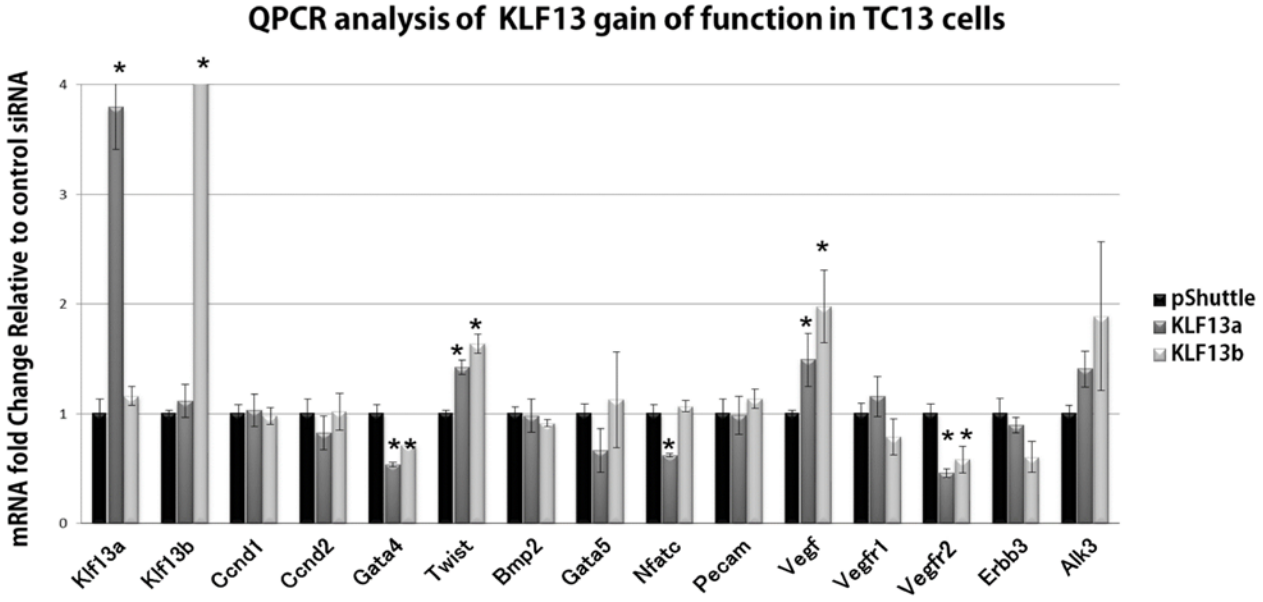
QPCR analysis of KLF13 gain of function in TC13 cells
mRNA fold Change Relative to control siRNA
0
1
2
3
4
Klf13a
Klf13b
Ccnd1
Ccnd2
Gata4
Twist
Bmp2
Gata5
Nfatc
Pecam
Vegf
Vegfr1
Vegfr2
Erbb3
Alk3
pShuttle
KLF13a
KLF13b

Figure 3.5: KLF13 isoforms activate distinct gene programs in cardiac cells.

QPCR analysis using RNA extracted from endocardial progenitor (TC13) cells (panel A) and atrial cardiomyocytes (HL-1) cells (panel B) infected with Flag-tagged KLF13a, KLF13b, or pShuttle adenoviral vectors ($n \geq 3$ for each group). *$p < 0.05$.

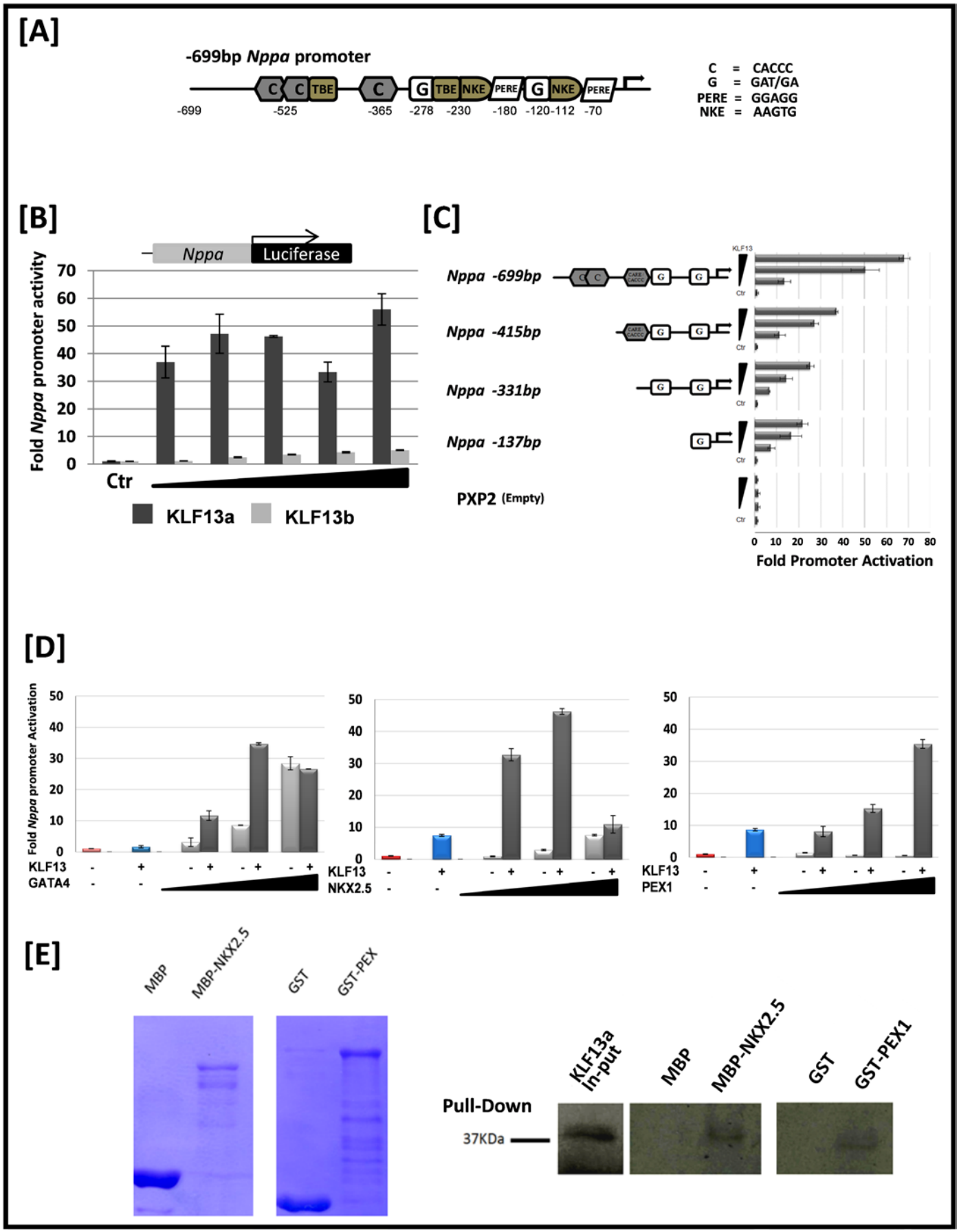
[A]
-699bp Nppa promoter
C TBE C G TBE NKE PERE G NKE PERE
-699 -525 -365 -278 -230 -180 -120-112 -70
C = CACCC
G = GAT/GA
PERE = GGAGG
NKE = AAGTG
[B]
Nppa
Luciferase
Fold Nppa promoter activity
70 60 50 40 30 20 10 0
Ctr
KLF13a
KLF13b
[C]
KLF13
Nppa -699bp
Nppa -415bp
Nppa -331bp
Nppa -137bp
PXP2 (Empty)
Ctr
0 10 20 30 40 50 60 70 80
Fold Promoter Activation
[D]
Fold Nppa promoter Activation
50 40 30 20 10 0
KLF13
GATA4
KLF13
NKX2.5
KLF13
PEX1
[E]
MBP
MBP-NKX2.5
GST
GST-PEX
Pull-Down
37KDa
KLF13a in-put
MBP
MBP-NKX2.5
GST
GST-PEX1

Figure 3.6: KLF13 isoforms differentially interact with novel co-activators.

A) Representation of the -699bp *Nppa* promoter showing known regulatory elements. CA/GT boxes are also shown. C is KLF CACCC binding sites, TBE is T-Box element, NKE is the NKX element, G is GATA element, and PERE is for Phenylephrine Response element. B) The transcriptional activity of the 2 KLF13 isoforms on the -699 bp *Nppa* promoter in NIH 3T3 cells. Increasing doses of KLF13 isoforms were used (25ng, 50ng, and 100ng). Note how only KLF13a activates the *Nppa* promoter. C) Transient co-transfections map several KLF13 response regions within the -699bp *Nppa* promoter. The different doses of KLF13 used were 25ng, 50ng, and 100ng. The data shown is from on representative out of three different experiments, each carried out in triplicates. D) KLF13 activates the *Nppa* promoter synergistically with GATA4, NKX2.5, and PEX1. Cells were transfected 2ug of -699bp *Nppa* promoter and a constant dose of KLF13 (either 50ng or 100ng), together with increasing doses of the indicated transcription factors (25ng, 50ng, and 100ng). E) KLF13 physically interacts with GATA4, NKX2.5 and PEX. The pull-down assay was performed using in vitro-translated ^{35}S-labeled-KLF13 and bacterially produced fusion proteins MBP-NKX2.5 and GST-PEX1. The left panel is the coomassie blue staining of SDS-PAGE gel showing the bacterially produced fusion proteins. Note how KLF13 is retained by MBP-NKX2.5, and GST-PEX1 but not on the control MBP and GST.

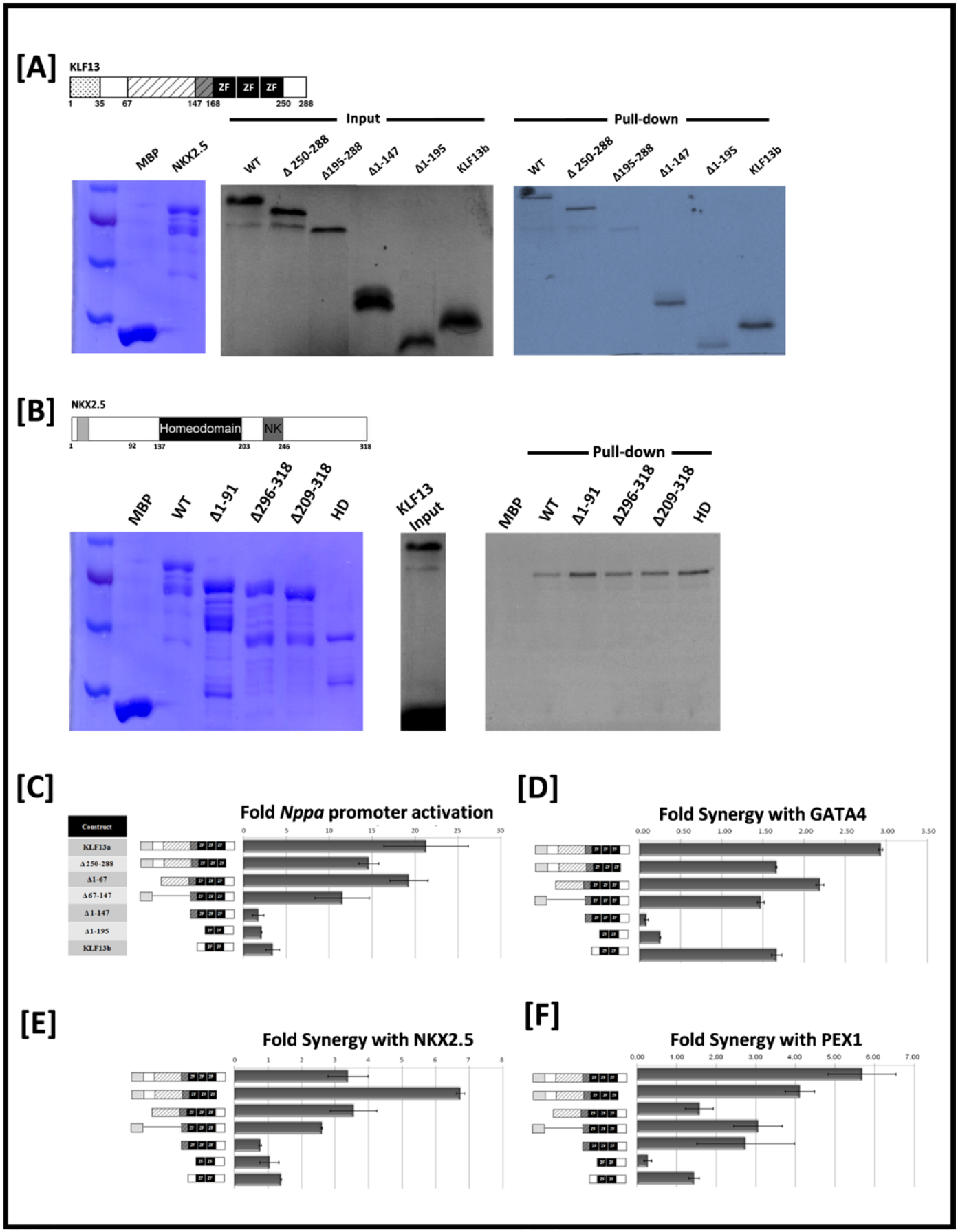
[A]
KLF13
ZF
ZF
ZF
1
35
67
147
168
250
288
Input
Pull-down
MBP
NKX2.5
WT
Δ 250-288
Δ195-288
Δ1-147
Δ1-195
KLF13b
[B]
NKX2.5
Homeodomain
NK
1
92
137
203
246
318
Pull-down
MBP
WT
Δ1-91
Δ296-318
Δ209-318
HD
KLF13 Input
[C]
Fold Nppa promoter activation
Construct
KLF13a
Δ250-288
Δ1-67
Δ67-147
Δ1-147
Δ1-195
KLF13b
[D]
Fold Synergy with GATA4
[E]
Fold Synergy with NKX2.5
[F]
Fold Synergy with PEX1

Figure 3.7: Mapping functional KLF13 domains involved in transcriptional activation and synergy.

A) The zinc finger domain of KLF13 is involved in physical interaction with NKX2.5. Note how Δ1-195 and KLF13b were retained by MBP-NKX2.5. B) The homeodomain (HD) of NKX2.5 is required for physical interaction with KLF13. In A and B, pull-down assays were performed using bacterially produced MBP-NKX2.5 constructs and in vitro-translated ^{35}S-labeled-KLF13 protein. In each case, the left panel is the coomassie blue staining of the SDS-PAGE gel showing the bacterially produced MBP-fusion constructs. Note how KLF13 was retained efficiently by MBP-HD (AA137-203). C, D , E an F) Structure-function analysis of KLF13 domains involved in transcriptional activation as well as synergy with GATA-4, NKX2.5, and PEX1 over the *Nppa* promoter. In (C), *Nppa* reporter was co-transfected with KLF13 expression vectors alone or in (D, E and F), in combination with GATA-4, NKX2.5, or PEX1 expression vectors, respectively. The fold synergy is calculated using the ratio of promoter activation by KLF13 in the presence of its functional partner over the sum of the individual promoter activation by KLF13 plus that of its partner.

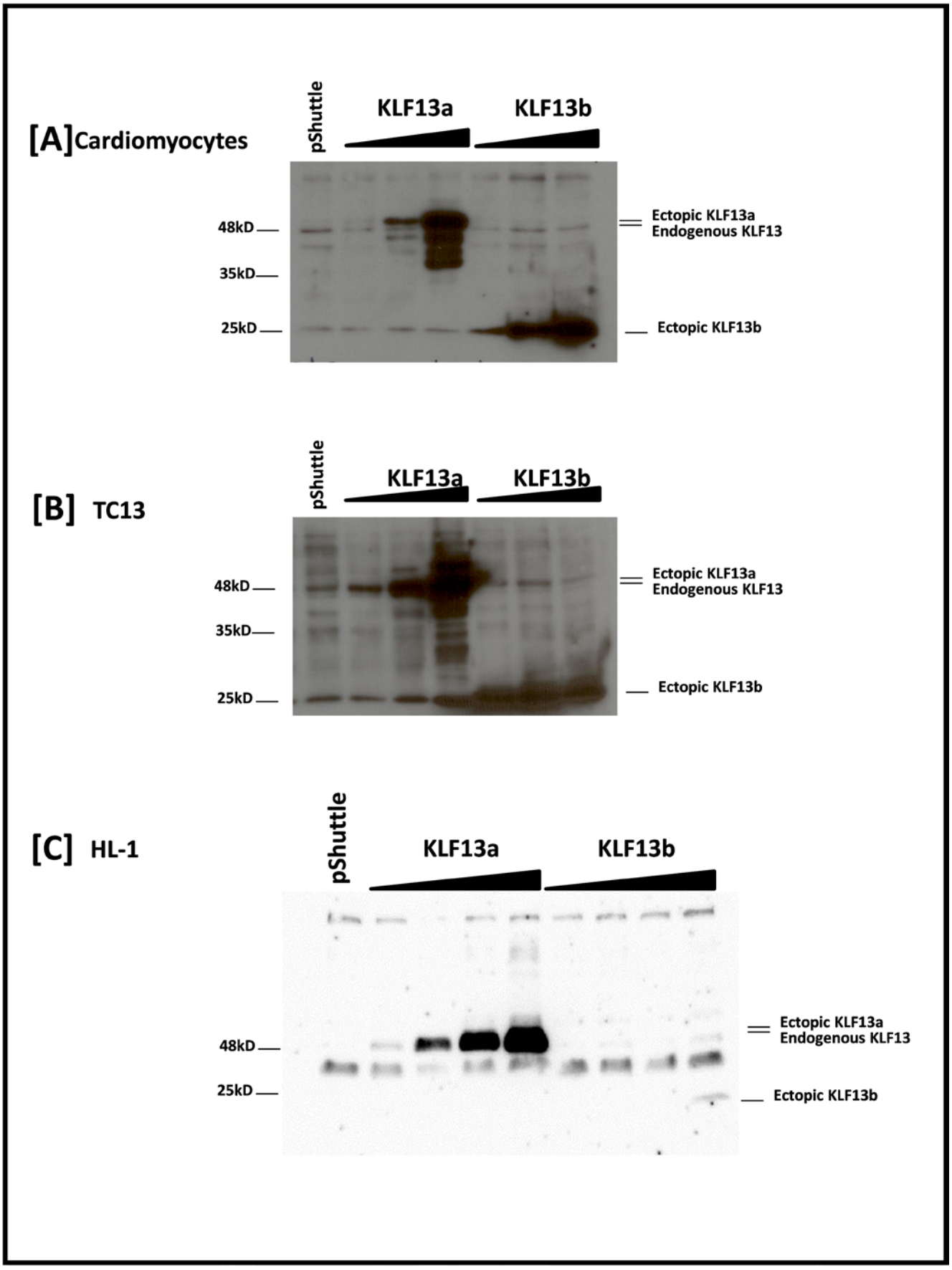
[A]Cardiomyocytes
pShuttle
KLF13a
KLF13b
48kD
35kD
25kD
Ectopic KLF13a
Endogenous KLF13
Ectopic KLF13b
[B] TC13
pShuttle
KLF13a
KLF13b
48kD
35kD
25kD
Ectopic KLF13a
Endogenous KLF13
Ectopic KLF13b
[C] HL-1
pShuttle
KLF13a
KLF13b
48kD
25kD
Ectopic KLF13a
Endogenous KLF13
Ectopic KLF13b

Supplemental Figure 3.1: Overexpression of KLF13 isoforms in different cardiac cell lines.

Western blot analysis of endogenous and exogenous (adenovirus mediated infection) Flag-tagged KLF13 isoforms in primary postnatal cardiomyocyte cultures (A), endocardial TC13 cells (B) and atrial cardiomyocyte (HL1) cell line (C). The KLF13 antibody directed against the common exon2 coding sequences was used.

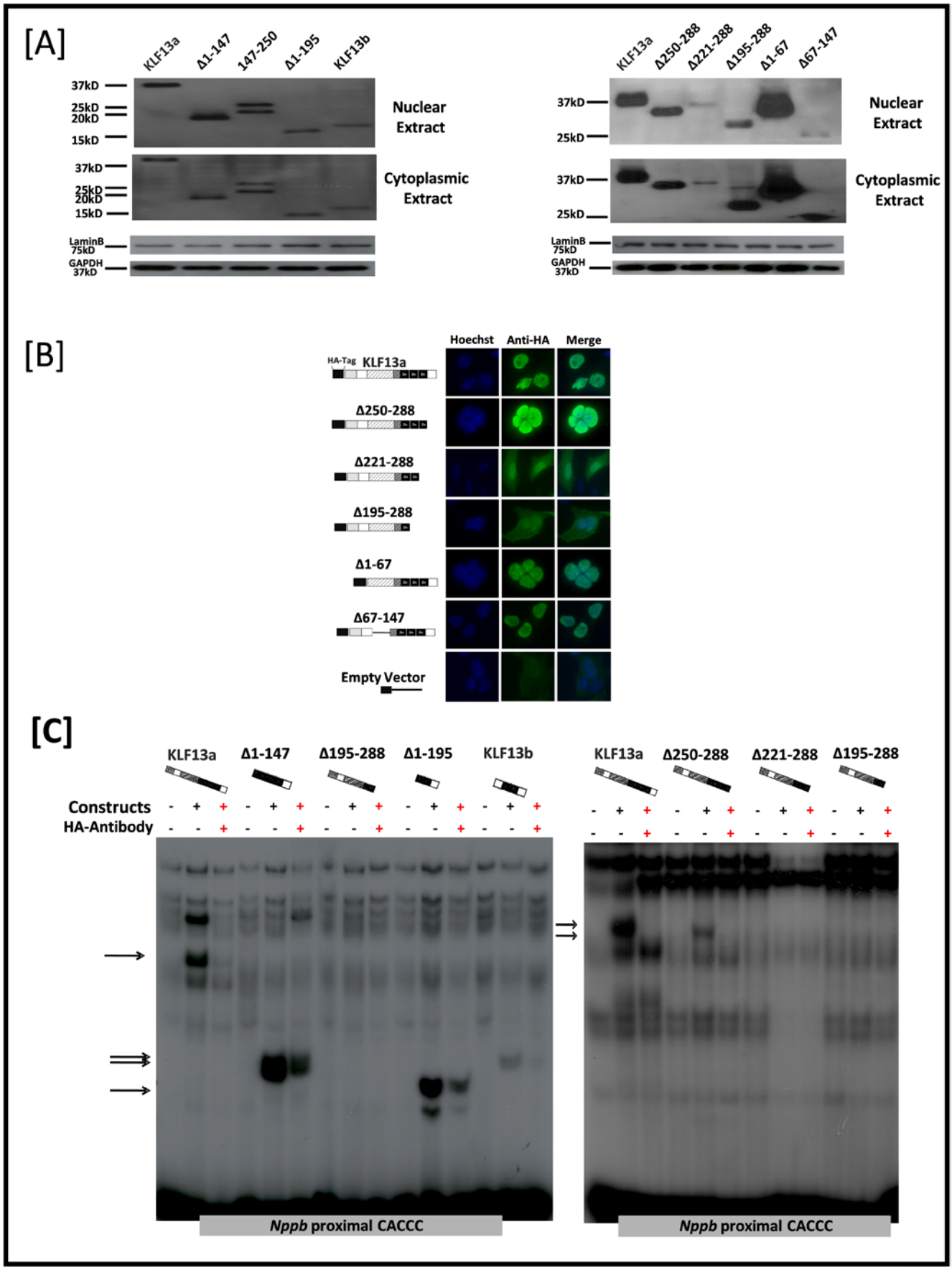
[A]
KLF13a
Δ1-147
147-250
Δ1-195
KLF13b
37kD
25kD
20kD
15kD
Nuclear Extract
Cytoplasmic Extract
LaminB 75kD
GAPDH 37kD
KLF13a
Δ250-288
Δ221-288
Δ195-288
Δ1-67
Δ67-147
[B]
Hoechst
Anti-HA
Merge
HA-Tag KLF13a
Δ250-288
Δ221-288
Δ195-288
Δ1-67
Δ67-147
Empty Vector
[C]
KLF13a
Δ1-147
Δ195-288
Δ1-195
KLF13b
Constructs
HA-Antibody
Nppb proximal CACCC
KLF13a
Δ250-288
Δ221-288
Δ195-288
Nppb proximal CACCC

Supplemental Figure 3.2: Structure function analysis of KLF13.

A) Western blot showing the expression of the recombinant KLF13 proteins in nuclear and cytoplasmic extracts of transfected AD293 cells. The expressed proteins were detected using anti-HA antibody. Lamin B was used as loading control for nuclear extracts and GAPDH for cytoplasmic extracts. B) Cellular localization of the HA-tagged KLF13 protein constructs transfected into AD293 cells. The green color shows the Alexa 488 conjugated secondary antibodies against the anti-HA antibody. The nuclei were visualized by Hoechst 33424 autofluorescence (blue). C) Binding properties of various KLF13a mutant and KLF13 to electrophoretic mobility shift assays (EMSA) of several HA-tagged KLF13 constructs as shown above the corresponding lanes. The DNA probe utilized is derived from the proximal CACCC element of the *Nppb* promoter. The arrowheads show KLF13 – DNA complexes.

Table 3.1: Summary of KLF13 structure function analysis.

	Construct	Cellular Localization	Activation of Nppa/b	DNA Binding	Synergy		
					GATA4	NKX2.5	PEX
	KLF13a	N>>C	+++	Yes	+++	+++	+++
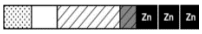	Δ250-288	N>>C	++	Yes	+	++++	++
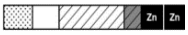	Δ221-288	N>C	+	No	NA	NA	NA
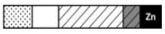	Δ C-Ter	N=C	+/-	No	NA	NA	NA
	Δ1-67	N>>C	++	NA	++	++	+
	Δ 67-147	N>>C	+	NA	+	++	++
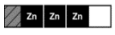	Δ 1-147	N>>C	+/-	Yes	-	-	++
	Δ N-Ter	N=C	+/-	Yes	-	-	-
	Klf13b	N>C	+	Yes	+	+/-	+/-

3.5. Discussion

KLF13 is a dosage sensitive regulator of hematopoiesis and heart development but the mechanisms regulating *Klf13* gene expression as well as protein levels and activity remain poorly understood. In this manuscript, we report that KLF13 exists as two distinct isoforms that have in common the last two zinc fingers and carboxyl-terminus but differ markedly in their N-terminal domain. These isoforms, which are the results of the use of alternative promoters and first exons, have differential cellular and target promoter activity. Additionally, we uncovered novel interactions between KLF13 and two cardiac enriched transcription factors, PEX1 and NKX2.5 belonging respectively to the Kruppel family of zinc fingers and the NK homeobox containing proteins. Through structure-function analysis we provide evidence for the existence of multiple transactivation domains on the known KLF13a protein which are differentially required for interaction with various KLF13 co-activators. Since KLF13b lacks all KLF13a N-terminal TADs, it is able to support some but not all physical or functional interactions with these co-activators. Thus, our work provides insight into two new regulatory mechanisms for KLF13, alternate exon1 usage leading to distinct protein isoforms and interaction with a new class of transcription factors, the NK family of homeobox proteins. Lastly, through gain of function studies, we demonstrate differential effects of KLF13a/b on proliferation and differentiation genes and on cell growth of endocardial progenitors and cardiomyocytes. Together, the data provide novel insight into an important regulator of homeostasis whose alteration is associated with human disease.

Alternate promoter usage generates distinct KLF13 isoforms.

Previous studies showed that *Klf13* transcripts are derived from two exons; exon1 contains the 5' untranslated region (5' UTR) as well as the coding sequence for an N-terminal transcriptionally active domain and the first zinc finger; exon2 contains the two additional zinc fingers and a short C-terminal domain. This genomic structure is conserved across species. Our data indicate that *Klf13* is transcribed from two distinct promoters. When the alternate transcription start site (TSS) is used a transcript containing exon1b and exon2 sequences is generated translating into a shorter protein with a novel 5'UTR and the last two zinc fingers along with the serine (Ser) rich carboxyl- domain (**Figure 3.1A**). Structure-function analysis on two target promoters activated by KLF13 revealed the presence of 3 distinct TADs within the N-terminal domain of KLF13a that are absent in KLF13b and one within the C-terminal domain common to both isoforms. Importantly, KLF13b retained the ability to bind DNA but was generally a weaker transcriptional activator that reduced KLF13a activity (**Figure 3.2B-D)**. Thus, the production of KLF13b may serve as a rheostat to maintain the proper level of KLF13 activity. Of note, the presence of both transcripts in several target organs and their changing relative abundance, with KLF13a/KLF13b ratio being greater in postnatal vs embryonic tissues (**Figure 3.1C**).

Multiple isoforms for other KLF family members have been reported recently (23); they include KLF5, 7, 8, 10 and 12. bKLF4 and 6 were also previously shown to exist as multiple isoforms with differential effect on cancer progression (24;25). In all cases, the isoforms were the result of alternative splicing producing shorter proteins with similar translational start and termination codons. While we cannot rule out the existence of alternative splicing in the *Klf13* locus, we didn't detect additional bands using our PCR strategy in any of the tissues tested. Thus, our data reveal an additional mechanism to

generate isoforms within the KLF family through alternative transcription start site. In silico analysis of promoter, TSS and transcripts data bases (e!Ensembl; EPD; FANTOM) suggest the conservation of this regulatory mechanism in humans (38-40). In both cases, the TSS for the shorter isoform is within the first intron, approximately 14 Kbp downstream of the other TSS. Alignment of the human and mouse genomic sequences revealed a high level of conservation in the first 500bp upstream of exon1b with clusters of transcription factor binding sites. Among other, is the presence of conserved CAAT, GATA, STAT and SP1/GC rich elements is noteworthy. Little is known regarding transcriptional regulation of KLF13 gene. Mitsuma et al reported that the first 500bp upstream of exon1 are sufficient to direct expression in erythroid cells and are activated by GATA1 (41). In the future, it will be interesting to analyze the two KLF13 promoters and determine common as well as divergent regulatory mechanisms.

Distinct role of KLF13 isoforms in cardiac cells.

In human, deletion of the chromosomal region that contains *KLF13* was associated with various heart defects (7). Similarly, loss of KLF13 in *Xenopus* leads to developmental cardiac defects that include hypoplastic myocardium and delayed atrioventricular cushion formation (6); this phenotype is suggestive of an important role for KLF13 in either one or both major cardiac cell types, cardiomyocytes and endocardial cells which both express KLF13a. We tested the effect of the two KLF13 isoforms on cardiomyocytes using quiescent postnatal cardiomyocytes as well as an established atrial cardiomyocyte cell line with embryonic-like features. Ectopic expression of KLF13 in postnatal cardiomyocytes indicated that KLF13a but not KLF13b increased expression of target genes including CyclinD2 (*Ccnd2*), *Nppb* and α-myosin heavy chain (*Myh6*), and

doubled the number of Ki67 positive myocytes indicative of a growth promoting effect. Interestingly, both isoforms significantly upregulated expression of serum response factor (*Srf*), which is a critical muscle regulatory transcription factor. In contrast, gain of KLF13 function in proliferating embryonic like cardiomyocytes was associated with growth arrest and downregulation of both *Ccnd1* and *Ccnd2*, but upregulation of the embryonic genes *Nppa* and β-myosin heavy chain (*Myh7*). While these effects were common to KLF13a and b, other changes in gene expression were isoform specific; for example, KLF13a but not KLF13b downregulated *Gata4* and *Gata5* transcripts and upregulated *Vegf* mRNA; conversely, only KLF13b downregulated *Tbx5*. Together, these results suggest differential temporally regulated functions for KLF13 isoforms on cardiomyocyte proliferation and differentiation. Analysis of KLF13 effects on the endocardial progenitor cell line TC13 was also consistent with a dual regulatory role for KLF13 on cell proliferation and differentiation. Interestingly, some of the genes that are common to endocardial and myocardial cells were differentially regulated by KLF13 proteins in a cell type specific manner. For example, whereas only KLF13a decreased *Gata4* transcripts in cardiomyocytes, both isoforms similarly inhibited Gata4 transcription in endocardial cells (**Figure 3.5 A and B**). On the other hand, *Nfatc* was inhibited by both isoforms in cardiomyocytes but only by KLF13a in endocardial cells. Others like *Vegfr2* were responsive to KLF13 in one but not the other cell type. Disruption of endocardial or myocardial cell proliferation or differentiation can alter critical endocardial-myocardial cell interactions and has profound consequences on heart morphogenesis and postnatal heart function. The data obtained in these *in vitro* cell systems warrant closer investigation of cell and isoform specific manipulation of KLF13 in transgenic mouse hearts.

KLF13 functional domains and interacting partners.

Like other members of the KLF family, KLF13a can act either as a transcriptional activator or repressor by recruiting to target promoters co-activators like p300/CBP, PCAF and Brg1 (21;42) or corepressors such as mSin3A and HDAC (43). GAL4 fusion assays indicated that the N-terminus of KLF13a contains both activation and repression autonomous domains (43;44). KLF13b lacks the entire KLF13a N-terminal domain and contains a novel 24 amino acid N-terminal region with no homology to known transcriptional activation/repression domains. Nonetheless, KLF13b retained the ability to activate several KLF13a target promoters. Interestingly, both PCAF and CBP interact with AA167-289 which contain the zinc fingers and Serine rich C-terminus (44). KLF13b is thus able to translocate to the nucleus, bind DNA and activate transcription, possibly through similar or distinct mechanisms to KLF13a.

Our structure-function analysis of KLF13 on the *Nppb* promoter revealed an important contribution of the C-terminus (AA 250-288) as well as two N-terminal domains (AA 1-67 and AA 67-147) in transcriptional activation. Of note, all three domains were needed for maximal synergy with GATA4 and KLF13b retained the ability to cooperate – albeit to lower extent – with this transcription factor. In contrast, the N-terminal TADs of KLF13a, which are absent in KLF13b were required for synergy with NKX2.5 and KLF13b retained the ability to physically associate with NKX2.5 but not to enhance NKX2.5 activation. These findings suggest that KLF13 proteins may have a subset of common cofactors but also isoform specific ones.

Lastly, the identification of NKX2.5 as a novel KLF13 coactivator is noteworthy. NKX2.5 is a key regulator of heart development and mutations in *NKX2.5* are

associated with human congenital heart disease (45;46). Few DNA binding transcription factors have so far been identified as KLF co-factors. They include the GATA family of zinc finger proteins (6), the MADS box containing SRF which was shown to cooperate with KLF3 in activating muscle creatine kinase (*McK*) (47) and more recently the leucine zipper cMAF transcription factor shown to cooperate with KLF13 for activation of the interleukin 4 (*Il4*) promoter in T-cells (48). KLF13 is co-expressed with other members of the NK family, for example NKX2.1 in T-cells (49) and NKX6.1 and NKX2.2 in the brain (50). Thus cooperativity between KLF13 and NK proteins may extend to other organs beyond the heart and may be worth further investigation.

Taken together, our data point to a possible mechanism for regulating *klf13* gene activity that involves the production of two isoforms, KLF13a and KLF13b, that have distinct spatiotemporal distributions and partially redundant activities. We suggest that the differential interactions with a distinct repertoire of cofactors not only allow *klf13* isoforms to regulate distinct subsets of genes, but also to participate in the divergent regulation of the same gene (4). Deciphering the role of cardiac transcription factors and their isoforms during development, as well as their effects on cell proliferation and differentiation, will contribute to our understating of genotype-phenotype relations in patients with CHD.

Acknowledgment

The authors are grateful to Dr. Georges Nemer and the members of the lab for discussion and suggestions and to Hélène Touchette for editorial assistance.

Funding

This work was supported by a grant from the Canadian Institute of Health Research [201009MOP]. Rami Darwich was a Canada-Vanier Scholar and recipient of a University of Ottawa and an Ontario Graduate scholarships. Funding for open access charge: [CIHR 201009MOP].

3.6. Reference List

1. Pearson,R., Fleetwood,J., Eaton,S., Crossley,M. and Bao,S. (2008) Kruppel-like transcription factors: a functional family. *Int. J Biochem. Cell Biol.*, **40**, 1996-2001.

2. Tetreault,M.P., Yang,Y. and Katz,J.P. (2013) Kruppel-like factors in cancer. *Nat Rev. Cancer*, **13**, 701-713.

3. Prosdocimo,D.A., Sabeh,M.K. and Jain,M.K. (2015) Kruppel-like factors in muscle health and disease. *Trends Cardiovasc. Med*, **25**, 278-287.

4. Lomberk,G. and Urrutia,R. (2005) The family feud: turning off Sp1 by Sp1-like KLF proteins. *Biochem. J*, **392**, 1-11.

5. Fisch,S., Gray,S., Heymans,S., Haldar,S.M., Wang,B., Pfister,O., Cui,L., Kumar,A., Lin,Z., Sen-Banerjee,S. *et al.* (2007) Kruppel-like factor 15 is a regulator of cardiomyocyte hypertrophy. *Proc Natl. Acad Sci U. S A*, **104**, 7074-7079.

6. Lavallée,G., Andelfinger,G., Nadeau,M., Lefebvre,C., Nemer,G., Horb,M. and Nemer,M. (2006) The Kruppel-like transcription factor KLF13 is a GATA-4 collaborator for heart development. *EMBO J*, **25**, 5201-5213.

7. van Bon,B.W., Mefford,H.C., Menten,B., Koolen,D.A., Sharp,A.J., Nillesen,W.M., Innis,J.W., de Ravel,T.J., Mercer,C.L., Fichera,M. *et al.* (2009) Further delineation of the 15q13 microdeletion and duplication syndromes: a clinical spectrum varying from non-pathogenic to a severe outcome. *J Med Genet*, **46**, 511-523.

8. Nemer,M. and Horb,M.E. (2007) The KLF family of transcriptional regulators in cardiomyocyte proliferation and differentiation. *Cell Cycle*, **6**, 117-121.

9. Outram,S.V., Gordon,A.R., Hager-Theodorides,A.L., Metcalfe,J., Crompton,T. and Kemp,P. (2008) KLF13 influences multiple stages of both B and T cell development. *Cell Cycle*, **7**, 2047-2055.

10. Pabona,J.M., Zeng,Z., Simmen,F.A. and Simmen,R.C. (2010) Functional differentiation of uterine stromal cells involves cross-regulation between bone morphogenetic protein 2 and Kruppel-like factor (KLF) family members KLF9 and KLF13. *Endocrinology*, **151**, 3396-3406.

11. Henson,B.J. and Gollin,S.M. (2010) Overexpression of KLF13 and FGFR3 in oral cancer cells. *Cytogenet. Genome Res.*, **128**, 192-198.

12. Stephens,S.H., Franks,A., Berger,R., Palionyte,M., Fingerlin,T.E., Wagner,B., Logel,J., Olincy,A., Ross,R.G., Freedman,R. *et al.* (2012) Multiple genes in the 15q13-q14 chromosomal region are associated with schizophrenia. *Psychiatr. Genet*, **22**, 1-14.

13. Tropeano,M., Andrieux,J., Vassos,E. and Collier,D. (2014) Clinical utility gene card for: 15q13.3 microdeletion syndrome. *Eur. J Hum Genetics*, **22, 1338**; doi:10.1038/ejhg.2014.88.

14. Banerjee,S., Cui,H., Xie,N., Tan,Z., Yang,S., Icyuz,M., Thannickal,V.J., Abraham,E. and Liu,G. (2013) miR-125a-5p regulates differential activation of macrophages and inflammation. *J Biol. Chem.*, **288**, 35428-35436.

15. Natesampillai,S., Kerkvliet,J., Leung,P.C. and Veldhuis,J.D. (2008) Regulation of Kruppel-like factor 4, 9, and 13 genes and the steroidogenic genes LDLR, StAR, and CYP11A in ovarian granulosa cells. *Am J Physiol Endocrinol. Metab*, **294**, E385-E391.

16. Asano,H., Li,X.S. and Stamatoyannopoulos,G. (2000) FKLF-2: a novel Kruppel-like transcriptional factor that activates globin and other erythroid lineage genes. *Blood*, **95**, 3578-3584.

17. Martin,K.M., Cooper,W.N., Metcalfe,J.C. and Kemp,P.R. (2000) Mouse BTEB3, a new member of the basic transcription element binding protein (BTEB) family, activates expression from GC-rich minimal promoter regions. *Biochem. J.*, **345 Pt 3**, 529-533.

18. Kaczynski,J., Cook,T. and Urrutia,R. (2003) Sp1- and Kruppel-like transcription factors. *Genome Biol.*, **4**, 206.

19. Zhou,M., McPherson,L., Feng,D., Song,A., Dong,C., Lyu,S.C., Zhou,L., Shi,X., Ahn,Y.T., Wang,D. *et al.* (2007) Kruppel-like transcription factor 13 regulates T lymphocyte survival in vivo. *J Immunol.*, **178**, 5496-5504.

20. Zhao,X., Tang,Y., Qu,B., Cui,H., Wang,S., Wang,L., Luo,X., Huang,X., Li,J., Chen,S. *et al.* (2010) MicroRNA-125a contributes to elevated inflammatory chemokine RANTES levels via targeting KLF13 in systemic lupus erythematosus. *Arthritis Rheum.*, **62**, 3425-3435.

21. Song,C.Z., Keller,K., Chen,Y. and Stamatoyannopoulos,G. (2003) Functional interplay between CBP and PCAF in acetylation and regulation of transcription factor KLF13 activity. *J Mol. Biol*, **329**, 207-215.

22. Huang,B., Ahn,Y.T., McPherson,L., Clayberger,C. and Krensky,A.M. (2007) Interaction of PRP4 with Kruppel-like factor 13 regulates CCL5 transcription. *J Immunol.*, **178**, 7081-7087.

23. Camacho-Vanegas,O., Till,J., Miranda-Lorenzo,I., Ozturk,B., Camacho,S.C. and Martignetti,J.A. (2013) Shaking the family tree: identification of novel and biologically active alternatively spliced isoforms across the KLF family of transcription factors. *FASEB J*, **27**, 432-436.

24. Wei,D., Wang,L., Kanai,M., Jia,Z., Le,X., Li,Q., Wang,H. and Xie,K. (2010) KLF4alpha up-regulation promotes cell cycle progression and reduces survival time of patients with pancreatic cancer. *Gastroenterology*, **139**, 2135-2145.

25. Narla,G., Difeo,A., Reeves,H.L., Schaid,D.J., Hirshfeld,J., Hod,E., Katz,A., Isaacs,W.B., Hebbring,S., Komiya,A. *et al.* (2005) A germline DNA polymorphism enhances alternative splicing of the KLF6 tumor suppressor gene and is associated with increased prostate cancer risk. *Cancer Res.*, **65**, 1213-1222.

26. Narla,G., Difeo,A., Yao,S., Banno,A., Hod,E., Reeves,H.L., Qiao,R.F., Camacho-Vanegas,O., Levine,A., Kirschenbaum,A. *et al.* (2005) Targeted inhibition of the KLF6 splice variant, KLF6 SV1, suppresses prostate cancer cell growth and spread. *Cancer Res.*, **65**, 5761-5768.

27. Charron,F., Paradis,P., Bronchain,O., Nemer,G. and Nemer,M. (1999) Cooperative interaction between GATA-4 and GATA-6 regulates myocardial gene expression. *Mol. Cell. Biol.*, **19**, 4355-4365.

28. Nemer,G. and Nemer,M. (2002) Cooperative interaction between GATA-5 and NF-ATc regulates endothelial-endocardial differentiation of cardiogenic cells. *Development*, **129**, 4045-4055.

29. Yamak,A., Latinkic,B.V., Dali,R., Temsah,R. and Nemer,M. (2014) Cyclin D2 is a GATA4 cofactor in cardiogenesis. *Proc Natl. Acad Sci U. S A*, **111**, 1415-1420.

30. Georges,R., Nemer,G., Morin,M., Lefebvre,C. and Nemer,M. (2008) Distinct expression and function of alternatively spliced Tbx5 isoforms in cell growth and differentiation. *Mol. Cell. Biol.*, **28**, 4052-4067.

31. Debrus,S., Rahbani,L., Marttila,M., Delorme,B., Paradis,S. and Nemer,M. (2005) The zinc finger-only protein Zfp260 is a novel cardiac regulator and a nuclear effector of a1-adrenergic signaling. *Mol. Cell. Biol.*, **25**, 8669-8682.

32. Yamak,A., Temsah,R., Maharsy,W., Caron,S., Paradis,P., Aries,A. and Nemer,M. (2012) Cyclin D2 rescues size and function of GATA4 haplo-insufficient hearts. *Am J Physiol Heart Circ. Physiol*, **303**, H1057-H1066.

33. Charron,F., Tsimiklis,G., Arcand,M., Robitaille,L., Liang,Q., Molkentin,J.D., Meloche,S. and Nemer,M. (2001) Tissue-specific GATA factors are transcriptional effectors of the small GTPase RhoA. *Genes Dev.*, **15**, 2702-2719.

34. Wang,J., Paradis,P., Lefebvre,C. and Nemer,M. (2005) Convergence of protein kinase C and JAK-STAT signaling on transcription factor GATA-4. *Mol. Cell. Biol.*, **25**, 9829-9844.

35. Ahuja,P., Sdek,P. and MacLellan,W.R. (2007) Cardiac myocyte cell cycle control in development, disease, and regeneration. *Physiol Rev.*, **87**, 521-544.

36. Durocher,D., Charron,F., Warren,R., Schwartz,R.J. and Nemer,M. (1997) The cardiac transcription factors Nkx2-5 and GATA-4 are mutual cofactors. *EMBO J.*, **16**, 5687-5696.

37. Bruneau,B.G., Nemer,G., Schmitt, J.P., Charron,F., Robitaille,L., Caron,S., Conner,D.A., Gessler,M., Nemer,M. *et al.* (2001) A murine model of Holt-Oram syndrome defines roles of the T-box transcription factor Tbx5 in cardiogenesis and disease. *Cell*, **106**, 709-721.

38. Haberle,V., Forrest,A.R., Hayashizaki,Y., Carninci,P. and Lenhard,B. (2015) CAGEr: precise TSS data retrieval and high-resolution promoterome mining for integrative analyses. *Nucleic Acids Res.*, **43**, e51.

39. Lizio,M., Harshbarger,J., Shimoji,H., Severin,J., Kasukawa,T., Sahin,S., Abugessaisa,I., Fukuda,S., Hori,F., Ishikawa-Kato,S. *et al.* (2015) Gateways to the FANTOM5 promoter level mammalian expression atlas. *Genome Biol.*, **16**, 22.

40. Dreos,R., Ambrosini,G., Cavin,P.R. and Bucher,P. (2013) EPD and EPDnew, high-quality promoter resources in the next-generation sequencing era. *Nucleic Acids Res.*, **41**, D157-D164.

41. Mitsuma,A., Asano,H., Kinoshita,T., Murate,T., Saito,H., Stamatoyannopoulos,G. and Naoe,T. (2005) Transcriptional regulation of FKLF-2 (KLF13) gene in erythroid cells. *Biochim. Biophys. Acta*, **1727**, 125-133.

42. Ahn,Y.T., Huang,B., McPherson,L., Clayberger,C. and Krensky,A.M. (2007) Dynamic interplay of transcriptional machinery and chromatin regulates "late" expression of the chemokine RANTES in T lymphocytes. *Mol Cell Biol.*, **27**, 253-266.

43. Kaczynski,J., Zhang,J.S., Ellenrieder,V., Conley,A., Duenes,T., Kester,H., van Der,B.B. and Urrutia,R. (2001) The Sp1-like protein BTEB3 inhibits transcription via the basic transcription element box by interacting with mSin3A and HDAC-1 co-repressors and competing with Sp1. *J Biol. Chem.*, **276**, 36749-36756.

44. Song,A., Patel,A., Thamatrakoln,K., Liu,C., Feng,D., Clayberger,C. and Krensky,A.M. (2002) Functional domains and DNA-binding sequences of RFLAT-1/KLF13, a Kruppel-like transcription factor of activated T lymphocytes. *J Biol Chem*, **277**, 30055-30065.

45. Reamon-Buettner,S.M. and Borlak,J. (2010) NKX2-5: an update on this hypermutable homeodomain protein and its role in human congenital heart disease (CHD). *Hum. Mutat.*, **31**, 1185-1194.

46. Nemer,M. (2008) Genetic insights into normal and abnormal heart development. *J. Cardiovasc. Pathol.*, **17**, 48-54.

47. Himeda,C.L., Ranish,J.A., Pearson,R.C., Crossley,M. and Hauschka,S.D. (2010) KLF3 regulates muscle-specific gene expression and synergizes with serum response factor on KLF binding sites. *Mol Cell Biol.*, **30**, 3430-3443.

48. Kwon,S.J., Crespo-Barreto,J., Zhang,W., Wang,T., Kim,D.S., Krensky,A. and Clayberger,C. (2014) KLF13 cooperates with c-Maf to regulate IL-4 expression in CD4+ T cells. *J Immunol.*, **192**, 5703-5709.

49. Homminga,I., Pieters,R., Langerak,A.W., de Rooi,J.J., Stubbs,A., Verstegen,M., Vuerhard,M., Buijs-Gladdines,J., Kooi,C., Klous,P. *et al.* (2011) Integrated transcript and genome analyses reveal NKX2-1 and MEF2C as potential oncogenes in T cell acute lymphoblastic leukemia. *Cancer Cell*, **19**, 484-497.

50. McMahon,A.P. (2000) Neural patterning: the role of Nkx genes in the ventral spinal cord. *Genes Dev*, **14**, 2261-2264.

51. Garg,V., Kathiriya,I.S., Barnes,R., Schluterman,M.K., King,I.N., Butler,C.A., Rothrock,C.R., Eapen,R.S., Hirayama-Yamada,K., Joo,K. *et al.* (2003) GATA4 mutations cause human congenital heart defects and reveal an interaction with TBX5. *Nature*, **424**, 443-447.

52. Stirnimann,C.U., Ptchelkine,D., Grimm,C. and Muller,C.W. (2010) Structural basis of TBX5-DNA recognition: the T-box domain in its DNA-bound and -unbound form. *J Mol Biol.*, **400**, 71-81.

53. Zaragoza,M.V., Lewis,L.E., Sun,G., Wang,E., Li,L., Said-Salman,I., Feucht,L. and Huang,T. (2004) Identification of the TBX5 transactivating domain and the nuclear localization signal. *Gene*, **330**, 9-18.

4. Experimental Chapter Three

KLF13 is a genetic modifier of the Holt-Oram Syndrome gene TBX5

Rami Darwich[1], Gregor Andelfinger, Abir Yamak, Mona Nemer[1,*]

[1] Molecular Genetics and Cardiac Regeneration Laboratory, Department of Biochemistry, Microbiology and Immunology, University of Ottawa, 550 Cumberland, Ottawa, K1N 6N5, Canada.

Corresponding author: Mona Nemer, University of Ottawa, 550 Cumberland, Ottawa, ON K1N 6N5 Tel: 1-613-562-5270; Fax: 1-613-562-5271; Email: mona.nemer@uottawa.ca

Contributions: In this chapter I have performed all the reported results with the exception of expression profile of TBX5 and KLF13 in consecutive heart sections at E11.5 and E15.5 (Figure 4.1) which was performed by Abir Yamak. The chapter was written with the contribution of my supervisor

4.1 Abstract

TBX5, a member of the T-box family of transcription factors, is a dosage sensitive regulator of heart development. Mutations in *TBX5* are responsible for Holt-Oram Syndrome, an autosomal dominant disease with variable and partially penetrant cardiac defects suggestive of the existence of genetic and environmental modifiers. KLF13, a member of the Krüppel-like family of zinc finger proteins is co-expressed with TBX5 in several cardiac cells including atrial cardiomyocytes and cells of the interatrial septum. We report that KLF13 interacts physically and functionally with TBX5 to synergistically activate transcription of cardiac genes. We show that TBX5 contacts KLF13 via its T-domain and find that several disease-causing mutations therein have decreased KLF13 interaction. Whereas Klf13 heterozygote mice have no detectable cardiac defects, loss of a *Klf13* allele in *Tbx5* heterozygote mice significantly increases the penetrance of TBX5-dependent cardiac abnormalities including atrial and ventricular septal defects. The results reveal for the first time combinatorial interaction between a T-box protein and a KLF family member and its importance for heart and possibly other organ development. The data also suggest that, in human, *KLF13* may be a genetic modifier of the Holt-Oram Syndrome gene *TBX5*.

4.2 Introduction

Congenital heart disease (CHD) represents the most common human birth defect with an incidence of 1-2% of all live births; CHD is a major cause of fetal loss and the leading cause of infant mortality (1;2). Septal defects, the most frequent CHDs, range in severity from the relatively minor patent foramen oval (PFO), to the complex and potentially fatal Tetralogy of Fallot (ToF). Although a subset of CHDs are etiologically monogenic, the majority of CHDs are multifactorial (2;3). Human genetic studies, which have linked several genomic loci to CHDs as well as genetic manipulations in animal models, revealed two important patterns: on the one hand, a given structural defect is often linked to more than one locus or gene; on the other hand, disease manifestation is often characterized by variable penetrance and expressivity. Variable penetrance can be attributed to the differences in the genetic buffering capacity of interconnected regulatory networks needed to compensate for both environmental and genetic variations. This buffering capacity is influenced by modifier genes, genetic polymorphisms, and environmental factors (1;4;5). This variability is even observed in the case of autosomal dominant diseases such as Holt-Oram Syndrome (HOS) which is caused by mutations in *TBX5* and where cardiac manifestation among affected family members can vary from asymptomatic conduction system defects to severe structural anomalies. Understanding the genotype-phenotype relationship is critical for improving patient care. This in turn necessitates deciphering the molecular basis of CHD including the identification of modifier genes and factors.

TBX5, the gene mutated in human Holt-Oram Syndrome (HOS), encodes a member of the T-box family of transcription factors, TBX5, one of the most extensively studied cardiac transcription factors. HOS is a dominant disorder characterised primarily by upper limb defects and heart abnormalities (6). The prevalent HOS-associated cardiac defects are

atrial and ventricular septal defects (ASD, VSD), hypoplastic left ventricle and conduction anomalies (7;8). TBX5 is expressed at the earliest stages of cardiogenesis, throughout the heart primordia, where it is co-expressed with other cardiac transcription factors such as NKX2.5 and GATA4. In mice, loss of both *Tbx5* alleles is embryonic lethal due to arrested cardiac morphogenesis (9). Interestingly, mice heterozygous for *Tbx5* or with hypomorphic Tbx5 alleles recapitulate many features of HOS (9;10) and represent unique tools to elucidate gene-gene and gene-environment interactions in the onset of CHD.

TBX5 mechanisms of action involves cooperative interactions with other conserved cardiac transcription factors such as GATA4, NKX2.5 and MEF2C (9;11;12). The relevance of these interactions is underscored by the finding that mutations that disrupt cooperativity between TBX5 and its cofactors are associated with CHD (7). Similarly, combined heterozygous loss of TBX5 and its GATA4 cofactor leads to increased penetrance of severe cardiac defects (13;14), confirming that GATA4 is a genetic modifier of TBX5. Several TBX5 cofactors were identified because of their shared transcription targets. This is best illustrated for NKX2.5 which binds the atrial natriuretic peptide (*Nppa)* promoter at juxtaposed NKE/TBE sites and synergises with TBX5 in transcriptional activation (9). The *Nppa* promoter contains binding sites for several key cardiac transcription factors and has been extensively used to characterise several regulatory pathways essential for heart development (15). We previously showed that *Nppa* is activated by KLF13, a member of the Krüppel-like family of important regulators of cell growth and differentiation (16). KLF13 binds evolutionary conserved regulatory elements known as CACC-box that are present on several cardiac promoters (*Nppb, Nppa, Myh6* and *Myh7*), and acts as a cardiac transcription activator; KLF13 functionally and physically interacts with GATA4, a critical regulator of cardiac development (16). In murine hearts, *Klf13* expression is detected as early as ED 9.5

in both myocardial and endocardial cells with higher expression in the developing atrial myocardium and ventricular trabeculae.

Here, we show KLF13 and TBX5 co-localize in several cardiac cells, and physically and functionally interact to synergistically activate the *Nppa* and other promoters. We find that several TBX5 mutations associated with congenital heart defects in HOS patients are impaired in their functional and physical interactions with KLF13. We also report that whereas *Klf13* heterozygosity is not associated with detectable cardiac defects, compound haploinsufficiency of *Klf13* and *Tbx5* is associated with decreased postnatal viability and significantly higher incidence of septal defects than observed in *Tbx5* heterozygous mice. These results identify KLF13 as a TBX5 cofactor and point to *KLF13* as a genetic modifier of Holt-Oram Syndrome and possibly other congenital heart diseases.

4.3 Materials and Method

Ethics statement. Research was performed in accordance with institutional guidelines and was approved by the Institutional Animal Care and Use Committee (IACUC) of the University of Ottawa. The guidelines of the IACUC conform to those of the US National Institute of Health (NIH) (Assurance number for University of Ottawa: A5043-01).

Mouse strains and genotyping. Mice heterozygous for null Tbx5 alleles were previously described (9). Klf13$^{+/-}$ mice were generated by targeted deletion of exon 2, which encodes the 2nd and 3rd zinc fingers as well as the entire C-terminus of KLF13. 129Sv ES cells were electroporated with the targeting vector and homologous recombination was tested by southern blot analysis in individually isolated ES clones. Two clones positive for the targeted *Klf13* deletion were then microinjected into C57/B6 blastocysts (3.5d) followed by implantation into pseudo pregnant CD1 females. Germline transmission was achieved through breeding the resulting chimeras to C57/B6 mice. Klf13$^{+/-}$ mice were confirmed by Southern blots and the level of Klf13 transcripts in the heart was confirmed by QPCR. Mice were kept on a C57/B6 background. To generate the double heterozygote mice used in this study, *Klf13* heterozygote mice were mated with *CMV-Cre* transgenic mice on the same C57BL6 background to produce *Klf13*$^{+/-}$ *CMV-Cre*$^{+/-}$ mice. *Klf13*$^{+/-}$ *CMV-Cre*$^{+/-}$ were then mated with mice homozygote for the floxed *Tbx5* alleles on Black Swiss/129 background to constitutively delete the sequences between the loxP sites. For embryo collection and analysis, pregnant mothers were sacrificed at various embryonic time points. Embryonic day 0.5 was marked the morning a vaginal plug was seen. Littermates were used as controls for the various studies performed.

Histology. For histological analysis, adult heart tissues or staged embryos (E11.5, E15.5 and E18.5) were fixed in 4% paraformaldehyde (PFA) at 4ºC overnight and paraffin embedded. Masson Trichrome staining and immunohistochemistry were conducted as previously described (17). The antibodies used were: N-terminal TBX5 (previously described: (13;18), KLF13 (previously described: (16).

Echocardiographic analysis. Mice were anesthetized (2.0% isoflurane, 80 ml/min 100% O_2) and shaved to facilitate two-dimensional guided M-mode echocardiography using a Visual-Sonics VEVO 2100 system (Visual Sonics, Amsterdam) with a 30-MHz linear array transducer. Images and videos were analyzed using the VEVO 2100 analysis software (Visual Sonics, Amsterdam).

Real-Time PCR analysis. Total RNA was isolated from mouse tissues using TRIZOL reagent (Invitrogen). Transcript levels of the various markers were determined by real-time PCR. Primer sequences are available on request.

Cell count. Image J software was used to count the endocardial and mesenchymal cushion cells.

Cell cultures. NIH3T3 cells were maintained and transfected as previously described (19). The Nppa-Luciferase reporter (9) was used for analyzing the transcriptional effects of KLF13 and TBX5. TBX5 mutants were introduced in the HA-tagged TBX5 expression vector (18) using PCR amplification and sequence confirmed.

Protein binding assays. Pull down assays were carried-out using bacterially expressed MBP-KLF13 or MBP-NKX2.5 and in vitro translated ^{35}S-labelled TBX5 protein using previously described protocols (16). For the bacterial expression, KLF13 and NKX2.5

cDNA constructs were cloned in-frame into the pMALC vector to produce MBP fusion proteins. These constructs were used to transform BL21 cells, and then bacterial cells were harvested in MBP binding buffer (MBP binding buffer: 20 mM Tris-HCl pH 7.5, 200 mM NaCl, 1 mM EDTA, 0.5 mM PMSF, 1 mM DTT) (GST binding buffer: 1XPBS, 100 mM Tris-HCl pH 7.5, 1 mM EDTA, 0.5 mM PMSF). The suspended cells were then sonicated and the cellular debris were then removed by centrifugation. The fusion proteins were then purified by binding to amylase/sepharose beads (New England Biolabs, Inc.). Immobilized fusion protein concentration estimation was conducted using 10%SDS-PAGE stained with Coomassie blue and BSA as a standard (1-2-5-10-15ug).

For in vitro translated TBX5, we used TNT coupled in vitro transcription-translation system (Promega Corp., Madison, Wis.) with [^{35}S] methionine. In vitro binding studies were performed by incubating 10 µl of ^{35}S-labeled TBX5 with 500 ng of immobilized KLF13 and NKX2.5 fusion proteins in 500 µl of binding buffer (150 mM NaCl, 50 mM Tris-Cl [pH 7.5], 10 mM ZnCl20.3% Nonidet P-40, 1 mM dithiothreitol [DTT], 0.5 mM PMSF, 0.25% bovine serum albumin [BSA]) overnight at 4°C with agitation and then centrifuged for 2 min at 15,000 rpm at room temperature. Beads were washed three times by vortexing in 500 µl of binding buffer at RT and three times by vortexing in 500 µl of binding buffer without BSA. The protein complexes were released after boiling in Laemmli buffer and resolved by sodium dodecyl sulfate-polyacrylamide gel electrophoresis. The gel was then dried and exposed to autoradiography film (Hyperfilm ECL, Amersham).

Statistics. The data are presented as mean ± SEM; $p<0.05$ by student two-tailed *t*-test is considered statistically significant.

4.4 Results

4.4.1. Functional and Physical Interaction between KLF13 and TBX5.

Previously, we reported that loss of klf13 in the African clawed frog (*Xenopus laevis*) causes CHD including atrial septal delay/defects and hypoplastic ventricles (16). These defects are reminiscent of those observed in mice with hypomorphic *Tbx5* alleles (9). KLF13 is enriched in atrial cardiomyocytes and in endocardial cells (16). Immuno-histochemical staining for KLF13 and TBX5 on consecutive mouse heart sections shows that the two proteins have a similar expression profile in certain regions of the heart (**Figure 4.1**). TBX5 and KLF13 are both expressed in the myocardium of the atrio-ventricular cushion (AVC) at E11.5. At E15.5, both proteins are expressed in the atria, atrial septum and ventricular trabeculae. KLF13 is also expressed in the interventricular septum and the ventricular walls at E15.5. Within these regions, several cells (see red arrows in **Figure 4.1**) co- stain for both TBX5 and KLF13 notably in the atrial septum. Interestingly, in silico sequence analysis reveals evolutionary conservation of juxtaposed TBX5 (TBE) and KLF13 binding sites (CACCC elements) on the *Nppa* promoter and on other cardiac/endocardial promoters such a *Nppb*, *Vegfa* , and *Nos3* promoters. This prompted us to test for functional cooperativity between KLF13 and TBX5.

The functional interaction between KLF13 and TBX5 was first assayed using luciferase co-transfection assays. When co-transfected into heterologous cells (NIH 3T3), the *Nppa*-luciferase promoter was activated 5-10 fold in the presence of either KLF13 or TBX5 expression plasmids; however, simultaneous presence of both factors produced a synergistic activation of up to 200 fold (**Figure 4.2**). This synergy was also observed over other TBX5 activated promoters, including *Vegfa* and *Nos3* (**Figure 4.2D** and data not shown).

To study the structure-function of the TBX5-KLF13 synergy, we utilized TBX5 constructs containing deletions of specific functional domains. We previously (20) reported the presence of two transactivation domains within the C-terminal of TBX5 between 400-518aa and 250-300aa. Deleting these two TADs and the N-terminal domain (Δ1-52aa) led to a significant decrease in *Nppa* promoter activation but did not abrogate the synergy between KLF13 and TBX5 suggesting that the T-domain is sufficient for supporting synergy with KLF13 (**Figure 4.2E)**. Next, we tested whether the 2 proteins physically interact. Pull-down assays were carried out using *in vitro*- translated ^{35}S-labeled-KLF13 and GST-TBX5 recombinants. As shown in **Figure 4.2F**, KLF13 was retained on the GST-TBX5 columns and the T-domain was sufficient for maintaining the physical interaction with KLF13. Reciprocally, we also sought to determine the KLF13 domains important for functional and physical interaction with TBX5 (**Figure 4.2G-H**). Deletion of the last 38 aa reduces KLF13 activity by half in presence or absence of TBX5. The N-terminal domain of KLF13 contains 2 discreet transactivation domains located between 1-67 and 67-147aa, and deletion of either one of them abrogates synergy with TBX5 (**Figure 4.2G**) on the *Nppa* promoter. Interestingly, a mutant protein containing the last 2 zinc-fingers and C-terminal domains as well as the KLF13b isoform that spans these sequences are able to support synergy, albeit to a lower extent than the full length KLF13a isoform. These results suggest that both sequence and conformation considerations are involved in KLF13 interaction with TBX5. To test which domains are required for physical contact with TBX5, pull-down assays were carried out using MBP- TBX5 and various *in vitro*- translated ^{35}S-labeled-KLF13 deletion constructs. (**Figure 4.2H**). Deletion of the last two zinc fingers (Δ195-288aa) severely reduced physical interaction with TBX5. Interestingly, constructs containing the last 2 zinc fingers (Δ 195-288 and KLF13b) were capable of physically

interacting with MBP-TBX5. Overall our structure function analysis indicates that the physical interaction between KLF13 and TBX5 is mediated via the last 2 DNA-binding zinc fingers of KLF13 and the T-box domain of TBX5.

4.4.2. Klf13 is a genetic modifier of Tbx5-dependent septal defects.

The functional interaction between KLF13 and TBX5 as well as the similarity of the cardiac phenotypes resulting from mammalian TBX5 haploinsufficiency and KLF13 loss of function in *Xenopus* (ASD, hypoplastic ventricle, AV defects) suggest the existence of genetic interaction between these pathways in heart morphogenesis. To test this in mammalian development, we generate *Klf13* heterozygote mice by targeting for deletion *Klf13* exon 2 using homologous recombination in ES cells as described in materials and methods. Mice lacking a functional *Klf13* allele were born at expected Mendelian ratios. Detailed histological examination of heart structure revealed no obvious defects. Functional analysis using echocardiography showed that all cardiac parameters were indistinguishable from control littermates (data not shown). To generate *Tbx5* and *Klf13* double heterozygote mice, *Tbx5* $^{flox/flox}$ mice were mated with *Klf13*$^{+/-}$ CMV-Cre$^{+/-}$ mice. An equal ratio of the following four genotypes would be expected: *Tbx5*$^{+/flox}$ *Klf13*$^{+/+}$, *Tbx5*$^{+/flox}$ *Klf13*$^{+/-}$, *Tbx5*$^{+/del}$ *Klf13*$^{+/+}$, and *Tbx5*$^{+/del}$ *Klf13*$^{+/-}$. However, and consistent with the reported perinatal lethality of *Tbx5* $^{+/del}$ mice, only 62% of the expected *Tbx5*$^{+/del}$ *Klf13*$^{+/+}$ were present at weaning (postnatal day 28) in comparison to the number of control mice; similarly, the observed ratio of double heterozygote mice at weaning was also lower than expected by almost 50% (**Figure 4.3 A**).

Despite their lower frequency, the surviving *Tbx5*$^{+/del}$ *Klf13*$^{+/+}$ (Tbx5 heterozygotes) and *Tbx5*$^{+/del}$ *Klf13*$^{+/-}$ (Tbx5-Klf13 double heterozygotes) mice appeared morphologically normal when compared with control littermates. *Tbx5*$^{+/del}$ mice were previously reported to

have smaller left ventricle (LV) end-diastolic diameter (EDD) and end-systolic diameter (ESD) which are indicative of impaired diastolic function (21). Using echocardiographic analysis on 150 day old mice the assessment of left ventricular mass over body weight (LV/BW) revealed that a subgroup (3/8) of *Tbx5*$^{+/del}$ *Klf13*$^{+/+}$ mice had a lower ratio than the littermate controls (**Figure 4.3 B**). Although analysis of cardiac fractional shortening (**Figure 4.3 C**) showed no significant changes in comparison to the controls, *Tbx5*$^{+/del}$ *Klf13*$^{+/-}$ mice and the *Tbx5-Klf13* double heterozygotes showed more heterogeneity within their group. Analysis of pulmonary and aortic valve mean gradients showed no significant difference among the various genotypes (**Figure 4.3 D** and data not shown). Consistent with previous reports (22), histological analysis by Masson Trichrome staining of the *Tbx5*$^{+/del}$ *Klf13*$^{+/+}$ hearts revealed 55% (6/11) prevalence of ASD compared to 0-0.5% in control littermates (0/20 for *Tbx5*$^{+/flox}$ *Klf13*$^{+/+}$ and 1/20 for *Tbx5*$^{+/flox}$ *Klf13*$^{+/-}$). Interestingly, *Tbx5*$^{+/del}$ *Klf13*$^{+/-}$ double heterozygotes had a higher prevalence of ASD (15/20, 75%) than *Tbx5* heterozygote littermates (**Figure 4.3 F-H**).

Although only 48% of the *Tbx5*$^{+/del}$ *Klf13*$^{+/-}$ were present at weaning, genotype analysis of E13.5 and E15.5 embryos showed no lethality at these embryonic stages **(Figure 4.4 A)** suggesting that loss of a *Klf13* allele affects later stages of development or postnatal survival. Consistent with previous reports, *Tbx5*$^{+/del}$ embryos had evidence of cardiac septal defects at E15.5 **(Figure 4.4 C and D)** (9). Atrial septal defects and membranous ventricular septal defects were observed in 42% (3/7) of the *Tbx5*$^{+/del}$ *Klf13*$^{+/+}$ embryos. At this stage, increased penetrance of atrial (75% or 6/8) and ventricular (63% or 5/8) septal defects were observed in *Tbx5*$^{+/del}$ *Klf13*$^{+/-}$ embryos but were not present in either *Klf13* heterozygotes or in littermates with functional *Tbx5* and *Klf13* alleles. **(Figure 4.4 E)**. Taken together, our results show that loss of a *Klf13* allele in a *Tbx5*$^{+/del}$ genetic background

is associated with higher rates of septal defects suggesting that *Klf13* is a genetic modifier of *Tbx5* in septal formation.

To analyse the consequences of the compound loss of a *Klf13* and a *Tbx5* allele on cardiac gene expression, we performed QPCR analysis (**Figure 4.5**) on E11.5-12.5 embryos. The selected genes analysed included known regulators of heart morphogenesis (eg: GATA4/5, MEF2) as well as reported TBX5 targets (eg, Slit2, Nos3, Myl7). These studies revealed interesting patterns of gene expression including that in morphologically normal *Klf13* heterozygotes where many transcripts were unexpectedly altered. In fact, the level of several transcripts were similarly upregulated in *Tbx5* and *Klf13* heterozygotes, albeit not to the same extent. They included *Gata4*, *Gata5*, *Mef2a*, *Erbb4*, *Vegfc*, *PlexinD1*, *Sema6d*, and *Myh7*. Interestingly, although transcripts of *Slit1* were upregulated only in embryos heterozygote for *Tbx5*, the double mutant embryos showed a significant upregulation in comparison to the littermate controls. Similarly, while transcript levels of *Dkk3* in either *Klf13* or *Tbx5* heterozygotes were not significantly different from control littermates, the double heterozygotes showed significant downregulation in comparison to the littermate controls. In other cases, such as *BMP10, Flt1, Scn5a* and *Hcn4* the upregulation observed in *Tbx5* heterozygotes was reversed by the loss of *Klf13*. These changes may reflect compensatory mechanisms that were no longer operative in the absence of both alleles, and may explain *Klf13* action as a *Tbx5* modifier.

2.4.3. Effect of disease causing TBX5 mutants on KLF13 interaction.

Analysis of point mutations is considered as the “Rosetta stone” in deciphering the genotype-phenotype relation and how disruption of the combinatorial interactions of transcription factors can lead to specific birth defects (51). To date, over 60 mutations in the

TBX5 gene have been associated with Holt-Oram syndrome; the majority introduce a premature stop codon or change an amino acid within the T- domain (52;53). To analyze the effect of TBX5 point mutants on the interaction with KLF13, we produced TBX5 constructs harboring thirteen HOS missense point mutations and tested them for physical and functional interaction with KLF13 and the known TBX5 co-factors NKX2.5 and GATA4. **Figure 4.6A** shows a schematic diagram of the TBX5 protein structure depicting the location of the mutations tested. First the expression and subcellular localization of all Flag-tagged-TBX5 point mutants were verified and compared to the wild type protein using Western blot and protein extracts prepared from transfected AD 293 cells (**Figure 4.6B**). While the wild-type Flag-TBX5 showed a preferential nuclear localization, several point mutants (G80Q, G169R, T223M, and R237Q) showed a predominant cytoplasmic localization, while others (A79V, L102P, W121G, T144I, and G195A) had an equal protein distribution in the 2 cellular compartments. We further ascertained our results at the cell level using immunofluorescence with anti-Flag-antibody in transfected cells (**Figure 4.6C**). The immunofluorescence generally confirmed the results obtained by Western blot analysis.

The transcriptional activities of the point mutants were analyzed using the *Nppa*-luciferase reporter. To account for the differential nuclear localization, a dose response study was conducted (25ng, 50ng, 100ng, 200ng, and 400ng). As shown in **Figure 4.6D**, in comparison to WT-TBX5, mutants G80Q, G169R, W121G, T223M, and R237Q showed drastic losses of transcriptional activity; G169R and G195A displayed a moderate but significant reduction (40%) in the ability to trans activate the *Nppa-luc* reporter. The reduced transcriptional activity of these point mutants might be due, in part, to defective nuclear localization. On the other hand, I45T whose expression and subcellular localisation are indistinguishable from those of native TBX5 showed a significant increase in

transcriptional activity. Intriguingly, despite their cytoplasmic leakiness, mutants A79V, L102P, and T144I, showed no significant deviation from the transcriptional activity of wild type TBX5. The activity of I54T, Y100C, and R134C was similar to that of intact TBX5. To evaluate the effect of all mutants on transcriptional synergy with KLF13, GATA4, and NKX2.5, we conducted luciferase co-transfection assays with *Nppa*-luciferase reporter **(Figure 4.7 B-D, respectively)**. Similar to the transcriptional analysis of the point mutants, 5 different dosages of TBX5 plasmids were used, thus minimizing artefacts due to the difference in their basal activity (25ng, 50ng, 100ng, 200ng, and 400ng). Given the variable transcriptional activity of the point mutants, we opted to express the results as fold synergy [activity when both proteins present/ additive effect of each protein] to better distinguish basal and synergistic effects. Point mutants G80Q, W121G, T223M, and R237Q showed no synergy with either KLF13, GATA4, or NKX2.5. Interestingly, despite an intact basal transcriptional activity, A79V and Y100C had reduced synergy with KLF13 but not with GATA4 or NKX2.5. In contrast, R134C and G169R affected only GATA4 synergy while G169R and G195A affected synergy with both GATA4 and KLF13 but not with NKX2.5. Mutants I54T, L102P, and T144I had similar activity as wild type TBX5 with all 3 co-factors. To test whether altered synergy is due to altered physical interactions, the binding of wild type and TBX5 mutants with KLF13 and NKX2.5 was carried out using MBP-KLF13/MBP-NKX2.5 and *in vitro*- translated ^{35}S-labeled-TBX5 protein. **Figure 4.7 F- G** show the quantitative analysis of the pull down assay presented in **Figure 4. 6E**. Mutants G80Q, T223M, and R237Q by MBP-KLF13 and -NKX2.5 were severely hindered in their interaction with both KLF13 and NKX2.5 indicating that, in addition to defective nuclear localisation, these mutations disrupt important protein-protein interactions. Interestingly, A79V and Y100C and G169R which show reduced synergy with KLF13 also have

decreased physical interaction with MBP-KLF13 while R134C ability to physically or functionally interact with KLF13 is unchanged. Our results indicate that the loss of function observed in TBX5 mutants are associated with selective disruption of physical and/or functional interaction with co-factors including with KLF13.

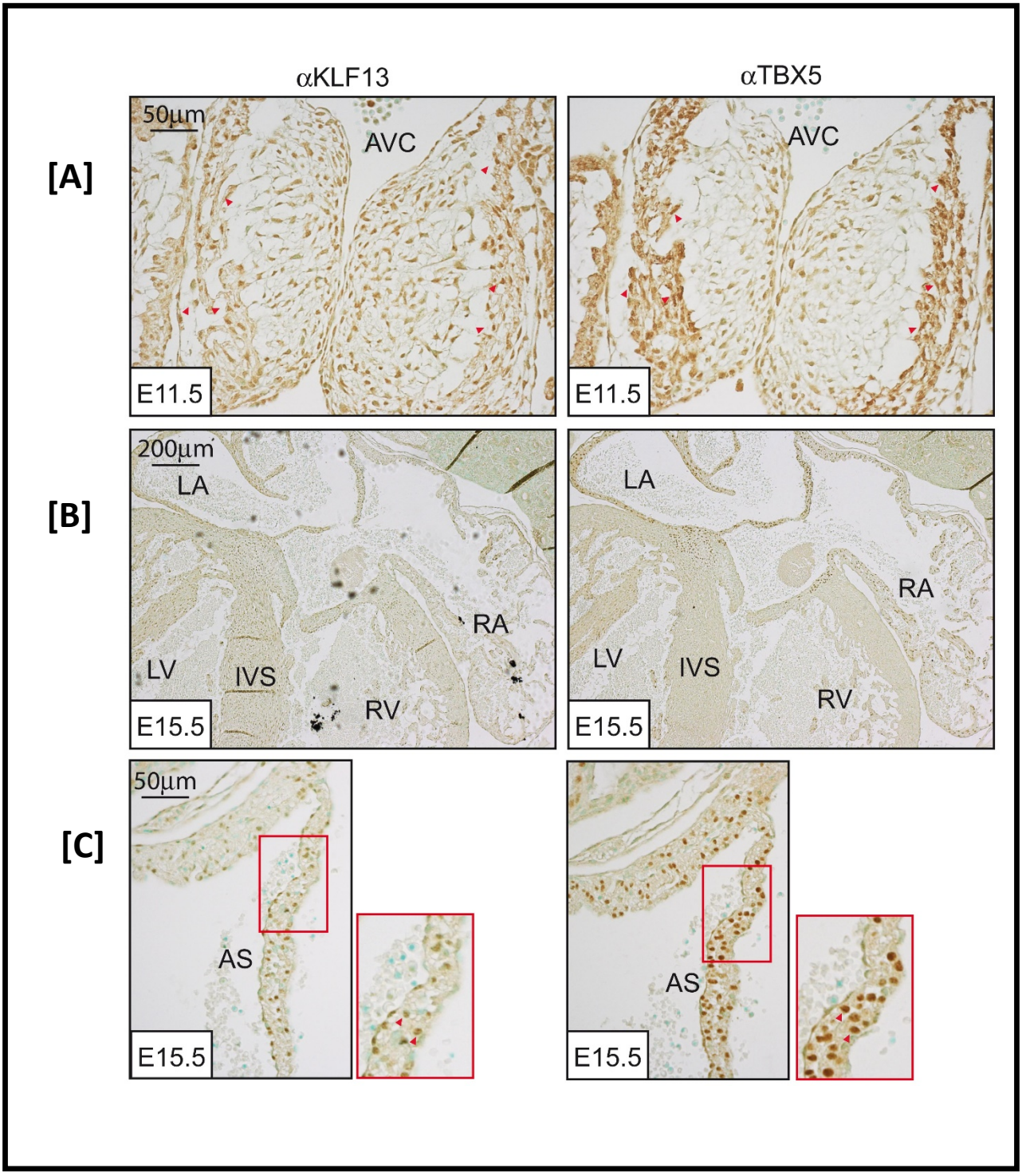
αKLF13
αTBX5
[A]
50μm
AVC
AVC
E11.5
E11.5
[B]
200μm
LA
LA
RA
RA
LV
IVS
RV
LV
IVS
RV
E15.5
E15.5
[C]
50μm
AS
AS
E15.5
E15.5

Figure 4. 1: Similar expression profile of TBX5 and KLF13 in consecutive heart sections at E11.5 and E15.5.

Both proteins are expressed in the myocardial wall of the AVC at E11.5 (A) and in the atria, atrial septum and ventricular trabeculae at E15.5 (B and C). Note that KLF13 is additionally expressed in the IVS and ventricular walls. Red arrowheads indicate individual cells stained for both proteins at E11.5 and in the AS of E15.5 hearts. AVC: atrioventricular cushion; LA: left atrium; RA: right atrium; LV: left ventricle; RV: right ventricle; IVS: interventricular septum; AS: atrial septum.

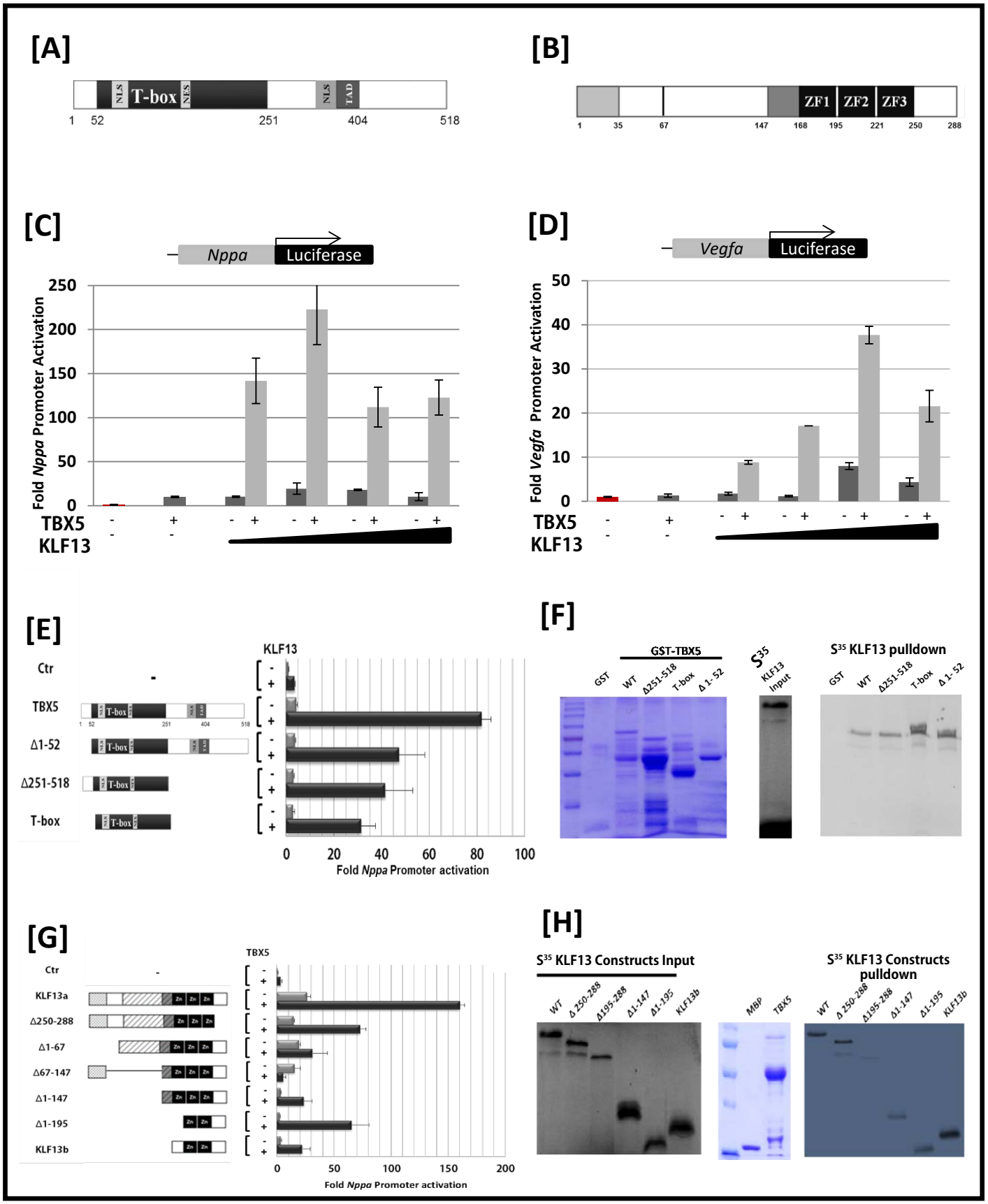
[A]
NLS
T-box
NES
NLS
TAD
1
52
251
404
518
[B]
ZF1
ZF2
ZF3
1
35
67
147
168
195
221
250
288
[C]
Nppa
Luciferase
Fold Nppa Promoter Activation
250
200
150
100
50
0
TBX5
KLF13
[D]
Vegfa
Luciferase
Fold Vegfa Promoter Activation
50
40
30
20
10
0
TBX5
KLF13
[E]
Ctr
TBX5
Δ1-52
Δ251-518
T-box
KLF13
0
20
40
60
80
100
Fold Nppa Promoter activation
[F]
GST-TBX5
GST
WT
Δ251-518
T-box
Δ 1- 52
S35
KLF13
Input
S35 KLF13 pulldown
GST
WT
Δ251-518
T-box
Δ 1- 52
[G]
Ctr
KLF13a
Δ250-288
Δ1-67
Δ67-147
Δ1-147
Δ1-195
KLF13b
TBX5
0
50
100
150
200
Fold Nppa Promoter activation
[H]
S35 KLF13 Constructs Input
WT
Δ 250-288
Δ195-288
Δ1-147
Δ1-195
KLF13b
MBP
TBX5
S35 KLF13 Constructs pulldown
WT
Δ 250-288
Δ195-288
Δ1-147
Δ1-195
KLF13b

Figure 4. 2: KLF13 and TBX5 functionally and physically interact to potentiate their activities on cardiac promoters.

A-B) Schematic representation of the TBX5 and KLF13 protein structures, respectively. C-D) KLF13 and TBX5 synergistic interaction on the *Nppa*- and *Vegfa*-reporters, respectively. The study was conducted by co-transfecting NIH 3T3 with 2µg of -699bp *Nppa* or *Vegfa* promoter and a constant dose of TBX5 (either 50ng or 100ng, respectively) without/with an increasing doses of KLF13 (25ng, 50ng,100ng, and 200ng). Note that the total amount of DNA was kept constant using an empty pCGN vector. Fold promoter activity is expressed as the fold change relative to the control. The data shown is a representation of two different experiments, each carried out in duplicates. E) Structure function analysis of the synergy between TBX5 and KLF13. Transfections were carried out using the -699bp *Nppa* promoter. The study was conducted by co-transfecting NIH 3T3 with 2ug of *Nppa* promoter, a constant dose of KLF13 (50ng), and five dosages of each of the TBX5 constructs. One representative dose is reported here. Note how the Tbox domain alone was sufficient to maintain synergy with TBX5. F) Pull-down assays (right panel) using *in vitro*-translated ^{35}S-labeled-KLF13 (middle panel) and the GST-TBX5 fusion proteins (left panel). Note how *in-vitro* translated KLF13 was retained by the T-box domain. G) Structure function analysis of KLF13 domains important for the synergy with TBX5 on the Nppa promoter. The study was conducted by co-transfecting NIH 3T3 with 2µg of *Nppa* promoter, a constant dose of Tbx5 (50ng), without/with five dosages of each of the KLF13 constructs. One representative dose is reported here. Note how the constructs containing only zinc-fingers (Δ1-147 and Δ1-195) as well as the second isoform were sufficient to maintain synergy with TBX5. H) Pull-down assays (right panel) using *in vitro*-translated ^{35}S-labeled-KLF13 constructs (left panel) and the MBP-TBX5 fusion protein (middle panel). Note how the region containing the last two zinc-fingers, amino acids 195-288, as well as the second isoform, were sufficiently retained by the MBP-TBX5 beads.

[A]

Tbx5 $^{Flox/Flox}$ x *CMV-Cre* $^{+/-}$ *Klf13* $^{+/-}$

Genotype at weaning		Observed	Expected
Tbx5 $^{+/flox}$	*Klf13* $^{+/+}$	21 (34.4%)	25%
Tbx5 $^{+/flox}$	*Klf13* $^{+/-}$	17 (27.9%)	25%
Tbx5 $^{+/del}$	*Klf13* $^{+/+}$	13 (21.3%)	25%
Tbx5 $^{+/del}$	*Klf13* $^{+/-}$	10 (16.4%)	25%
		Total: 61	

[B] LV/BW

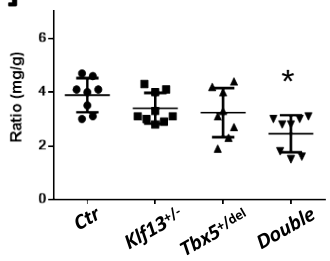

[C] FC

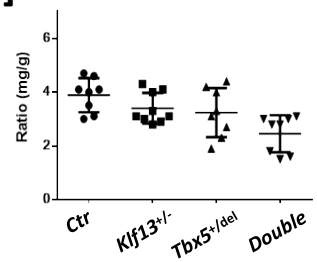

[D] PV

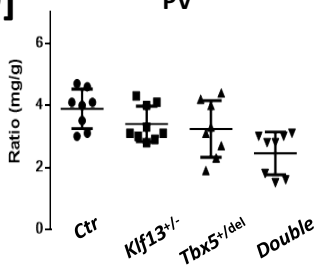

[E]

[F]

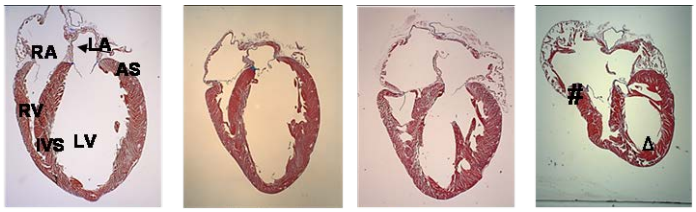

[G]

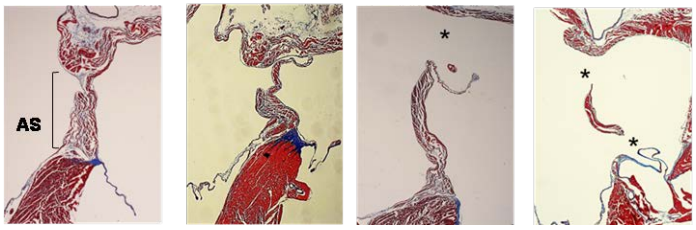

[H]

Genotype		ASD
Tbx5 $^{+/flox}$	*Klf13* $^{+/+}$	0/12
Tbx5 $^{+/flox}$	*Klf13* $^{+/-}$	1/20
Tbx5 $^{+/del}$	*Klf13* $^{+/+}$	6/12
Tbx5 $^{+/del}$	*Klf13* $^{+/-}$	15/19

Figure 4. 3: Reduced viability and higher frequency of cardiac defects in compound Tbx5$^{+/del}$ Klf13$^{+/-}$ heterozygotes adult mice.

A) Frequency of genotypes obtained from intercrossing *Tbx5*$^{flox/flox}$ with *Klf13*$^{+/-}$ CMV-Cre$^{+/-}$ mice at weaning. B-D) Echocardiography of *Tbx*5$^{+/del}$ *Klf13*$^{+/-}$ mice at 150 days of age. B-D) Echocardiography analysis assessing the cardiac function in the *Tbx5 Klf13* mutant mice. The parameters assessed were Ventricular Mass / Body Weight (LV/BW), Fractional Shortening (FS), and Pulmonary Valve Mean Gradient (PV), respectively. B) Shows a decrease in the ratio of Left Ventricular Mass / Body Weight (LV/BW) which is indicative of left ventricular hypotrophy (n=8 per group). * $P < 0.05$ in comparison to the control. E) Gross morphologies of freshly dissected hearts from 150 day-old control, *Klf13*$^{+/-}$, *Tbx5*$^{+/del}$, and *Tbx5*$^{+/del}$ *Klf13*$^{+/-}$ mice. Note how significantly smaller *Tbx5*$^{+/del}$ *Klf13*$^{+/-}$ hearts are with signs of right atrial hypertrophy. F-G) Trichrome staining of a frontal section from hearts of 150 day-old mice showing the normal septum in control and *Klf13*$^{+/-}$ hearts whereas *Tbx5*$^{+/del}$ and *Tbx5*$^{+/del}$ *Klf13*$^{+/-}$ hearts are afflicted with atrial septal defects (*). The *Tbx5*$^{+/del}$ *Klf13*$^{+/-}$ also exhibited signs of left ventricular hypotrophy (Δ). H) Quantitative analysis of the atrial septal defects frequency in the our genotypes. Note the increased incidents of ASDs in *Tbx5*$^{+/del}$ *Klf13*$^{+/-}$ mice in comparison to *Tbx5*$^{+/del}$. AS, Atrial Septum; RA, Right Atria; LA, Left Atria; IVS, Interventricualr Septum; LV, Left Ventricle; RV, Right ventricle.

[A]

Tbx5 $^{Flox/Flox}$ x ***CMV-Cre*** $^{+/-}$ ***Klf13*** $^{+/-}$

Genotype		Observed Frequency at E15.5	Observed Frequency at E11.5	Expected
Tbx5 $^{+/flox}$	*Klf13* $^{+/+}$	7 (25%)	10 (27.8%)	25%
Tbx5 $^{+/flox}$	*Klf13* $^{+/-}$	6 (22%)	8 (22.2%)	25%
Tbx5 $^{+/del}$	*Klf13* $^{+/+}$	7(25%)	8 (22.2%)	25%
Tbx5 $^{+/del}$	*Klf13* $^{+/-}$	8(28%)	10 (27.2%)	25%
		Total: 28	Total: 36	

[B]

[C]

[D]

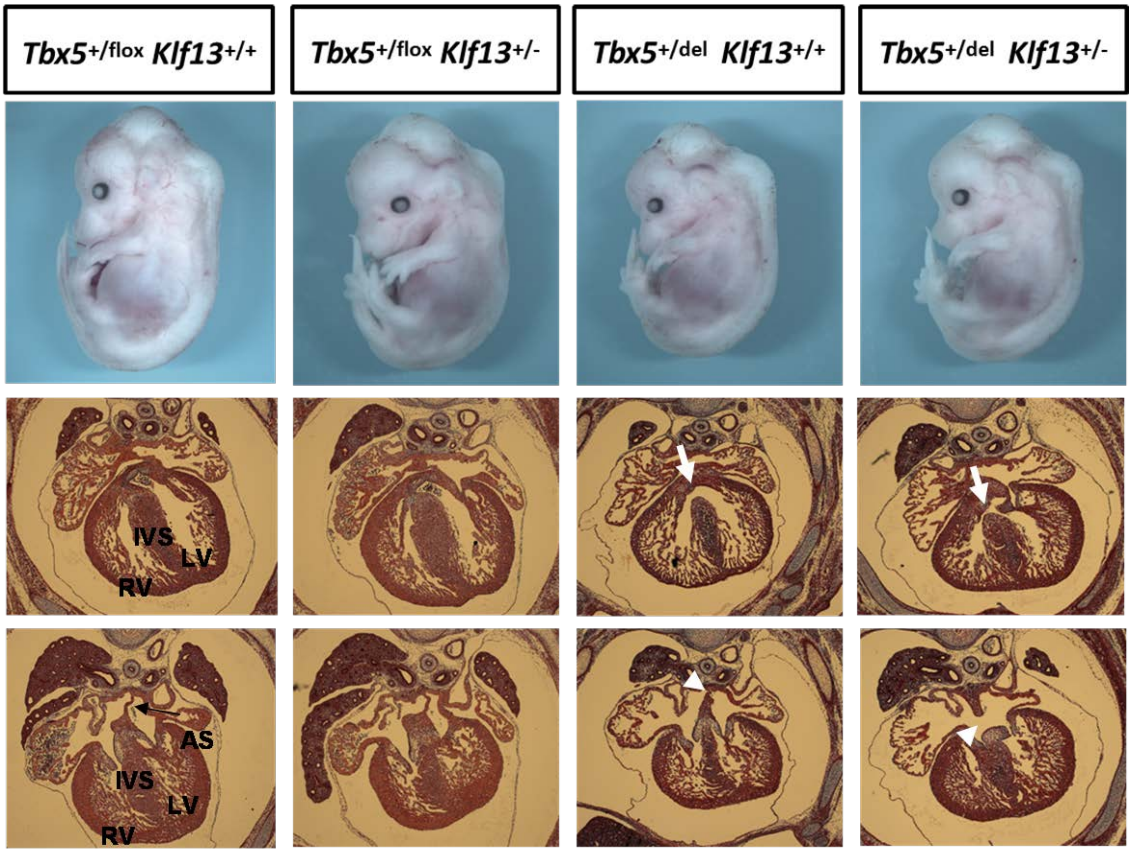

[E]

Genotype at E15.5		ASD	VSD
Tbx5 $^{+/}$	*Klf13* $^{+/+}$	0/7	0/7
Tbx5 $^{+/}$	*Klf13* $^{+/-}$	0/6	0/6
Tbx5	*Klf13* $^{+/+}$	3/7	3/7
Tbx5	*Klf13* $^{+/-}$	6/8	5/8

Figure 4. 4: Higher frequency of cardiac defects in compound *Tbx5*$^{+/del}$ *Klf13*$^{+/-}$ heterozygotes E15.5 embryos.

A) Frequency of genotypes obtained from intercrossing *Tbx5*$^{flox/flox}$ with *Klf13*$^{+/-}$ CMV-Cre$^{+/-}$ mice at E15.5 and E11.5. Note that no significant deviation was noticed between the genotypes. **B)** Representative images of E15.5 *Tbx5*$^{+/del}$ *Klf13*$^{+/-}$ heterozygotes as compared to their littermates. **C)** Coronal sections through E15.5 embryonic hearts at the level of the interventricular septum. In *Tbx5*$^{+/del}$ and *Tbx5*$^{+/del}$ *Klf13*$^{+/-}$ double heterozygotes, interventricular septation defects (white arrow) are demonstrated. Normal interventricular septation is seen in control and *Klf13*$^{+/-}$. **D)** Coronal sections through E15.5 embryonic hearts at the level of the atrial septum. Atrial septal defects (white arrow head) were found in hearts of *Tbx5*$^{+/del}$ and *Tbx5*$^{+/del}$ *Klf13*$^{+/-}$ double heterozygote embryos. AS, Atrial Septum; RA, Right Atria; LA, Left Atria; IVS, Interventricular Septum, LV, Left Ventricle; RV, Right ventricle. **D)** Table representing the frequency of cardiac abnormalities identified in each genotype at E15.5. ASD, atrial septal defect; VSD, ventricular septal defect.

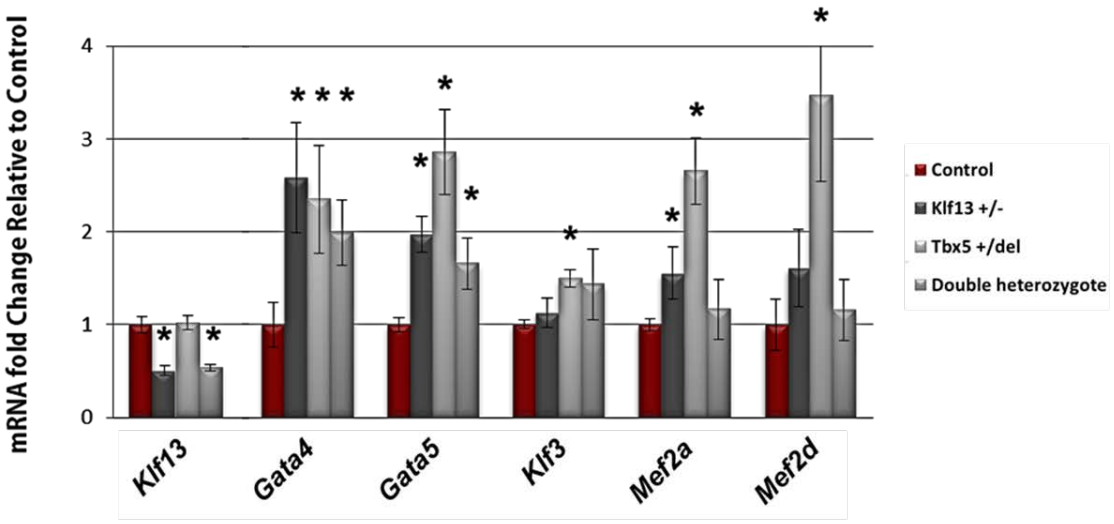
mRNA fold Change Relative to Control
Control
Klf13 +/-
Tbx5 +/del
Double heterozygote
Klf13
Gata4
Gata5
Klf3
Mef2a
Mef2d

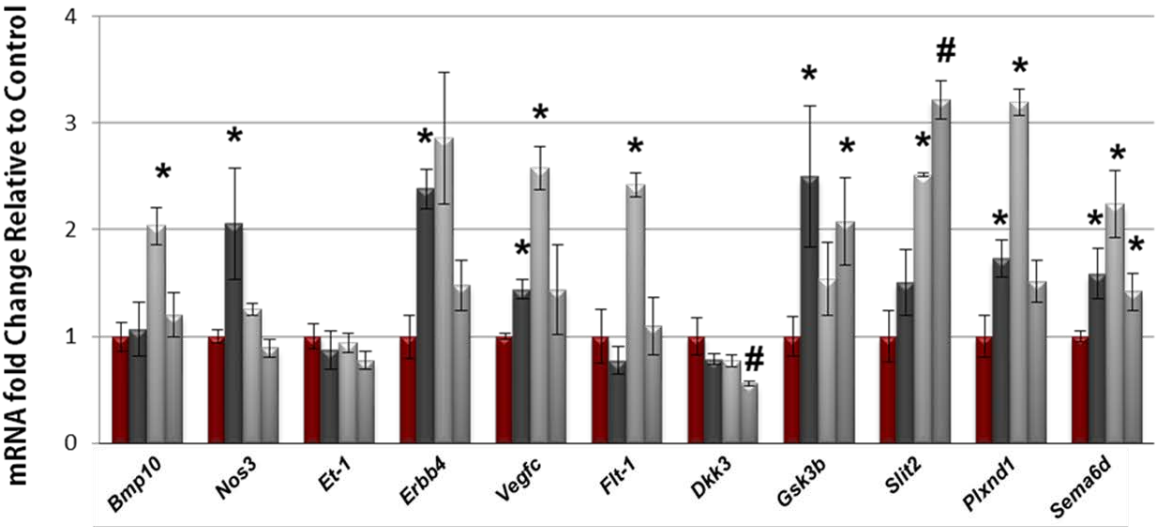
mRNA fold Change Relative to Control
Bmp10
Nos3
Et-1
Erbb4
Vegfc
Flt-1
Dkk3
Gsk3b
Slit2
Plxnd1
Sema6d

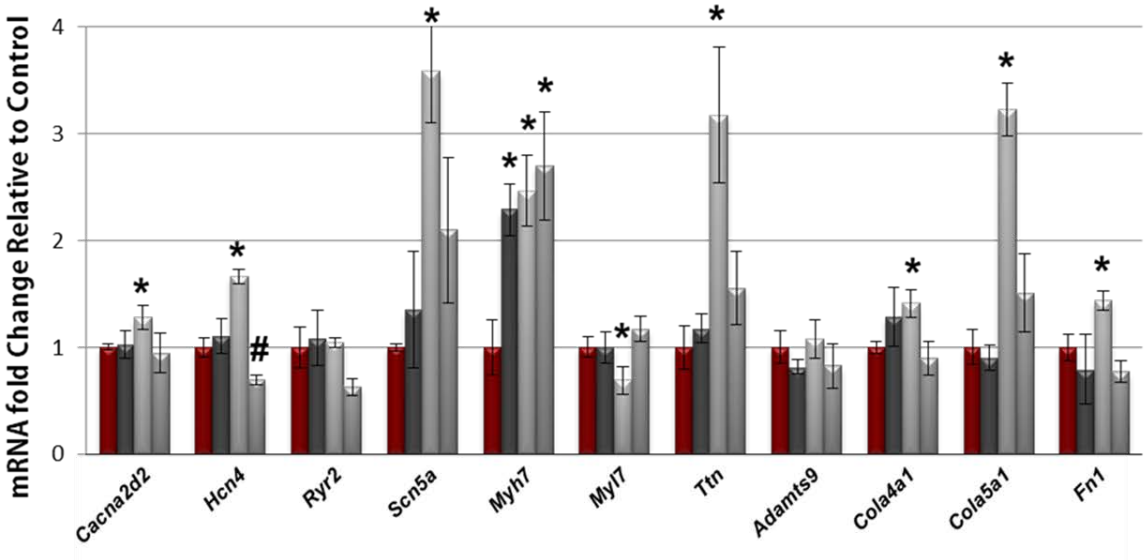
mRNA fold Change Relative to Control
Cacna2d2
Hcn4
Ryr2
Scn5a
Myh7
Myl7
Ttn
Adamts9
Cola4a1
Cola5a1
Fn1

Figure 4. 5: Quantitative real-time PCR comparing expression of selected cardiac genes in Klf13 and Tbx5 mutant embryos (E11.5-12.5).

QPCR analysis using RNA extracted from hearts of E11.5-12.5 mouse embryos. N=3-5 for each genotype. * $P < 0.05$ in comparison to the control. # $P < 0.05$ in comparison to *Tbx5* $^{+/del}$ and *Klf13* $^{+/-}$.

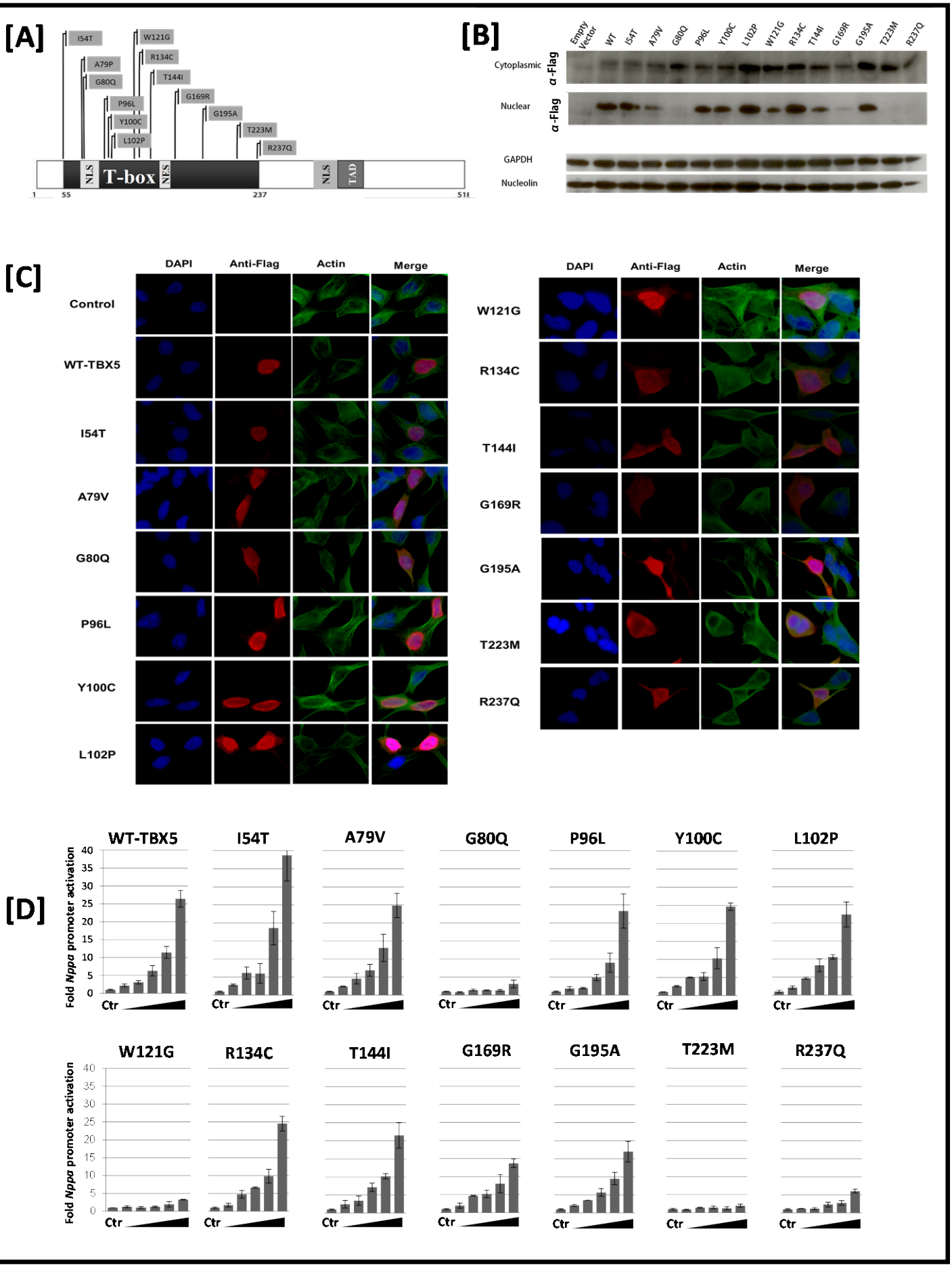
[A]
I54T
A79P
G80Q
P96L
Y100C
L102P
W121G
R134C
T144I
G169R
G195A
T223M
R237Q
NLS
T-box
NES
NLS
TAD
1
55
237
518
[B]
Empty Vector
WT
I54T
A79V
G80Q
P96L
Y100C
L102P
W121G
R134C
T144I
G169R
G195A
T223M
R237Q
Cytoplasmic
α-Flag
Nuclear
α-Flag
GAPDH
Nucleolin
[C]
DAPI
Anti-Flag
Actin
Merge
Control
WT-TBX5
I54T
A79V
G80Q
P96L
Y100C
L102P
W121G
R134C
T144I
G169R
G195A
T223M
R237Q
[D]
WT-TBX5
I54T
A79V
G80Q
P96L
Y100C
L102P
W121G
R134C
T144I
G169R
G195A
T223M
R237Q
Fold Nppa promoter activation
0
5
10
15
20
25
30
35
40
Ctr

Figure 4. 6: Functional analysis of CHD linked TBX5 point mutants.

A) Schematic representation of the Tbx5 protein structure showing the location of the germline mutations related to human incident CHDs. The majority of mutations are located in the DNA-binding domain of TBX5. Intronic and somatic (non-familial) mutations are not included. NLS: Nuclear localization signal, NES: Nuclear export signal, TAD: Transactivation domain. The mutations are located according to reference (1). B) Western blot showing the expression the expression and cellular localization of each of the TBX5 point mutant produced. 10μg of each of the plasmid expressing a mutant Flag-tagged-TBX5 were transfected into AD293 cells, and cellular extracts were prepared 48 h post-transfection. Expression of the proteins was monitored using an anti-Flag antibody. C) Immunocytochemistry staining for flag-tagged TBX5 point mutants showing their cellular localization. AD293 cells were transfected by 10μg of each of the Flag-TBX5 point mutant proteins indicated on the left side. The green color shows the Alexa 488 conjugated secondary antibodies against the anti-actin antibody. The red colour shows the Alexa 546 conjugated secondary antibodies against the anti-Flag antibody. The nuclei were visualized by Hoechst 33424 autofluorescence. Staining of cells transfected with the backbone pCDNA3 (empty vector) were used as background controls. D) The transcriptional activities of TBX5 point mutations on the Nppa promoter. Transfections were carried out using the -699bp *Nppa* promoter and increasing dosages (25, 50, 100, 200, and 400ng) of each point mutant. Each dosage was conducted in duplicate and the experiment was conducted twice. The data shown are for one representative experiment.

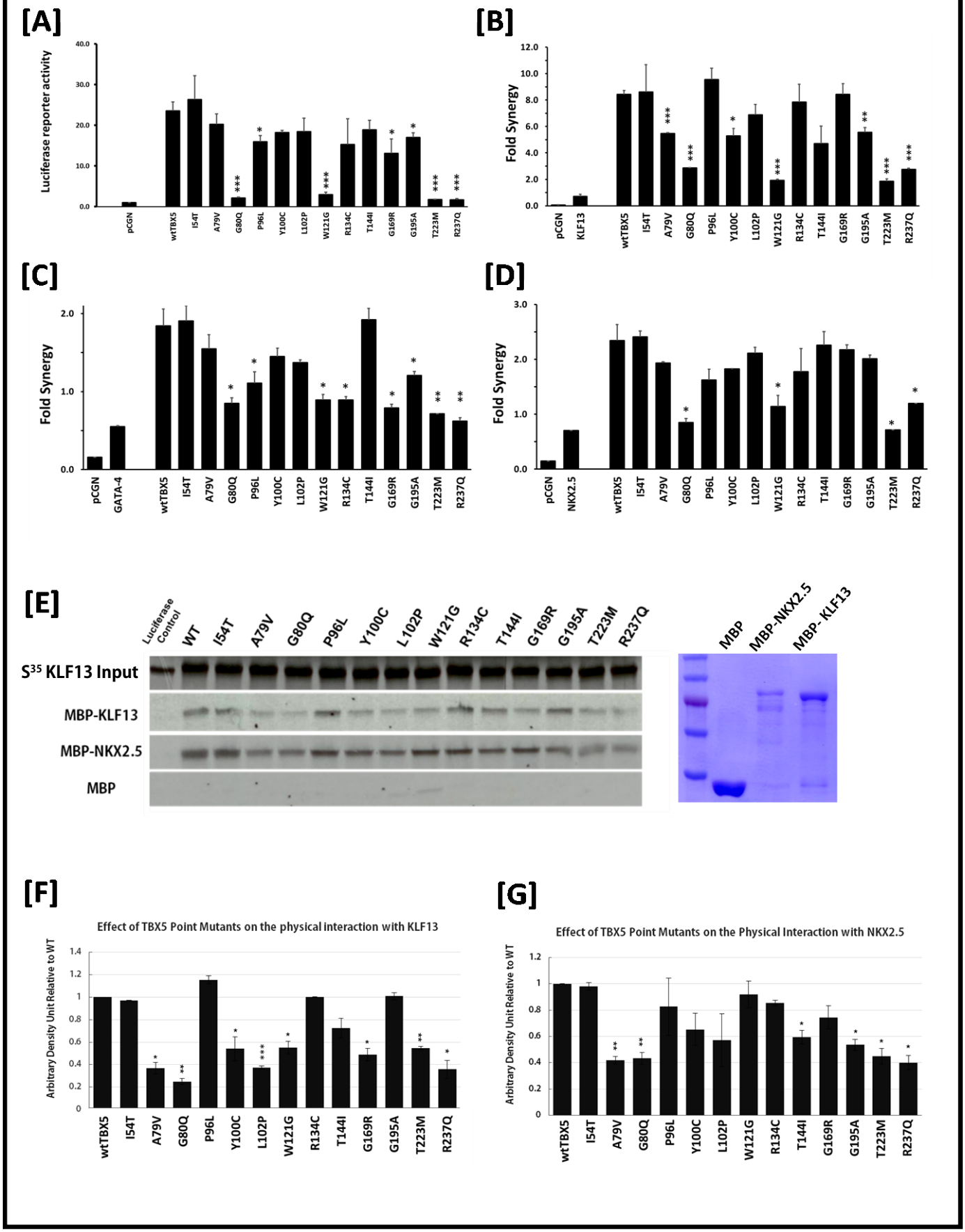
[A]
Luciferase reporter activity
pCGN
wtTBX5
I54T
A79V
G80Q
P96L
Y100C
L102P
W121G
R134C
T144I
G169R
G195A
T223M
R237Q
[B]
Fold Synergy
pCGN
KLF13
[C]
GATA-4
[D]
NKX2.5
[E]
Luciferase Control
WT
S35 KLF13 Input
MBP-KLF13
MBP-NKX2.5
MBP
MBP-NKX2.5
MBP- KLF13
[F]
Effect of TBX5 Point Mutants on the physical interaction with KLF13
Arbitrary Density Unit Relative to WT
[G]
Effect of TBX5 Point Mutants on the Physical Interaction with NKX2.5

Figure 4. 7: Effect of TBX5 point mutations on the on the interaction with KLF13, GATA4, and NKX2.5.

A-D) effects TBX5 point mutations on the on the synergy with KLF13, GATA4, and NKX2.5 on the *Nppa* promoter. Transfections were carried out using the -699bp *Nppa* promoter. In (A) TBX5 point mutants were co-transfected with the *Nppa* reporter, whereas in (B, C, and D) KLF13, GATA4, and NKX2.5 expression vectors was also included, respectively. The synergy results represent the ratio of promoter activation by TBX5 point mutants in the presence of its functional partner over the sum of promoter activation by TBX5 point mutants and their partners alone. Note that different dosages (25, 50, 100, 200, and 400ng) of each point mutant were also used. Each dosage was conducted in duplicate and the trend was confirmed at least in three dosages. The data shown are for one representative dosage. **E-G)** The effect of TBX5 point mutations on the physical interaction with KLF13 and NKX2.5**.** In vitro translated 35S radio-labelled TBX5 point mutants were incubated with MBP-KLF13, MBP-NKX2.5, or MBP proteins on Dextrin Sepharose beads. The bound TBX5 mutants were resolved by SDS/PAGE and revealed by autoradiography. Right panel is coomassie blue staining of SDS-PAGE gel showing the bacterially produced KLF13 and NKX2.4-MBP fusion proteins. F-G) Quantification analysis of the pull-down of TBX5 point mutants by KLF13 (F) and NKX2.5 (G). The quantification was carried on two radiographs using the open access program ImageJ. * $P < 0.05$ in comparison to the wild type TBX5.

4.5. Discussion

In this paper, we show that KLF13 and TBX5 are mutual cofactors and that they interact physically and functionally to synergistically activate expression of common downstream targets. Additionally, we find that loss of one *Klf13* allele in a *Tbx5* heterozygote genetic background potentiates the penetrance of *Tbx5*-dependent septal defects suggesting that *Klf13* is a genetic modifier of *Tbx5* in congenital heart disease.

We previously uncovered the functional importance of the KLF13 protein, a member of the kruppel-like factors (KLFs), during cardiac morphogenesis in the African clawed frog (*Xenopus laevis*). Knocking-down *Klf13* alleles in *Xenopus* embryos led to delayed cushion formation and valve maturation, septal defects, and hypotrabeculation, suggesting that the KLF13 protein is important for amphibian heart morphogenesis (16). Gene expression analysis using *Xenopus* embryos with *Klf13* loss of function, at stage 30 of development which is prior to the formation of the cardiac tube, indicated significant reduction in the gene expression of several cardiac specific transcription factors, including *Gata4*, *Gata5*, and *Tbx5*. Our present work suggests that KLF13 function in heart developmental is evolutionary conserved and that *KLF13* may be a CHD causing gene or a genetic modifier of CHD. Interestingly, whereas loss of one *Klf13* allele does not produce any overt structural or functional cardiac alteration, transcript analysis suggests significant alteration of gene expression that may not affect heart development or steady state heart function or that may reflect compensatory changes to loss of one *Klf13* allele. Nonetheless, combined loss of a *Klf13* and a *Tbx5* allele have profound consequences on postnatal viability as well as heart structure and function. These results have profound implications for human genetic studies and for deciphering genes whose alteration can cause CHD. In an independent study, we generated and analysed *Klf13* null mice. These mice are born at

reduced frequencies owing to severe heart defects due to abnormal endocardial cushion development. The surviving *Klf13*$^{-/-}$ mice have several partially penetrant structural cardiac abnormalities including aortic and atrio-ventricular septal defects. Consistent with a conserved role in heart development, heterozygous micro-deletion or duplication of the chromosomal band harboring *KLF13* (15q13.3) in human are associated with a wide range of cardiac defects that include Tetralogy of Fallot, mitral valve prolapse, and hypoplasia of the right side of the heart (26-28). Together with the work shown in this manuscript, the data strongly support an evolutionary conserved role for KLF13 in heart morphogenesis.

Several studies have correlated abnormal endocardial cushion cell proliferation and apoptosis to the aforementioned structural cardiac defects; however, the molecules and pathways regulating endocardial cell survival are not fully understood (13,29,30). In a previous study (13), we showed that TBX5 is a marker of a subset of endocardial cells destined to form the atrial septum and its loss of function is associated with excessive apoptosis and fully penetrant ASDs. On the other hand, in our unpublished report, KLF13 was shown to be robustly expressed in the endocardial cushions and its loss of function in mice was associated with altered endothelial-mesenchymal transformation (EMT) in the AV cushion with reduced endothelial cell proliferation and enhanced mesenchymal differentiation. KLF13 was also found to be a potent activator of cyclin D1/2 as well as VEGF which are important for cardiac cell proliferation (16). Taken together, we suggest that KLF13 and TBX5 genetic interaction plays an important role in regulating proper endocardial cushion development. Furthermore, our reported QPCR analysis using E11.5 showed an overlap among the transcripts that was disrupted by the heterozygote deletion of either Tbx5 or Klf13. Many of the affected transcripts were shown to be genes important for proper endocardial cushion development (Gata5, Mef2a, Erbb4, Vegfc, PlexinD1, and

Sema6D) (31-34). Interestingly, in the double mutant mice transcripts of Slit1 showed a significant upregulation and transcripts of Dickkopf3 (Dkk3) and Hcn4 were significantly downregulated in comparison to littermate controls. Interestingly, many members of the Slit and Dkk gene family were shown to be suppressors of Wnt/β-catenin signalling (35-40). The Wnt/β-catenin signaling pathway plays an important role in embryonic cardiac specification, cardiovascular progenitor expansion, endocardial cushion formation, and cardiomyocyte proliferation (41,42). While SLIT1 protein enhances β-catenin complex formation with E-cadherin, DKK3 reduces the cytoplasmic accumulation of β-catenin (35-38). Although the role of Dkk3 in cardiac development and the etiology of congenital heart disease is yet to be investigated (43), loss of function of Slit2 or Slit3 were associated with several congenital heart defects that were endocardial in nature (39,40). Our results support that Klf13 and Tbx5 participate in common cardiac genetic programmes that are important for proper endocardial cushion development and septation of the heart.

Concerning structure-function, the physical interaction between KLF13 and TBX5 was found to be mediated via the three zinc-finger domain and the T-box domain of KLF13 and TBX5, respectively. To our knowledge, this transcriptional interaction is the first one reported to date between the TBX and KLF families. However, TBX5 was shown to interact with other zinc-finger-containing transcription factors including GATA4 (a two C4-type zinc-finger-containing protein) and SALL4 (an eight C2H2-type zinc-finger-containing protein) (44-46). Similarly, TBX5 interaction with SALL4 and GATA4 was mediated by their zinc-finger domains - the first zinc-finger and second zinc-finger, respectively. However, while TBX5 - GATA4 interaction was mediated via the T-box domain of TBX5, TBX5 -SALL4 interaction was mediated by the C-terminal domain of TBX5 [28, 30, 46]. Interestingly, mutations in these two factors, GATA4 and SALL4, were also correlated with

cardiac septal defects similar to those found in Holt-Oram syndrome (46). Our report complements the previous reported combinatorial interactions between GATA4, KLF13, and TBX5 (47,48) and suggests that KLF13 and TBX5 might be involved in a multifactorial complex that controls cardiac gene expression by both direct protein-protein and protein-DNA interaction.

More than 60 single point or deletion mutations of human TBX5 are associated with Holt–Oram syndrome, and the majority are within the T-box domain (49,50). Mechanistically, the deleterious effect of some of the TBX5 mutations on the physical and functional interactions with GATA4 and NKX2.5 supported the existence of a tri-complex composed of the three TFs to regulate the expression of a subset of genes required for cardiac septal formation (44, 45, 51). Here we showed that among thirteen missense point mutations localized to the T-box domain and associated with Holt-Oram syndrome, at least nine (A79V, G80Q, Y100C, L102P, W121G, G169R, G195A, T223M, and R237Q) had reduced functional and/or physical interaction with KLF13. Interestingly, the majority of the mutants were also associated with other basic biochemical defects (nuclear localization, DNA-binding, and promoter activation) as well as defective interaction with NKX2.5 and GATA4. The effects of TBX5 mutations on interactions with KLF13, GATA4, and NKX2.5 support the existence of a multifactorial complex composed of these transcription factors to regulate the expression of a subset of genes required for cardiac septal formation. Analysis of TBX5 point mutations can function as a Rosetta Stone in understanding how disruption of the combinatorial interactions of transcription factors can lead to specific birth defects (48).

The mechanism of action of Klf13 as a genetic modifier of Tbx5 will need to be further clarified. However, notwithstanding the mechanistic uncertainty, the novel finding that a member of the KLF family is a co-factor of a T-domain protein involved in human congenital heart disease is important for developmental biology and translational medicine.

Acknowledgements

We are indebted to members of the Nemer Lab for discussions and interesting suggestions. We thank Drs Komati and Maharsy for advice and Janie Beauregard and Megan Fortier for technical assistance. We are grateful to the core histology facility at the University of Ottawa for expert help. This work is supported by grants from the Heart and Stroke Foundation of Canada, the Canadian Institute for Health Research and the McCain Family Foundation. RD was a Canada Vanier Scholar and Gregor Andelfinger a Clinician Scientist of the FRSQ, Quebec, Canada.

4.6. References:

1. Fahed,A.C., Gelb,B.D., Seidman,J.G. and Seidman,C.E. (2013) Genetics of congenital heart disease: the glass half empty. *Circ. Res.*, **112**, 707-720.

2. Bruneau,B.G. (2008) The developmental genetics of congenital heart disease. *Nature*, **451**, 943-948.

3. Lage,K., Greenway,S.C., Rosenfeld,J.A., Wakimoto,H., Gorham,J.M., Segre,A.V., Roberts,A.E., Smoot,L.B., Pu,W.T., Pereira,A.C. *et al.* (2012) Genetic and environmental risk factors in congenital heart disease functionally converge in protein networks driving heart development. *Proc Natl. Acad Sci U. S A*, **109**, 14035-14040.

4. Nemer,M. (2008) Genetic insights into normal and abnormal heart development. *J. Cardiovasc. Pathol.*, **17**, 48-54.

5. Wang,G.Z., Liu,J., Wang,W., Zhang,H.Y. and Lercher,M.J. (2011) A gene's ability to buffer variation is predicted by its fitness contribution and genetic interactions. *PLoS One*, **6**, e17650.

6. Basson,C.T., Bachinsky,D.R., Lin,R.C., Levi,T., Elkins,J.A., Soults,J., Grayzel,D., Kroumpouzou,E., Traill,T.A., Leblanc-Straceski,J. *et al.* (1997) Mutations in human TBX5 [corrected] cause limb and cardiac malformation in Holt-Oram syndrome. *Nat Genet*, **15**, 30-35.

7. Al-Qattan,M.M. and Abou Al-Shaar,H. (2015) Molecular basis of the clinical features of Holt-Oram syndrome resulting from missense and extended protein mutations of the TBX5 gene as well as TBX5 intragenic duplications. *Gene*, **560**, 129-136.

8. McDermott,D.A., Bressan,M.C., He,J., Lee,J.S., Aftimos,S., Brueckner,M., Gilbert,F., Graham,G.E., Hannibal,M.C., Innis,J.W. *et al.* (2005) TBX5 genetic testing validates strict clinical criteria for Holt-Oram syndrome. *Pediatr. Res.*, **58**, 981-986.

9. Bruneau,B.G., Nemer,G., Schmitt, J.P., Charron,F., Robitaille,L., Caron,S., Conner,D.A., Gessler,M., Nemer,M. *et al.* (2001) A murine model of Holt-Oram syndrome defines roles of the T-box transcription factor Tbx5 in cardiogenesis and disease. *Cell*, **106**, 709-721.

10. Mori,A.D., Zhu,Y., Vahora,I., Nieman,B., Koshiba-Takeuchi,K., Davidson,L., Pizard,A., Seidman,J.G., Seidman,C.E., Chen,X.J. *et al.* (2006) Tbx5-dependent rheostatic control of cardiac gene expression and morphogenesis. *Dev Biol.*, **297**, 566-586.

11. Garg,V., Kathiriya,I.S., Barnes,R., Schluterman,M.K., King,I.N., Butler,C.A., Rothrock,C.R., Eapen,R.S., Hirayama-Yamada,K., Joo,K. *et al.* (2003) GATA4 mutations cause human congenital heart defects and reveal an interaction with TBX5. *Nature*, **424**, 443-447.

12. Ghosh,T.K., Song,F.F., Packham,E.A., Buxton,S., Robinson,T.E., Ronksley,J., Self,T., Bonser,A.J. and Brook,J.D. (2009) Physical interaction between TBX5 and MEF2C is required for early heart development. *Mol Cell Biol.*, **29**, 2205-2218.

13. Nadeau,M., Georges,R.O., Laforest,B., Yamak,A., Lefebvre,C., Beauregard,J., Paradis,P., Bruneau,B.G., Andelfinger,G. and Nemer,M. (2010) An endocardial pathway involving Tbx5, Gata4, and Nos3 required for atrial septum formation. *Proc Natl. Acad Sci U. S A*, **107**, 19356-19361.

14. Maitra,M., Schluterman,M.K., Nichols,H.A., Richardson,J.A., Lo,C.W., Srivastava,D. and Garg,V. (2009) Interaction of Gata4 and Gata6 with Tbx5 is critical for normal cardiac development. *Dev Biol.*, **326**, 368-377.

15. Hayek,S. and Nemer,M. (2011) Cardiac natriuretic peptides: from basic discovery to clinical practice. *Cardiovasc. Ther.*, **29**, 362-376.

16. Lavallée,G., Andelfinger,G., Nadeau,M., Lefebvre,C., Nemer,G., Horb,M. and Nemer,M. (2006) The Kruppel-like transcription factor KLF13 is a GATA-4 collaborator for heart development. *EMBO J*, **25**, 5201-5213.

17. Laforest,B., Andelfinger,G. and Nemer,M. (2011) Loss of Gata5 in mice leads to bicuspid aortic valve. *J Clin. Invest*, **121**, 2876-2887.

18. Yamak,A., Georges,R.O., Sheikh-Hassani,M., Morin,M., Komati,H. and Nemer,M. (2015) Novel exons in the tbx5 gene locus generate protein isoforms with distinct expression domains and function. *J Biol. Chem.*, **290**, 6844-6856.

19. Yamak,A., Latinkic,B.V., Dali,R., Temsah,R. and Nemer,M. (2014) Cyclin D2 is a GATA4 cofactor in cardiogenesis. *Proc Natl. Acad Sci U. S A*, **111**, 1415-1420.

20. Georges,R., Nemer,G., Morin,M., Lefebvre,C. and Nemer,M. (2008) Distinct expression and function of alternatively spliced Tbx5 isoforms in cell growth and differentiation. *Mol. Cell. Biol.*, **28**, 4052-4067.

21. Zhu,Y., Gramolini,A.O., Walsh,M.A., Zhou,Y.Q., Slorach,C., Friedberg,M.K., Takeuchi,J.K., Sun,H., Henkelman,R.M., Backx,P.H. *et al.* (2008) Tbx5-dependent pathway regulating diastolic function in congenital heart disease. *Proc Natl Acad Sci U. S A*, **105**, 5519-5524.

22. Xie,L., Hoffmann,A.D., Burnicka-Turek,O., Friedland-Little,J.M., Zhang,K. and Moskowitz,I.P. (2012) Tbx5-hedgehog molecular networks are essential in the second heart field for atrial septation. *Dev Cell*, **23**, 280-291.

23. Garg,V., Kathiriya,I.S., Barnes,R., Schluterman,M.K., King,I.N., Butler,C.A., Rothrock,C.R., Eapen,R.S., Hirayama-Yamada,K., Joo,K. *et al.* (2003) GATA4 mutations cause human congenital heart defects and reveal an interaction with TBX5. *Nature*, **424**, 443-447.

24. Stirnimann,C.U., Ptchelkine,D., Grimm,C. and Muller,C.W. (2010) Structural basis of TBX5-DNA recognition: the T-box domain in its DNA-bound and -unbound form. *J Mol Biol.*, **400**, 71-81.

25. Zaragoza,M.V., Lewis,L.E., Sun,G., Wang,E., Li,L., Said-Salman,I., Feucht,L. and Huang,T. (2004) Identification of the TBX5 transactivating domain and the nuclear localization signal. *Gene*, **330**, 9-18.

26. van Bon,B.W., Mefford,H.C., Menten,B., Koolen,D.A., Sharp,A.J., Nillesen,W.M., Innis,J.W., de Ravel,T.J., Mercer,C.L., Fichera,M. *et al.* (2009) Further delineation of the 15q13 microdeletion and duplication syndromes: a clinical spectrum varying from non-pathogenic to a severe outcome. *J Med Genet*, **46**, 511-523.

27. Lepichon,J.B., Bittel,D.C., Graf,W.D. and Yu,S. (2010) A 15q13.3 homozygous microdeletion associated with a severe neurodevelopmental disorder suggests putative functions of the TRPM1, CHRNA7, and other homozygously deleted genes. *Am J Med Genet A*, **152A**, 1300-1304.

28. Derwinska,K., Bartnik,M., Wisniowiecka-Kowalnik,B., Jagla,M., Rudzinski,A., Pietrzyk,J.J., Kawalec,W., Ziolkowska,L., Kutkowska-Kazmierczak,A., Gambin,T. *et al.* (2012) Assessment of the role of copy-number variants in 150 patients with congenital heart defects. *Med Wieku. Rozwoj.*, **16**, 175-182.

29. Abdelwahid, E., Rice, D., Pelliniemi, L.J. and Jokinen, E. (2001) Overlapping and differential localization of Bmp-2, Bmp-4, Msx-2 and apoptosis in the endocardial cushion and adjacent tissues of the developing mouse heart. *Cell Tissue Res*, **305**, 67-78.

30. Keyes, W.M. and Sanders, E.J. (2002) Regulation of apoptosis in the endocardial cushions of the developing chick heart. *Am J Physiol Cell Physiol*, **282**, C1348-1360.

31. Dor, Y., Camenisch, T.D., Itin, A., Fishman, G.I., McDonald, J.A., Carmeliet, P. and Keshet, E. (2001) A novel role for VEGF in endocardial cushion formation and its potential contribution to congenital heart defects. *Development*, **128**, 1531-1538.

32. Nemer, G. and Nemer, M. (2002) Cooperative interaction between GATA5 and NF-ATc regulates endothelial-endocardial differentiation of cardiogenic cells. *Development*, **129**, 4045-4055.

33. Laforest, B., Andelfinger, G. and Nemer, M. (2011) Loss of Gata5 in mice leads to bicuspid aortic valve. *The Journal of Clinical Investigation*, **121**, 2876-2887.

34. Gitler, A.D., Lu, M.M. and Epstein, J.A. (2004) PlexinD1 and Semaphorin Signaling Are Required in Endothelial Cells for Cardiovascular Development. *Developmental Cell*, **7**, 107-116.

35. Das, D.S., Wadhwa, N., Kunj, N., Sarda, K., Pradhan, B.S. and Majumdar, S.S. (2013) Dickkopf Homolog 3 (<italic>DKK3</italic>) Plays a Crucial Role Upstream of

WNT/β-CATENIN Signaling for Sertoli Cell Mediated Regulation of Spermatogenesis. *PLoS ONE*, **8**, e63603.

36. Yue, W., Sun, Q., Dacic, S., Landreneau, R.J., Siegfried, J.M., Yu, J. and Zhang, L. (2008) Downregulation of Dkk3 activates β-catenin/TCF-4 signaling in lung cancer. *Carcinogenesis*, **29**, 84-92.

37. Dickinson, R.E. and Duncan, W.C. (2010) The SLIT–ROBO pathway: a regulator of cell function with implications for the reproductive system. *Reproduction*, **139**, 697-704.

38. Biankin, A.V., Waddell, N., Kassahn, K.S., Gingras, M.-C., Muthuswamy, L.B., Johns, A.L., Miller, D.K., Wilson, P.J., Patch, A.-M., Wu, J. *et al.* (2012) Pancreatic cancer genomes reveal aberrations in axon guidance pathway genes. *Nature*, **491**, 399-405.

39. Mommersteeg, M.T., Yeh, M.L., Parnavelas, J.G. and Andrews, W.D. (2015) Disrupted Slit-Robo signalling results in membranous ventricular septum defects and bicuspid aortic valves. *Cardiovasc Res*, **106**, 55-66.

40. Medioni, C., Bertrand, N., Mesbah, K., Hudry, B., Dupays, L., Wolstein, O., Washkowitz, A.J., Papaioannou, V.E., Mohun, T.J., Harvey, R.P. *et al.* (2010) Expression of Slit and Robo Genes in the Developing Mouse Heart. *Developmental dynamics : an official publication of the American Association of Anatomists*, **239**, 3303-3311.

41. Klaus, A., Saga, Y., Taketo, M.M., Tzahor, E. and Birchmeier, W. (2007) Distinct roles of Wnt/β-catenin and Bmp signaling during early cardiogenesis. *Proceedings of the National Academy of Sciences*, **104**, 18531-18536.

42. Combs, M.D. and Yutzey, K.E. (2009) Heart Valve Development: Regulatory Networks in Development and Disease. *Circulation Research*, **105**, 408-421.

43. Bao, M.-W., Cai, Z., Zhang, X.-J., Li, L., Liu, X., Wan, N., Hu, G., Wan, F., Zhang, R., Zhu, X. *et al.* (2015) Dickkopf-3 protects against cardiac dysfunction and ventricular remodelling following myocardial infarction. *Basic Res Cardiol*, **110**, 1-17.

44. Basson, C.T. (1997) Mutations in human TBX5 cause limb and cardiac malformation in Holt-Oram syndrome. *Nature Genet.*, **15**, 30-35.

45. Basson, C.T. (1999) Different TBX5 interactions in heart and limb defined by Holt-Oram syndrome mutations. *Proc. Natl Acad. Sci. USA*, **96**, 2919-2924.

46. Koshiba-Takeuchi, K., Takeuchi, J.K., Arruda, E.P., Kathiriya, I.S., Mo, R., Hui, C.-c., Srivastava, D. and Bruneau, B.G. (2006) Cooperative and antagonistic interactions between Sall4 and Tbx5 pattern the mouse limb and heart. *Nat Genet*, **38**, 175-183.
47. Lavallee, G., Andelfinger, G., Nadeau, M., Lefebvre, C., Nemer, G., Horb, M.E. and Nemer, M. (2006) The Kruppel-like transcription factor KLF13 is a novel regulator of

heart development. *EMBO J*, **25**, 5201-5213.

48. Garg, V., Kathiriya, I.S., Barnes, R., Schluterman, M.K., King, I.N., Butler, C.A., Rothrock, C.R., Eapen, R.S., Hirayama-Yamada, K., Joo, K. *et al.* (2003) GATA4 mutations cause human congenital heart defects and reveal an interaction with TBX5. *Nature*, **424**, 443-447.

49. Stirnimann, C.U., Ptchelkine, D., Grimm, C. and Müller, C.W. (2010) Structural Basis of TBX5–DNA Recognition: The T-Box Domain in Its DNA-Bound and -Unbound Form. *Journal of Molecular Biology*, **400**, 71-81.

50. Zaragoza, M.V., Lewis, L.E., Sun, G., Wang, E., Li, L., Said-Salman, I., Feucht, L. and Huang, T. (2004) Identification of the TBX5 transactivating domain and the nuclear localization signal. *Gene*, **330**, 9-18.

51. Ghosh, T.K., Song, F.F., Packham, E.A., Buxton, S., Robinson, T.E., Ronksley, J., Self, T., Bonser, A.J. and Brook, J.D. (2009) Physical Interaction between TBX5 and MEF2C Is Required for Early Heart Development. *Mol. Cell. Biol.*, **29**, 2205-2218.

5. Discussion:

In this thesis we show that KLF13, a member of the kruppel-like factors (KLFs) family, is important for the proper development of the heart. Mice lacking both *Klf13* alleles are born at reduced frequency and are afflicted with severe heart defects that could be endocardial or myocardial in nature. We also report that *Klf13* gives rise to two KLF13 isoforms (i.e., KLF13a and KLF13b) through the use of an alternative transcription start site (TSS). The two isoforms have distinct biochemical properties and spatiotemporal expression. We also identified TBX5, NKX2.5, and PEX1 as novel transcriptional partners of KLF13. Furthermore, we uncovered a role for *Klf13* as a genetic modifier for the septal defects associated with *Tbx5* heterozygosity.

5.1. Kruppel like transcription factors and Cardiac development

Identifying the molecular and genetic pathways important for heart development and the causes of CHD are still a challenging puzzle. Dissection of the cis-elements that control the complex spatiotemporal cardiac gene expression is important in deciphering the molecular mechanisms controlling cardiac-development. Analysis of several cardiac promoters revealed the presence of CACCC boxes (putative binding sites of the KLF family) within their regulatory domains. Among these promoters are those of the genes *Nppa*, *Nppb*, Myh7, and cardiac troponin C (cTnC) (34). The presence of these putative sites suggests a regulatory function for the KLF family in the heart. Our lab was first in describing the role of a KLF member, KLF13, during cardiac development by reporting KLF13's contribution to *Nppb* gene regulation and Xenopus cardiogenesis (34). The knockdown of *Klf13* in *Xenopus* embryos leads to a cardiac phenotype with ventricular

hypotrabeculation, atrial septal defects, delayed atrioventricular cushion formation and maturation of valves. Interestingly, microdeletion/microduplication of the chromosomal region 15q13.3 in human, which contains *Klf13* is also associated with human cardiac malformations (194). Here we show that KLF13 loss of function is embryonically lethal in mice and surviving mice are afflicted with endocardial cushion related defects that include "Goose-neck" deformity, AV valvular anomalies, and patent foramen ovale. Surviving *Klf13*$^{-/-}$ mice have several structural cardiac abnormalities and the expression of several genes involved in epithelial-mesenchymal transformation (EMT) is altered. Embryonically, the endocardium in these mutant mice have altered EMT with reduced endothelial cell proliferation and excessive mesenchymal differentiation in the AV cushion. Noteworthy, our RNA sequencing analysis of E11.5 mouse embryonic heart, showed that *Klf13* knock-out hearts are associated with dysregulated expression of several endocardial cushions genes (e.g. *Nos3, Tbx20, Jag1/2*) as well as genes important for cell migration and adhesion (e.g. *Adamts, Bmpr2, Notch1/2, Fibrillin, Erbb4, VEGF, Flt1*, and *Elk4*), actin cytoskeleton organization, and microtubule organizing center. These dysregulated processes ascertain our finding of altered EMT and implicate cellular migration and adhesion as one possible mechanism for the associated endocardial cushion defects. Our results support an evolutionary conserved role for *Klf13* in cardiac morphogenesis.

Recently, two other members of the KLF family, KLF2(191) and KLF3(192), were reported to have a role during cardiac development and were specifically correlated with endocardial cushion defects. Knockdown of klf2a in zebrafish, a homolog of KLF2 in mouse and human, using morpholino antisense oligonucleotides (MOs) was associated with valvular dysgenesis characterized with thicker and less flexible valves and increased regurgitation (224). In mice, KLF2 loss of function was associated with atrial septal defects

and abnormal EMT in the endocardial cushions of the AV canal (191). On the other hand, the role of KLF3 was recognized in a screen for dominant mutations affecting cardiovascular function in N-ethyl-N-nitrosourea (ENU) mutagenized mice. Loss of KLF3 function was correlated with various defects including ventricular and atrial septal defects, abnormal thickness and disorganization of the ventricular and septal myocardium, and abnormal hyperplasia of atrioventricular cushion tissue. Noteworthy, our RNA sequencing analysis of the *Klf13* knock-out embryos showed a significant decrease in both the transcripts of Klf3 and Klf7 (0.6 and 0.75 reduction) in comparison to control embryos. In light of these recent reports, our results emphasize the role of the KLF family as important regulators of endocardial cushion development.

5.2. The transcriptional activities of KLF13

The Sp1-like/KLF family is characterized by the presence of three Cys2/His2 zinc fingers that bestow preferential binding to GC/GT rich sequences in gene promoters and enhancer regions in order to mediate activation and/or repression of transcription (187,188). On the other hand, members of the KLFs diverge beyond their zinc finger domain. The heterogeneity beyond the zinc finger domain, especially that of the N-terminal domain, may explain in part the diverse biochemical mechanisms by which KLFs regulate transcription, which, together with their specific spatiotemporal expression can explain their influence on diverse cellular processes (187,195). Several activation and repression domains that interact with various co-activators and co-repressors, determined by the cellular environment, were localized within the amino-terminal region in several KLFs. Here we report that KLF13

contains at least three transactivation domains (TAD); two within the N-terminal domain (TAD1: AA1-67 and TAD2:AA67-147) and one in the C-terminal (TAD3) at AA 250-288. It is worth mentioning that while KLF13 acts as an activator on many promoters including *Nppa*, *Nppb*, *Sv40*, *Hbg*, and *Sm22a* (34,189,208,211), it also acts as a repressor for low density lipoprotein receptor (*Ldlr*) and cytochrome P450 1A1 (*Cyp1a1*) promoters in vitro (189). Thus, it is most likely that the transcriptional activities of KLF13 are cell and promoter context dependent. Several members of the Sp1-like/KLF family were identified as having bi-functional activities by interacting with different co-repressors or co-activators to regulate transcription.

The endocardial defects associated with KLF2, KLF3, and KLF13 loss of function in mice are indicative of a convergent role for the KLF/Sp family in regulating endocardial gene expression. The existence of multiple KLF proteins with distinct spatiotemporal expression, diverse biochemical interactions, and preferential binding to GC/GT rich sequences grant the nucleus a bio-molecular rheostat to control gene expression at each stage of cardiac development. For example, while Sp1 and KLF13 can activate the *Nppa* promoter in cardiomyocytes, Sp3 has opposing negative effects on *Nppa* expression (34,225). In addition, while KLF13 was shown to potentiate GATA transactional activities on several cardiac promoters (34), KLF15 repressed GATA4 DNA-binding and its transcriptional activity (226). The distinct biochemical properties of the KLF family not only allow them to regulate a distinct subset of genes, but also to participate in the divergent regulation of the same gene (195). In addition, we report that KLF13 is implicated in an additional layer of gene regulation during development via isoform production. The isoforms, KLF13a and KLF13b, have differential expression during development as well as distinct cellular and target promoter activity. They are the results of the use of alternative

promoters and first exons. Although KLF13b lacks all KLF13a N-terminal TADs, it was able to translocate to the nucleus, bind DNA, and activate transcription possibly through a similar or distinct mechanism to KLF13a. Furthermore, KLF13b was able to support some but not all physical or functional interactions with KLF13a co-activators (e.g. GATA4 and TBX5). Thus, the production of distinct isoforms may serve as a bio-molecular transistor to control *Klf13* gene activities. Interestingly, while our knock out mice were generated by the targeted deletion of the common exon 2 and thus knocking out both isoforms, Gordon *et al* generated their *Klf13* knock out mice by the targeted deletion of exon 1a and thus only deleting KLF13a. While Gordon *et al* knock out mice were produced with the expected Mendelian ratio, they reported that fewer mice were present at weaning (213). Phenotypically, their mice were characterized by splenomegaly, modified Erythropoiesis, and enlarged hearts. On the other hand, our knock out model mice were born at reduced frequency owing to severe congenital heart defects. The earlier onset of death and our congenital heart defects might be due to the additional loss in KLF13b function. Interestingly, the production of isoforms with differential functions and distinct effects on gene expression is not unique to KLF13. The best studied example is that of *Klf6* - while KLF6 acts as a classic tumor suppressor, the nuclear localization signal lacking isoform KLF6 SV1 exhibits an opposite effect on cell proliferation, colony formation, and invasion (197). Other KLF family members that have been reported to exist as different isoforms include KLF4, 5, 7, 8, 10 and 12 (197,227,228). Thus, the importance of KLF13 isoform production may extend to other organs beyond the heart and may be worth further investigation.

5.3. Identification of new KLF13 transcriptional partners.

The morphological changes that take place during cardiac development require the proper expression of different structural, metabolic, regulatory, and signaling genes (229). The use of experimental animals in genetic screens, expression analysis, transgenic and knockout models, and transplantation/ablation studies was indispensable to the discovery and the investigation of many genes essential for cardiac development. Transcription factors are major regulators of embryonic developmental processes by virtue of controlling the genetic programs proper to the different stages of development. A wealth of knowledge was collected from the identification of transcription factors linked to CHDs. Two patterns emerged from the associated defects: first, the defects are polygenic in nature meaning that a given structural defect is often linked to more than one locus; second, the mutation-linked genes are polymorphic - they are linked to multiple cardiac defects. These patterns can be explained by the overlap in function and spatiotemporal expression and the combinatorial interaction between transcription factors during cardiac development. The aforementioned explanation provided the framework for the discovery of the importance of KLF13 during cardiac development. During cardiac development in *Xenopous*, KLF3 and GATA4 expression overlap at the heart tube stage in both the myocardial and endocardial cells (34). This overlap, together with KLF13 functional and physical interaction with GATA4 on several cardiac promoters including *Nppa*, suggested that both are part of the regulatory network required for early stages of cardiogenesis. The importance of KLF13 was supported by the phenotype associated with its knockdown in *Xenopus*, which produced atrial septal defects, hypotrabeculation, and hypoplastic myocardium.

In a step towards analyzing KLF13's mechanism of action and deciphering its role in the genetic networks regulating cardiac development, we pursued the identification of the

factor(s) that might cooperate with KLF13 on the *Nppa* promoter. Our use of *Nppa* as the primary model with which to study KLF13's cardiac-specific transcription was prompted by its early expression during development and its atrial co-prevalence with KLF13. We found three KLF13 binding sites (centered at -365, -515 and -535) on the *Nppa* promoter were juxtaposed to several cardiac response elements including GATA, PERE, NKE, and TBE. Using a candidate approach based on the overlap in spatiotemporal expression during cardiac development as well as associated cardiac defects upon loss of function, we tested for possible cooperation of KLF13 with TBX5, NKX2.5, and PEX1. KLF13 was able to synergistically activate the *Nppa* promoter in the presence of the cardiac transcription factors GATA4, TBX5, NKX2.5, and PEX1 (**Figure 5. 1**). A direct physical interaction was also shown between KLF13 and TBX5, NKX2.5 and PEX1. Interestingly, the loss of function in either TBX5 or NKX2.5 was associated with similar septal defects and reduced heart mass as to those seen with KLF13 loss-of-function (214). Thus, our results show that KLF13 is an important member of the genetic network that patterns the embryonic heart. The interaction of KLF13 with other members of the GATA, TBX and NKX families in the context of other organs is worth investigating. For example, KLF13 is co-expressed with other members of the NK family including NKX2.1 in T-cells (230) and NKX6.1 and NKX2.2 in the brain (231). Thus cooperativity between KLF13 and NK proteins may extend to other organs beyond the heart and may be worth further investigation.

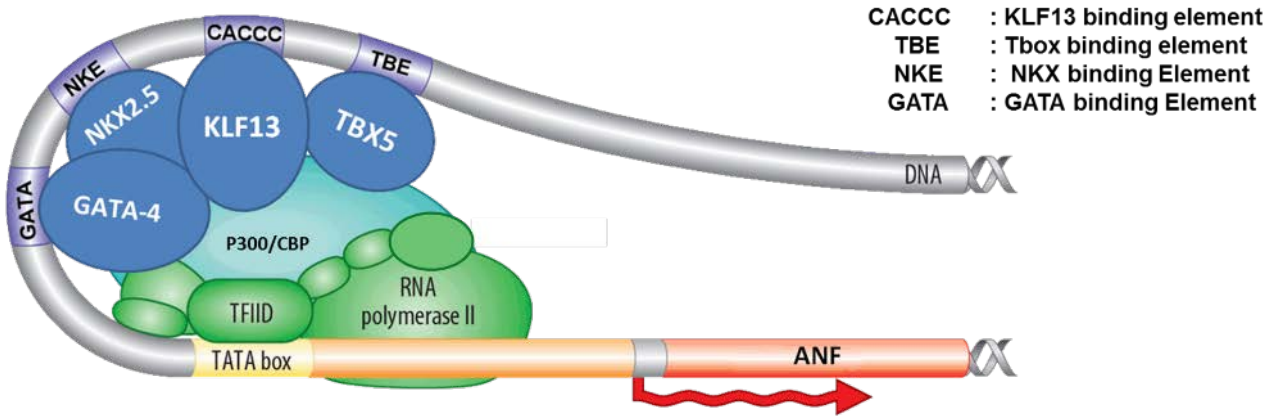

Figure 5. 1: A hypothetical model for the molecular mechanism of KLF13 synergy with the transfection factors NKX2.5, TBX5, and GATA-4. The model illustrates the bridging functionality of p300/CBP. In addition, the figure shows the acetylation of several residues in NKX2.5, GATA-4 and KLF13.

5.4. Klf13 as a genetic modifier for congenital heart diseases.

Cardiac defects often display variable penetrance and expressivity due to the influence of modifier genes as well as the contribution of non-genetic factors including environmental exposures, epigenetics, and stochastic effects (232). Epidemiological analysis suggests that genetic factors are the predominant cause of variable penetrance and expressivity in CHD (233). For example, variable penetrance and expressivity is observed at the level of autosomal dominant diseases such as Holt-Oram Syndrome (HOS), linked to the *Tbx5* gene, where the associated cardiac manifestation among affected family members can vary from asymptomatic conduction system defects to severe structural anomalies (12). Unfortunately the genetic basis of CHD is known for only minority of afflicted patients (less than 25%)(234). Therefore, the discovery of genes linked with CHD remains an important and clinically relevant endeavor. Here, we show that compound haploinsufficiency of *Klf13* and *Tbx5* alleles is associated with higher mortality and an increased incidence of atrial septal defects. The increased incidence in ASD point to *Klf13* as a candidate modifier gene for atrial septal defects in mice. Of note, the incomplete penetrance of ASD, points to an additional regulatory factors influencing both *Klf13* and *Tbx5*. Although not reported here, we also found that *Klf13* is a genetic modifier for bicuspid aortic valves associated with *Gata5* mutant mice. A buffering model might explain the penetrance variability of CHD in which a compensatory mechanism might exist through the function of a second allele, a duplicated gene, a pathway that maintains residual function, and/or from epigenetic and environmental mechanisms. For example, we previously showed that injection of GATA4 RNA rescued the cardiac defects in KLF13 knockdown embryos in a dose-dependent manner (34). However, a buffering capacity and tolerant window of loss of function of a particular gene becomes narrower by increased

mutation loading on different components of a particular network. We hypothesize that the loss of tolerance window is the cause of the increased septal defects associated with *Klf13 Tbx5* double heterozygote mice.

5.5. Conclusion and future studies

In the current study, using *in vivo* and *in vitro* approaches, we examined KLF13's mechanisms of action and the cardiac defects associated with its loss of function in mouse. Variable cardiac phenotypes were observed in Klf13 null mice and most were endocardial cushion defects including "Goose-neck" deformity and atrioventricular (AV) valvular abnormalities. Furthermore, epithelial-mesenchymal transformation (EMT) was found to be altered in these mice with reduced endothelial cell proliferation and dysregulated EMT regulatory genes. Further analysis is needed to establish the exact nature of these defects and whether it is due to defective myocardium, endocardium, or cardiac jelly. An *ex vivo* collagen gel assay is a relatively quick method to ascertain our findings of altered EMT with abnormal cellular migration and adhesion as a possible mechanism for the associated endocardial cushion defects (235). Furthermore, a modified method that uses pre-EMT endocardial cells from E9.0 embryos might be useful to study endocardial cell EMT in isolation of myocardial signaling defects (236). Long term goals would be to generate a tissue-specific deletion mouse model to decipher the tissue specific role of *Klf13* in the development of the endocardium and the myocardium. Furthermore, it would be interesting to examine the postnatal role of *Klf13* in the heart following angiotensin II (Ang II) infusion. This is of a particular interest as loss of function of the family member *Klf15* in mice is associated with the development of severe heart failure and aortopathy in response to stress.

Here we also report that alternate promoter usage gives rise to two KLF13 isoforms, KLF13a and KLF13b, which have distinct spatiotemporal distribution and biochemical properties. The isoforms share 2 of the 3 zinc finger domains but diverge in their N-terminal regions. Elucidating the specific function of KLF13 isoforms will require an isoform specific deletion or inducible disruptions of *Klf13* isoforms. Beside the heart, it would be interesting to evaluate the effect of KLF13b loss of function in tissues that were previously effected by KLF13a loss of function such as the hematopoietic system. Also, detailed analysis of each isoform promoter will provide valuable insight to the mechanisms of KLF13 expression and activity control.

In human, heterozygous microdeletions and duplications of the chromosomal bands 15q13.3 (harboring *KLF13 along with at least another 7 genes*) are associated with a wide range of cardiac defects that include Tetralogy of Fallot, mitral valve prolapse, and hypoplasia of the right side of the heart (237,238). Taken together, it is highly probable that *KLF13* is a critical component of human cardiac development and screening for mutations in *KLF13* in patients with congenital heart diseases will be of clinical relevance. Given the synergistic partnership between KLF13 and the cardiac transcription factors GATA4, TBX5, and NKX2.5, it would also be interesting to see the effect of *KLF13* mutation on the penetrance of CHD in human associated with the aforementioned transcriptional partners.

Taken together, the analysis of KLF13's role in the genetic architecture of CHD and its underlying transcriptional networks may provide new insights to the elucidation of the genetic architecture of CHD. In addition, our studies may provide a new paradigm that may help to decipher the genotype-phenotype relationship in patients with congenital heart diseases.

6. References

1. Martin-Puig, S., Wang, Z. and Chien, K.R. (2008) Lives of a Heart Cell: Tracing the Origins of Cardiac Progenitors. *Cell stem cell*, **2**, 320-331.
2. Cohen, E.D., Miller, M.F., Wang, Z., Moon, R.T. and Morrisey, E.E. (2012) Wnt5a and Wnt11 are essential for second heart field progenitor development. *Development*, **139**, 1931-1940.
3. Buckingham M, M.S., Zaffran S. (2005) Building the mammalian heart from two sources of myocardial cells. *Nat Rev Genet.*, **6**, 826-835.
4. Srivastava, D. (2006) Making or Breaking the Heart: From Lineage Determination to Morphogenesis. *Cell*, **126**, 1037-1048.
5. Wu, S.M., Chien, K.R. and Mummery, C. (2008) Origins and Fates of Cardiovascular Progenitor Cells. *Cell*, **132**, 537-543.
6. Bruneau, B.G. (2008) The developmental genetics of congenital heart disease. *Nature*, **451**, 943-948.
7. Koshiba-Takeuchi, K., Takeuchi, J., Arruda, E., Kathiriya, I., Mo, R. and Hui, C. (2006) Cooperative and antagonistic interactions between Sall4 and Tbx5 pattern the mouse limb and heart. *Nat Genet*, **38**, 175 - 183.
8. Abraham, D., Clive, H., Dashwood, M., Coghlan, G. and Ponticos, M., *Advances in Vascular Medicine*. Springer London, pp. 113-130.
9. Linask, K.K.a.L., J. W. . (1993) Early heart development: Dynamics of endocardial cell sorting suggests a common origin with cardiomyocytes. *American Journal of Anatomy*, **196**, 62-69.
10. Packham, E.A. and David Brook, J. (2003) Interaction makes the heart grow stronger. *Trends in Molecular Medicine*, **9**, 407-409.
11. Olson, E.N. and Srivastava, D. (1996) Molecular Pathways Controlling Heart Development. *Science*, **272**, 671-676.
12. Nemer, M. Genetic insights into normal and abnormal heart development. *Cardiovascular Pathology*, **17**, 48-54.
13. Darwich, R. (2010) Research Thesis, University of Ottawa, Ottawa.
14. Laforest, B. and Nemer, M. (2011) A Hand for the Epicardium. *Circulation Research*, **108**, 900-902.
15. Jensen, B., Wang, T., Christoffels, V.M. and Moorman, A.F.M. (2013) Evolution and development of the building plan of the vertebrate heart. *Biochimica et Biophysica Acta (BBA) - Molecular Cell Research*, **1833**, 783-794.
16. Laforest, B. (2011), McGill, Montreal.
17. Camenisch, T.D., Runyan, R.B. and Markwald, R.R. (2010) In Rosenthal, N. and Harvey, R. P. (eds.), *Heart Development and Regeneration*. Academic Press, Boston, pp. 363-387.
18. Carpentier A, A.D., Filsoufi F. . (2010) *Carpentier's Reconstructive Valve Surgery. From Valve Analysis to Valve Reconstruction*. Saunders Elsevier.
19. von Gise, A. and Pu, W.T. (2012) Endocardial and Epicardial Epithelial to Mesenchymal Transitions in Heart Development and Disease. *Circulation Research*, **110**, 1628-1645.
20. Combs, M.D. and Yutzey, K.E. (2009) Heart Valve Development: Regulatory Networks in Development and Disease. *Circulation Research*, **105**, 408-421.

21. Lin, C.-J., Lin, C.-Y., Chen, C.-H., Zhou, B. and Chang, C.-P. (2012) Partitioning the heart: mechanisms of cardiac septation and valve development. *Development*, **139**, 3277-3299.
22. Webb, S., Brown, N.A. and Anderson, R.H. (1998) Formation of the Atrioventricular Septal Structures in the Normal Mouse. *Circulation Research*, **82**, 645-656.
23. Anderson, R.H., Webb, S., Brown, N.A., Lamers, W. and Moorman, A. (2003) Development of the heart: (2) Septation of the atriums and ventricles. *Heart*, **89**, 949-958.
24. Verzi, M.P., McCulley, D.J., De Val, S., Dodou, E. and Black, B.L. (2005) The right ventricle, outflow tract, and ventricular septum comprise a restricted expression domain within the secondary/anterior heart field. *Developmental Biology*, **287**, 134-145.
25. Contreras-Ramos, A., Sánchez-Gómez, C., García-Romero, H.L. and Cimarosti, L.O. (2008) Normal Development of the Muscular Region of the Interventricular Septum – I. The Significance of the Ventricular Trabeculations. *Anatomia, Histologia, Embryologia*, **37**, 344-351.
26. Posch, M., Perrot, A., Berger, F. and Özcelik, C. Molecular genetics of congenital atrial septal defects. *Clinical Research in Cardiology*, **99**, 137-147.
27. de Los Reyes, E. and Roach, E.S. (2014) Neurologic complications of congenital heart disease and its treatment. *Handb Clin Neurol*, **119**, 49-59.
28. Olson, E.N. (2004) A decade of discoveries in cardiac biology. *Nat Med*, **10**, 467-474.
29. Joziasse, I., van de Smagt, J., Smith, K., Bakkers, J., Sieswerda, G.-J., Mulder, B. and Doevendans, P. (2008) Genes in congenital heart disease: atrioventricular valve formation. *Basic Research in Cardiology*, **103**, 216-227.
30. Hartman, J.L., IV, Garvik, B. and Hartwell, L. (2001) Principles for the Buffering of Genetic Variation. *Science*, **291**, 1001-1004.
31. Rutherford, S.L. (2003) Between genotype and phenotype: protein chaperones and evolvability. *Nat Rev Genet*, **4**, 263-274.
32. Bentham, J. and Bhattacharya, S. (2008) Genetic Mechanisms Controlling Cardiovascular Development. *Annals of the New York Academy of Sciences*, **1123**, 10-19.
33. Xin, M., Davis, C.A., Molkentin, J.D., Lien, C.-L., Duncan, S.A., Richardson, J.A. and Olson, E.N. (2006) A threshold of GATA4 and GATA6 expression is required for cardiovascular development. *Proceedings of the National Academy of Sciences*, **103**, 11189-11194.
34. Lavallee, G., Andelfinger, G., Nadeau, M., Lefebvre, C., Nemer, G., Horb, M.E. and Nemer, M. (2006) The Kruppel-like transcription factor KLF13 is a novel regulator of heart development. *EMBO J*, **25**, 5201-5213.
35. Armstrong, E.J. and Bischoff, J. (2004) Heart valve development: endothelial cell signaling and differentiation. *Circ Res*, **95**, 459-470.
36. Boyer, A.S. and Raymond, B.R. (2001) TGFβ Type III and TGFβ Type II receptors have distinct activities during epithelial–mesenchymal cell transformation in the embryonic heart. *Developmental Dynamics*, **221**, 454-459.
37. Dünker, N. and Krieglstein, K. (2002) Tgfß2 –/– Tgfß3 –/– double knockout mice display severe midline fusion defects and early embryonic lethality. *Anat Embryol*, **206**, 73-83.

38. Luna-Zurita, L., Prados, B., Grego-Bessa, J., Luxan, G., del Monte, G., Benguria, A., Adams, R.H., Perez-Pomares, J.M. and de la Pompa, J.L. (2010) Integration of a Notch-dependent mesenchymal gene program and Bmp2-driven cell invasiveness regulates murine cardiac valve formation. *Journal of Clinical Investigation*, **120**, 3493-3507.
39. Okagawa, H., Markwald, R.R. and Sugi, Y. (2007) Functional BMP receptor in endocardial cells is required in atrioventricular cushion mesenchymal cell formation in chick. *Developmental Biology*, **306**, 179-192.
40. Kim, R.Y., Robertson, E.J. and Solloway, M.J. (2001) Bmp6 and Bmp7 Are Required for Cushion Formation and Septation in the Developing Mouse Heart. *Developmental Biology*, **235**, 449-466.
41. Niessen, K. and Karsan, A. (2008) Notch Signaling in Cardiac Development. *Circulation Research*, **102**, 1169-1181.
42. Niessen, K.K.A. (2007) Notch signaling in the developing cardiovascular system. *American Journal of Physiology - Cell Physiology*, **293**, C1-C11.
43. Loomes, K.M., Taichman, D.B., Glover, C.L., Williams, P.T., Markowitz, J.E., Piccoli, D.A., Baldwin, H.S. and Oakey, R.J. (2002) Characterization of Notch receptor expression in the developing mammalian heart and liver. *American Journal of Medical Genetics*, **112**, 181-189.
44. Timmerman, L.A., Grego-Bessa, J., Raya, A., Bertran, E., Perez-Pomares, J.M., Diez, J., Aranda, S., Palomo, S., McCormick, F., Izpisua-Belmonte, J.C. *et al.* (2004) Notch promotes epithelial-mesenchymal transition during cardiac development and oncogenic transformation. *Genes Dev*, **18**, 99-115.
45. Donovan, J., Kordylewska, A., Jan, Y.N. and Utset, M.F. Tetralogy of Fallot and Other Congenital Heart Defects in Hey2 Mutant Mice. *Current Biology*, **12**, 1605-1610.
46. Dor, Y., Camenisch, T.D., Itin, A., Fishman, G.I., McDonald, J.A., Carmeliet, P. and Keshet, E. (2001) A novel role for VEGF in endocardial cushion formation and its potential contribution to congenital heart defects. *Development*, **128**, 1531-1538.
47. Armstrong, E.J. and Bischoff, J. (2004) Heart Valve Development: Endothelial Cell Signaling and Differentiation. *Circulation Research*, **95**, 459-470.
48. Zachary, I. (2003) VEGF signalling: integration and multi-tasking in endothelial cell biology. *Biochem Soc Trans*, **31**, 1171-1177.
49. Taimeh, Z., Loughran, J., Birks, E.J. and Bolli, R. (2013) Vascular endothelial growth factor in heart failure. *Nat Rev Cardiol*, **10**, 519-530.
50. Stankunas, K., Ma, G.K., Kuhnert, F.J., Kuo, C.J. and Chang, C.-P. (2010) VEGF signaling has distinct spatiotemporal roles during heart valve development. *Developmental Biology*, **347**, 325-336.
51. Miquerol, L., Langille, B.L. and Nagy, A. (2000) Embryonic development is disrupted by modest increases in vascular endothelial growth factor gene expression. *Development*, **127**, 3941-3946.
52. Carmeliet, P., Ferreira, V., Breier, G., Pollefeyt, S., Kieckens, L., Gertsenstein, M., Fahrig, M., Vandenhoeck, A., Harpal, K., Eberhardt, C. *et al.* (1996) Abnormal blood vessel development and lethality in embryos lacking a single VEGF allele. *Nature*, **380**, 435-439.
53. Chang, C.-P., Neilson, J.R., Bayle, J.H., Gestwicki, J.E., Kuo, A., Stankunas, K., Graef, I.A. and Crabtree, G.R. A Field of Myocardial-Endocardial NFAT Signaling Underlies Heart Valve Morphogenesis. *Cell*, **118**, 649-663.

54. Beals, C.R., Clipstone, N.A., Ho, S.N. and Crabtree, G.R. (1997) Nuclear localization of NF-ATc by a calcineurin-dependent, cyclosporin-sensitive intramolecular interaction. *Genes & Development*, **11**, 824-834.
55. Wolfe, S.A., Zhou, P., Dotsch, V., Chen, L., You, A., Ho, S.N., Crabtree, G.R., Wagner, G. and Verdine, G.L. (1997) Unusual Rel-like architecture in the DNA-binding domain of the transcription factor NFATc. *Nature*, **385**, 172-176.
56. De La Pompa, J.L., Timmerman, L.A., Takimoto, H., Yoshida, H., Elia, A.J., Samper, E., Potter, J., Wakeham, A., Marengere, L., Langille, B.L. *et al.* (1998) Role of the NF-ATc transcription factor in morphogenesis of cardiac valves and septum. *Nature*, **392**, 182-186.
57. Schulz, R.A. and Yutzey, K.E. (2004) Calcineurin signaling and NFAT activation in cardiovascular and skeletal muscle development. *Developmental Biology*, **266**, 1-16.
58. Bourajjaj, M., Armand, A.S., da Costa Martins, P.A., Weijts, B., van der Nagel, R., Heeneman, S., Wehrens, X.H. and De Windt, L.J. (2008) NFATc2 is a necessary mediator of calcineurin-dependent cardiac hypertrophy and heart failure. *J Biol Chem*, **283**, 22295-22303.
59. Wilkins, B.J., De Windt, L.J., Bueno, O.F., Braz, J.C., Glascock, B.J., Kimball, T.F. and Molkentin, J.D. (2002) Targeted disruption of NFATc3, but not NFATc4, reveals an intrinsic defect in calcineurin-mediated cardiac hypertrophic growth. *Mol Cell Biol*, **22**, 7603-7613.
60. Graef, I.A., Chen, F., Chen, L., Kuo, A. and Crabtree, G.R. (2001) Signals transduced by Ca(2+)/calcineurin and NFATc3/c4 pattern the developing vasculature. *Cell*, **105**, 863-875.
61. Chang, C.-P., Neilson, J.R., Bayle, J.H., Gestwicki, J.E., Kuo, A., Stankunas, K., Graef, I.A. and Crabtree, G.R. (2004) A Field of Myocardial-Endocardial NFAT Signaling Underlies Heart Valve Morphogenesis. *Cell*, **118**, 649-663.
62. Odiete, O., Hill, M.F. and Sawyer, D.B. (2012) Neuregulin in Cardiovascular Development and Disease. *Circulation Research*, **111**, 1376-1385.
63. Vasti, C. and Hertig, C.M. (2014) Neuregulin-1/erbB activities with focus on the susceptibility of the heart to anthracyclines. *World J Cardiol*, **6**, 653-662.
64. Esper, R.M. and Loeb, J.A. (2009) Neurotrophins Induce Neuregulin Release through Protein Kinase Cδ Activation. *Journal of Biological Chemistry*, **284**, 26251-26260.
65. Erickson, S.L., O'Shea, K.S., Ghaboosi, N., Loverro, L., Frantz, G., Bauer, M., Lu, L.H. and Moore, M.W. (1997) ErbB3 is required for normal cerebellar and cardiac development: a comparison with ErbB2-and heregulin-deficient mice. *Development*, **124**, 4999-5011.
66. Gassmann, M., Casagranda, F., Orioli, D., Simon, H., Lai, C., Klein, R. and Lemke, G. (1995) Aberrant neural and cardiac development in mice lacking the ErbB4 neuregulin receptor. *Nature*, **378**, 390-394.
67. Camenisch, T.D., Spicer, A.P., Brehm-Gibson, T., Biesterfeldt, J., Augustine, M.L., Calabro, A., Jr., Kubalak, S., Klewer, S.E. and McDonald, J.A. (2000) Disruption of hyaluronan synthase-2 abrogates normal cardiac morphogenesis and hyaluronan-mediated transformation of epithelium to mesenchyme. *J Clin Invest*, **106**, 349-360.
68. Alsan, B.H. and Schultheiss, T.M. (2002) Regulation of avian cardiogenesis by Fgf8 signaling. *Development*, **129**, 1935-1943.

69. Frank, D.U., Fotheringham, L.K., Brewer, J.A., Muglia, L.J., Tristani-Firouzi, M., Capecchi, M.R. and Moon, A.M. (2002) An Fgf8 mouse mutant phenocopies human 22q11 deletion syndrome. *Development*, **129**, 4591-4603.
70. Lee, Y., Shioi, T., Kasahara, H., Jobe, S.M., Wiese, R.J., Markham, B.E. and Izumo, S. (1998) The Cardiac Tissue-Restricted Homeobox Protein Csx/Nkx2.5 Physically Associates with the Zinc Finger Protein GATA4 and Cooperatively Activates Atrial Natriuretic Factor Gene Expression. *Mol. Cell. Biol.*, **18**, 3120-3129.
71. Garg, V., Kathiriya, I.S., Barnes, R., Schluterman, M.K., King, I.N., Butler, C.A., Rothrock, C.R., Eapen, R.S., Hirayama-Yamada, K., Joo, K. *et al.* (2003) GATA4 mutations cause human congenital heart defects and reveal an interaction with TBX5. *Nature*, **424**, 443-447.
72. Morin, S., Charron, F., Robitaille, L. and Nemer, M. (2000) GATA-dependent recruitment of MEF2 proteins to target promoters. *EMBO J*, **19**, 2046-2055.
73. Belaguli, N.S., Sepulveda, J.L., Nigam, V., Charron, F., Nemer, M. and Schwartz, R.J. (2000) Cardiac Tissue Enriched Factors Serum Response Factor and GATA-4 Are Mutual Coregulators. *Mol. Cell. Biol.*, **20**, 7550-7558.
74. Dai, Y.-S., Cserjesi, P., Markham, B.E. and Molkentin, J.D. (2002) The Transcription Factors GATA4 and dHAND Physically Interact to Synergistically Activate Cardiac Gene Expression through a p300-dependent Mechanism. *Journal of Biological Chemistry*, **277**, 24390-24398.
75. Moorman, A.F.M. and Christoffels, V.M. (2003) Cardiac Chamber Formation: Development, Genes, and Evolution. *Physiol. Rev.*, **83**, 1223-1267.
76. Bruneau, B.G. (2002) Transcriptional Regulation of Vertebrate Cardiac Morphogenesis. *Circ Res*, **90**, 509-519.
77. Takeuchi, J.K., Mileikovskaia, M., Koshiba-Takeuchi, K., Heidt, A.B., Mori, A.D., Arruda, E.P., Gertsenstein, M., Georges, R., Davidson, L., Mo, R. *et al.* (2005) Tbx20 dose-dependently regulates transcription factor networks required for mouse heart and motoneuron development. *Development*, **132**, 2463-2474.
78. Bernstein, B.E., Meissner, A. and Lander, E.S. (2007) The Mammalian Epigenome. *Cell*, **128**, 669-681.
79. Simone, C. (2006) SWI/SNF: The crossroads where extracellular signaling pathways meet chromatin. *Journal of Cellular Physiology*, **207**, 309-314.
80. Kouzarides, T. (2007) Chromatin Modifications and Their Function. *Cell*, **128**, 693-705.
81. Kawamura, T., Ono, K., Morimoto, T., Wada, H., Hirai, M., Hidaka, K., Morisaki, T., Heike, T., Nakahata, T., Kita, T. *et al.* (2005) Acetylation of GATA-4 Is Involved in the Differentiation of Embryonic Stem Cells into Cardiac Myocytes. *Journal of Biological Chemistry*, **280**, 19682-19688.
82. Haberland, M., Montgomery, R.L. and Olson, E.N. (2009) The many roles of histone deacetylases in development and physiology: implications for disease and therapy. *Nat Rev Genet*, **10**, 32-42.
83. de Bold, A.J., Borenstein, H.B., Veress, A.T. and Sonnenberg, H. (1981) A rapid and potent natriuretic response to intravenous injection of atrial myocardial extract in rats. *Life Sciences*, **28**, 89-94.
84. Sudoh, T., Kangawa, K., Minamino, N. and Matsuo, H. (1988) A new natriuretic peptide in porcine brain. *Nature*, **332**, 78-81.
85. Hayek, S. and Nemer, M. (2010) Cardiac Natriuretic Peptides: From Basic Discovery to Clinical Practice. *Cardiovascular Therapeutics*, no-no.

86. de Bold, A.J., Bruneau, B.G. and Kuroski de Bold, M.L. (1996) Mechanical and neuroendocrine regulation of the endocrine heart. *Cardiovascular Research*, **31**, 7-18.
87. Suo, M. (2002), University of Oulu, Oulu.
88. Nishikimi, T., Maeda, N. and Matsuoka, H. (2006) The role of natriuretic peptides in cardioprotection. *Cardiovasc Res*, **69**, 318-328.
89. John, S., Krege, J., Oliver, P., Hagaman, Hodgin, J., Pang, S., Flynn, T. and Smithies, O. (1995) Genetic decreases in atrial natriuretic peptide and salt-sensitive hypertension. *Science*, **267**, 679-681.
90. Y Ogawa, H.I., N Tamura, S Suga, T Yoshimasa, M Uehira, S Matsuda, S Shiono, H Nishimoto, and K Nakao. (1994) Molecular cloning of the complementary DNA and gene that encode mouse brain natriuretic peptide and generation of transgenic mice that overexpress the brain natriuretic peptide gene. *J Clin Invest.*, **93**, 1911–1921.
91. McBride, K. and Nemer, M. (2001) Regulation of the ANF and BNP promoters by GATA factors: Lessons learned for cardiac transcription. *Canadian Journal of Physiology and Pharmacology*, **79**, 673-681.
92. Argentin, S., Ardati, A., Tremblay, S., Lihrmann, I., Robitaille, L., Drouin, J. and Nemer, M. (1994) Developmental stage-specific regulation of atrial natriuretic factor gene transcription in cardiac cells. *Mol. Cell. Biol.*, **14**, 777-790.
93. R T Lee, K.D.B., J M Pfeffer, M A Pfeffer, E J Neer, and C E Seidman. (1988) Atrial natriuretic factor gene expression in ventricles of rats with spontaneous biventricular hypertrophy. *J Clin Invest.*, **81**, 431–434.
94. Ruskoaho, H. (1992) Atrial natriuretic peptide: synthesis, release, and metabolism. *Pharmacological Reviews*, **44**, 479-602.
95. Hunyady, B., Hipkin, R.W., Schonbrunn, A. and Mezey, E. (1997) Immunohistochemical Localization of Somatostatin Receptor SST2A in the Rat Pancreas. *Endocrinology*, **138**, 2636-2639.
96. Zhou, P., He, A. and Pu, W.T. (2012) In Benoit, G. B. (ed.), *Current Topics in Developmental Biology*. Academic Press, Vol. Volume 100, pp. 143-169.
97. Evans, T. and Felsenfeld, G. (1989) The erythroid-specific transcription factor eryf1: A new finger protein. *Cell*, **58**, 877-885.
98. Martin, D.I.K. and Orkin, S.H. (1990) Transcriptional activation and DNA binding by the erythroid factor GF-1/NF-E1/Eryf 1. *Genes and Development*, **4**, 1886-1898.
99. Kuo, C.T., Morrisey, E.E., Anandappa, R., Sigrist, K., Lu, M.M., Parmacek, M.S., Soudais, C. and Leiden, J.M. (1997) GATA4 transcription factor is required for ventral morphogenesis and heart tube formation. *Genes & Development*, **11**, 1048-1060.
100. Biben, C. and Harvey, R.P. (1997) Homeodomain factor Nkx2-5 controls left/right asymmetric expression of bHLH gene eHand during murine heart development. *Genes & Development*, **11**, 1357-1369.
101. Habets, P.E.M.H., Moorman, A.F.M., Clout, D.E.W., van Roon, M.A., Lingbeek, M., van Lohuizen, M., Campione, M. and Christoffels, V.M. (2002) Cooperative action of Tbx2 and Nkx2.5 inhibits ANF expression in the atrioventricular canal: implications for cardiac chamber formation. *Genes & Development*, **16**, 1234-1246.
102. Jay, P.Y., Harris, B.S., Maguire, C.T., Buerger, A., Wakimoto, H., Tanaka, M., Kupershmidt, S., Roden, D.M., Schultheiss, T.M., Oâ€™Brien, T.X. *et al.* (2004) Nkx2-5 mutation causes anatomic hypoplasia of the cardiac conduction system. *The Journal of Clinical Investigation*, **113**, 1130-1137.

103. Lyons, I., Parsons, L.M., Hartley, L., Li, R., Andrews, J.E., Robb, L. and Harvey, R.P. (1995) Myogenic and morphogenetic defects in the heart tubes of murine embryos lacking the homeo box gene Nkx2-5. *Genes & Development*, **9**, 1654-1666.
104. Pashmforoush, M., Lu, J.T., Chen, H., Amand, T.S., Kondo, R., Pradervand, S., Evans, S.M., Clark, B., Feramisco, J.R., Giles, W. *et al.* (2004) Nkx2-5 Pathways and Congenital Heart Disease: Loss of Ventricular Myocyte Lineage Specification Leads to Progressive Cardiomyopathy and Complete Heart Block. *Cell*, **117**, 373-386.
105. Tanaka, M., Chen, Z., Bartunkova, S., Yamasaki, N. and Izumo, S. (1999) The cardiac homeobox gene Csx/Nkx2.5 lies genetically upstream of multiple genes essential for heart development. *Development*, **126**, 1269-1280.
106. Watt, A.J., Battle, M.A., Li, J. and Duncan, S.A. (2004) GATA4 is essential for formation of the proepicardium and regulates cardiogenesis. *Proceedings of the National Academy of Sciences of the United States of America*, **101**, 12573-12578.
107. Reiter, J.F., Alexander, J., Rodaway, A., Yelon, D., Patient, R., Holder, N. and Stainier, D.Y.R. (1999) Gata5 is required for the development of the heart and endoderm in zebrafish. *Genes & Development*, **13**, 2983-2995.
108. Laforest, B., Andelfinger, G. and Nemer, M. (2011) Loss of Gata5 in mice leads to bicuspid aortic valve. *The Journal of Clinical Investigation*, **121**, 2876-2887.
109. Crispino, J.D., Lodish, M.B., Thurberg, B.L., Litovsky, S.H., Collins, T., Molkentin, J.D. and Orkin, S.H. (2001) Proper coronary vascular development and heart morphogenesis depend on interaction of GATA-4 with FOG cofactors. *Genes & Development*, **15**, 839-844.
110. Vong, L., Bi, W., O'Connor-Halligan, K.E., Li, C., Cserjesi, P. and Schwarz, J.J. (2006) MEF2C is required for the normal allocation of cells between the ventricular and sinoatrial precursors of the primary heart field. *Developmental Dynamics*, **235**, 1809-1821.
111. Marguerie, A., Bajolle, F., Zaffran, S., Brown, N.A., Dickson, C., Buckingham, M.E. and Kelly, R.G. (2006) Congenital heart defects in Fgfr2-IIIb and Fgf10 mutant mice. *Cardiovascular Research*, **71**, 50-60.
112. Cai, C.-L., Liang, X., Shi, Y., Chu, P.-H., Pfaff, S.L., Chen, J. and Evans, S. (2003) Isl1 Identifies a Cardiac Progenitor Population that Proliferates Prior to Differentiation and Contributes a Majority of Cells to the Heart. *Developmental Cell*, **5**, 877-889.
113. Firulli, A.B., McFadden, D.G., Lin, Q., Srivastava, D. and Olson, E.N. (1998) Heart and extra-embryonic mesodermal defects in mouse embryos lacking the bHLH transcription factor Hand1. *Nat Genet*, **18**, 266-270.
114. Srivastava, D. and Olson, E.N. (2000) A genetic blueprint for cardiac development. *Nature*, **407**, 221-226.
115. Yamagishi, H. (2003) Tbx1 is regulated by tissue-specific forkhead proteins through a common Sonic hedgehog-responsive enhancer. *Genes Dev.*, **17**, 269-281.
116. Christoffels, V.M., Habets, P.E.M.H., Franco, D., Campione, M., de Jong, F., Lamers, W.H., Bao, Z.-Z., Palmer, S., Biben, C., Harvey, R.P. *et al.* (2000) Chamber Formation and Morphogenesis in the Developing Mammalian Heart. *Developmental Biology*, **223**, 266-278.
117. Mommersteeg, M.T.M., Hoogaars, W.M.H., Prall, O.W.J., de Gier-de Vries, C., Wiese, C., Clout, D.E.W., Papaioannou, V.E., Brown, N.A., Harvey, R.P., Moorman,

A.F.M. *et al.* (2007) Molecular Pathway for the Localized Formation of the Sinoatrial Node. *Circ Res*, **100**, 354-362.
118. Mori, A.D., Zhu, Y., Vahora, I., Nieman, B., Koshiba-Takeuchi, K., Davidson, L., Pizard, A., Seidman, J.G., Seidman, C.E., Chen, X.J. *et al.* (2006) Tbx5-dependent rheostatic control of cardiac gene expression and morphogenesis. *Developmental Biology*, **297**, 566-586.
119. Ko, L.J. and Engel, J.D. (1993) DNA-binding specificities of the GATA transcription factor family. *Mol. Cell. Biol.*, **13**, 4011-4022.
120. Grepin, C., Dagnino, L., Robitaille, L., Haberstroh, L., Antakly, T. and Nemer, M. (1994) A hormone-encoding gene identifies a pathway for cardiac but not skeletal muscle gene transcription. *Mol. Cell. Biol.*, **14**, 3115-3129.
121. Molkentin, J.D. (2000) The Zinc Finger-containing Transcription Factors GATA-4, -5, and -6: Ubiquitously Expressed Regulators of Tissue-Specific Gene Expression. *Journal of Biological Chemistry*, **275**, 38949-38952.
122. Oka, T., Maillet, M., Watt, A.J., Schwartz, R.J., Aronow, B.J., Duncan, S.A. and Molkentin, J.D. (2006) Cardiac-Specific Deletion of Gata4 Reveals Its Requirement for Hypertrophy, Compensation, and Myocyte Viability. *Circulation Research*, **98**, 837-845.
123. Arceci, R.J., King, A.A., Simon, M.C., Orkin, S.H. and Wilson, D.B. (1993) Mouse GATA-4: a retinoic acid-inducible GATA-binding transcription factor expressed in endodermally derived tissues and heart. *Mol. Cell. Biol.*, **13**, 2235-2246.
124. Grepin, C., Robitaille, L., Antakly, T. and Nemer, M. (1995) Inhibition of transcription factor GATA-4 expression blocks in vitro cardiac muscle differentiation. *Mol. Cell. Biol.*, **15**, 4095-4102.
125. Bartlett, H., Veenstra, G. and Weeks, D. Examining the Cardiac NK-2 Genes in Early Heart Development. *Pediatric cardiology*, **31**, 335-341.
126. Molkentin, J.D., Lin, Q., Duncan, S.A. and Olson, E.N. (1997) Requirement of the transcription factor GATA4 for heart tube formation and ventral morphogenesis. *Genes & Development*, **11**, 1061-1072.
127. Clark KL, Y.K., and Benson DW. (2006) Transcription factors and congenital heart defects. *Annu Rev Physiol*, 97-121.
128. David J.Whyatt, E.d.a.F.G. (1993) The two zinc finger-like domains of GATA-1 have different DNA binding specificities. *The EMBO Journal*, **12**, 4993-5005.
129. Pikkarainen, S., Tokola, H., KerkelÃ¤, R. and Ruskoaho, H. (2004) GATA transcription factors in the developing and adult heart. *Cardiovascular Research*, **63**, 196-207.
130. Durocher, D., Charron, F., Warren, R., Schwartz, R.J. and Nemer, M. (1997) The cardiac transcription factors Nkx2-5 and GATA-4 are mutual cofactors. *EMBO J*, **16**, 5687-5696.
131. Svensson, E.C., Huggins, G.S., Dardik, F.B., Polk, C.E. and Leiden, J.M. (2000) A Functionally Conserved N-terminal Domain of the Friend of GATA-2 (FOG-2) Protein Represses GATA4-Dependent Transcription. *Journal of Biological Chemistry*, **275**, 20762-20769.
132. Morrisey, E.E., Ip, H.S., Tang, Z. and Parmacek, M.S. (1997) GATA-4 activates transcription via two novel domains that are conserved within the GATA-4/5/6 subfamily. *J. Biol. Chem.*, **272**, 8515-8524.
133. Potthoff, M.J. and Olson, E.N. (2007) MEF2: a central regulator of diverse developmental programs. *Development*, **134**, 4131-4140.

134. Edmondson, D.G., Lyons, G.E., Martin, J.F. and Olson, E.N. (1994) Mef2 gene expression marks the cardiac and skeletal muscle lineages during mouse embryogenesis. *Development*, **120**, 1251-1263.
135. Lin, Q., Lu, J., Yanagisawa, H., Webb, R., Lyons, G.E., Richardson, J.A. and Olson, E.N. (1998) Requirement of the MADS-box transcription factor MEF2C for vascular development. *Development*, **125**, 4565-4574.
136. Naya, F.J., Black, B.L., Wu, H., Bassel-Duby, R., Richardson, J.A., Hill, J.A. and Olson, E.N. (2002) Mitochondrial deficiency and cardiac sudden death in mice lacking the MEF2A transcription factor. *Nat Med*, **8**, 1303-1309.
137. Karamboulas, C., Dakubo, G.D., Liu, J., De Repentigny, Y., Yutzey, K., Wallace, V.A., Kothary, R. and Skerjanc, I.S. (2006) Disruption of MEF2 activity in cardiomyoblasts inhibits cardiomyogenesis. *J Cell Sci*, **119**, 4315-4321.
138. Xu, J., Gong, N.L., Bodi, I., Aronow, B.J., Backx, P.H. and Molkentin, J.D. (2006) Myocyte enhancer factors 2A and 2C induce dilated cardiomyopathy in transgenic mice. *J Biol Chem*, **281**, 9152-9162.
139. Azpiazu, N. and Frasch, M. (1993) tinman and bagpipe: two homeo box genes that determine cell fates in the dorsal mesoderm of Drosophila. *Genes Dev*, **7**, 1325-1340.
140. Harvey, R.P. (1996) NK-2Homeobox Genes and Heart Development. *Developmental Biology*, **178**, 203-216.
141. Hiroi, Y., Kudoh, S., Monzen, K., Ikeda, Y., Yazaki, Y., Nagai, R. and Komuro, I. (2001) Tbx5 associates with Nkx2-5 and synergistically promotes cardiomyocyte differentiation. *Nat Genet*, **28**, 276-280.
142. Akazawa, H. and Komuro, I. (2005) Cardiac transcription factor Csx/Nkx2-5: Its role in cardiac development and diseases. *Pharmacology & Therapeutics*, **107**, 252-268.
143. Chen, C. and Schwartz, R. (1996) Recruitment of the tinman homolog Nkx-2.5 by serum response factor activates cardiac alpha-actin gene transcription. *Mol. Cell. Biol.*, **16**, 6372-6384.
144. Pradhan, L., Genis, C., Scone, P., Weinberg, E.O., Kasahara, H. and Nam, H.J. (2012) Crystal structure of the human NKX2.5 homeodomain in complex with DNA target. *Biochemistry*, **51**, 6312-6319.
145. Yu, H., Xu, J.H., Song, H.M., Zhao, L., Xu, W.J., Wang, J., Li, R.G., Xu, L., Jiang, W.F., Qiu, X.B. *et al.* (2014) Mutational spectrum of the NKX2-5 gene in patients with lone atrial fibrillation. *Int J Med Sci*, **11**, 554-563.
146. Liu, Z. and Karmarkar, V. (2008) Groucho/Tup1 family co-repressors in plant development. *Trends in Plant Science*, **13**, 137-144.
147. Muhr, J., Andersson, E., Persson, M., Jessell, T.M. and Ericson, J. (2001) Groucho-Mediated Transcriptional Repression Establishes Progenitor Cell Pattern and Neuronal Fate in the Ventral Neural Tube. *Cell*, **104**, 861-873.
148. Li, T., Li, Y.-M., Jia, Z.-Q., Chen, P., Ma, K.-T. and Zhou, C.-Y. (2007) Carboxyl Terminus of NKX2.5 Impairs its Interaction with p300. *Journal of Molecular Biology*, **370**, 976-992.
149. Chen, Y.-Z., Ying, H., Zhang, J., Cheng, W., Kang, Y.-X. and Hua, Z.-C. (2007) Biochemical Analyses of Csx/Nkx2.5 Mutants and Their Structure–Function Relationship. *International Journal of Molecular Sciences*, **8**, 284-294.
150. Lee, J.-c., Kim, K.-H., Lee, Y. and Yoo, S. (2014) NK2-specific domain is responsible for cell death upon ectopic expression of VND in various Drosophila tissues. *Genes Genom*, **36**, 1-10.

151. Jamali, M., Rogerson, P.J., Wilton, S. and Skerjanc, I.S. (2001) Nkx2-5 activity is essential for cardiomyogenesis. *J Biol Chem*, **276**, 42252-42258.
152. Stennard, F.A. and Harvey, R.P. (2005) T-box transcription factors and their roles in regulatory hierarchies in the developing heart. *Development*, **132**, 4897-4910.
153. Singh, R. and Kispert, A. (2010) Tbx20, Smads, and the Atrioventricular Canal. *Trends in Cardiovascular Medicine*, **20**, 109-114.
154. Ryan, K. and Chin, A.J. (2003) T-box genes and cardiac development. *Birth Defects Research Part C: Embryo Today: Reviews*, **69**, 25-37.
155. Greulich, F., Rudat, C. and Kispert, A. (2011) Mechanisms of T-box gene function in the developing heart. *Cardiovasc Res*, **91**, 212-222.
156. Clabby, M.L., Robison, T.A., Quigley, H.F., Wilson, D.B. and Kelly, D.P. (2003) Retinoid X Receptor Î± Represses GATA-4-mediated Transcription via a Retinoid-dependent Interaction with the Cardiac-enriched Repressor FOG-2. *Journal of Biological Chemistry*, **278**, 5760-5767.
157. Dai, Y.-S. and Markham, B.E. (2001) p300 Functions as a Coactivator of Transcription Factor GATA-4. *Journal of Biological Chemistry*, **276**, 37178-37185.
158. Charron, F., Paradis, P., Bronchain, O., Nemer, G. and Nemer, M. (1999) Cooperative Interaction between GATA-4 and GATA-6 Regulates Myocardial Gene Expression. *Mol. Cell. Biol.*, **19**, 4355-4365.
159. Nadeau, M., Georges, R.O., Laforest, B., Yamak, A., Lefebvre, C., Beauregard, J., Paradis, P., Bruneau, B.G., Andelfinger, G. and Nemer, M. (2010) An endocardial pathway involving Tbx5, Gata4, and Nos3 required for atrial septum formation. *Proc Natl Acad Sci U S A*, **107**, 19356-19361.
160. Rallis, C., Bruneau, B.G., Del Buono, J., Seidman, C.E., Seidman, J.G., Nissim, S., Tabin, C.J. and Logan, M.P.O. (2003) Tbx5 is required for forelimb bud formation and continued outgrowth. *Development*, **130**, 2741-2751.
161. Liberatore, C.M., Searcy-Schrick, R.D. and Yutzey, K.E. (2000) Ventricular Expression of tbx5 Inhibits Normal Heart Chamber Development. *Developmental Biology*, **223**, 169-180.
162. Liu, J. and Stainier, D.Y. (2010) Tbx5 and Bmp signaling are essential for proepicardium specification in zebrafish. *Circ Res*, **106**, 1818-1828.
163. Liberatore, C.M., Searcy-Schrick, R.D. and Yutzey, K.E. (2000) Ventricular expression of tbx5 inhibits normal heart chamber development. *Dev Biol*, **223**, 169-180.
164. Yamak, A., Georges, R.O., Sheikh-Hassani, M., Morin, M., Komati, H. and Nemer, M. (2015) Novel exons in the tbx5 gene locus generate protein isoforms with distinct expression domains and function. *J Biol Chem*, **290**, 6844-6856.
165. Zaragoza, M.V., Lewis, L.E., Sun, G., Wang, E., Li, L., Said-Salman, I., Feucht, L. and Huang, T. (2004) Identification of the TBX5 transactivating domain and the nuclear localization signal. *Gene*, **330**, 9-18.
166. Stirnimann, C.U., Ptchelkine, D., Grimm, C. and Müller, C.W. (2010) Structural Basis of TBX5–DNA Recognition: The T-Box Domain in Its DNA-Bound and -Unbound Form. *Journal of Molecular Biology*, **400**, 71-81.
167. Ghosh, T.K., Packham, E.A., Bonser, A.J., Robinson, T.E., Cross, Stephen J. and Brook, J.D. (2001) Characterization of the TBX5 binding site and analysis of mutations that cause Holt–Oram syndrome. *Human Molecular Genetics*, **10**, 1983-1994.

168. Stirnimann, C.U., Ptchelkine, D., Grimm, C. and Müller, C.W. Structural Basis of TBX5-DNA Recognition: The T-Box Domain in Its DNA-Bound and -Unbound Form. *Journal of Molecular Biology*, **400**, 71-81.
169. Kulisz, A. and Simon, H.-G. (2008) An Evolutionarily Conserved Nuclear Export Signal Facilitates Cytoplasmic Localization of the Tbx5 Transcription Factor. *Mol. Cell. Biol.*, **28**, 1553-1564.
170. Hiroi, Y. (2001) Tbx5 associates with Nkx2-5 and synergistically promotes cardiomyocyte differentiation. *Nature Genet.*, **28**, 276-280.
171. ZHOU Zhu-ren, G.L.-g., GENG Wen-qing, QIU Guang-rong, SUN Kai-lai. (2008) Functional implications of C-terminus of TBX5 with high homology to C-terminal domain of yeast DNA-directed RNA polymerase II largest subunit. *Chinese Medical Journal*, **121** 762-765.
172. Murakami, M., Nakagawa, M., Olson, E. and Nakagawa, O. (2005) A WW domain protein TAZ is a critical coactivator for TBX5, a transcription factor implicated in Holt-Oram syndrome. *Proc Natl Acad Sci USA*, **102**, 18034 - 18039.
173. Vaughan, C.J. and Basson, C.T. (2000) Molecular determinants of atrial and ventricular septal defects and patent ductus arteriosus. *American Journal of Medical Genetics*, **97**, 304-309.
174. Koshiba-Takeuchi, K., Mori, A.D., Kaynak, B.L., Cebra-Thomas, J., Sukonnik, T., Georges, R.O., Latham, S., Beck, L., Henkelman, R.M., Black, B.L. *et al.* (2009) Reptilian heart development and the molecular basis of cardiac chamber evolution. *Nature*, **461**, 95-98.
175. Garg, V., Kathiriya, I.S., Barnes, R., Schluterman, M.K., King, I.N., Butler, C.A., Rothrock, C.R., Eapen, R.S., Hirayama-Yamada, K., Joo, K. *et al.* (2003) GATA4 mutations cause human congenital heart defects and reveal an interaction with TBX5. *Nature*, **424**, 443-447.
176. Ghosh, T.K., Song, F.F., Packham, E.A., Buxton, S., Robinson, T.E., Ronksley, J., Self, T., Bonser, A.J. and Brook, J.D. (2009) Physical Interaction between TBX5 and MEF2C Is Required for Early Heart Development. *Mol. Cell. Biol.*, **29**, 2205-2218.
177. Krause, A., Zacharias, W., Camarata, T., Linkhart, B., Law, E., Lischke, A., Miljan, E. and Simon, H.-G. (2004) Tbx5 and Tbx4 transcription factors interact with a new chicken PDZ-LIM protein in limb and heart development. *Developmental Biology*, **273**, 106-120.
178. Basson, C.T. (1997) Mutations in human TBX5 cause limb and cardiac malformation in Holt-Oram syndrome. *Nature Genet.*, **15**, 30-35.
179. Basson, C.T. (1999) Different TBX5 interactions in heart and limb defined by Holt-Oram syndrome mutations. *Proc. Natl Acad. Sci. USA*, **96**, 2919-2924.
180. Debrus, S., Rahbani, L., Marttila, M., Delorme, B., Paradis, P. and Nemer, M. (2005) The Zinc Finger-Only Protein Zfp260 Is a Novel Cardiac Regulator and a Nuclear Effector of α1-Adrenergic Signaling. *Molecular and Cellular Biology*, **25**, 8669-8682.
181. Komati, H., Maharsy, W., Beauregard, J., Hayek, S. and Nemer, M. (2011) ZFP260 is an inducer of cardiac hypertrophy and a nuclear mediator of endothelin-1 signaling. *Journal of Biological Chemistry*.
182. A. Ardati, a.M.N. (1993) A nuclear pathway for alpha 1-adrenergic receptor signaling in cardiac cells. *EMBO J*, **12**, 5131-5139.

183. Debrus, S., Rahbani, L., Marttila, M., Delorme, B., Paradis, P. and Nemer, M. (2005) The Zinc Finger-Only Protein Zfp260 Is a Novel Cardiac Regulator and a Nuclear Effector of {alpha}1-Adrenergic Signaling. *Mol. Cell. Biol.*, **25**, 8669-8682.
184. Besnar, N., Persuy, M.A., Stinnakre, M.G., Lepourry, L., Da Silva, J.C., Goubin, G. and Vilotte, J.L. (2002) Targeted expression of the only zinc finger gene in transgenic mice is associated with impaired mammary development. *Transgenic Res*, **11**, 505-513.
185. Antoine, K., Prosperi, M.T., Ferbus, D., Boule, C. and Goubin, G. (2005) A Kruppel zinc finger of ZNF 146 interacts with the SUMO-1 conjugating enzyme UBC9 and is sumoylated in vivo. *Mol Cell Biochem*, **271**, 215-223.
186. Pearson, R., Fleetwood, J., Eaton, S., Crossley, M. and Bao, S. (2008) Kruppel-like transcription factors: A functional family. *The International Journal of Biochemistry & Cell Biology*, **40**, 1996-2001.
187. Song, A., Patel, A., Thamatrakoln, K., Liu, C., Feng, D., Clayberger, C. and Krensky, A.M. (2002) Functional Domains and DNA-binding Sequences of RFLAT-1/KLF13, a Kruppel-like Transcription Factor of Activated T Lymphocytes. *Journal of Biological Chemistry*, **277**, 30055-30065.
188. Simmen, R.C.M., Pabona, J.M.P., Velarde, M.C., Simmons, C., Rahal, O. and Simmen, F.A. The emerging role of Kruppel-like factors in endocrine-responsive cancers of female reproductive tissues. *J Endocrinol*, **204**, 223-231.
189. Kaczynski, J., Cook, T. and Urrutia, R. (2003) Sp1- and Kruppel-like transcription factors. *Genome Biology*, **4**, 206.
190. Jain, M.K., Sangwung, P. and Hamik, A. (2014) Regulation of an Inflammatory Disease: Krüppel-Like Factors and Atherosclerosis. *Arteriosclerosis, Thrombosis, and Vascular Biology*, **34**, 499-508.
191. Chiplunkar, A.R., Lung, T.K., Alhashem, Y., Koppenhaver, B.A., Salloum, F.N., Kukreja, R.C., Haar, J.L. and Lloyd, J.A. (2013) Krüppel-Like Factor 2 Is Required for Normal Mouse Cardiac Development. *PLoS ONE*, **8**, e54891.
192. Kelsey, L., Flenniken, A.M., Qu, D., Funnell, A.P.W., Pearson, R., Zhou, Y.-Q., Voronina, I., Berberovic, Z., Wood, G., Newbigging, S. *et al.* (2013) ENU-induced Mutation in the DNA-binding Domain of KLF3 Reveals Important Roles for KLF3 in Cardiovascular Development and Function in Mice. *PLoS Genet*, **9**, e1003612.
193. Haldar, S.M., Lu, Y., Jeyaraj, D., Kawanami, D., Cui, Y., Eapen, S.J., Hao, C., Li, Y., Doughman, Y.Q., Watanabe, M. *et al.* (2010) Klf15 deficiency is a molecular link between heart failure and aortic aneurysm formation. *Sci Transl Med*, **2**, 3000502.
194. LePichon, J.-B., Bittel, D.C., Graf, W.D. and Yu, S. (2010) A 15q13.3 homozygous microdeletion associated with a severe neurodevelopmental disorder suggests putative functions of the TRPM1, CHRNA7, and other homozygously deleted genes. *American Journal of Medical Genetics Part A*, **152A**, 1300-1304.
195. Lomberk, G. and Urrutia, R. (2005) The family feud: turning off Sp1 by Sp1-like KLF proteins. *Biochem. J.*, **392**, 1-11.
196. Saptarsi, M.H., Osama, A.I. and Mukesh, K.J. (2007) Kruppel-like Factors (KLFs) in muscle biology. *Journal of molecular and cellular cardiology*, **43**, 1-10.
197. Narla, G., DiFeo, A., Yao, S., Banno, A., Hod, E., Reeves, H.L., Qiao, R.F., Camacho-Vanegas, O., Levine, A., Kirschenbaum, A. *et al.* (2005) Targeted Inhibition of the KLF6 Splice Variant, KLF6 SV1, Suppresses Prostate Cancer Cell Growth and Spread. *Cancer Research*, **65**, 5761-5768.

198. Yoshida, T., Gan, Q., Franke, A.S., Ho, R., Zhang, J., Chen, Y.E., Hayashi, M., Majesky, M.W., Somlyo, A.V. and Owens, G.K. Smooth and Cardiac Muscle-selective Knock-out of KrÃ¼ppel-like Factor 4 Causes Postnatal Death and Growth Retardation. *Journal of Biological Chemistry*, **285**, 21175-21184.
199. Shindo, T., Manabe, I., Fukushima, Y., Tobe, K., Aizawa, K., Miyamoto, S., Kawai-Kowase, K., Moriyama, N., Imai, Y., Kawakami, H. *et al.* (2002) Kruppel-like zinc-finger transcription factor KLF5/BTEB2 is a target for angiotensin II signaling and an essential regulator of cardiovascular remodeling. *Nat Med*, **8**, 856-863.
200. Rajamannan, N.M., Subramaniam, M., Abraham, T.P., Vasile, V.C., Ackerman, M.J., Monroe, D.G., Chew, T.-L. and Spelsberg, T.C. (2007) TGFβ inducible early gene-1 (TIEG1) and cardiac hypertrophy: Discovery and characterization of a novel signaling pathway. *Journal of Cellular Biochemistry*, **100**, 315-325.
201. Fisch, S., Gray, S., Heymans, S., Haldar, S.M., Wang, B., Pfister, O., Cui, L., Kumar, A., Lin, Z., Sen-Banerjee, S. *et al.* (2007) Kruppel-like factor 15 is a regulator of cardiomyocyte hypertrophy. *Proceedings of the National Academy of Sciences*, **104**, 7074-7079.
202. Prosdocimo, D.A., John, J.E., Zhang, L., Efraim, E.S., Zhang, R., Liao, X. and Jain, M.K. (2015) KLF15 and PPARα Cooperate to Regulate Cardiomyocyte Lipid Gene Expression and Oxidation. *PPAR Research*, **2015**, 201625.
203. Liu, Y., Sinha, S., McDonald, O.G., Shang, Y., Hoofnagle, M.H. and Owens, G.K. (2005) Kruppel-like Factor 4 Abrogates Myocardin-induced Activation of Smooth Muscle Gene Expression. *Journal of Biological Chemistry*, **280**, 9719-9727.
204. Richard, B., Xin Xin, S., Grace, W. and Michael, C. (2006) Angiotensin II and tumor necrosis factor-alpha upregulate survivin and Kruppel-like factor 5 in smooth muscle cells: Potential relevance to vein graft hyperplasia. *Surgery*, **140**, 289-296.
205. Martin, K.M., Ellis, P.D., Metcalfe, J.C. and Kemp, P.R. (2003) Selective modulation of the SM22alpha promoter by the binding of BTEB3 (basal transcription element-binding protein 3) to TGGG repeats. *Biochem. J.*, **375**, 457-463.
206. Gray, S., Wang, B., Sakuma, M., Croce, K., Fisch, S., Haldar, S., Lu, P., Zhu, Y., Simon, D.I. and Jain, M.K. (2006) Abstract 1393: Targeting of KLF15 Reveals a Critical Role in the Vascular Smooth Muscle Cell Response to Injury. *Circulation*, **114**, II_266-a-.
207. Matsumoto, N., Laub, F., Aldabe, R., Zhang, W., Ramirez, F., Yoshida, T. and Terada, M. (1998) Cloning the cDNA for a New Human Zinc Finger Protein Defines a Group of Closely Related KrÃ¼ppel-like Transcription Factors. *Journal of Biological Chemistry*, **273**, 28229-28237.
208. Asano, H., Li, X.S. and Stamatoyannopoulos, G. (2000) FKLF-2: a novel Kruppel-like transcriptional factor that activates globin and other erythroid lineage genes. *Blood*, **95**, 3578-3584.
209. Yamamoto, J., Ikeda, Y., Iguchi, H., Fujino, T., Tanaka, T., Asaba, H., Iwasaki, S., Ioka, R.X., Kaneko, I.W., Magoori, K. *et al.* (2004) A KrÃ¼ppel-like factor KLF15 Contributes Fasting-induced Transcriptional Activation of Mitochondrial Acetyl-CoA Synthetase Gene AceCS2. *Journal of Biological Chemistry*, **279**, 16954-16962.
210. Song, A., Chen, Y.-F., Thamatrakoln, K., Storm, T.A. and Krensky, A.M. (1999) RFLAT-1: A New Zinc Finger Transcription Factor that Activates RANTES Gene Expression in T Lymphocytes. *Immunity*, **10**, 93-103.

211. Martin, K.M., Cooper, W.N., Metcalfe, J.C. and Kemp, P.R. (2000) Mouse BTEB3, a new member of the basic transcription element binding protein (BTEB) family, activates expression from GC-rich minimal promoter regions. *Biochem. J.*, **345**, 529-533.
212. Martin, K.M., Metcalfe, J.C. and Kemp, P.R. (2001) Expression of Klf9 and Klf13 in mouse development. *Mechanisms of Development*, **103**, 149-151.
213. Gordon, A.R., Outram, S.V., Keramatipour, M., Goddard, C.A., Colledge, W.H., Metcalfe, J.C., Hager-Theodorides, A.L., Crompton, T. and Kemp, P.R. (2008) Splenomegaly and Modified Erythropoiesis in KLF13â€"/â€" Mice. *Journal of Biological Chemistry*, **283**, 11897-11904.
214. Nemer M, H.M. (2007) The KLF family of transcriptional regulators in cardiomyocyte proliferation and differentiation. *Cell Cycle*, **6**, 117-121.
215. Toshio, N.F., H. Takashi, U. Shigeyuki, Y. . (2009) In Nagai, R. F., Scott L.; Kasuga, Masato (ed.), *The Biology of Krüppel-like Factors*. Springer, Tokyo, Japan, pp. 268.
216. Wolfe SA, N.L., Pabo CO. (1999) DNA recognition by Cys2His2 zinc finger proteins. *Annu Rev Biophys Biomol Struct*, **29**, 183–212.
217. Nedved, M.L. and Moe, G.R. (1994) Cooperative, non-specific binding of a Zinc finger peptide to DNA. *Nucleic Acids Research*, **22**, 4705-4711.
218. Zhou, M., McPherson, L., Feng, D., Song, A., Dong, C., Lyu, S.-C., Zhou, L., Shi, X., Ahn, Y.-T., Wang, D. *et al.* (2007) KrÃ¼ppel-Like Transcription Factor 13 Regulates T Lymphocyte Survival In Vivo. *The Journal of Immunology*, **178**, 5496-5504.
219. Song, C.-Z., Keller, K., Murata, K., Asano, H. and Stamatoyannopoulos, G. (2002) Functional Interaction between Coactivators CBP/p300, PCAF, and Transcription Factor FKLF2. *Journal of Biological Chemistry*, **277**, 7029-7036.
220. Grzenda, A., Lomberk, G., Zhang, J.-S. and Urrutia, R. Sin3: Master scaffold and transcriptional corepressor. *Biochimica et Biophysica Acta (BBA) - Gene Regulatory Mechanisms*, **1789**, 443-450.
221. Kaczynski, J., Zhang, J.-S., Ellenrieder, V., Conley, A., Duenes, T., Kester, H., van der Burg, B. and Urrutia, R. (2001) The Sp1-like Protein BTEB3 Inhibits Transcription via the Basic Transcription Element Box by Interacting with mSin3A and HDAC-1 Co-repressors and Competing with Sp1. *Journal of Biological Chemistry*, **276**, 36749-36756.
222. Huang, B., Ahn, Y.-T., McPherson, L., Clayberger, C. and Krensky, A.M. (2007) Interaction of PRP4 with KrÃ¼ppel-Like Factor 13 Regulates CCL5 Transcription. *The Journal of Immunology*, **178**, 7081-7087.
223. Nikolcheva, T., Pyronnet, S., Chou, S.Y., Sonenberg, N., Song, A., Clayberger, C. and Krensky, A.M. (2002) A translational rheostat for RFLAT-1 regulates RANTES expression in T lymphocytes. *J Clin Invest*, **110**, 119-126.
224. Vermot, J., Forouhar, A.S., Liebling, M., Wu, D., Plummer, D., Gharib, M. and Fraser, S.E. (2009) Reversing Blood Flows Act through <italic>klf2a</italic> to Ensure Normal Valvulogenesis in the Developing Heart. *PLoS Biol*, **7**, e1000246.
225. Hu, X., Li, T., Zhang, C., Liu, Y., Xu, M., Wang, W., Jia, Z., Ma, K., Zhang, Y. and Zhou, C. (2011) GATA4 regulates ANF expression synergistically with Sp1 in a cardiac hypertrophy model. *J Cell Mol Med*, **15**, 1865-1877.

226. Fisch, S., Gray, S., Heymans, S., Haldar, S.M., Wang, B., Pfister, O., Cui, L., Kumar, A., Lin, Z., Sen-Banerjee, S. *et al.* (2007) Kruppel-like factor 15 is a regulator of cardiomyocyte hypertrophy. *Proc Natl Acad Sci U S A*, **104**, 7074-7079.
227. Camacho-Vanegas, O., Till, J., Miranda-Lorenzo, I., Ozturk, B., Camacho, S.C. and Martignetti, J.A. (2013) Shaking the family tree: identification of novel and biologically active alternatively spliced isoforms across the KLF family of transcription factors. *The FASEB Journal*, **27**, 432-436.
228. Wei, D., Wang, L., Kanai, M., Jia, Z., Le, X., Li, Q., Wang, H. and Xie, K. (2010) KLF4α Up-regulation Promotes Cell Cycle Progression and Reduces Survival Time of Patients With Pancreatic Cancer. *Gastroenterology*, **139**, 2135-2145.
229. Rodeck, C.H. and Whittle, M.J. (2009) *Fetal Medicine: Basic Science and Clinical Practice*. Churchill Livingstone.
230. Homminga, I., Pieters, R., Langerak, A.W., de Rooi, J.J., Stubbs, A., Verstegen, M., Vuerhard, M., Buijs-Gladdines, J., Kooi, C., Klous, P. *et al.* (2011) Integrated transcript and genome analyses reveal NKX2-1 and MEF2C as potential oncogenes in T cell acute lymphoblastic leukemia. *Cancer Cell*, **19**, 484-497.
231. McMahon, A.P. (2000) Neural patterning: the role of Nkx genes in the ventral spinal cord. *Genes Dev*, **14**, 2261-2264.
232. Gelb, B.D. and Chung, W.K. (2014) Complex genetics and the etiology of human congenital heart disease. *Cold Spring Harb Perspect Med*, **4**.
233. Øyen, N., Poulsen, G., Boyd, H.A., Wohlfahrt, J., Jensen, P.K.A. and Melbye, M. (2009) Recurrence of Congenital Heart Defects in Families. *Circulation*, **120**, 295-301.
234. Nemer, M. (2008) Genetic insights into normal and abnormal heart development. *Cardiovasc Pathol*, **17**, 48-54.
235. Xiong, Y., Zhou, B. and Chang, C.P. (2012) Analysis of the endocardial-to-mesenchymal transformation of heart valve development by collagen gel culture assay. *Methods Mol Biol*, **843**, 101-109.
236. Mahler, G., Gould, R. and Butcher, J. (2010) Isolation and culture of avian embryonic valvular progenitor cells. *J Vis Exp*, **27**.
237. van Bon, B.W.M., Mefford, H.C., Menten, B., Koolen, D.A., Sharp, A.J., Nillesen, W.M., Innis, J.W., de Ravel, T.J.L., Mercer, C.L., Fichera, M. *et al.* (2009) Further delineation of the 15q13 microdeletion and duplication syndromes: a clinical spectrum varying from non-pathogenic to a severe outcome. *Journal of Medical Genetics*, **46**, 511-523.
238. Derwińska K, B.M., Wiśniowiecka-Kowalnik B, Jagła M, Rudziński A, Pietrzyk JJ, Kawalec W, Ziółkowska L, Kutkowska-Kaźmierczak A, Gambin T, Sykulski M, Shaw CA, Gambin A, Mazurczak T, Obersztyn E, Bocian E, Stankiewicz P. (2012) Assessment of the role of copy-number variants in 150 patients with congenital heart defects. *Med Wieku Rozwoj*, **16**, 175-182.